COMPREHENSIVE RISK PREDICTION IN CARDIOMYOPATHIES. NEW GENETIC AND IMAGING MARKERS OF RISK

EDITED BY: Luis Lopes, Nuno Cardim, Juan R. Gimeno and Giovanni Quarta

PUBLISHED IN: Frontiers in Cardiovascular Medicine

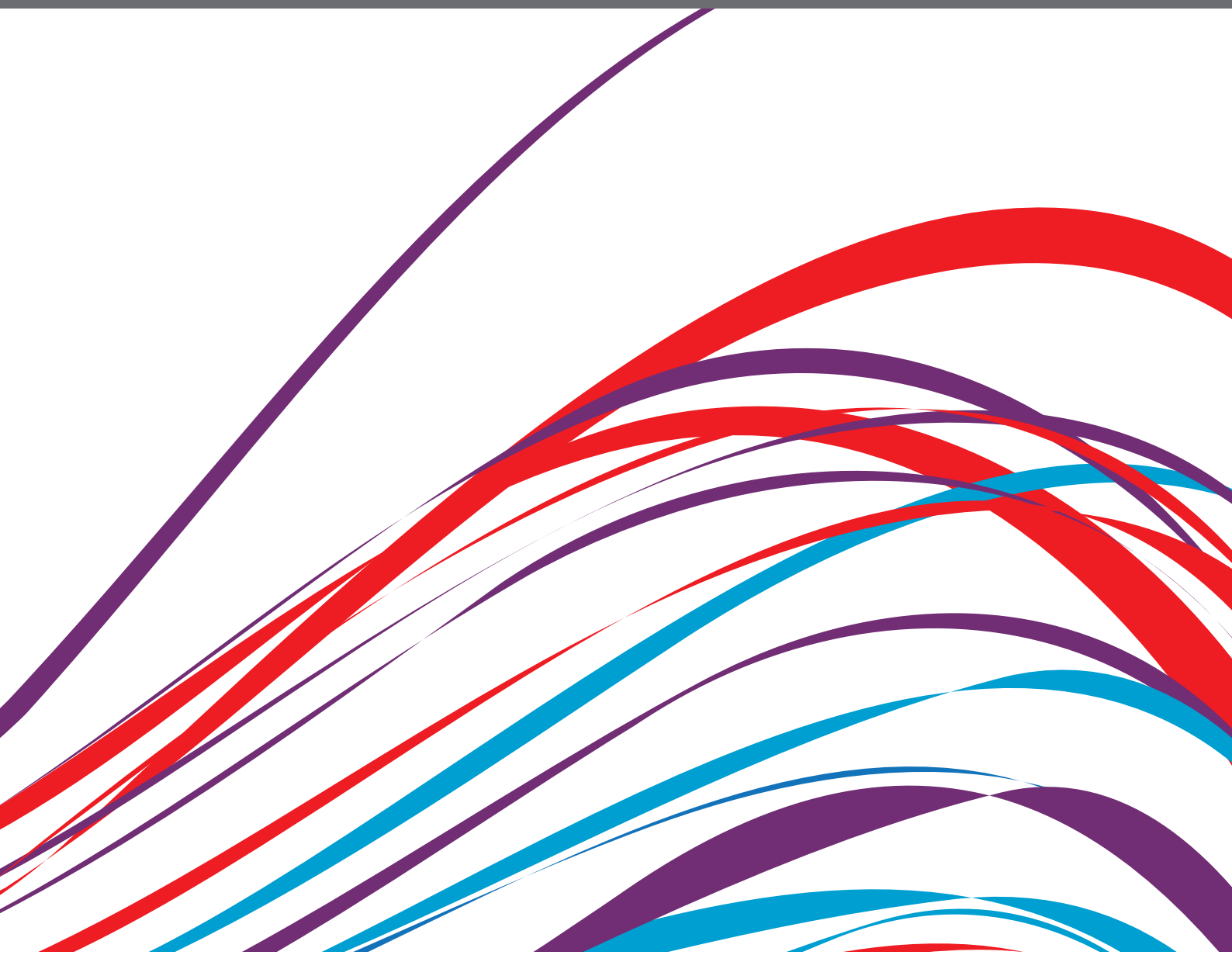

frontiers Research Topics

frontiers

ISSN 1664-8714
ISBN 978-2-88974-789-4
DOI 10.3389/978-2-88974-789-4

About Frontiers

Frontiers is more than just an open-access publisher of scholarly articles: it is a pioneering approach to the world of academia, radically improving the way scholarly research is managed. The grand vision of Frontiers is a world where all people have an equal opportunity to seek, share and generate knowledge. Frontiers provides immediate and permanent online open access to all its publications, but this alone is not enough to realize our grand goals.

Frontiers Journal Series

The Frontiers Journal Series is a multi-tier and interdisciplinary set of open-access, online journals, promising a paradigm shift from the current review, selection and dissemination processes in academic publishing. All Frontiers journals are driven by researchers for researchers; therefore, they constitute a service to the scholarly community. At the same time, the Frontiers Journal Series operates on a revolutionary invention, the tiered publishing system, initially addressing specific communities of scholars, and gradually climbing up to broader public understanding, thus serving the interests of the lay society, too.

Dedication to Quality

Each Frontiers article is a landmark of the highest quality, thanks to genuinely collaborative interactions between authors and review editors, who include some of the world's best academicians. Research must be certified by peers before entering a stream of knowledge that may eventually reach the public - and shape society; therefore, Frontiers only applies the most rigorous and unbiased reviews.
Frontiers revolutionizes research publishing by freely delivering the most outstanding research, evaluated with no bias from both the academic and social point of view. By applying the most advanced information technologies, Frontiers is catapulting scholarly publishing into a new generation.

What are Frontiers Research Topics?

Frontiers Research Topics are very popular trademarks of the Frontiers Journals Series: they are collections of at least ten articles, all centered on a particular subject. With their unique mix of varied contributions from Original Research to Review Articles, Frontiers Research Topics unify the most influential researchers, the latest key findings and historical advances in a hot research area! Find out more on how to host your own Frontiers Research Topic or contribute to one as an author by contacting the Frontiers Editorial Office: frontiersin.org/about/contact

COMPREHENSIVE RISK PREDICTION IN CARDIOMYOPATHIES. NEW GENETIC AND IMAGING MARKERS OF RISK

Topic Editors:
Luis Lopes, University College London, United Kingdom
Nuno Cardim, Hospital da Luz Lisboa, Portugal
Juan R. Gimeno, Hospital Universitario Virgen de la Arrixaca, Spain
Giovanni Quarta, Papa Giovanni XXIII Hospital, Italy

Citation: Lopes, L., Cardim, N., Gimeno, J. R., Quarta, G., eds. (2022). Comprehensive Risk Prediction in Cardiomyopathies. New Genetic and Imaging Markers of Risk. Lausanne: Frontiers Media SA. doi: 10.3389/978-2-88974-789-4

Table of Contents

frontiers in Cardiovascular Medicine

EDITORIAL
published: 08 March 2022
doi: 10.3389/fcvm.2022.849882

Editorial: Comprehensive Risk Prediction in Cardiomyopathies: New Genetic and Imaging Markers of Risk

Luis Rocha Lopes[1,2]*, *Giovanni Quarta*[3], *Nuno Cardim*[4,5] *and Juan Ramon Gimeno*[6]

[1] Barts Heart Centre, St. Bartholomew's Hospital, London, United Kingdom, [2] Institute of Cardiovascular Science, University College London, London, United Kingdom, [3] Papa Giovanni XXIII Hospital, Bergamo, Italy, [4] Hospital da Luz, Lisbon, Portugal, [5] Universidade Nova de Lisboa, Lisbon, Portugal, [6] Unidad Centros, Servicios y Unidades de Referencia/European Reference Networks Cardiopatías Familiares, Hospital Clínico Universitario Virgen Arrixaca, Murcia, Spain

Keywords: risk, cardiomyopathies, imaging, genetics, strain, cardiac magnetic resonance (CMR), cardiac computed tomographic (CT) imaging, histology

Editorial on the Research Topic

Comprehensive Risk Prediction in Cardiomyopathies: New Genetic and Imaging Markers of Risk

Hypertrophic, (HCM), dilated (DCM), and arrhythmogenic cardiomyopathies (ACM) are major causes of heart failure and sudden death (1). Current management guidelines recommend the use of risk stratification algorithms and more recently scores, to help with important decisions regarding medication initiation/uptitration and device use, including implantable cardioverter-defibrillators or cardiac resynchronization therapy (2–5). These algorithms and scores are mainly comprised of symptomatic status and a few imaging and/or ambulatory ECG markers.

A significant proportion of heart muscle disease is genetically caused and a pathogenic/likely pathogenic variant can be found in around 40–50% of index cases (1). Advances in genetics have allowed for an increasing diagnostic certainty and optimized family screening processes. An influence of genetics in prognosis and outcomes has also been reported in the last few years, but it is yet to be integrated into decision-making recommendations (6).

Great advances in cardiac imaging have also been described in the context of heart muscle disease, including myocardial deformation techniques, scar imaging, perfusion imaging, and tissue characterization (7). These have provided new insights regarding previously unknown phenotypes, including early disease, and already help with differential diagnosis dilemmas in the daily clinical practice. However, unlike old markers such as ejection fraction and wall thickness, these new imaging parameters have not yet been fully integrated in risk prediction algorithms, despite a number of publications describing associations with events (8).

The aim of this Research Topic was to gather contributions from researchers working in the fields of cardiomyopathy genetics and/or cardiomyopathy imaging, who have an interest in establishing a role for new genetics and imaging markers in comprehensive risk prediction in cardiomyopathies.

Segura-Rodriguez et al. described an association between epicardial global longitudinal strain (GLS), non-sustained ventricular tachycardia (NSVT), and late gadolinium enhancement (LGE) on cardiac magnetic resonance in 45 ACM patients, suggesting that a layer-specific GLS approach might offer better acuity compared to overall GLS.

In another paper focusing on myocardial deformation, Kim et al. assessed GLS in 300 patients after pacemaker implantation and found that lower LGS was associated with cardiovascular death and hospitalization for heart failure at 44 ± 28 months follow-up.

OPEN ACCESS

Edited and reviewed by:
Carla Sousa,
São João University Hospital Center, Portugal

***Correspondence:**
Luis Rocha Lopes
luis.lopes.10@ucl.ac.uk

Specialty section:
This article was submitted to Cardiovascular Imaging, a section of the journal Frontiers in Cardiovascular Medicine

Received: *06 January 2022*
Accepted: *31 January 2022*
Published: *08 March 2022*

Citation:
Lopes LR, Quarta G, Cardim N and Gimeno JR (2022) Editorial: Comprehensive Risk Prediction in Cardiomyopathies: New Genetic and Imaging Markers of Risk. Front. Cardiovasc. Med. 9:849882. doi: 10.3389/fcvm.2022.849882

In a different and original approach, Bueno-Beti and Asimaki described novel markers of ACM in surrogate tissues, such as the blood and the buccal epithelium, which may represent a non-invasive, safe and inexpensive alternative for diagnosis and cascade screening.

Also on the theme of ACM, Martinez-Sole et al. conducted a very timely systematic review of the exercise influence on the phenotype, concluding that sports may accelerate ACM phenotype either with structural and/or arrhythmic features, and restriction may soften the progression; data on phenotype-negative mutation carriers was also explored, as well as gaps in the current evidence.

Lopez-Ayala et al. analyzed 42 genotype positive-phenotype negative ACM carriers and found that a flattened ST segment may be an early sign of electrical remodeling that precedes T- wave inversion in healthy genetic carriers.

Conte et al. focused their contribution on a less explored imaging modality in the context of cardiomyopathies – when compared to magnetic resonance or echocardiography – by reviewing novel applications of cardiac computed tomography (CT) for a newly diagnosed cardiomyopathy, mainly DCM, including coronary imaging, function assessment, and tissue characterization, but also novel CT applications in HCM and ACM.

Two other articles addressed HCM. Qin et al. described a potential incremental value of T1 mapping to predicted SCD in addition to current guidelines.

An article by Aguiar Rosa et al. described that ischemia was associated with morphological markers of severity of disease, fibrosis, arrhythmia, and functional capacity.

Finally, in a non-genetic heart muscle disease context, Arcari et al. reviewed strain and CMR tissue characterization mapping parameters that have shown recent promise as prognostic predictors for takotsubo syndrome and reviewed the current limited evidence for a possible genetic predisposition.

Overall, the several manuscripts published in this Research Topic demonstrate some of the current trends on cardiomyopathies research: the promising prognostic value of myocardial deformation imaging and tissue characterization for ACM and HCM; the role of myocardial ischemia as a new imaging risk marker in HCM; the value of CT in the diagnosis of cardiomyopathies; new diagnostic approaches for family screening based on the ECG and buccal epithelium for ACM; and the impact of exercise in ACM, including mutation carriers.

AUTHOR CONTRIBUTIONS

LL drafted the editorial and approved the final content. All authors reviewed the drafted editorial and approved the final version.

REFERENCES

1. McKenna WJ, Judge DP. Epidemiology of the inherited cardiomyopathies. *Nat Rev Cardiol.* (2020). doi: 10.1038/s41569-020-0428-2
2. Authors/Task Force, Elliott PM, Anastasakis A, Borger MA, Borggrefe M, Cecchi F, et al. 2014 ESC Guidelines on diagnosis and management of hypertrophic cardiomyopathy: the task force for the diagnosis and management of hypertrophic cardiomyopathy of the European Society of Cardiology (ESC). *Eur Heart J.* (2014) 35:2733–79. doi: 10.1093/eurheartj/ehu284
3. Writing Committee M, Ommen SR, Mital S, Burke MA, Day SM, Deswal A, et al. 2020 AHA/ACC guideline for the diagnosis and treatment of patients with hypertrophic cardiomyopathy: a report of the American College of Cardiology/American Heart Association Joint Committee on Clinical Practice Guidelines. *Circulation.* (2020) 142:e533–e557. doi: 10.1161/CIR.0000000000000938
4. Towbin JA, McKenna WJ, Abrams DJ, Ackerman MJ, Calkins H, Darrieux FCC, et al. 2019 HRS expert consensus statement on evaluation, risk stratification, and management of arrhythmogenic cardiomyopathy: executive summary. *Heart Rhythm.* (2019) 16:e373–407. doi: 10.1016/j.hrthm.2019.09.019
5. Cadrin-Tourigny J, Bosman LP, Wang W, Tadros R, Bhonsale A, Bourfiss M, et al. Sudden cardiac death prediction in arrhythmogenic right ventricular cardiomyopathy: a multinational collaboration. *Circ Arrhythm Electrophysiol.* (2021) 14:e008509. doi: 10.1161/CIRCEP.120.008509
6. Semsarian C, Ingles J, Ross SB, Dunwoodie SL, Bagnall RD, Kovacic JC. Precision medicine in cardiovascular disease: genetics and impact on phenotypes: JACC focus seminar 1/5. *J Am Coll Cardiol.* (2021) 77:2517–30. doi: 10.1016/j.jacc.2020.12.071
7. Cardim N, Galderisi M, Edvardsen T, Plein S, Popescu BA, D'Andrea A, et al. Role of multimodality cardiac imaging in the management of patients with hypertrophic cardiomyopathy: an expert consensus of the European Association of Cardiovascular Imaging Endorsed by the Saudi Heart Association. *Eur Heart J Cardiovasc Imaging.* (2015) 16:280. doi: 10.1093/ehjci/jeu291
8. Tower-Rader A, Mohananey D, To A, Lever HM, Popovic ZB, Desai MY. Prognostic value of global longitudinal strain in hypertrophic cardiomyopathy: a systematic review of existing literature. *JACC Cardiovasc Imaging.* (2019) 12:1930–42. doi: 10.1016/j.jcmg.2018.07.016

Conflict of Interest: The authors declare that the research was conducted in the absence of any commercial or financial relationships that could be construed as a potential conflict of interest.

frontiers in Cardiovascular Medicine

ORIGINAL RESEARCH
published: 07 May 2021
doi: 10.3389/fcvm.2021.646391

Electrocardiographic Screening of Arrhythmogenic Cardiomyopathy in Genotype-Positive and Phenotype-Negative Relatives

Jose Maria Lopez-Ayala[1]*, *Javier Gimeno-Blanes*[2], *David Lopez-Cuenca*[3], *Maria Sabater Molina*[3] and *Juan Ramon Gimeno-Blanes*[3]

[1] Department of Cardiology, San Juan General University Hospital, Alicante, Spain, [2] Department of Signal Theory and Communications, Miguel Hernández University, Alicante, Spain, [3] Department of Cardiology, Virgen de la Arrixaca University Hospital, Murcia, Spain

OPEN ACCESS

Edited by:
Matteo Cameli, University of Siena, Italy

Reviewed by:
Alexandros Protonotarios, University College London, United Kingdom
Emmanuel Androulakis, Royal Brompton & Harefield NHS Foundation Trust, United Kingdom

***Correspondence:**
Jose Maria Lopez-Ayala
josemaria_lopezayala@yahoo.es

Specialty section:
This article was submitted to Cardiovascular Imaging, a section of the journal Frontiers in Cardiovascular Medicine

Received: *26 December 2020*
Accepted: *22 March 2021*
Published: *07 May 2021*

Citation:
Lopez-Ayala JM, Gimeno-Blanes J, Lopez-Cuenca D, Molina MS and Gimeno-Blanes JR (2021) Electrocardiographic Screening of Arrhythmogenic Cardiomyopathy in Genotype-Positive and Phenotype-Negative Relatives. Front. Cardiovasc. Med. 8:646391. doi: 10.3389/fcvm.2021.646391

Background: Arrhythmogenic cardiomyopathy is a hereditary cause of ventricular arrhythmias and sudden death. Identifying the healthy genetic carriers who will develop the disease remains a challenge. A novel approach to the analysis of the digital electrocardiograms of mutation carriers through signal processing may identify early electrocardiographic abnormalities.

Methods: A retrospective case–control study included a population of healthy genetics carriers and their wild-type relatives. Genotype-positive/phenotype-negative individuals bore mutations associated with the development of arrhythmogenic cardiomyopathy. The relatives included had a non-pathological 12-lead electrocardiogram, echocardiogram, and a cardiac magnetic resonance. Automatic digital electrocardiographic analyses comprised QRS and terminal activation delay duration, the number of QRS fragmentations, ST slope, and T-wave voltage.

Results: Digital 12-lead electrocardiograms from 41 genotype-positive/phenotype-negative (29 simple carriers and 12 double mutation carriers) and 73 wild-type relatives were analyzed. No differences in the QRS length, the number of QRS fragmentations, and the voltage of the T-wave were observed. After adjusting for potential confounders, double carriers showed an average ST-slope flatter than those of the simple carriers and wild type [5.18° (0.73–8.01), 7.15° (5.14–11.05), and 11.46° (3.94–17.49), respectively, $p = 0.005$]. There was a significant negative correlation between the ST slope and the age in genotype-positive/phenotype-negative relatives ($r = 0.376$, $p = 0.021$) not observed in their wild-type counterparts ($r = 0.074$, $p = 0.570$).

Conclusions: A flattened ST segment may be an early sign of electrical remodeling that precedes T-wave inversion in healthy genetic carriers. A thorough analysis of the digital electrocardiographic signal may help identify and measure early electrical abnormalities.

Keywords: arrhythmogenic right ventricular cardiomyopathy, electrocardiogram, genetic carrier, early diagnosis, familiar screening

INTRODUCTION

Arrhythmogenic cardiomyopathy is a cause of unexpected sudden death and ventricular arrhythmias in the general population including the youth and competitive athletes (1, 2). This umbrella term encompasses a broad phenotypic spectrum of disease that may predominantly affect one of the ventricles or both (3). The underlying cause of the disease is usually a mutation in a desmosomal gene, although mutations in other genes have been also described (4). Most common forms of arrhythmogenic cardiomyopathy are classically inherited in a dominant trait with incomplete penetrance and a variable clinical phenotype. The natural history of the disease encompasses a concealed, an electric, and a late structural phase, being sinister arrhythmias and sudden death a potential outcome at any stage even in the absence of overt structural abnormalities (5).

Once the diagnosis of arrhythmogenic cardiomyopathy is established, carrying out a complete family screening is recommended. As electrocardiographic changes usually precede the development of subsequent structural abnormalities, it is paramount to identify early electrocardiographic abnormalities that herald an initial electric phase of the disease. Thus far, predicting the individuals who will develop a severe phenotype remains a challenge.

As desmosomal disruption results in cell-to-cell mechanical and electrical uncoupling and fibrofatty replacement that slow down the electrical propagation (6), we hypothesized that genotype-positive/phenotype-negative relatives may show longer QRS terminal activation delays and minor ST/T-wave abnormalities preceding the development of the overt electrocardiographic abnormalities included in the current diagnostic criteria (7). The goal of this research is, therefore, to identify early electrocardiographic abnormalities in genotype-positive/phenotype-negative relatives.

MATERIALS AND METHODS

We carried out a retrospective electrocardiographic evaluation in genotype-positive/phenotype-negative relatives of families with a previous diagnosis of arrhythmogenic cardiomyopathy. All individuals had been previously assessed in a monographic cardiomyopathy clinic, were above 18 years of age, and consented to undergo genetic testing. None of the included individuals reported a previous history of heart disease. Participants showed normal imaging findings (non-dilated left and right ventricles, normal ejection fraction, no regional wall motion abnormalities, and no late gadolinium enhancement on cardiac magnetic resonance, **Table 2**). Mutation carriers and controls showing inverted T-waves in precordial leads beyond V1 were excluded from the analysis.

Genetic Testing

A panel of genes associated with arrhythmogenic cardiomyopathy was tested in the proband of each family (defined as the first member to be diagnosed with the disease). Genetic confirmation tests were performed through Sanger sequencing in all the relatives. The frequency of the mutations in the general population was evaluated with the Genome Aggregation Database (gnomAD) (RRID:SCR_014964) Frequencies < 0.001 supports the pathogenicity of the included

TABLE 1 | List of the 41 identified mutations in the desmosomal genes and *LDB3*.

Gene	Mutation	*N*	Mechanism	Affected carriers	MAF in gnomAD (genome)	ACMG score
JUP	c.56C>T (p.Thr19Ile)	3	Missense	3	3.234E−5	Uncertain significance
PKP-2	c.419C>T (p.Ser140Phe)	2	Missense	7	0.0019	Uncertain significance
	c.1253C>A (p.Ala418Asp)	1	Missense	1	–	Uncertain significance
DSC-2	c.2686_2687dup (p.Ala897Lysfs*900)	4	Nonsense/truncation	5	–	Pathogenic
	c.397G>A (p.Ala133Thr)	1	Missense	1	6.459E−5	Uncertain significance
	c.1350A>G (p.Arg450=)	1	Missense	2	0.0019	Likely benign
DSP	c.5773C>T (p.Gln1925*)	2	Nonsense/truncation	1	–	Pathogenic
	c.3219_3220insA (p.Ala1074Serfs*1087)	5	Nonsense/truncation	5	–	Pathogenic
	c.2631-1G>A (IVS18-1G>A)	1	Splicing/intronic	1	–	Pathogenic
	c.1339C>T (p.Q447X)	4	Nonsense/truncation	20	–	Pathogenic
	c.4609C>T (p.Arg1537Cys)	7	Missense	6	0.0087	Benign
	c.4372C>G (p.Arg1458Gly)	3	Missense	3	0.0009	Uncertain significance
DSG-2	c.2759T>G (p.Val920Gly)	3	Missense	7	0.0033	Benign
	c.166G>A (p.Val56Met)	2	Missense	1	0.0016	Likely benign
LDB3	c.1051A>G (p.Thr351Ala)	2	Missense	6	0.0003	Likely benign

Nucleotide and the protein changes are shown along with the predicted effect of the mutation. The mechanism of the mutation is classified as missense, nonsense, or truncation and boundary mutations affecting the splicing. Affected carriers represents the total number of probands and relatives bearing the mutation. Minor allele frequency (MAF) in the gnomAD database.

JUP, junctional plakoglobin; PKP-2, plakophilin-2; DSC-2, desmocollin-2; DSP, desmoplakin; DSG-2, desmoglein-2; LDB3, LIM domain binding 3; ACMG score, American College of Medical Genetics Score.

variants. American College of Medical Genetics Score (ACMG) score and familiar cosegregation were also used to establish the clinical significance of the mutations.

Digital Electrocardiographic Analysis

Digital 12-lead electrocardiograms were obtained with a GE MAC 5000 System. Fiducial points were independently set for each beat in the 12 leads with MATLAB 2010 [Version 7.10.0 (R2010a), Natick, Massachusetts: The MathWorks Inc, MATLAB, RRID: SCR_001622]. The cardiology analyst (JL) was blinded to the genetic data at the time of evaluation. Details about signal processing have been published elsewhere (8). In summary, fiducial points were set at the beginning of the P-wave, QRS onset, QRS offset, and at the end of the T-wave. The terminal activation delay of the QRS was measured from the nadir of the S-wave to the J-point. The T-wave voltage (mV) and area (μV·s) were calculated through changes in the slope of the electrocardiographic signal. The ST slope was defined as the averaged angle between the ST tangent with the baseline in the 12 leads. The investigated electrocardiographic variables were the median QRS duration, terminal activation delay in V1–V3, the number of QRS fragmentations, the presence of bundle branch blocks, ST-slope, and T-wave voltage and area.

Statistical Analysis

Qualitative variables were expressed in percentage and compared with Pearson's χ^2-test (or Fisher's test when appropriate). Quantitative variables are described as mean ± standard deviation (or median and interquartile rank should they do not follow a normal distribution), and they were compared with the Student's *t*-test or ANOVA (or the non-parametric Wilcoxon's and Kruskal–Wallis tests). Normality was tested with the Shapiro–Wilk test. The correlation between two quantitative variables was determined with Pearson's *r* coefficient.

The effect of genetic status (wild type, a single mutation, or double mutation) on the ST slope and the effect of potential confounding variables (age, sex, body mass index, predicted effect of the mutation) was determined with a linear regression model. Wild-type status and female sex were set as reference categories. Statistical analysis was performed with the package Stata 13.1 (Copyright 1985-2013 Stata Corp Texas 77845 USA, RRID: SCR_012763).

RESULTS

Genetic Results

A total of 41 genotype-positive/phenotype-negative relatives with a digital electrocardiogram were included in the study. Pathogenic mutations were identified in five desmosomal genes (*DSP*, *PKP-2*, *DSG-2*, *DSC-2*, *JUP*) and *LDB3*. The frequency and the proposed mechanism of each mutation are described in **Table 1**.

Electrocardiographic Characterization in Mutation Carriers

Basal characteristics and electrocardiographic findings are summarized in **Table 2**. No significant differences were observed in the median QRS length, QRS terminal activation delay, or the number of fragmentations in the QRS between genotype-positive/phenotype-negative and wild-type relatives. Despite the ST slope being flatter in mutation carriers compared to wild type, this difference was not significant, 6.24° (4.11–9.81) vs. 11.94° (6.19–17.53), $p = 0.187$. No differences were observed either in the T-wave voltage, T-wave area, or T-wave dispersion between groups.

TABLE 2 | Quantitative analysis of the electrocardiographic parameters through digital analysis in gene carriers and wild-type relatives.

	Mutation carriers ($N = 41$)	Wild type ($N = 73$)	*p*
Sex (male)	22 (53.7%)	45 (61.64%)	0.939
Age (years)	38.5 (25–50.5)	34 (26–47)	0.514
BMI (kg/m^2)	23.67 (22.66–25.50)	23.41 (21.80–26.85)	0.880
LVED volume (ml)	137 ± 19	132 ± 9	0.854
LVEF (%)	63 ± 8	61 ± 5	0.756
RVED volume (ml)	132 ± 9	134 ± 6	0.698
RVEF (%)	60 ± 6	59 ± 7	0.921
ECG			
IRBBB	14 (34.15%)	23 (31.51%)	0.977
CRBBB	3 (6.82%)	3 (4.11%)	0.166
QRS (ms)	84 (78–90)	84 (80–84)	0.803
QRS V1–3 (S-offset) (ms)	38 (32–44)	38 (34–42)	0.474
QRS fragmentation (*n*)	1 (0–2)	1 (0–1)	0.268
ST slope (°)	6.24 (4.11–9.81)	11.46 (3.94–17.49)	0.187
TWI (*n*)	1 (1, 2)	1 (1, 2)	0.896
T-wave amplitude (mV)	0.20 (0.11–0.30)	0.214 (0.139–0.285)	0.348
T-wave area (μV·s)	18.58 (9.13–30.42)	22.35 (12.77–32.98)	0.478
T-wave dispersion (μV·s)	2.50 (1.48–5.02)	1.82 (0.81–4.79)	0.742

Values are expressed in percentage, median, and interquartile range.
IRBBB, incomplete right bundle branch block; CRBBB, complete right bundle branch block; TWI, T-wave inversion.

Electrocardiographic Findings in Double-Mutation Carriers

Digital electrocardiograms were obtained from carriers of 15 different mutations (5 pathogenic, 5 VUS, 5 benign or likely benign, **Table 1**). Among 41 genotype-positive/phenotype-negative individuals, 12 bore 2 different mutations in desmosomal genes. Their electrocardiographic parameters were compared with those of single-mutation carriers and the wild-type relatives (**Table 3**). The averaged ST slope showed a significant difference between the three groups: 7.15° (5.14–11.05), 5.18° (0.73–8.01), and 11.46° (3.94–17.49) (single mutation, double mutation, and wild type, respectively), $p = 0.005$ (**Figure 1**).

The ST slope significantly correlated with the T-wave voltage in mutation carriers ($r = 0.376$, $p = 0.021$) but not in the wild-type group ($r = 0.074$, $p = 0.570$). Other electrocardiographic variables did not demonstrate any correlation with the ST slope.

Of note, a negative correlation between the ST slope and age was present in mutation carriers ($r = -0.353$, $p = 0.022$) but not in wild-type individuals ($r = -0.053$, $p = 0.672$) (**Figure 2**).

TABLE 3 | Quantitative analysis of the main electrocardiographic parameters in single- and double-mutation carriers and wild-type relatives.

	Simple carriers (*N* = 29)	Double carriers (*N* = 12)	Wild type (*N* = 73)	*p*
Sex (male)	14 (48.27%)	8 (66.67%)	45 (61.64%)	0.5590
Age (years)	36 (28–48)	35 (25–56)	34 (26–47)	0.8080
BMI (kg/m^2)	24.01 (21.48–25.50)	23.67 (22.66–26.40)	23.41 (21.80–26.85)	0.7919
ECG				
IRBBB	14 (48.27%)	0 (0%)	23 (31.51%)	0.012
CRBBB	0 (0%)	0 (0%)	3 (4.11%)	0.0382
QRS (ms)	84 (78–94)	86 (76–100)	84 (80–84)	0.9288
QRS V1–3 (S-offset) (ms)	38 (36–44)	38 (28–42)	38 (34–42)	0.5667
QRS fragmentation (*n*)	1 (0–2)	0	1 (0–1)	0.9579
ST slope (°)	7.15 (5.14–11.05)	5.18 (0.73–8.01)	11.46 (3.94–17.49)	0.0054
TWI (*n*)	1 (1,2)	1 (0–2.5)	1 (1,2)	0.8822
T-wave amplitude (mV)	0.223 (0.119–0.277)	0.171 (0.11–0.30)	0.214 (0.139–0.285)	0.7696
T-wave area (μVs)	18.91 (12.30–29.18)	11.03 (6.37–33.44)	22.35 (12.77–32.98)	0.4965
T-wave dispersion (μVs)	2.36 (1.13–4.96)	2.96 (2.41–10.38)	1.82 (0.81–4.79)	0.1936

BMI, body mass index; IRBBB, incomplete right bundle branch block; CRBBB, complete right bundle branch block; TWI, T-wave inversion.

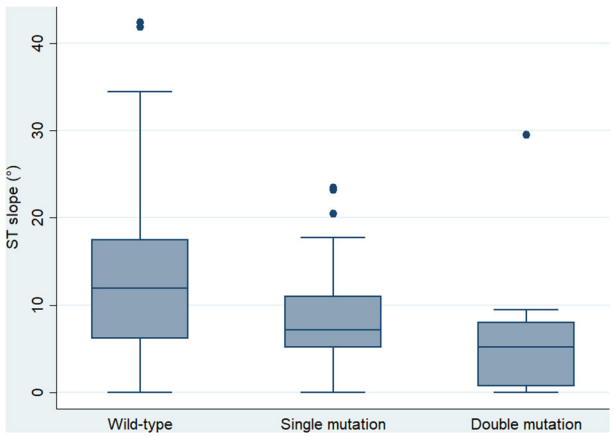

FIGURE 1 | Box plot showing the median and interquartile range of the ST slope in wild-type controls and single- and double-mutation carriers ($p = 0.001$).

The effect of the genetic mutations on the ST slope was estimated with a linear regression model. Potential confounding variables such as age, sex, body mass index, and the type of mutation (classified into truncating or no truncating mutations) were included in the model. The presence of double mutations was independently associated with a flatter ST slope (b = −7.86, $p = 0.002$), while this effect was not significant in the case of single mutation carriers (b = −2.344, $p = 0.206$) (**Table 4**).

DISCUSSION

The diagnosis of arrhythmogenic cardiomyopathy poses a challenge in the clinical practice due to a wide phenotypic spectrum that encompasses right-sided (1) and left-sided or biventricular forms (9, 10). Despite current efforts to stratify the risk of sudden death in these patients, it is well-recognized that affected individuals may die suddenly at an early phase of the disease when electrocardiographic and structural abnormalities are usually absent.

Therefore, the identification of the mutation carriers who will develop the disease is challenging. Magnetic resonance imaging (11) and speckle tracking (12) have shown minor abnormalities in healthy mutation carriers, although they are not routinely used in the family screening due to the lack of reproducibility of the speckle tracking and the cost and risk of overdiagnosis of non-pathological findings such as subtle wall motion abnormalities in cardiac magnetic resonance.

Once the diagnosis of arrhythmogenic cardiomyopathy is established, carrying out a genetic study, as well as a complete cascade family screening, is recommended to identify relatives at risk. This strategy also helps make a definitive diagnosis in probands with a thus far borderline phenotype (7).

As electrocardiographic abnormalities usually precede the development of overt structural cardiomyopathy, we aimed to identify signs of the electric "concealed stage" of the cardiomyopathy through a detailed analysis of digital electrocardiograms. Despite the presence of complete right bundle branch block, negative anterior T-waves, terminal activation delay > 55 ms in V1–V3 being frequently found in arrhythmogenic cardiomyopathy patients (13, 14), data on the prevalence of these electrocardiographic abnormalities in genotype-positive/phenotype-negative individuals are lacking. Furthermore, studies that compare mutation carriers with non-mutation carriers from the same family are pertinent to understand the phenotypic effect of mutations and variants.

We retrospectively evaluated the digital electrocardiograms of carriers of pathogenic mutations that did not show either evidence of structural disease on imaging or electrocardiographic abnormalities included in the current diagnostic criteria. Accurate QRS, ST, and T-wave measurements were obtained through digital electrocardiographic analysis thereby allowing a more sensitive approach to that provided by the analysis

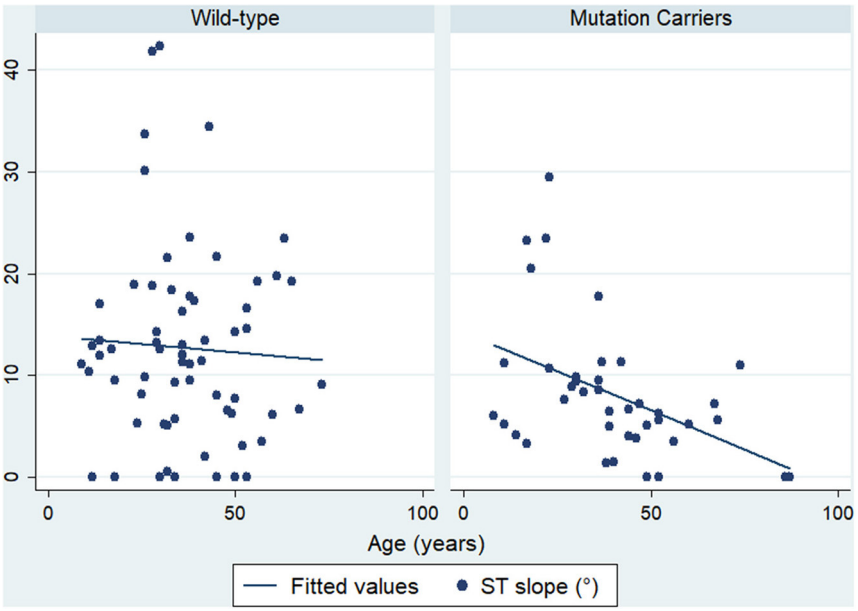

FIGURE 2 | Correlation between ST slope and age. Mutation carriers are presented on the right side and wild-type on the left side.

TABLE 4 | Linear regression models.

	Model 1 ST slope	Model 2 ST slope
Genetic status		
0. Control	0	0
1. Simple mutation	−2.344	−1.904
	(1.839)	(1.955)
2. Double mutation	−7.862**	−7.641**
	(2.416)	(2.678)
Sex		
0. Female	0	0
1. Male	3.781*	3.516*
	(1.614)	(1.737)
BMI (kg/m^2)	0.161	0.115
	(0.261)	(0.271)
Age (years)	−0.0705	−0.0701
	(0.0587)	(0.0638)
Type of mutation		
0. Non-truncating		0
1. Truncating		−0.843
		(1.872)
Constant	8.730	10.06
	(5.373)	(5.600)
N	84	75
R^2	0.194	0.180

The included variables were ST slope (dependent variable), genetic status (independent variable) and sex, body mass index, and age (as potential confounders). A second model (on the right) added the type of mutation (truncating/non-truncating). Non-carriers and female sex are considered the reference for the variables sex and type of mutation, respectively. Standard errors are shown in parentheses.
*$p < 0.05$, **$p < 0.01$.*

of conventionally recorded electrocardiograms. QRS terminal activation delay, averaged ST slope in the 12 leads, and T-wave voltage were therefore quantitatively assessed, which should overcome the subjectivity in the interpretation of subtle electrocardiographic abnormalities.

The initial hypothesis of the study was that of healthy genotype-positive/phenotype-negative individuals showing a longer QRS duration and terminal activation delay, a flatter ST slope, and smaller T-wave amplitude than wild-type relatives. We hypothesize that mutations and variants associated with the development of arrhythmogenic cardiomyopathy may play a role in early GAP junctions and connexin-43 remodeling (15) as well as intracellular ion mishandling (16), which may precede the development of electrocardiographic abnormalities (right bundle branch block and T-wave inversion) and further gross structural abnormalities as the clinical phenotype progresses. A proportion of the carriers included in the study bore non-pathogenic variants, which may either act as modulators of the phenotypic expression of the disease or cause subtle electrocardiographic abnormalities.

Our study demonstrated the trend of genotype-positive/phenotype-negative relatives to show a flatter ST slope, more pronounced in the case of double-mutation carriers. The effect of a double-hit mutation on the ST slope remained significant after correction for potential confounders such as age, sex, and body mass index. Interestingly, we did not find differences between mutation carriers and wild-type individuals in any of the parameters included in the current of former diagnostic criteria, the number of QRS fragmentations, or the T-wave amplitude. In view of these findings, we propose that

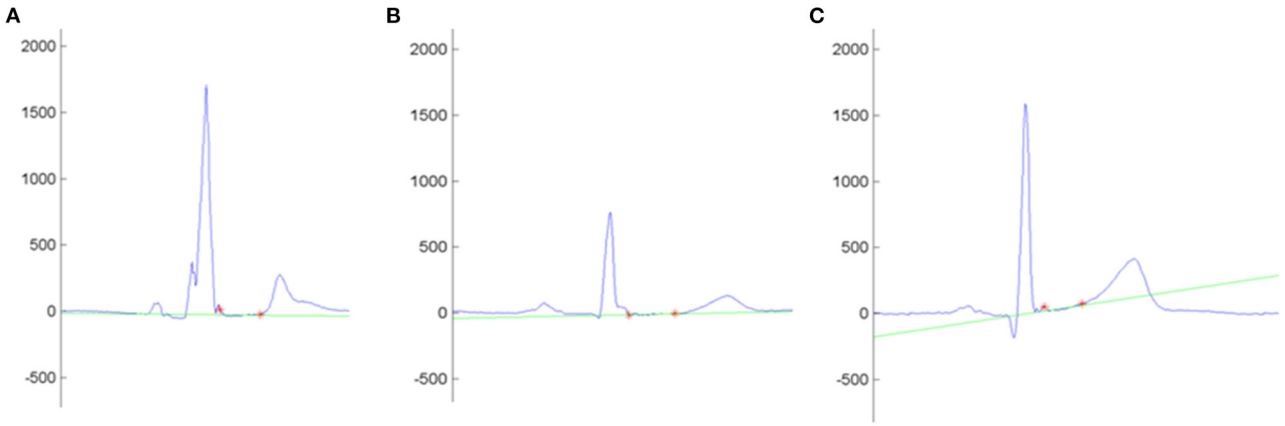

FIGURE 3 | Example of the automatic measurement of the ST slope in the lead I. Y-Axis shows the voltage (mV). Red asterisks mark the QRS offset and the T-wave onset. The intersection line (green) determines the ST-slope angle with the isoelectric line. **(A–C)** shows the ST slope of an arrhythmogenic cardiomyopathy patient (−0.4°), a non-affected mutation carrier (1.9°), and a control (9.3°), respectively.

ST-slope flattening is an early electrical abnormality in relatives with a significant genetic burden (**Figure 3**). Gene carriers bearing this repolarization pattern may benefit from a thorough cardiological study [including cardiac magnetic resonance, Holter monitoring and exercise test (17)] and a more frequent follow-up than other healthy relatives.

The analysis of the ST-segment morphology has proved to be a useful tool in the differential diagnosis between arrhythmogenic cardiomyopathy and the physiological adaptation to competitive sport commonly known as athlete's heart. Of note, a convex upward morphology (positive ST slope) in anterior leads suggests a physiological remodeling, whereas a flat or down-sloping ST (negative ST slope) suggests the diagnosis of arrhythmogenic cardiomyopathy (18). Repolarization abnormalities in arrhythmogenic cardiomyopathy patients classically involves right precordial leads. However, as biventricular or left-sided phenotypes may also affect inferior and left precordial leads, the average ST slope of the 12 leads was included in the analysis.

In order to evaluate the ST slope beyond the dichotomic classification between positive or flat/negative slope, we support a quantitative approach rendered by the processing of digital electrocardiograms, which eliminates the interobserver bias.

As arrhythmogenic cardiomyopathy typically shows an incomplete penetrance, it would be reasonable to expect a progressive flattening of the ST slope during follow-up, which is beyond the scope of this research. Whether ST flattening precedes a future T-wave inversion will require further investigations. In this regard, we observed a negative correlation between age and ST slope in mutation carriers, which supports that hypothesis.

This research has several limitations. First, this is a non-matched case–control study that includes a small number of individuals. Second, it was not possible to identify the mutation carriers who will develop further electrical or structural abnormalities on the basis of ST. This hypothesis will require further investigations. Third, the interpretation of the genetic analysis is challenging in arrhythmogenic cardiomyopathy due to a significant prevalence of desmosomal variants in the general population. Some of the variants included are not disease causing by themselves although may contribute to the phenotype of the disease.

In conclusion, we proposed that a detailed and thorough analysis of digital electrocardiograms in genotype-positive/phenotype-negative individuals renders the identification of early electrocardiographic abnormalities, which may portend an early phase of the disease. ST-slope flattening is the earliest abnormality found in double-hit mutation carriers.

DATA AVAILABILITY STATEMENT

The raw data supporting the conclusions of this article will be made available by the authors, without undue reservation.

ETHICS STATEMENT

The studies involving human participants were reviewed and approved by Virgen de la Arrixaca Ethics Committee. The patients/participants provided their written informed consent to participate in this study.

AUTHOR CONTRIBUTIONS

JL-A: conceptualization, methodology, writing-original draft, and formal analysis. DL-C: resources and conceptualization. MM: methodology and genetic testing. JaG-B: conceptualization, software, methodology, and formal analysis. JuG-B: conceptualization, data curation, and writing—original draft, resources. All authors contributed to the article and approved the submitted version.

ACKNOWLEDGMENTS

We would like to thank the Department of Cardiology, Inherited Cardiac Diseases Unit and the Cardiogenetic Laboratory of the Virgen de la Arrixaca University Hospital, and the Department of Signal Theory and Communications of the Miguel Hernández University and Health in Code for their contributions.

REFERENCES

1. Marcus FI, Fontaine GH, Guiraudon G, Frank R, Laurenceau JL, Malergue C, et al. Right ventricular dysplasia: a report of 24 adult cases. *Circulation.* (1982) 65:384–98. doi: 10.1161/01.CIR.65.2.384
2. Corrado D, Basso C, Rizzoli G, Schiavon M, Thiene G. Does sports activity enhance the risk of sudden death in adolescents and young adults? *J Am Coll Cardiol.* (2003) 42:1959–63. doi: 10.1016/j.jacc.2003.03.002
3. Sen-Chowdhry S, Syrris P, Prasad SK, Hughes SE, Merrifield R, Ward D, et al. Left-dominant arrhythmogenic cardiomyopathy. An under-recognized clinical entity. *J Am Coll Cardiol.* (2008) 52:2175–87. doi: 10.1016/j.jacc.2008.09.019
4. Austin KM, Trembley MA, Chandler SF, Sanders SP, Saffitz JE, Abrams DJ, et al. Molecular mechanisms of arrhythmogenic cardiomyopathy. *Nat Rev Cardiol.* (2019) 16:519–37. doi: 10.1038/s41569-019-0200-7
5. Basso C, Corrado D, Marcus FI, Nava A, Thiene G. Arrhythmogenic right ventricular cardiomyopathy. *Lancet.* (2009) 373:1289–300. doi: 10.1016/S0140-6736(09)60256-7
6. Saffitz JE. Arrhythmogenic cardiomyopathy and abnormalities of cell-to-cell coupling. *Heart Rhythm.* (2009) 6 (8 Suppl.) S62–5. doi: 10.1016/j.hrthm.2009.03.003
7. Marcus FI, McKenna WJ, Sherrill D, Basso C, Bauce B, Bluemke DA, et al. Diagnosis of arrhythmogenic right ventricular cardiomyopathy/dysplasia: proposed modification of the task force criteria. *Circulation.* (2010) 121:1533–41. doi: 10.1161/CIRCULATIONAHA.108.840827
8. Casanez-Ventura, A., Gimeno-Blanes, F. J., Rojo-Alvarez, J. L., Flores-Yepes, J. A., Gimeno-Blanes, J. R., Lopez-Ayala, J. M. and Garcia-Alberola, A. QRS delineation algorithms comparison and model fine tuning for automatic clinical classification. In: *Computing in Cardiology,* Vol 40 (2013). p. 1163–6.
9. Norman M, Simpson M, Mogensen J, Shaw A, Hughes S, Syrris P, et al. Novel mutation in desmoplakin causes arrhythmogenic left ventricular cardiomyopathy. *Circulation.* (2005) 112:636–42. doi: 10.1161/CIRCULATIONAHA.104.532234
10. López-Ayala JM, Gómez-Milanés I, Sánchez Muñoz JJ, Ruiz-Espejo F, Ortíz M, González-Carrillo J, et al. Desmoplakin truncations and arrhythmogenic left ventricular cardiomyopathy: characterizing a phenotype. *Europace.* (2014) 16:1838–46. doi: 10.1093/europace/euu128
11. Bauce B, Rampazzo A, Basso C, Mazzotti E, Rigato I, Steriotis A, et al. Clinical phenotype and diagnosis of arrhythmogenic right ventricular cardiomyopathy in pediatric patients carrying desmosomal gene mutations. *Heart Rhythm.* (2011) 8:1686–95. doi: 10.1016/j.hrthm.2011.06.026
12. Mast TP, Taha K, Cramer MJ, Lumens J, van der Heijden JF, Bouma BJ, et al. The prognostic value of right ventricular deformation imaging in early arrhythmogenic right ventricular cardiomyopathy. *JACC Cardiovasc Imaging.* (2019) 12:446–55. doi: 10.1016/j.jcmg.2018.01.012
13. Marcus FI, Zareba W. The electrocardiogram in right ventricular cardiomyopathy/dysplasia. How can the electrocardiogram assist in understanding the pathologic and functional changes of the heart in this disease? *J Electrocardiol.* (2009) 42:136.e1-136.e5. doi: 10.1016/j.jelectrocard.2008.12.011
14. Cox MGPJ, Nelen MR, Wilde AAM, et al. Activation delay and VT parameters in arrhythmogenic right ventricular dysplasia/cardiomyopathy: toward improvement of diagnostic ECG criteria. *J Cardiovasc Electrophysiol.* (2008) 19:775–81. doi: 10.1111/j.1540-8167.2008.01140.x
15. Hauer RNW, Cox MGPJ. The challenge of early diagnosis in arrhythmogenic right ventricular dysplasia/cardiomyopathy. *J Cardiovasc Electrophysiol.* (2008) 19:1135–6. doi: 10.1111/j.1540-8167.2008.01262.x
16. Kim JC, Pérez-Hernández M, Alvarado FJ, Maurya SR, Montnach J, Yin Y, et al. Disruption of Ca(2+)(i) homeostasis and connexin 43 hemichannel function in the right ventricle precedes overt arrhythmogenic cardiomyopathy in plakophilin-2-deficient mice. *Circulation.* (2019) 140:1015–30. doi: 10.1161/CIRCULATIONAHA.119.039710
17. Towbin JA, McKenna WJ, Abrams DJ, Ackerman MJ, Calkins H, Darrieux FC, et al. 2019 HRS expert consensus statement on evaluation, risk stratification, and management of arrhythmogenic cardiomyopathy: executive summary. *Heart Rhythm.* (2019) 16:e373–407. doi: 10.1016/j.hrthm.2019.09.019
18. Zaidi A, Sheikh N, Jongman JK, Gati S, Panoulas VF, Carr-White G, et al. Clinical differentiation between physiological remodeling and arrhythmogenic right ventricular cardiomyopathy in athletes with marked electrocardiographic repolarization anomalies. *J Am Coll Cardiol.* (2015) 65:2702–11. doi: 10.1016/j.jacc.2015.04.035

Conflict of Interest: The authors declare that the research was conducted in the absence of any commercial or financial relationships that could be construed as a potential conflict of interest.

frontiers in Cardiovascular Medicine

ORIGINAL RESEARCH
published: 08 June 2021
doi: 10.3389/fcvm.2021.661673

Incremental Values of T1 Mapping in the Prediction of Sudden Cardiac Death Risk in Hypertrophic Cardiomyopathy: A Comparison With Two Guidelines

*Le Qin[1], Jiehua Min[1], Chihua Chen[1], Lan Zhu[1], Shengjia Gu[1], Mi Zhou[2], Wenjie Yang[1] and Fuhua Yan[1]**

[1] Department of Radiology, Ruijin Hospital, Shanghai Jiao Tong University School of Medicine, Shanghai, China, [2] Department of Cardiac Surgery, Ruijin Hospital, Shanghai Jiao Tong University School of Medicine, Shanghai, China

OPEN ACCESS

Edited by:
Juan R. Gimeno, Hospital Universitario Virgen de la Arrixaca, Spain

Reviewed by:
Josefa Gonzalez, European Society of Cardiology, France
Jose Maria Lopez Ayala, San Juan de Alicante University Hospital, Spain

***Correspondence:**
Fuhua Yan
yfh11655@rjh.com.cn

Specialty section:
This article was submitted to Cardiovascular Imaging, a section of the journal Frontiers in Cardiovascular Medicine

Received: 31 January 2021
Accepted: 28 April 2021
Published: 08 June 2021

Citation:
Qin L, Min J, Chen C, Zhu L, Gu S, Zhou M, Yang W and Yan F (2021) Incremental Values of T1 Mapping in the Prediction of Sudden Cardiac Death Risk in Hypertrophic Cardiomyopathy: A Comparison With Two Guidelines. Front. Cardiovasc. Med. 8:661673. doi: 10.3389/fcvm.2021.661673

Background: MRI native T1 mapping and extracellular volume fraction (ECV) are quantitative values that could reflect various myocardial tissue characterization. The role of these parameters in predicting the risk of sudden cardiac death (SCD) in hypertrophic cardiomyopathy (HCM) is still poorly understood.

Aim: This study aims to investigate the ability of native T1 mapping and ECV values to predict major adverse cardiovascular events (MACE) in HCM, and its incremental values over the 2014 European Society of Cardiology (ESC) and enhanced American College of Cardiology/American Heart Association (ACC/AHA) guidelines.

Methods: Between July 2016 and October 2020, HCM patients and healthy individuals with sex and age matched who underwent cardiac MRI were prospectively enrolled. The native T1 and ECV parameters were measured. The SCD risk was evaluated by the 2014 ESC guidelines and enhanced ACC/AHA guidelines. MACE included cardiac death, transplantation, heart failure admission, and implantable cardioverter-defibrillator implantation.

Results: A total of 203 HCM patients (54.2 ± 14.9 years) and 101 healthy individuals (53.2 ± 14.7 years) were evaluated. During a median follow-up of 15 months, 25 patients (12.3%) had MACE. In multivariate Cox regression analysis, global native T1 mapping (hazard ratio (HR): 1.446; 95% confidence interval (CI): 1.195–1.749; $P < 0.001$) and non-sustained ventricular tachycardia (NSVT) (HR: 4.949; 95% CI, 2.033–12.047; $P < 0.001$) were independently associated with MACE. Ten of 86 patients (11.6%) with low SCD risk assessed by the two guidelines had MACE. In this subgroup of patients, multivariate Cox regression analysis showed that global native T1 mapping was independently associated with MACE (HR: 1.532; 95% CI: 1.221–1.922; $P < 0.001$). In 85 patients with conflicting results assessed by the two guidelines, end-stage systolic dysfunction was independently associated with MACE (HR: 7.942, 95% CI: 1.322–47.707, $P = 0.023$). In 32 patients with high SCD risk assessed by the two guidelines, NSVT was independently associated with MACE (HR: 9.779, 95% CI: 1.953–48.964, $P = 0.006$).

Conclusion: The global native T1 mapping could provide incremental values and serve as potential supplements to the current guidelines in the prediction of MACE.

Keywords: hypertrophic cardiomyopathy, sudden cardiac death, magnetic resonance imaging, native T1 mapping, ECV, guideline

INTRODUCTION

Hypertrophic cardiomyopathy (HCM) is a common genetic disease with a prevalence of 1/200 to 500 people (1–3). Although a majority of HCM patients have normal life expectancy, sudden cardiac death (SCD) remains to be the most common adverse outcome (4). Implantable cardioverter-defibrillator (ICD) is recommended as the only effective way to prevent from SCD and increase lifespan (5). However, placement of ICDs is sometimes companied by complications such as infections (6). Thus, it is important but challenging to identify patients who are at high risk of SCD and likely benefit from ICDs.

Two strategies are widely used for assessing SCD risk in HCM patients in clinical settings, which often leads to conflicting results (7). One is the 2014 European Society of Cardiology (ESC) guidelines in which a 5-year SCD risk predictive model was proposed (8), and the other is the enhanced American College of Cardiology/American Heart Association (ACC/AHA) guidelines that included seven binary biomarkers to judge SCD risk (9). In the enhanced ACC/AHA guidelines, the percentage of late gadolinium enhancement (LGE) to left ventricular (LV) mass representing the myocardial characterization is included as a new biomarker. This feature makes the two guidelines very different. LGE could be non-invasively acquired by cardiac MRI and has been a reference standard for evaluating myocardial fibrosis (10). In the past decade, LGE has been confirmed as an independent predictor of SCD and adverse outcomes in HCM (11–13). However, it is often confusing to define diffuse interstitial expansion by LGE (14). The amount of LGE also differs based on the chosen thresholding techniques (15).

MRI mapping technique can non-invasively reflect tissue physiology and pathophysiology in multiple cardiovascular diseases alternative to myocardial biopsies (16). Native T1 mapping and extracellular volume fraction (ECV) derived from native and contrast-enhanced T1 values are quantitative methods that enable the detection of myocardial tissue characterization (17). These intrinsic quantitative parameters can reflect the states of focal and diffuse interstitial fibrosis, as well as iron overload, lipid deposition, edema, and protein infiltration (18–20). Compared with LGE, native T1 mapping and ECV could potentially provide more information about myocardial tissue. However, the predictive value of these parameters has not been fully understood.

Hence, this study was conducted to evaluate the ability of native T1 and ECV values to predict major adverse cardiovascular events (MACE) in HCM patients, and its incremental values over the current 2014 ESC guidelines and enhanced ACC/AHA guidelines.

Abbreviations: HCM, hypertrophic cardiomyopathy; SCD, sudden cardiac death; ICD, implantable cardioverter-defibrillator; ESC, European Society of Cardiology; ACC/AHA, American College of Cardiology/American Heart Association; LGE, late gadolinium enhancement; LV, left ventricular; ECV, extracellular volume fraction; LVWT, left ventricular wall thickness; LVEF, left ventricular ejection fraction; LVOT, left ventricular outflow tract; NSVT, non-sustained ventricular tachycardia; MACE, major adverse cardiovascular events; HR, hazard ratio; CI, confidence interval.

MATERIALS AND METHODS

This prospective study was approved by our local Institutional Review Board, and written informed consents of all patients were obtained. From July 2016 to October 2020, 308 HCM patients who underwent cardiac MRI in our institution were enrolled. Clinical diagnosis of HCM was done based on the LV wall thickness (LVWT) $\geq$15 mm by echocardiography or MRI without LV dilation that could not be explained by loading conditions or LVWT of 13–14 mm supported by family history of HCM, non-cardiac symptoms, electrocardiogram, laboratory tests, and other cardiac imaging (1, 8). Differentiation from hypertensive heart diseases were summarized in **Supplementary Material 1**. Exclusion criteria are shown in **Figure 1**. Follow-up data was acquired by telephone interview, outpatient visit, and the record of inpatient data. The primary endpoint was set as the incidence of MACE, including all cardiac-caused death, the placement of ICDs, cardiac transplantation, myocardial infarction, and heart failure hospitalization. One hundred one healthy volunteers with age- and sex-matched distribution with HCM patients were enrolled as control group, with no history of cardiovascular diseases and symptoms, and with normal electrocardiogram and echocardiography. The control group was included to define the normal ranges of native T1 mapping and ECV values.

Cardiac MRI Protocols

All cardiac MRI examinations were performed on a 3.0-T MRI scanner (Ingenia, Philips Healthcare). The cine (voxel: 2 × 2 × 8 mm, field of view: 350 × 350 × 8 mm, time repetition/time echo: 3.1/1.55 ms, flip angle: 45°, matrix: 176 × 168, sense factor: 2) and LGE (voxel: 1.6 × 1.9 × 10 mm, field of view: 300 × 300 × 10 mm, time repetition/time echo: 6.1/3.0 ms, flip angle: 25°, matrix: 188 × 135, sense factor: 2) sequences included two-, three-, and four-chamber and short-axis images covering the whole LV myocardium. Native and enhanced T1 mapping were acquired by MOdified Look-Locker recovery sequence using "5s(3s)3s" and "4s(1s)3s(1s)2s" scheme, respectively (voxel: 2 × 2 × 8 mm, FOV: 300 × 300 × 8 mm, TR/TE: 2.3/1.07 ms, flip angle: 20°, matrix: 152 × 150) (**Supplementary Material 2**). Mapping image acquisition was in short-axis slices with a gap of 2 mm covering the whole LV myocardium. LGE and enhanced

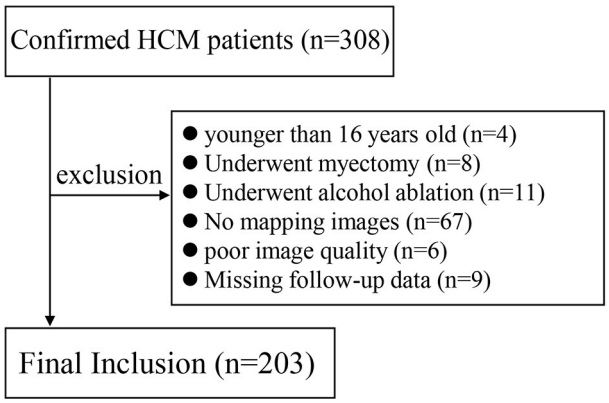

FIGURE 1 | Flow diagram of patient selection.

T1 mapping were performed 10–15 min after intravenous administration of gadolinium contrast agent (Magnevist, Bayer Healthcare Pharmaceuticals) of 0.2 mmol/kg.

MRI Analysis

Cardiac structure, function, and LGE imaging were analyzed on a commercial postprocessing software QMass (version8.1, Medis Medical Imaging). Phenotypes of HCM were evaluated on four-chamber cine images as previously described (4). The maximal LVWT was measured on cine images of all planes at the end-diastolic phase. The anterior-posterior left atrium (LA) diameter was measured on four-chamber cine images. Cardiac function was calculated by manually tracing the endocardial and epicardial borders of LV myocardium at the end-diastolic and end-systolic phases on short-axis cine images, excluding papillary muscles. The quantitative LGE was performed by manually adjusting the grayscale intensity threshold slider to fill in the visually apparent hyperintense as described previously (21). Global and regional native T1 mapping and ECV values were acquired on a commercial post-processing software (CVI^{42}, Circle Cardiovascular Imaging) by manually tracing endocardial and epicardial borders of LV myocardium on motion-corrected mapping images. The reference points were set at the superior and inferior LV insertion to generate a 16-segment AHA model (22). Hematocrit was recorded by obtaining venous blood sample within 24 h prior to MRI. The ECV values were generated by equations reported previously (18). The minimal and maximal mapping values of all 16 segments were also selected for analysis.

Risk Models

The family history of SCD and unexplained syncope were recorded. The standard echocardiography was used to measure an instantaneous peak Doppler LV outflow tract (LVOT) pressure gradient at rest (8). The 24-h ambulatory electrocardiogram monitoring was performed to detect the presence of non-sustained ventricular tachycardia (NSVT) in a standard fashion (5, 8).

A 5-year estimated SCD risk was calculated according to the formulation of "1-0.998$^{\exp(\text{Prognostic index})}$" proposed in the 2014 ESC guidelines (8). Prognostic index = [0.15939858 × maximal LVWT (mm)]–[0.00294271 × maximal LVWT^2 (mm^2)] + [0.0259082 × left atrial diameter (mm)] + [0.00446131 × maximal (rest/Valsalva) LVOT gradient (mmHg)] + [0.4583082 × family history of SCD] + [0.82639195 × NSVT] + [0.71650361 × unexplained syncope]–[0.01799934 × age at clinical evaluation (years)]. Patients with 5-year risk of <4 and ≥4% were classified as lower and higher SCD risk groups, respectively. According to the enhanced ACC/AHA guidelines, patients were considered at high risk for SCD if at least one of the following major risk markers was present: family history of SCD, maximal LVWT ≥30 mm, unexplained syncope, NSVT, LGE/LV mass ≥15%, end-stage LV ejection fraction (LVEF) <50%, and LV apical aneurysm (9).

Statistical Analysis

All continuous data were expressed as mean ± standard deviation if normally distributed, and median (interquartile range) if non-normally distributed. The normality of data was determined by Kolmogorov-Smirnov test. Independent *t*-test and Mann-Whitney *U*-test were used to compare the normally and non-normally distributed data between two groups, respectively. The ordinal variables were compared by χ^2 test or Fisher's exact test, when appropriate. ANOVA test and Kruskal–Wallis *H*-test were used to compare the normally and non-normally distributed data among three groups, respectively, with Bonferroni test for paired *post-hoc* test. Univariate and multivariate Cox regression analyses were used to estimate the relationship between cardiac MRI and major SCD risk, with the incidence of MACE. "Forward: LR" was used to select variables in the multivariate analysis. Kaplan-Meier methods and log-rank tests were used to compare the MACE-free survival between two groups. Pearson (r) and Spearman (r_s) correlation coefficient were used to analyze the correlation of continuous data and ranking data, respectively. All statistical analyses were performed by SPSS (version22.0, IBM) and GraphPad Prism (version8.0.2, GraphPad Software). $P < 0.05$ was considered to be statistically significant.

RESULTS

Study Population

A total of 203 HCM patients (120 males, 59.1%; age, 54.2 ± 14.9 years) and 101 healthy individuals (59 males, 58.4%; age, 53.2 ± 14.7 years) were included. Eighty-six patients (42.4%) were older than 60 years. Hypertension was common in 126 HCM patients (62.1%), and LVOT pressure gradient of 30 mmHg or greater was present in 105 patients (51.7%). Thirteen patients had SCD family history, 28 underwent unexplained syncope, and 11 had NSVT. All baseline demographics are summarized in **Table 1**.

Compared with the control group, end-systolic volume (ESV) was lower, while LVEF and LV myocardial mass were higher in HCM patients (all $P < 0.001$). Of all HCM patients, LVEF <50% and LV apical aneurysm were observed in seven (3.4%) and four patients (2.0%), respectively. The median maximal LVWT was 22.2 mm

TABLE 1 | Baseline demographics of HCM patients and healthy individuals.

Baseline demographics	HCM patients (*N* = 203)	Control group (*N* = 101)	*P*-value
Clinical data			
Male (*N*, %)	120, 59.1%	59, 58.4%	0.907
Age (years)$^{+}$	54.2 ± 14.9	53.2 ± 14.7	0.592
BMI (kg/m^2)$^{+}$	24.8 ± 3.7	23.5 ± 2.5	<0.001*
Heart rate (beats/min)$^{\#}$	70 (18)	67 (15)	0.001*
Systolic blood pressure (mmHg)$^{\#}$	132 (27)	117 (15)	<0.001*
Diastolic blood pressure (mmHg)$^{\#}$	74 (14)	71 (11)	0.043
Hypertension (*N*, %)	126, 62.1%	0, 0%	<0.001*
Hyperlipidemia (*N*, %)	59, 29.1%	0, 0%	<0.001*
Diabetes mellitus (*N*, %)	24, 11.8%	0, 0%	<0.001*
Atrial fibrillation (*N*, %)	22, 10.8%	0, 0%	<0.001*
SCD family history (*N*, %)	13, 6.4%	0, 0%	0.009*
Unexplained syncope (*N*, %)	28, 13.8%	0, 0%	<0.001*
NSVT (*N*, %)	11, 5.4%	0, 0%	0.017*
Mitral regurgitation	157, 77.3%	0, 0%	<0.001*
NYHA classification (I/II/III/IV)	18/82/100/3	101/0/0/0	<0.001*
Echocardiography			
LOVT pressure gradient (mmHg)$^{\#}$	32 (49)	–	–
Laboratory test			
NT-pro BNP (pg/ml)	1,216.4 (1,196.1)	–	–
CK-MB (ng/ml)	3.5 (2.7)	–	–
Myoglobin (ng/ml)	21.6 (11.5)	–	–
cTnI (ng/ml)	0.03 (0.06)	–	–
Therapy			
Septal myectomy (*N*, %)	99, 48.8%	–	–
ICD (*N*, %)	8, 3.9%		
Drug therapy$^{\$}$			
β-Blocker (*N*, %)	87, 42.9%	–	–
ACEi/ARB (*N*, %)	92, 45.3%	–	–
Calcium antagonists (*N*, %)	62, 30.5%	–	–
Diuretics (*N*, %)	9, 0.4%	–	–

HCM, hypertrophic cardiomyopathy; BMI, body mass index; SCD, sudden cardiac death; NSVT, non-sustained ventricular tachycardia; LVOT, left ventricular outflow tract; NYHA, New York Heart Association; NT-pro ICD, implantable cardioverter-defibrillator; BNP, N-terminal pro-B-type natriuretic peptide; CK-MB, creatine kinase isomer-myoglobin; cTnI, cardiac troponin I; ACEi, angiotensin-converting enzyme inhibitors; ARB, angiotensin receptor blocker.

$^{+}$*Expressed as mean ± standard deviation.*

$^{\#}$*Expressed as median (interquartile range).*

$^{\$}$*Postoperative drug therapy was not included.*

**With statistically significant difference.*

(interquartile range, 9.2) in patients with HCM. The global, minimal, and maximal native T1 and ECV values were significantly higher in patients with HCM (all $P < 0.001$). The median LGE/LV mass was 13.6% (21.3), with non-LGE in 15 patients (7.4%) and LGE/LV mass ≥15% in 88 patients (43.3%). According to the results of the control group, normal ranges of global native T1 mapping and ECV values in our institution were 1,180.4–1,299.6 ms and 21.4–29.4%, respectively. Increased global native T1 mapping (>1,299.6 ms) and increased global ECV (>29.4%) were found in 110 and 81 patients, respectively. The MRI parameters of HCM patients and control group are described in **Table 2**. Furthermore, phenotypes of HCM are presented in **Table 3**.

Major SCD Risk Factors and Cardiac MRI Parameters in Two Guidelines

The 5-year SCD probability derived from the 2014 ESC guidelines for all HCM patients was 2.25% (1.73), in which 32 patients (15.8%) were classified as high risk. A total of 117 patients (57.6%) were ranked as high risk by the enhanced ACC/AHA guidelines. Differences between patients with low and high SCD risk assessed by the 2014 ESC guidelines and enhanced ACC/AHA guidelines are described in **Supplementary Table 1**.

The global native T1 and ECV showed a significant correlation ($r = 0.307$, $P = 0.002$ and $r = 0.495$, $P < 0.001$, respectively) in both the control group and HCM patients. In the HCM patients, the LGE/LV mass showed a significant correlation with

TABLE 2 | Comparison of cardiac MRI data among healthy individuals and HCM patients.

MRI parameters	Control group (*N* = 101)	HCM patients (*N* = 203)	*P*-value
EDV (ml)[#]	103.7 (31.1)	103.5 (40.1)	0.467
EDV/BSA (ml/m^2)[#]	61.2 (12.4)	58.9 (18.7)	0.987
ESV (ml)[#]	29.4 (14.3)	23.9 (15.7)	<0.001*
ESV/BSA (ml/m^2)[#]	17.8 (7.2)	13.7 (8.6)	<0.001*
LVEF (%)[#]	70.6 (6.5)	76.8 (12.3)	<0.001*
LVEF <50% (*N*, %)	0, 0%	7, 3.4%	0.059
Mass (g)[#]	92.4 (34.3)	184.4 (104.4)	<0.001*
Mass/BSA (g/m^2)[#]	55.5 (16.0)	105.8 (56.2)	<0.001*
Maximal LVWT (mm)[#]	9.0 (2.0)	22.2 (9.2)	<0.001*
Maximal LVWT ≥30 mm (*N*, %)	0, 0%	40, 19.7%	<0.001*
LA diameter (mm)[#]	36.0 (5.5)	44.0 (6.0)	<0.001*
LGE/LV mass (%)[#]	0 (0, 0)	13.6 (21.3)	<0.001*
LGE/LV mass ≥15% (*N*, %)	0, 0%	88, 43.3%	<0.001*
Apical aneurysm (*N*, %)	0, 0%	4, 2.0%	0.156
Global native T1 (ms)[+]	1,240.0 ± 29.8	1,308.0 ± 55.5	<0.001*
Minimal native T1 (ms)[+]	1,185.2 ± 31.0	1,231.5 ± 70.9	<0.001*
Maximal native T1 (ms)[+]	1,320.1 ± 112.6	1,393.4 ± 140.4	<0.001*
Global ECV (%)[+]	25.4 ± 2.0	29.6 ± 6.0	<0.001*
Minimal ECV (%)[+]	22.5 ± 1.9	24.2 ± 3.5	<0.001*
Maximal ECV (%)[+]	29.2 ± 3.8	36.4 ± 9.6	<0.001*

EDV, end diastolic volume; BSA, body surface area; ESV, end systolic volume; LVEF, left ventricular ejection fraction; LGE, late gadolinium enhancement; ECV, extracellular volume fraction; HCM, hypertrophic cardiomyopathy.
[+]Expressed as mean ± standard deviation.
[#]Expressed as median (interquartile range).
**With statistically significant difference.*

TABLE 3 | Phenotype of HCM.

Phenotype	Number of patients
Focal basal septum HCM	67
Diffuse septum HCM	85
Concentric and diffuse HCM	6
Burned out phase HCM	4
Midventricular HCM	5
Apical HCM	27
Focal midseptum HCM	9

HCM, hypertrophic cardiomyopathy.

TABLE 4 | Correlation between SCD risk factors and global T1 mapping parameters.

Major risk factor	Global native T1		Global ECV	
	r or r_s	*P* value	*r* or r_s	*P*-value
2014 ESC guidelines major risk factors				
Maximal LVWT	0.180	0.010*	0.163	0.020*
LA diameter	0.202	0.004*	0.219	0.002*
LVOT gradient pressure	−0.002	0.980	−0.151	0.032*
SCD family history	0.084	0.236	0.107	0.128
NSVT	0.212	0.002*	0.200	0.004*
Unexplained syncope	−0.026	0.714	0.047	0.507
Age	0.021	0.767	−0.123	0.081
Enhanced ACC/AHA guidelines major risk factors				
Maximal LVWT ≥30 mm	0.147	0.037*	0.205	0.003*
LGE/LV mass ≥15%	0.538	<0.001*	0.608	<0.001*
End-stage systolic dysfunction	0.248	<0.001*	0.293	<0.001*
LV apical aneurysm	0.051	0.466	0.135	0.055

ECV, extracellular volume fraction; r, Pearson correlation coefficient; r_s, Spearman correlation coefficient; ESC, European Society of Cardiology; LVWT, left ventricular wall thickness; LV, left ventricular; LA, left atrium; LVOT, left ventricular outflow tract; SCD, sudden cardiac death; NSVT, non-sustained ventricular tachycardia; ACC/AHA, American College of Cardiology/American Heart Association; LGE, late gadolinium enhancement.
**With statistically significant difference.*

global native T1 ($r = 0.448$, $P < 0.001$) and global ECV ($r = 0.684$, $P < 0.001$). Similarly, LGE/LV mass ≥15% also showed significant correlation with global native T1 ($r_s = 0.538$, $P < 0.001$) and ECV ($r_s = 0.608$, $P < 0.001$), respectively. Besides, the maximal LVWT, LA diameter, NSVT, and end-stage systolic dysfunction showed a significant correlation with global native T1 and ECV ($P < 0.05$; **Table 4**).

Cardiac MRI Between Two Guidelines

All 203 patients were grouped into three subgroups according to the 2014 ESC guidelines and the enhanced ACC/AHA guidelines. Subgroup 1 consisted of 86 patients (42.4%) and had lower risk according to both guidelines. Subgroup 2 comprised 85 patients (41.9%) and demonstrated conflicting results as evaluated by the two guidelines. The patients were classified as lower risk by the 2014 ESC guidelines but higher risk by the enhanced ACC/AHA

guidelines. Subgroup 3 consisted of the remaining 32 patients (15.7%) evaluated as higher risk by both guidelines. Since none of the patients was considered to be high risk by the 2014 ESC guidelines and low risk by the enhanced ACC/AHA guidelines, the patients of subgroup 1 were patients ranked as lower risk by the enhanced ACC/AHA guidelines, and the patients of subgroups 2 and 3 were patients ranked as higher risk by the enhanced ACC/AHA guidelines.

All cardiac MRI parameters and T1 mapping values were significantly different among subgroups 1 to 3 except maximal native T1 and the presence of LV apical aneurysm ($P < 0.05$; **Supplementary Table 2**). Subgroup 3 had the highest EDV and LA diameter, while subgroup 1 had the least ESV, LV myocardial mass, maximal LVWT, and LGE/LV (all $P < 0.05$). All four cases with LV apical aneurysm were in subgroup 2. Subgroups 2 and 3 had higher global native T1 and ECV values than subgroup 1 did (all $P < 0.05$).

Predictive Values of Native T1 Mapping and ECV

During a median follow-up of 15 months (interquartile range, 19 months; range, 1–46 months), a total of 25 patients (12.3%) had MACE, including five cardiac death (three SCD), 10 placement of ICDs, two cardiac transplantation, two myocardial infarction, and six heart failure hospitalization. Placement of ICDs was due to III° atrial-ventricular block (four patients), sinus arrest (one patient), and NSVT (five patients). Median interval time between cardiac MRI and MACE was 6 months (interquartile range, 16.5 months; range, 1–35 months). In a total of 203 patients with HCM, Kaplan–Meier curves demonstrated that lower MACE-free survival was significantly associated with increased global native T1 mapping, increased global ECV, and high SCD risk assessed by the 2014 ESC guidelines ($P < 0.001$; **Figure 2**). However, SCD risk stratification assessed by the

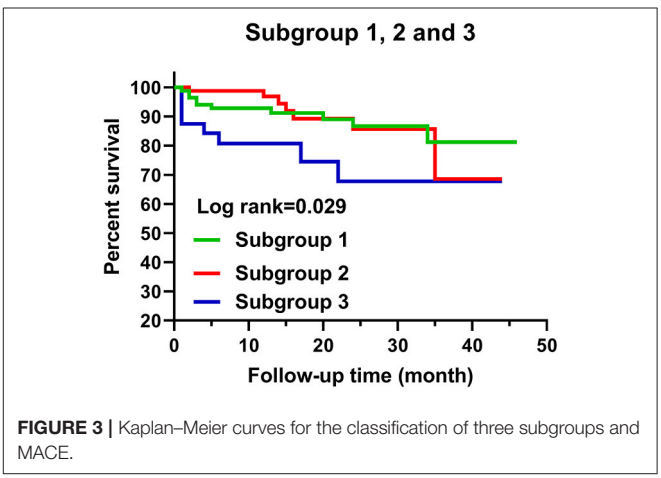

FIGURE 3 | Kaplan–Meier curves for the classification of three subgroups and MACE.

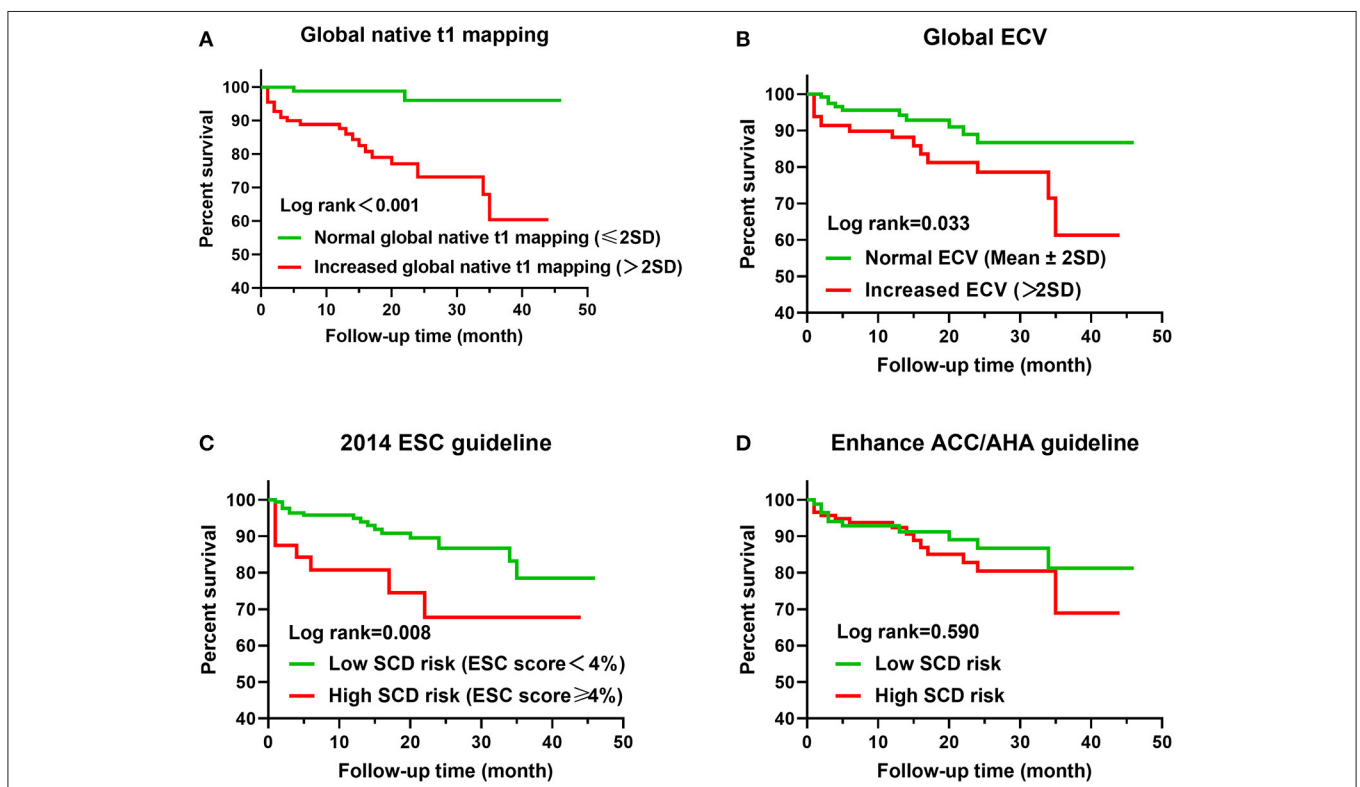

FIGURE 2 | Kaplan–Meier curves for T1 mapping values, risk stratification of guidelines, and MACE. **(A)** Global native T1 mapping >2SD (60 ms) vs. ≤2SD. **(B)** Global ECV >2SD (4%) vs. ≤2SD. **(C)** ESC score <4 vs. ≥4%. **(D)** Low SCD risk assessed by enhanced ACC/AHA guidelines vs. high SCD risk.

TABLE 5 | Univariate and multivariate Cox regression analysis of major SCD risks and MRI parameters for the prediction of MACE in all patients with HCM.

	Patients without MACE (*N* = 178)	Patients with MACE (*N* = 25)	HR (95% CI)	*P*-value
Univariate cox regression analysis				
Major risk factors				
Maximal LVWT (mm)	22.0 (9.3)	19.1 (8.8)	0.979 (0.911–1.053)	0.570
LA diameter (mm)	43.0 (6.0)	45.0 (8.5)	1.059 (0.998–1.123)	0.058
LVOT gradient pressure (mmHg)	31.5 (52.3)	15.0 (47.5)	0.995 (0.983–1.008)	0.458
SCD family history (*N*, %)	12, 6.7%	1, 4.0%	0.809 (0.109–6.011)	0.835
NSVT (*N*, %)	4, 2.2%	7, 28.0%	7.901 (3.293–18.953)	<0.001*
Unexplained syncope (*N*, %)	25, 14.0%	3, 12.0%	0.888 (0.266–2.970)	0.848
Age (years)	53.3 ± 15.2	60.1 ± 11.6	1.030 (0.999–1.062)	0.059
ESC score (%)	2.27 (1.69)	1.70 (3.49)	1.122 (0.907–1.390)	0.289
High SCD risk by 2014 ESC guideline (*N*, %)	24, 13.5%	8, 32.0%	2.954 (1.271–6.862)	0.012*
Maximal LVWT ≥30 mm (*N*, %)	36, 20.2%	4, 16.0%	0.892 (0.305–2.604)	0.834
LGE/LV mass ≥15% (*N*, %)	75, 42.1%	13, 52.0%	1.694 (0.770–3.726)	0.190
LGE/LV mass (%)	13.3 (18.7)	16.3 (35.8)	1.025 (1.005–1.046)	0.015*
End-stage systolic dysfunction (*N*, %)	1, 0.6%	6, 24.0%	8.687 (3.449–21.878)	<0.001*
LV apical aneurysm (*N*, %)	3, 1.7%	1, 4.0%	3.387 (0.449–25.554)	0.237
High SCD risk by enhanced ACC/AHA guideline (*N*, %)	102, 57.3%	15, 60.0%	1.368 (0.611–3.061)	0.446
Cardiac MRI parameters[$]				
EDV (ml)[#]	104.5 (37.8)	100.8 (84.1)	1.009 (1.002–1.015)	0.006*
EDV/BSA (ml/m^2)[#]	58.8 (18.3)	61.1 (34.7)	1.016 (1.006–1.025)	0.001*
ESV (ml)[#]	24.0 (14.8)	23.0 (66.0)	1.011 (1.006–1.016)	<0.001*
ESV/BSA (ml/m^2)[#]	13.8 (8.2)	13.3 (33.96)	1.017 (1.009–1.026)	<0.001*
LVEF (%)[#]	76.9 (11.7)	75.9 (32.3)	0.957 (0.936–0.979)	<0.001*
MASS (g)[#]	188.6 (97.6)	158.5 (160.8)	1.001 (0.996–1.005)	0.833
MASS/BSA (g/m^2)[#]	106.8 (54.0)	100.0 (68.8)	1.001 (0.992–1.010)	0.805
Global native T1 (ms)[+]	1,301.5 ± 53.1	1,356.2 ± 47.3	1.492 (1.259–1.769)	<0.001*
Increased global native T1 (*N*, %)	87, 48.9%	23, 92.0%	10.750 (2.533–45.623)	0.001*
Minimal native T1 (ms)[+]	1,225.2 ± 71.0	1,274.1 ± 52.3	1.505 (1.231–1.840)	<0.001*
Maximal native T1 (ms)[+]	1,388.4 ± 146.9	1,430.2 ± 71.0	1.046 (0.987–1.109)	0.126
Global ECV (%)[+]	29.0 ± 5.4	34.3 ± 8.0	1.150 (1.074–1.230)	<0.001*
Increased global ECV (*N*, %)	66, 37.1%	15, 60.0%	2.323 (1.043–5.174)	0.039*
Minimal ECV (%)[+]	23.9 ± 3.3	26.3 ± 3.8	1.290 (1.103–1.508)	0.001*
Maximal ECV (%)[+]	35.3 ± 8.6	43.7 ± 13.1	1.104 (1.051–1.160)	<0.001*
Multivariate cox regression analysis				
Global native T1	–	–	1.446 (1.195–1.749)	<0.001*
NSVT	–	–	4.949 (2.033–12.047)	<0.001*

SCD, sudden cardiac death; MACE, major adverse cardiovascular events; HCM, hypertrophic cardiomyopathy; HR, hazard ratio; CI, confidence interval; LVWT, left ventricular wall thickness; LA, left atrial; LVOT, left ventricular outflow tract; NSVT, non-sustained ventricular tachycardia; ESC, European Society of Cardiology; LGE, late gadolinium enhancement; LV, left ventricular; ACC/AHA, American College of Cardiology/American Heart Association; MRI, magnetic resonance imaging; ECV, extracellular volume fraction.

[+] *Expressed as mean ± standard deviation.*

[#] *Expressed as median (interquartile range).*

[$] *Native T1 values were set as per SD (30 ms) increase; ECV values were set as per SD (2%) increase.*

**With statistically significant difference.*

enhanced ACC/AHA guidelines was not associated with MACE-free survival. In addition, MACE-free survival was significantly different among the three subgroups (**Figure 3**).

Univariate Cox regression analysis showed that NSVT, LGE/LV mass, and end-stage systolic dysfunction were 7.901, 1.025, and 8.687 times higher in patients with MACE, respectively ($P < 0.05$; **Table 5**). In addition, global native T1 mapping, minimum native T1 mapping, global ECV, minimum ECV, and maximum ECV were 1.104–1.505 times higher in patients with MACE ($P < 0.05$). Furthermore, multivariate Cox regression analysis demonstrated that global native T1 mapping (hazard ratio (HR): 1.446; 95% confidence interval (CI): 1.195–1.749; $P < 0.001$) and NSVT (HR: 4.949; 95% CI: 2.033–12.047; $P < 0.001$) were independently associated with the incidence of MACE (**Figure 4**). It is worth noting that the presence of increased global native T1 mapping and ECV were excluded from the multivariate analysis due to their colinearity with global native T1 mapping and ECV values.

To further investigate the extra values of native T1 mapping and ECV in the prediction of MACE, Cox regression analysis were performed in three subgroups of patients. Ten patients in subgroup 1 (11.6%), seven patients in subgroup 2 (8.2%), and eight patients in subgroup 3 (25%) underwent MACE. In subgroup 1, univariate Cox regression analysis showed that global and minimum native T1 mapping and ECV, and age were 1.110–1.785 times higher in patients with MACE ($P < 0.05$; **Table 6**). Multivariate Cox regression analysis demonstrated that global native T1 mapping (HR: 1.532; 95% CI: 1.221–1.922; $P < 0.001$) was independently associated with the occurrence of MACE (**Figure 5**). In subgroup 2, univariate regression analysis showed that global native T1 mapping and end-stage systolic dysfunction were 1.518 and 6.472 times higher in patients with MACE ($P < 0.05$; **Table 7**). However, multivariate regression analysis revealed that only end-stage systolic dysfunction was independently associated with MACE (HR: 7.942; 95% CI: 1.322–47.707; $P = 0.023$; **Figure 6**). In subgroup 3, univariate Cox regression analysis showed that several parameters were significantly associated with MACE, but multivariate regression revealed that only NSVT was independently associated with MACE (HR: 9.779; 95% CI: 1.953–48.964; $P = 0.006$; **Table 8**).

DISCUSSION

Our study has demonstrated several important findings: (1) global native T1 mapping and NSVT are independent risk factors associated with MACE; (2) in patients stratified as low SCD risk by the two guidelines, global native T1 mapping has incremental predictive values over the two guidelines and is independently associated with poor outcomes; and (3) in patients with conflicting results assessed by the two guidelines, although end-stage systolic dysfunction is a powerful predictor, global native T1 mapping could also be helpful to indicate the poor outcome.

The 2014 ESC guidelines and enhanced ACC/AHA guidelines are currently the most two common guidelines to judge the risk for SCD and select patients for ICDs. However, there is no consensus reached as to which guideline is better and the evaluation of SCD risk is still challenging. In a study of 3,703 HCM patients, O'Mahony et al. have evidenced that the 2014 ESC guidelines demonstrated good discrimination between patients who should and should not receive ICDs (24). However, another large study involving 2,094 HCM patients conducted by Maron et al. revealed that the enhanced ACC/AHA guidelines had a higher sensitivity (79–93%) but lower specificity (76–80%) in discriminating patients with and without SCD events, whereas the 2014 ESC guidelines had a much lower sensitivity (47–69%) but slightly higher specificity (79–82%) (9). Liu et al. have demonstrated that the enhanced ACC/AHA guidelines assisted

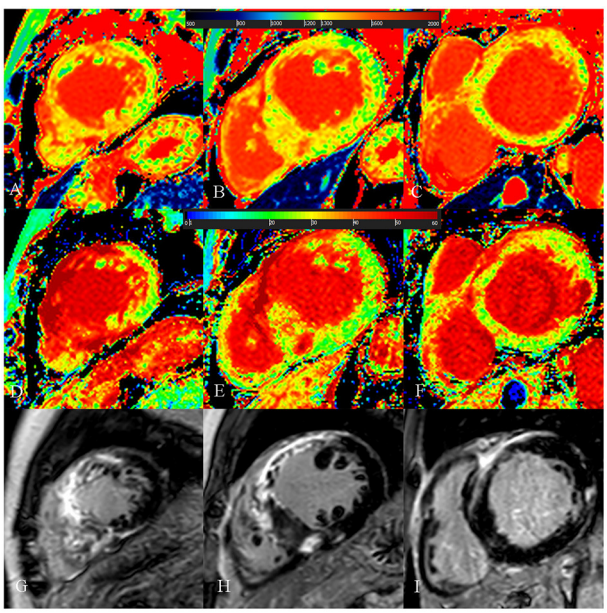

FIGURE 4 | A 54-year-old male with diffuse septum hypertrophic cardiomyopathy. **(A–C)** Native T1 mapping of the apical, mid-, and basal portions of the left ventricular (LV) myocardium revealed higher global native T1 (1,359.67 ms). **(D–F)** Extracellular volume fraction (ECV) of the apical, mid-, and basal portions of the LV myocardium showed higher ECV (38.9%). **(G–I)** Late gadolinium enhancement (LGE) images of the apical, mid-, and basal portions of the LV myocardium showed multiple LGE. The maximal LV wall thickness was 24.3 mm, left atrial diameter was 55 mm, and the LV outflow tract gradient pressure was normal. He had non-sustained ventricular tachycardia but no family history of sudden cardiac death (SCD) and unexplained syncope. He had LGE/LV mass ≥15% (LGE/LV mass: 46.3%) and end-stage systolic dysfunction but no apical aneurysm. He was stratified as having high SCD risk under the 2014 European Society of Cardiology guidelines (5-year SCD probability: 5.93%) and enhanced American College of Cardiology/American Heart Association guidelines. He underwent the placement of ICD 6 months after cardiac MRI examinations. Higher global native T1 mapping and ECV values also indicated poor outcome.

TABLE 6 | Univariate and multivariate Cox regression analysis of T1 mapping values for the prediction of MACE in subgroup 1.

	Patients without MACE (*N* = 76)	Patients with MACE (*N* = 10)	HR (95% CI)	*P*-value
Univariate cox regression analysis				
Major SCD risk factor				
Maximal LVWT (mm)[#]	19.0 (6.1)	19.1 (3.5)	0.977 (0.825–1.157)	0.977
LA diameter (mm)[#]	43.0 (6.0)	42.5 (4.5)	1.024 (0.905–1.158)	0.711
LVOT gradient pressure (mmHg)[#]	30.0 (47.3)	47.5 (74.0)	1.011 (0.993–1.029)	0.238
Age (years)[+]	55.3 ± 14.3	69.0 ± 7.7	1.110 (1.030–1.196)	0.006*
LGE/LV mass (%)[#]	8.0 (6.4)	7.6 (7.8)	0.953 (0.821–1.107)	0.529
Cardiac MRI mapping parameters[$]				
Global native T1 (ms)[+]	1,277.9 ± 45.2	1,341.2 ± 39.6	1.532 (1.221–1.922)	<0.001*
Increased global native T1 (*N*, %)	18, 23.7%	9, 90.0%	19.812 (2.508–156.495)	0.005*
Minimal native T1 (ms)[+]	1,208.4 ± 72.9	1,281.4 ± 54.6	1.635 (1.259–2.125)	<0.001*
Maximal native T1 (ms)[+]	1,368.3 ± 172.8	1,407.9 ± 47.8	1.033 (0.951–1.121)	0.445
Global ECV (%)[+]	26.0 ± 2.9	28.8 ± 1.7	1.785 (1.146–2.780)	0.010*
Increased global ECV (*N*, %)	9, 11.8%	3, 30.0%	2.314 (0.590–9.075)	0.229
Minimal ECV (%)[+]	22.4 ± 3.9	24.8 ± 2.2	1.540 (1.056–2.244)	0.025*
Maximal ECV (%)[+]	31.4 ± 5.7	34.3 ± 4.8	1.100 (0.946–1.280)	0.215
Multivariate cox regression analysis				
Global native T1	–	–	1.532 (1.221–1.922)	<0.001*

SCD, sudden cardiac death; MACE, major adverse cardiovascular events; HR, hazard ratio; CI, confidence interval; LVWT, left ventricular wall thickness; LA, left atrial; LVOT, left ventricular outflow tract; LGE, late gadolinium enhancement; LV, left ventricular; ECV, extracellular volume fraction.

[+]*Expressed as mean ± standard deviation.*

[#]*Expressed as median (interquartile range).*

[$]*Native T1 values were set as per SD (30 ms) increase; ECV values were set as per SD (2%) increase.*

**With statistically significant difference.*

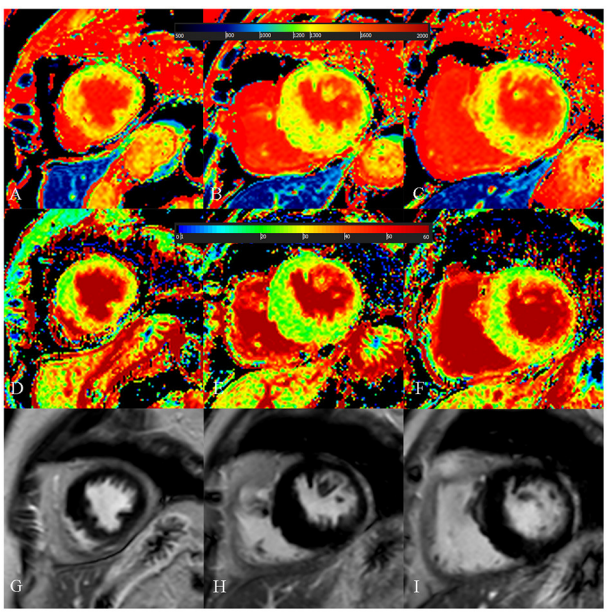

FIGURE 5 | A 73-year-old female with focal midseptum hypertrophic cardiomyopathy. **(A–C)** Native T1 mapping of the apical, mid-, and basal *(Continued)*

FIGURE 5 | portions of the left ventricular (LV) myocardium showed increased global native T1 (1,335.03 ms). **(D–F)** Extracellular volume fraction (ECV) of the apical, mid-, and basal portions of the LV myocardium showed normal global ECV (26.9%). **(G–I)** Late gadolinium enhancement (LGE) images of the apical, mid-, and basal portions of the LV myocardium showed no LGE. The maximal LV wall thickness was 19.8 mm, left atrial diameter was 40 mm, and the LV outflow tract gradient pressure was 95 mmHg. She had no family history of sudden cardiac death (SCD), non-sustained ventricular tachycardia, unexplained syncope, LGE/LV mass ≥15%, end-stage systolic dysfunction, and apical aneurysm. She was stratified as having low SCD risk under the 2014 European Society of Cardiology guidelines (5-year SCD probability: 1.70%) and enhanced American College of Cardiology/American Heart Association guidelines. However, she underwent cardiac-caused death 26 months after cardiac MRI examination. The elevated global native T1 mapping values could help indicate poor outcome in patients with low risk according to the two guidelines.

in better predicting for SCD risk stratification than the 2014 ESC guidelines did in 1,369 HCM patients (25). These uncertainties urge the need to introduce novel biomarkers to supplement the current guidelines (26). In this study, during a median follow-up of 15 months, we revealed that the global native T1 mapping was an independent predictor of MACE in HCM. It was not confounded by the traditional imaging risk factors, including maximal LVWT, LA diameter, and LGE/LV mass. Our findings

TABLE 7 | Univariate and multivariate Cox regression analysis of T1 mapping values for the prediction of MACE in subgroup 2.

	Patients without MACE (*N* = 78)	Patients with MACE (*N* = 7)	HR (95% CI)	*P*-value
Univariate cox regression analysis				
Major SCD risk factor				
Maximal LVWT (mm)[#]	24.3 (9.5)	22.3 (14.1)	1.003 (0.891–1.129)	0.957
LA diameter (mm)[#]	43.0 (6.0)	48.0 (11.0)	1.104 (0.955–1.275)	0.182
LVOT gradient pressure (mmHg)[#]	24.0 (50.5)	15.0 (45.0)	0.991 (0.966–1.017)	0.485
SCD family history (*N*, %)	7, 9.0%	0, 0%	–	–
NSVT (*N*, %)	1, 1.3%	1, 14.3%	2.249 (0.250–20.257)	0.470
Unexplained syncope (*N*, %)	13, 16.7%	0, 0%	–	–
Age (years)[+]	54.8 ± 15.2	57.1 ± 12.0	0.999 (0.946–1.055)	0.972
Maximal LVWT ≥30 mm (*N*, %)	26, 33.3%	2, 28.6%	0.948 (0.182–4.937)	0.949
LGE/LV mass ≥15% (*N*, %)	59, 75.6%	6, 85.7%	1.670 (0.201–13.884)	0.635
End-stage systolic dysfunction (*N*, %)	1, 1.3%	3, 42.9%	6.472 (1.397–29.976)	0.017*
LV apical aneurysm (*N*, %)	3, 3.8%	1, 14.3%	7.318 (0.809–66.202)	0.077
Cardiac MRI mapping parameters[$]				
Global native T1 (ms)[+]	1,319.1 ± 54.7	1,368.0 ± 66.5	1.518 (1.048–2.199)	0.027*
Increased global native T1 (*N*, %)	52, 66.7%	7, 100.0%	33.058 (0.014–77,171.798)	0.377
Minimal native T1 (ms)[+]	1,236.1 ± 70.5	1,275.8 ± 65.9	1.373 (0.852–2.212)	0.193
Maximal native T1 (ms)[+]	1,412.0 ± 136.8	1,451.6 ± 91.8	1.074 (0.926–1.245)	0.348
Global ECV (%)[+]	31.2 ± 6.2	36.9 ± 5.8	1.107 (0.975–1.257)	0.117
Increased global ECV (*N*, %)	42, 53.8%	6, 85.7%	3.629 (0.432–30.514)	0.235
Minimal ECV (%)[+]	24.8 ± 3.4	27.3 ± 4.5	1.186 (0.891–1.579)	0.243
Maximal ECV (%)[+]	38.7 ± 9.7	48.4 ± 9.6	1.087 (0.995–1.188)	0.064
Multivariate cox regression analysis				
End-stage systolic dysfunction (*N*, %)	–	–	7.942 (1.322–47.707)	0.023*

SCD, sudden cardiac death; MACE, major adverse cardiovascular events; HR, hazard ratio; CI, confidence interval; ECV, extracellular volume fraction.

[+]*Expressed as mean ± standard deviation.*

[#]*Expressed as median (interquartile range).*

[$]*Native T1 values were set as per SD (30 ms) increase; ECV values were set as per SD (2%) increase.*

**With statistically significant difference.*

are important because the global native T1 mapping might have the potential to be a supplement to the current guidelines and a new biomarker for SCD risk stratification. It could assist in the clinical decision making to prevent adverse outcomes in HCM, especially when the stratification and management could not be determined by the current guidelines.

To deeply excavate the incremental values of T1 mapping values over the current guidelines, we analyzed these parameters in the three subgroups stratified according to the two guidelines. It is noteworthy that we discover the strong independent association between native T1 mapping and the incidence of 10 MACE in 86 patients (11.6%, subgroup 1) assessed as low SCD risk according to the two guidelines. Choi et al. have also reported that seven SCD events happened in 615 patients with HCM in low-risk group assessed by the 2014 ESC guidelines (27). They suggested that the 2014 ESC guidelines might not be suitable in Asian patients and would unprotect the low-risk patients. Compared with their study, our results emphasize the extra values of the global native T1 mapping over the current two guidelines in the prediction of adverse outcomes. In this subgroup of patients who are not likely to receive the advanced therapies according to the current guidelines, increased global native T1 mapping could be helpful in the prediction of poor outcomes and the identification of patients who might benefit from ICDs. On the other hand, native T1 mapping and ECV values were not included in the multivariate analysis in patients of groups 2 and 3 due to the much stronger impact of end-stage systolic dysfunction and NSVT on the outcomes. However, these values were associated with the prediction of adverse outcomes in the univariate analysis and might be a supplement in the clinical decision when the traditional risk factors are not present.

There were limited studies with regard to the relationship between T1 mapping and ECV with the adverse outcomes in HCM patients (3). Li et al. have reported that ECV was a strong biomarker in predicting the adverse outcomes in 263 HCM patients during a mean follow-up of 28.3 months (23).

Xu et al. found that both native T1 mapping and ECV values were associated with SCD in 258 patients with HCM without the presence of LGE and LVOT obstruction (14). Two baseline studies of small sample size also revealed the relationship between ECV and SCD risks (28, 29). Compared with the previous few studies, our results have added new evidence regarding the prognostic significance of global native T1 mapping and ECV in the evaluation of HCM.

Similar to our study, the importance of native T1 mapping values on the prognosis has been revealed by studies about other cardiovascular diseases. In two studies of non-ischemic dilated cardiomyopathy, native T1 mapping was an independent predictor for MACE-related endpoints (30, 31). In a meta-analysis by Pan et al., native T1 mapping had the similar sensitivity and specificity with ECV in the prediction of prognosis in cardiac amyloidosis (32). We speculate that some explanations might be responsible for the increased native T1 mapping in HCM. First, this quantitative parameter is prone to T2 decay and more sensitive to the change of water content within myocardium than ECV (33). The myocardial edema can be resulted by microvascular ischemia which is a commonplace in HCM (34). In addition, chronic heart failure is also characterized by myocardial edema (35, 36). This is particularly important in our study because quite a few patients are over 60 years and more related with the adverse outcome caused by heart failure (37). Alternatively, native T1 mapping is a robust biomarker indicating the pathologic hypertrophic remodeling in HCM (38, 39). The myocardial tissue remodeling including cardiomyocyte disarray is also a risk factor for malignant arrhythmia (15, 32, 40). Furthermore, native T1 mapping is important for the detection of focal and diffuse fibrosis without the administration of contrast (14). It is particularly useful when the diffuse fibrosis is negative and undetectable on LGE images.

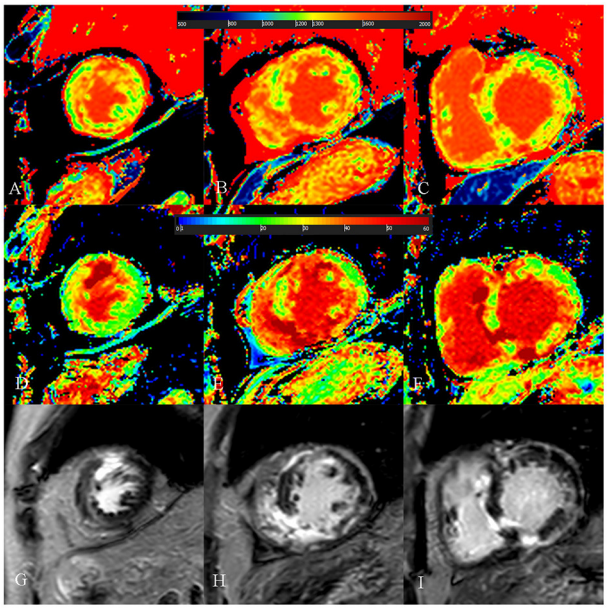

FIGURE 6 | A 52-year-old male with burned out phase hypertrophic cardiomyopathy. **(A–C)** Native T1 mapping of the apical, mid-, and basal portions of the left ventricular (LV) myocardium revealed higher global native T1 (1,380.7 ms). **(D–F)** Extracellular volume fraction (ECV) of the apical, mid-, and basal portions of the LV myocardium showed higher global ECV (32.8%). **(G–I)** Late gadolinium enhancement (LGE) images of the apical, mid-, and basal portions of the LV myocardium showed multiple LGE. The maximal LV wall thickness was 13 mm, left atrial diameter was 53 mm, and the LV outflow tract gradient pressure was 2 mmHg. He had non-sustained ventricular tachycardia, but no family history of sudden cardiac death (SCD), and unexplained syncope. He had LGE/LV mass ≥15% (elevated LGE/LV mass: 56.2%) and end-stage systolic dysfunction but no apical aneurysm. He was stratified with low SCD risk under the 2014 European Society of Cardiology guidelines (5-year SCD probability: 3.39%) and high SCD risk under the enhanced American College of Cardiology/American Heart Association guidelines. He underwent cardiac transplantation 35 months after cardiac MRI examination. End-stage systolic dysfunction strongly indicated poor outcome in this patient. However, increased global native T1 mapping and ECV values could also suggest that the patient was likely to be at high risk of SCD and needs further treatment.

LIMITATIONS

Our study had some limitations. Firstly, this study was performed in a single center where T1 mapping sequences were scanned on a 3.0-T MRI scanner. Future study was required to validate whether our results could be used in other centers. Secondly, the occurrence of MACE rather than SCD was considered the primary endpoint in our study. The prevalence of SCD and placement of ICD is rare in our population, and this would cause a big problem of underestimation or overestimation in the statistical power if we set SCD as the only primary endpoint. Moreover, MACE such as myocardial infarction and acute heart failure would put patients at high risk of SCD (1, 9). SCD-free survival due to the timely rescue should not exclude these patients from the high-risk stratification. Thirdly, our follow-up period is relatively short and the sample size of three subgroups is small. Future studies should investigate the predictive ability of T1 mapping values in larger samples during the long-term follow-up. Fourthly, genetic tests were not performed in our study. This would preclude the enrollment of genotype-positive but hypertrophy-negative patients. In addition, the influence of various genotypes on the endpoints has not been analyzed in our study. However, as an update to the 2011 ACC/AHA guidelines, the enhanced ACC/AHA guidelines have removed genetic mutations as a high-risk factor (5, 9). Finally, the proportion of patients with LGE/LV mass ≥15% is relatively high (88, 43.3%). This might be the reason that the enhanced ACC/AHA guideline was not associated with MACE-free survival. However, the new guidelines detected more patients (15 patients) with MACE than the 2014 ESC guidelines did (eight patients). Therefore, our results should be cautiously interpreted in generalized HCM patients.

CONCLUSION

Cardiac MRI T1 mapping, especially global native T1 mapping, could provide incremental values and serve as potential supplements to the current guidelines in the evaluation of high MACE risk and guide advanced therapies.

TABLE 8 | Univariate and multivariate cox regression analysis of T1 mapping values for the prediction of MACE in subgroup 3.

	Patients without MACE ($N = 24$)	Patients with MACE ($N = 8$)	HR (95% CI)	*P*-value
Univariate cox regression analysis				
Major SCD risk factor				
Maximal LVWT (mm)[#]	26.0 (6.9)	17.9 (8.3)	0.861 (0.735–1.009)	0.064
LA diameter (mm)[#]	47.0 (9.0)	50.0 (8.5)	1.011 (0.924–1.107)	0.811
LVOT gradient pressure (mmHg)[#]	44.0 (57.0)	2.0 (25.9)	0.954 (0.917–0.992)	0.019*
SCD family history (*N*, %)	6, 22.2%	0, 0%	0.629 (0.077–5.121)	0.665
NSVT (*N*, %)	5, 18.5%	4, 80.0%	9.779 (1.953–48.964)	0.006*
Unexplained syncope (*N*, %)	13, 48.1%	2, 40.0%	0.630 (0.150–2.644)	0.528
Age (years)	43.0 ± 12.9	52.8 ± 9.3	1.046 (0.990–1.105)	0.106
Maximal LVWT ≥30 mm (*N*, %)	11, 40.7%	1, 20.0%	0.381 (0.098–2.426)	0.381
LGE/LV mass ≥15% (*N*, %)	19, 70.4%	4, 80.0%	2.981 (0.366–24.273)	0.307
End-stage systolic dysfunction (*N*, %)	1, 3.7%	2, 40.0%	13.104 (2.546–67.440)	0.002*
Cardiac MRI mapping parameters[$]				
Global native T1 (ms)[+]	1,318.6 ± 43.2	1,358.3 ± 50.6	1.741 (1.038–2.921)	0.036*
Increased global native T1 (*N*, %)	17, 70.8%	7, 87.5%	3.634 (0.433–30.517)	0.235
Minimal native T1 (ms)[+]	1,243.0 ± 56.7	1,269.8 ± 41.6	1.308 (0.887–1.930)	0.175
Maximal native T1 (ms)[+]	1,375.6 ± 51.4	1,435.5 ± 83.9	1.409 (1.058–1.875)	0.019*
Global ECV (%)[+]	31.0 ± 3.9	38.9 ± 10.6	1.236 (1.059–1.442)	0.007*
Increased global ECV (*N*, %)	15, 62.5%	6, 75.0%	1.728 (0.347–8.596)	0.504
Minimal ECV (%)[+]	25.4 ± 2.7	27.2 ± 4.6	1.333 (0.875–2.030)	0.180
Maximal ECV (%)[+]	37.0 ± 7.5	51.3 ± 16.4	1.150 (1.044–1.267)	0.005*
Multivariate cox regression analysis				
NSVT	–	–	9.779 (1.953–48.964)	0.006*

SCD, sudden cardiac death; MACE, major adverse cardiovascular events; HR, hazard ratio; CI, confidence interval; ECV, extracellular volume fraction.

[+]*Expressed as mean ± standard deviation.*

[#]*Expressed as median (interquartile range).*

[$]*Native T1 values were set as per SD (30 ms) increase; ECV values were set as per SD (2%) increase.*

**With statistically significant difference.*

DATA AVAILABILITY STATEMENT

The datasets presented in this article are not readily available because our dataset is only available to our research team. Requests to access the datasets should be directed to Fuhua Yan, yfh11655@rjh.com.cn.

ETHICS STATEMENT

The studies involving human participants were reviewed and approved by Ruijin Hospital Ethics Committee Shanghai JiaoTong University School of Medicine. Written informed consent to participate in this study was provided by the participants' legal guardian/next of kin.

AUTHOR CONTRIBUTIONS

LQ, JM, and CC drafted the manuscript, figures, and tables. LZ, SG, and MZ helped for figure and case preparation. FY and WY made a careful review of the manuscript. All authors contributed to this study by conceiving and designing the study, performing the data collection and the statistical analysis or assisting in data interpretation, and approved the submitted version.

FUNDING

This study was supported by Shanghai Rising Stars of Medical Talent Youth Development Program, Youth Medical Talents—Medical Imaging Practitioner Program: SHWRS(2020)_087 and Innovative research team of high-level local universities in Shanghai.

SUPPLEMENTARY MATERIAL

The Supplementary Material for this article can be found online at: https://www.frontiersin.org/articles/10.3389/fcvm.2021.661673/full#supplementary-material

REFERENCES

1. Maron BJ. Clinical course and management of hypertrophic cardiomyopathy. *N Engl J Med*. (2018) 379:655–68. doi: 10.1056/NEJMra1710575
2. Semsarian C, Ingles J, Maron MS, Maron BJ. New perspectives on the prevalence of hypertrophic cardiomyopathy. *J Am Coll Cardiol.* (2015) 65:1249–54. doi: 10.1016/j.jacc.2015.01.019
3. Tower-Rader A, Kramer CM, Neubauer S, Nagueh SF, Desai MY. Multimodality imaging in hypertrophic cardiomyopathy for risk stratification. *Circ Cardiovasc Imaging.* (2020) 13:e009026. doi: 10.1161/CIRCIMAGING.119.009026
4. Baxi AJ, Restrepo CS, Vargas D, Marmol-Velez A, Ocazionez D, H M. Hypertrophic cardiomyopathy from A to Z genetics, pathophysiology, imaging, and management. *Radiographics.* (2016) 36:335–54. doi: 10.1148/rg.2016150137
5. Gersh BJ, Maron BJ, Bonow RO, Dearani JA, Fifer MA, Link MS, et al. 2011 ACCF/AHA guideline for the diagnosis and treatment of hypertrophic cardiomyopathy: executive summary: a report of the American College of Cardiology Foundation/American Heart Association Task Force on Practice Guidelines. *J Am Coll Cardiol*. (2011) 58:2703–38. doi: 10.1161/CIR.0b013e318223e2bd
6. Ho CY, Link MS. Predicting the future in hypertrophic cardiomyopathy. *Circulation.* (2018) 137:1024–6. doi: 10.1161/CIRCULATIONAHA.117.032627
7. Ommen SR. Sudden cardiac death risk in hypertrophic cardiomyopathy: wither our cognitive miser. *JAMA Cardiol*. (2019) 4:657–8. doi: 10.1001/jamacardio.2019.1438
8. Elliott PM, Anastasakis A, Borger MA, Borggrefe M, Cecchi F, Charron P, et al. 2014 ESC guidelines on diagnosis and management of hypertrophic cardiomyopathy: the task force for the diagnosis and management of hypertrophic cardiomyopathy of the European society of cardiology (ESC). *Eur Heart J*. (2014) 35:2733–79. doi: 10.1093/eurheartj/ehu284
9. Maron MS, Rowin EJ, Wessler BS, Mooney PJ, Fatima A, Patel P, et al. Enhanced American college of cardiology/American heart association strategy for prevention of sudden cardiac death in high-risk patients with hypertrophic cardiomyopathy. *JAMA Cardiol.* (2019) 4:644–57. doi: 10.1001/jamacardio.2019.1391
10. Maron MS, Rowin EJ, Maron BJ. How to image hypertrophic cardiomyopathy. *Circ Cardiovasc Imaging.* (2017) 10:e005372. doi: 10.1161/CIRCIMAGING.116.005372
11. Freitas P, Ferreira AM, Arteaga-Fernandez E, de Oliveira Antunes M, Mesquita J, Abecasis J, et al. The amount of late gadolinium enhancement outperforms current guideline-recommended criteria in the identification of patients with hypertrophic cardiomyopathy at risk of sudden cardiac death. *J Cardiovasc Magn Reson.* (2019) 21:50. doi: 10.1186/s12968-019-0561-4
12. Green JJ, Berger JS, Kramer CM, Salerno M. Prognostic value of late gadolinium enhancement in clinical outcomes for hypertrophic cardiomyopathy. *JACC Cardiovasc Imaging.* (2012) 5:370–7. doi: 10.1016/j.jcmg.2011.11.021
13. Mentias A, Raeisi-Giglou P, Smedira NG, Feng K, Sato K, Wazni O, et al. Late gadolinium enhancement in patients with hypertrophic cardiomyopathy and preserved systolic function. *J Am Coll Cardiol.* (2018) 72:857–70. doi: 10.1016/j.jacc.2018.05.060
14. Xu J, Zhuang B, Sirajuddin A, Li S, Huang J, Yin G, et al. MRI T1 mapping in hypertrophic cardiomyopathy: evaluation in patients without late gadolinium enhancement and hemodynamic obstruction. *Radiology.* (2020) 294:275–86. doi: 10.1148/radiol.2019190651
15. Schelbert EB, Moon JC. Exploiting differences in myocardial compartments with native T1 and extracellular volume fraction for the diagnosis of hypertrophic cardiomyopathy. *Circ Cardiovasc Imaging.* (2015) 8:e004232. doi: 10.1161/CIRCIMAGING.115.004232
16. Taylor AJ, Salerno M, Dharmakumar R, Jerosch-Herold M. T1 mapping basic techniques and clinical applications. *JACC: Cardiovasc Imaging*. (2016) 9:67–81. doi: 10.1016/j.jcmg.2015.11.005
17. Ando K, Nagao M, Watanabe E, Sakai A, Suzuki A, Nakao R, et al. Association between myocardial hypoxia and fibrosis in hypertrophic cardiomyopathy: analysis by T2* BOLD and T1 mapping MRI. *Eur Radiol.* (2020) 30:4327–36. doi: 10.1007/s00330-020-06779-9
18. Robinson AA, Chow K, Salerno M. Myocardial T1 and ECV measurement. *JACC Cardiovasc Imaging.* (2019) 12:2332–44. doi: 10.1016/j.jcmg.2019.06.031
19. Ferreira VM, Piechnik SK. CMR parametric mapping as a tool for myocardial tissue characterization. *Korean Circ J.* (2020) 50:658–76. doi: 10.4070/kcj.2020.0157
20. Bull S, White SK, Piechnik SK, Flett AS, Ferreira VM, Loudon M, et al. Human non-contrast T1 values and correlation with histology in diffuse fibrosis. *Heart.* (2013) 99:932–7. doi: 10.1136/heartjnl-2012-303052
21. Chan RH, Maron BJ, Olivotto I, Pencina MJ, Assenza GE, Haas T, et al. Prognostic value of quantitative contrast-enhanced cardiovascular magnetic resonance for the evaluation of sudden death risk in patients with hypertrophic cardiomyopathy. *Circulation.* (2014) 130:484–95. doi: 10.1161/CIRCULATIONAHA.113.007094
22. Manuel D Cerqueira, Neil J Weissman, Vasken Dilsizian, Alice K Jacobs, Sanjiv Kaul, Warren K Laskey, et al. Standardized myocardial segmentation and nomenclature for tomographic imaging of the heart. A statement for healthcare professionals from the cardiac imaging committee of the council on clinical cardiology of the American heart association. *Circulation.* (2002) 105:539–42. doi: 10.1161/hc0402.102975
23. Li Y, Liu X, Yang F, Wang J, Xu Y, Fang T, et al. Prognostic value of myocardial extracellular volume fraction evaluation based on cardiac magnetic resonance T1 mapping with T1 long and short in hypertrophic cardiomyopathy. *Eur Radiol.* (2021). doi: 10.1007/s00330-020-07650-7. [Epub ahead of print].
24. O'Mahony C, Jichi F, Ommen SR, Christiaans I, Arbustini E, Garcia-Pavia P, et al. International external validation study of the 2014 European society of cardiology guidelines on sudden cardiac death prevention in hypertrophic cardiomyopathy (EVIDENCE-HCM). *Circulation.* (2018) 137:1015–23. doi: 10.1161/CIRCULATIONAHA.117.030437
25. Liu J, Wu G, Zhang C, Ruan J, Wang D, Zhang M, et al. Improvement in sudden cardiac death risk prediction by the enhanced American college of cardiology/american heart association strategy in Chinese patients with hypertrophic cardiomyopathy. *Heart Rhythm.* (2020) 17:1658–63. doi: 10.1016/j.hrthm.2020.04.017
26. Pelliccia F, Gersh BJ, Camici PG. Gaps in evidence for risk stratification for sudden cardiac death in hypertrophic cardiomyopathy. *Circulation.* (2021) 143:101–3. doi: 10.1161/CIRCULATIONAHA.120.051968
27. You-Jung Choi, Hyung-Kwan Kim, Sang Chol Lee, Jun-Bean Park, Inki Moon, Jiesuck Park, et al. Validation of the hypertrophic cardiomyopathy risk-sudden cardiac death calculator in Asians. *Heart.* (2019) 105:1892–7. doi: 10.1136/heartjnl-2019-315160
28. Levine J, Collins JD, Ogele E, Murtagh G, Carr JC, Bonow RO, et al. Relation of late gadolinium enhancement and extracellular volume fraction to ventricular arrhythmias in hypertrophic cardiomyopathy. *Am J Cardiol.* (2020) 131:104–8. doi: 10.1016/j.amjcard.2020.06.040
29. Avanesov M, Münch J, Weinrich J, Well L, Säring D, Stehning C, et al. Prediction of the estimated 5-year risk of sudden cardiac death and syncope or non-sustained ventricular tachycardia in patients with hypertrophic cardiomyopathy using late gadolinium enhancement and extracellular volume CMR. *Eur Radiol.* (2017) 27:5136–45. doi: 10.1007/s00330-017-4869-x
30. Puntmann VO, Carr-White G, Jabbour A, Yu CY, Gebker R, Kelle S, et al. T1-Mapping and outcome in nonischemic cardiomyopathy: all-cause mortality and heart failure. *JACC Cardiovasc Imaging.* (2016) 9:40–50. doi: 10.1016/j.jcmg.2015.12.001
31. Nakamori S, Ngo LH, Rodriguez J, Neisius U, Manning WJ, Nezafat R. T1 mapping tissue heterogeneity provides improved risk stratification for ICDs without needing gadolinium in patients with dilated cardiomyopathy. *JACC Cardiovasc Imaging.* (2020) 13:1917–30. doi: 10.1016/j.jcmg.2020.03.014
32. Pan JA, Kerwin MJ, Salerno M. Native T1 mapping, extracellular volume mapping, and late gadolinium enhancement in cardiac amyloidosis: a meta-analysis. *JACC Cardiovasc Imaging.* (2020) 13:1299–310. doi: 10.1016/j.jcmg.2020.03.010
33. Peter Kellman, Hansen MS. T1-mapping in the heart accuracy and precision. *J Cardiovasc Magn Reson.* (2014) 16:2. doi: 10.1186/1532-429X-16-2
34. Villa AD, Sammut E, Zarinabad N, Carr-White G, Lee J, Bettencourt N, et al. Microvascular ischemia in hypertrophic cardiomyopathy: new insights from high-resolution combined quantification of perfusion and late gadolinium enhancement. *J Cardiovasc Magn Reson.* (2016) 18:4. doi: 10.1186/s12968-016-0223-8

35. Liang K, Baritussio A, Palazzuoli A, Williams M, De Garate E, Harries I, et al. Cardiovascular magnetic resonance of myocardial fibrosis, edema, and infiltrates in heart failure. *Heart Fail Clin.* (2021) 17:77–84. doi: 10.1016/j.hfc.2020.08.013
36. Henri O, Pouehe C, Houssari M, Galas L, Nicol L, Edwards-Levy F, et al. Selective stimulation of cardiac lymphangiogenesis reduces myocardial edema and fibrosis leading to improved cardiac function following myocardial infarction. *Circulation.* (2016) 133:1484–97; discussion 97. doi: 10.1161/CIRCULATIONAHA.115.020143
37. Maron BJ, Maron MS. Hypertrophic cardiomyopathy. *Lancet.* (2013) 381:242–55. doi: 10.1016/S0140-6736(12)60397-3
38. Arcari L, Hinojar R, Engel J, Freiwald T, Platschek S, Zainal H, et al. Native T1 and T2 provide distinctive signatures in hypertrophic cardiac conditions - comparison of uremic, hypertensive and hypertrophic cardiomyopathy. *Int J Cardiol.* (2020) 306:102–8. doi: 10.1016/j.ijcard.2020.03.002
39. Hinojar R, Varma N, Child N, Goodman B, Jabbour A, Yu CY, et al. T1 mapping in discrimination of hypertrophic phenotypes: hypertensive heart disease and hypertrophic cardiomyopathy: findings from the international T1 multicenter cardiovascular magnetic resonance study. *Circ Cardiovasc Imaging.* (2015) 8:e003285. doi: 10.1161/CIRCIMAGING.115.003285
40. Lu Huang, Lingping Ran, Peijun Zhao, Dazhong Tang, Rui Han, Tao Ai, et al. MRI native T1 and T2 mapping of myocardial segments in hypertrophic cardiomyopathy: tissue remodeling manifested prior to structure changes. *Br J Radiol.* (2019) 92:20190634. doi: 10.1259/bjr.20190634

Conflict of Interest: The authors declare that the research was conducted in the absence of any commercial or financial relationships that could be construed as a potential conflict of interest.

frontiers in Cardiovascular Medicine

ORIGINAL RESEARCH
published: 30 July 2021
doi: 10.3389/fcvm.2021.705778

Left Ventricular Global Longitudinal Strain Is Associated With Cardiovascular Outcomes in Patients Who Underwent Permanent Pacemaker Implantation

*Dae-Young Kim, Purevjargal Lkhagvasuren, Jiwon Seo, Iksung Cho, Geu-Ru Hong, Jong-Won Ha and Chi Young Shim**

Division of Cardiology, Severance Cardiovascular Hospital, Yonsei University College of Medicine, Seoul, South Korea

OPEN ACCESS

Edited by:
Juan R. Gimeno, Hospital Universitario Virgen de la Arrixaca, Spain

Reviewed by:
Piyush M. Srivastava, University of Melbourne, Australia
Carmen Muñoz-Esparza, Ciudad Sanitaria Virgen de la Arrixaca, Spain

***Correspondence:**
Chi Young Shim
cysprs@yuhs.ac

Specialty section:
This article was submitted to Cardiovascular Imaging, a section of the journal Frontiers in Cardiovascular Medicine

Received: *06 May 2021*
Accepted: *06 July 2021*
Published: *30 July 2021*

Citation:
Kim D-Y, Lkhagvasuren P, Seo J, Cho I, Hong G-R, Ha J-W and Shim CY (2021) Left Ventricular Global Longitudinal Strain Is Associated With Cardiovascular Outcomes in Patients Who Underwent Permanent Pacemaker Implantation. Front. Cardiovasc. Med. 8:705778. doi: 10.3389/fcvm.2021.705778

Background: Patients who underwent permanent pacemaker (PM) implantation have a potential risk of left ventricular (LV) systolic dysfunction. However, assessment of LV ejection fraction (LVEF) shows a limited role in identifying subclinical LV systolic dysfunction and predicting cardiovascular (CV) outcomes.

Methods: We reviewed 1,103 patients who underwent permanent PM implantation between January 2007 and December 2017. After excluding patients who did not undergo echocardiograms before or after PM implantation and those with LV ejection fraction (LVEF) <50%, significant valve dysfunction, and history of cardiac surgery before PM implantation, 300 (67 ± 13 years, 119 men) were finally analyzed. LV mechanical function was assessed with LV global longitudinal strain (LV-GLS) using 2-dimensional speckle-tracking echocardiography. CV outcomes were defined as a composite of CV death and hospitalization for heart failure.

Results: At 44 ± 28 months after post-PM echocardiogram, 23 patients (7.7%) had experienced CV outcomes. Patients with CV outcomes were older and had more comorbidities and a lower baseline |LV-GLS| than those without CV outcomes. LV mechanical function worsened after PM implantation in patients with CV outcomes. The cut-off value of 11.2% in |LV-GLS| on post-PM echocardiogram had a better predictive value for CV outcomes (AUC; 0.784 vs. 0.647, $p = 0.012$). CV outcome in patients with |LV-GLS|<11.2% was worse than that in those with |LV-GLS| ≥ 11.2% (log-rank $p < 0.001$). Multivariate Cox model revealed that reduced |LV-GLS| was independently associated with CV outcomes.

Conclusions: Pacing deteriorates LV mechanical function. Impaired LV-GLS is associated with poor CV outcomes in patients who underwent PM implantation.

Keywords: pacemaker, left ventricular global longitudinal strain, left ventricular ejection fraction (LVEF), cardiomyopahty, outcome

INTRODUCTION

Patients who have undergone permanent pacemaker (PM) implantation have a potential risk of left ventricular (LV) systolic dysfunction (1–3). PM-induced cardiomyopathy (PMIC) is generally defined as a decrease in LV systolic function after right ventricular (RV) pacing with no other independent triggering factors (4) and is associated with worse cardiovascular (CV) outcomes (5). Theoretically, increasing RV pacing causes LV mechanical dyssynchrony and consequently leads to a decrease in LV ejection fraction (LVEF) and CV events related to worsening heart failure (6–8). Although LVEF is the most widely used echocardiographic parameter representing LV systolic function, its measurement can be less reliable in patients with PM because of LV dyssynchronous contraction (9). Moreover, assessment of LVEF shows a limited role in identifying subclinical LV systolic dysfunction, both in patients at risk of PMIC and in the early stages of PMIC.

Assessment of LV mechanical function using LV-global longitudinal strain (LV-GLS) by 2-dimensional speckle-tracking echocardiography can detect subclinical LV dysfunction in the early stages of cardiomyopathy to provide prognostic information (10–12). A previous study demonstrated that LV-GLS could provide better risk stratification than could LVEF among patients with LV dyssynchrony caused by left bundle branch block (13). Therefore, we hypothesized that there would be a significant relationship between LV-GLS measured by 2D speckle-tracking echocardiography and the occurrence of CV outcomes in patients with permanent PM.

MATERIALS AND METHODS

Study Population

A total of 1,103 patients who underwent permanent PM implantation at a single tertiary hospital between January 2007 and December 2017 was identified retrospectively. Among them, we selected patients who underwent both baseline transthoracic echocardiography within 1 year before PM implantation and follow-up echocardiography between 6 months and 5 years after PM implantation. We excluded patients who had overt LV systolic dysfunction (LVEF $<$50%) before PM implantation, had at least a moderate degree of any valve dysfunction on baseline echocardiography, had a history of cardiac surgery, acute myocardial infarction within 3 months before PM implantation, and single-lead right atrial PM. All patients who had cardiovascular events in time between baseline and post-implantation echocardiogram were also excluded from this study cohort. Finally, 300 patients were included in the analysis. Patients' clinical data, medications, PM characteristics, echocardiographic characteristics, and clinical outcomes were reviewed retrospectively. The study was approved by the Institutional Review Board of Yonsei University Health System (approval number: 4-2020-0032) and conducted according to the Declaration of Helsinki.

Follow-Up and Outcomes

Patients were scheduled to visit the PM clinic every 6 months after PM implantation. Follow-up data, including pacing percentage and clinical events, were obtained by reviewing medical records. Data of pacing percentage was gathered at the time of the first interrogation after 2 months of PM implantation. Based on the echocardiographic data between 6 months and 5 years after PM implantation, PMIC was defined as a $\geq$10% decrease in LVEF compared with baseline echocardiography with resultant LVEF $<$50% (14). We reviewed all medical records after PM implantation through total follow-up periods, and patients who had an event of myocardial infarction, acute coronary syndrome, and who had severe valvular stenosis/regurgitation on post-PM echocardiogram were excluded from later analysis. CV outcomes were defined as a composite of admission for heart failure and CV death and the event was included only after the time of post-PM echocardiography. Admission of heart failure was defined when following conditions were met: the patient's symptom of dyspnea at least 3 of New York Heart Association (NYHA) class, required medication such as diuretics or vasodilators, elevated N-terminal pro-brain natriuretic peptide (NT-proBNP), and pulmonary edema or pleural effusion in chest X-ray. CV death was defined as the cause of the death was acute myocardial infarction, heaft failure, sudden cardiac death, lethal ventricular arrhythmia, or stroke, and we determined the CV death by review the patient's medical record and the death certificate. If a patient had at least two clinical outcomes, the first event was included for outcome analyses.

Echocardiography

Standard 2D and Doppler measurements were performed using a standard ultrasound machine (Vivid E9; GE Medical Systems, Chicago, IL; Philips iE33; Philips Healthcare, Netherlands) with a 2.5–3.5 MHz probe. Standard echocardiographic measurements were performed according to recommendations from the European association of cardiovascular imaging (15). LVEF was measured using the biplane Simpson's method in apical four- and two-chamber views. Left atrial volume index was measured by the biplane method in both the apical four- and two-chamber views and indexed on the body surface area. The severity of tricuspid regurgitation was graded with multi-parametric methods. (16).

Speckle-Tracking Echocardiography

The two-dimensional images from both baseline echocardiogram and echocardiogram after PM implantation were used for analyses of LV mechanical function. Three apical four-, three-, and two-chamber images for each echocardiographic study were stored and exported to the off-line data storage device, and speckle-tracking echocardiography was performed using a vendor-independent software package (TomTec software; Image Arena 4.6, Munich, Germany) as described previously (17). After that, LV-GLS and segmental longitudinal strain values were measured in a blinded method from the clinical data by experienced cardiologists, according to the practical guidance in assessing strain (18, 19). LV endocardial borders were traced at the end-diastolic and end-systolic frames in each apical view. TomTec software tracked the speckle on three endocardial

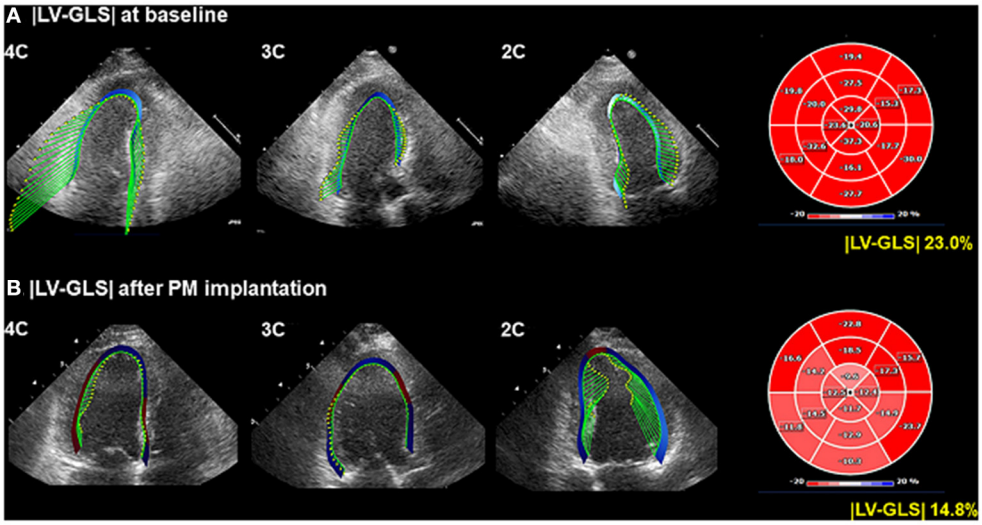

FIGURE 1 | Representative LV-GLS measurements. **(A)** LV-GLS was calculated from three standard apical views at baseline echocardiogram (left). The absolute value of LV-GLS was 23.0% (right). **(B)** LV-GLS was assessed after PM implantation. |LV-GLS| was 14.8% (right). LV-GLS, left ventricular global longitudinal strain; PM, pacemaker.

borders during the whole cardiac cycle. For analysis of segmental strain, we used the 16-segment model that divided the base and mid area into six segments (antero-septum, anterior, antero-lateral, infero-lateral, inferior, and infero-septal) and the apex into four segments (septal, inferior, lateral, and anterior), and LV-GLS was calculated by averaging the values at each segmental level as mentioned above. |LV-GLS| was defined as the absolute value of LV-GLS (removing the conventional negative value of LV-GLS data) (**Figure 1**). The LV-global circumferential strain (GCS) was calculated by averaging the values of segmental circumferential strains from the parasternal short-axis view in the basal-, mid-, and apical-LV levels. |LV-GLS| was defined as the absolute value of LV-GCS. We randomly selected 20 patients from the study population and analyzed the intra- and inter-observer reproducibility of LV-GLS measurement by Bland–Altman analysis. The intra-class correlation coefficients for |LV-GLS| were 0.987 and 0.963 for intra- and inter-observer variation, respectively. The Bland–Altman analysis showed the limits of agreement (LOA) across a broad range of LV-GLS values; the bias for intra- and inter-observer measurements of LV-GLS was 0.47% (range: −0.91 to −0.04%, 95% LOA) and 0.37% (range: −0.71 to 0.78%), respectively.

Statistical Analysis

Continuous variables are presented as mean ± standard deviation (SD), and categorical variables are presented as frequency and percentage. Comparisons of baseline clinical and echocardiographic parameters between the two groups were analyzed using Student's *t*-test for continuous data and chi-square ($\chi 2$) and Fisher's exact test for categorical data. Correlations between pacing percentage and echocardiographic variables including the strain of each segment were obtained using simple linear regression analysis and multiple linear regression analysis for adjusting other confounding factors. Predictive values of LV-GLS for CV outcomes were calculated using receiver operating characteristic (ROC) analysis. Clinical outcomes were constructed using Kaplan–Meier methods, and comparisons among groups were performed using a log-rank test. The predictors of CV outcomes were evaluated using multivariate nested Cox proportional hazard regression models. The independence of |LV-GLS| was examined using three models. Initially, three subgroups divided by |LV-GLS| tertile were included in the Cox model as a covariate, with adjustment for age and sex. Then, chronic kidney disease and coronary artery disease were included in the second model. Finally, LVEF and left atrial volume index were included in the last model. Significant differences were considered at $P < 0.05$. All statistical analyses were performed using SPSS 25.0 software (IBM Corp., Armonk, NY), and Medcalc statistical package (Medcalc software, Mariakerke, Belgium) was used for comparison of ROC curves.

RESULTS

Baseline Characteristics

During a mean 44 ± 28 months of follow-up after post-PM echocardiography, 23 of 300 patients (7.7%) experienced CV events. Clinical characteristics, medications, and data related to PM in patients with or without CV outcomes are presented in **Table 1**. Patients with CV outcomes were older and had a higher prevalence of chronic kidney disease, coronary artery disease than did those without CV outcomes. More heart failure medications including renin-angiotensin-aldosterone system blockade and diuretics were used by patients with CV outcomes compared to those without CV outcomes. The ventricular lead

TABLE 1 | Baseline characteristics.

	Total ($n = 300$)	Without CV outcomes ($n = 277$)	With CV outcomes ($n = 23$)	*P*-value
Age, years	67.1 ± 13.2	66.2 ± 13.8	74.5 ± 9.9	0.005
Male sex, *n* (%)	119 (39.7)	107 (38.6)	12 (52.2)	0.202
BMI, kg/m^2	24.3 ± 3.6	24.3 ± 3.6	25.0 ± 3.6	0.357
Hypertension, *n* (%)	171 (57.0)	155 (56.0)	16 (69.6)	0.205
Diabetes mellitus, *n* (%)	61 (20.3)	54 (19.5)	7 (30.4)	0.210
CKD, *n* (%)	22 (7.3)	16 (5.8)	6 (26.1)	<0.001
AF, *n* (%)	54 (18.0)	48 (17.3)	6 (26.1)	0.293
CAD, *n* (%)	39 (13.0)	30 (10.8)	9 (39.1)	<0.001
HFpEF, *n* (%)	5 (1.7)	4 (1.4)	1 (4.3)	0.296
Medications, *n* (%)				
RAAS blockers	141 (47.0)	122 (44.0)	19 (82.6)	<0.001
Beta blockers	39 (13.0)	36 (13.0)	3 (13.0)	0.995
CCB	69 (23.0)	64 (23.1)	5(21.7)	0.881
Diuretics	78 (26.0)	68 (24.5)	10 (43.5)	0.047
Statin	89 (29.7)	81 (29.2)	8 (34.8)	0.576
V lead position, *n* (%)				
Apex	273 (91.0)	250 (90.3)	23 (100.0)	0.117
Septum	27 (9.0)	27 (9.7)	0 (0.0)	
Pacing percentage, %	60.4 ± 42.4	61.3 ± 42.3	49.7 ± 42.6	0.211

CV, cardiovascular; BMI, body mass index; CKD, chronic kidney disease; AF, atrial fibrillation; CAD, coronary artery disease; HFpEF, heart failure with preserved ejection fraction; RAAS, renin-angiotensin-aldosterone system; CCB, calcium channel blockers; V, ventricular.

position and pacing percentage were not different between the groups.

Baseline and post-PM echocardiographic variables are presented in **Table 2**. On baseline echocardiogram, patients with CV outcomes showed lower e' and S' velocities, higher E/e', and lower |LV-GLS| than did those without CV outcomes. On post-PM echocardiogram, more dilated chambers, relatively low LVEF (even though mean LVEF was within the normal range), higher LV mass index, lower S' velocity, higher E/e', and lower |LV-GLS| and |LV-GCS| were shown in patients with CV outcomes compared to patients without CV outcomes. Timing of post-PM echocardiogram after PM implantation was not different between the groups.

Relationship Between RV Pacing and LV Mechanical Dysfunction

The correlations between RV pacing percentage on the first PM interrogation results and the parameters on post-PM echocardiogram are presented in **Table 3**. As RV pacing percentage increased, functional and structural deterioration was observed. The correlation between RV pacing percentage and |LV-GLS| was significant ($r = 0.257$, $p < 0.001$) compared to that of other global functional parameters and this phenomenon was strengthened especially with RV apical pacing, compared with RV septal pacing ($p < 0.001$ vs. $p = 0.248$). In terms of LV segmental strain, RV pacing percentage was significantly associated with impaired strain at all segments in the LV apex and at inferior and septal segments in the mid-LV. Multiple linear regression analysis revealed that RV pacing percentage was independently associated with impaired |LV-GLS| and |Apical septal strain| after adjusting for age, sex, HTN, and DM in all the study subjects (both $p < 0.001$) (**Supplementary Table 1**). When compared the subgroup with RV pacing percentage divided by 50%, the subgroup with the RV pacing under 50% had better event-free survival than those who were not (log rank p = 0.047) (**Supplementary Figure 1**).

Occurrence of PMIC and CV Outcomes Based on LV-GLS Levels

The changes in LVEF and |LV-GLS| according to the CV outcomes at the baseline echocardiogram and post-PM follow-up study are shown in **Figure 2**. LVEF and |LV-GLS| were decreased after PM implantation in the group without CV outcomes and the group with CV outcomes. However, LVEF after PM implantation maintained normal values in both groups, whereas |LV-GLS| decreased more noticeably in patients with CV outcomes. When compared the subgroup which was divided by the degree of |LV-GLS| change, the subgroup with the |LV-GLS| reduction under 10% had better event-free survival than those who were not (log rank $p = 0.035$) (**Supplementary Figure 2**).

ROC analysis of predictive values of LVEF and |LV-GLS| for PMIC and CV outcomes are shown in **Figure 3**. The |LV-GLS| on baseline echocardiogram revealed a significant predictive value for PMIC (area under the curve, AUC: 0.622, $p = 0.024$, cut-off 21.4%, sensitivity 81.3%, specificity 53.7%) after PM implantation. In terms of CV outcomes, the cut-off value of 11.2% in |LV-GLS| on post-PM echocardiogram showed a better predictive value than did LVEF (AUC; 0.784 vs. 0.647, $p = 0.012$), with acceptable sensitivity (60.9 %) and specificity (88.1%).

TABLE 2 | Echocardiographic characteristics.

	Total ($n = 300$)	Without CV outcomes ($n = 277$)	With CV outcomes ($n = 23$)	*P*-value
Baseline echocardiogram				
LVEDD, mm	50.3 ±4.7	50.2 ±4.6	51.4 ±5.5	0.250
LVESD, mm	32.3 ±4.3	32.2 ±4.2	33.7 ±5.4	0.120
LVEF. %	67.8 ±6.8	67.9 ±6.7	66.0 ±7.5	0.191
LV mass index, g/m^2	104.4 ±22.5	103.8 ±22.3	112.1 ±25.0	0.130
LA volume index, ml/m^2	35.8 ±12.6	35.4 ±12.5	40.4 ±14.0	0.068
e' velocity, cm/s	6.1 ±2.4	6.2 ±2.5	4.7 ±1.5	0.012
S' velocity, cm/s	6.7 ±1.6	6.8 ±1.6	5.8 ±1.4	0.007
E/e'	13.7 ±6.3	13.3 ±5.9	19.4 ±8.7	0.007
|LV-GLS|, %	21.0 ±5.3	21.2 ±5.3	18.5 ±4.7	0.016
|LV-GCS|, %	29.1 ±7.0	29.2 ±7.0	27.6 ±6.8	0.292
Post-PM echocardiogram				
Time after PM implantation, years	2.2 ±1.2	2.2 ±1.2	2.4 ±1.4	0.730
LVEDD, mm	49.6 ±5.1	49.4 ±5.0	51.7 ±6.2	0.035
LVESD, mm	33.4 ±5.7	33.1 ±5.5	36.4 ±7.5	0.047
LVEF. %	62.2 ±10.3	62.7 ±9.7	55.1 ±14.1	0.018
PMIC, n (%)	32 (10.7)	22 (7.9)	10 (43.5)	<0.001
LV mass index, g/m^2	101.4 ±25.3	100.0 ±24.6	120.0 ±27.7	<0.001
LA volume index, ml/m^2	34.8 ±13.4	34.0 ±12.9	44.8 ±15.3	<0.001
e' velocity, cm/s	5.3 ±1.9	5.3 ±1.9	5.0 ±1.3	0.476
S' velocity, cm/s	5.9 ±1.4	5.9 ±1.4	4.9 ±0.9	<0.001
E/e'	13.4 ±5.9	13.0 ±5.5	19.1 ±8.4	0.007
Significant TR (≥grade 2)	18 (6.0)	17 (6.1)	1 (4.3)	0.728
|LV-GLS|, %	16.6 ±5.3	17.0 ±5.0	11.2 ±5.5	<0.001
|LV-GCS|, %	24.5 ±7.1	24.9 ±6.9	19.1 ±7.7	<0.001

CV, cardiovascular; LVEDD, left ventricular end-diastolic dimension; LVESD, left ventricular end-systolic dimension; LVEF, left ventricular ejection fraction; LV, left ventricle; LA, left atrium; e', early diastolic mitral annular tissue velocity; S', systolic mitral annular tissue velocity; E/e', ratio of early diastolic mitral inflow velocity to early diastolic mitral annular tissue velocity; |LV-GLS|, absolute value of left ventricular global longitudinal strain; |LV-GCS|, absolute value of left ventricular global circumferential strain; PM, pacemaker; PMIC, pacemaker-induced cardiomyopathy; TR, tricuspid regurgitation.

Figure 4 shows the Kaplan–Meier survival curves for the two groups divided by an |LV-GLS| of 11.2 % and for three subgroups divided by |LV-GLS| tertile. At a mean 44 ± 28 months of follow-up after post-PM echocardiogram, the lowest |LV-GLS| group revealed a significantly worse CV outcome than did the others (log-rank $p < 0.001$). In multivariate nested Cox proportional hazard models, the lower |LV-GLS| showed an independent association with poor CV outcomes in age and sex adjusted analysis (hazard ratio, HR: 14.8; 95% confidence interval, CI: 1.93–112.70, $p = 0.009$). Multivariate models including comorbidities and conventional echocardiographic variables also revealed that the lower |LV-GLS| had a statistically significant association with poor CV outcomes (Model 2; HR: 15.18; CI: 1.96–117.61; $p = 0.009$) (Model 3; HR: 13.97; CI: 1.72–113.39; $p = 0.014$) (**Table 4**).

DISCUSSION

The principal findings of the present study were as follows: (1) RV pacing deteriorated global and segmental LV mechanical function, (2) |LV-GLS| at baseline echocardiogram showed a good predictive value for PMIC after PM implantation, (3) |LV-GLS| at post-PM echocardiogram revealed a better predictive value of CV outcomes than did LVEF, and (4) reduced |LV-GLS| was independently associated with poor CV outcomes in patients with permanent PM. These results imply that, for patients who undergo permanent PM implantation, serial assessments of LV-GLS by speckle-tracking echocardiography before and after PM implantation are beneficial for early detection of PMIC and prediction of clinical outcomes.

Usefulness of LV-GLS in Patients Who Underwent PM Implantation

As the population ages, not only is the number of patients receiving permanent PM implantation increasing, but so is the occurrence of heart failure after PM implantation. (20, 21). PMIC has emerged as one of the most important complications of PM implantation, and its incidence is increasing, increasing the need to upgrade to cardiac resynchronization therapy (4). PMIC is usually defined as a decrease of LVEF, but there are many limitations in predicting PMIC before LV systolic dysfunction. The present study demonstrated that the cut-off value of 21.4 % in |LV-GLS| on baseline echocardiogram before PM implantation revealed a significant predictive value for

TABLE 3 | Simple correlations between pacing percentage and echocardiographic variables after PM implantation.

		Correlation coefficient	*P*-value
LVEDD, mm		0.162	0.005
LVESD, mm		0.189	0.001
LVEF. %		−0.210	<0.001
LV mass index, g/m^2		0.116	0.048
LA volume index, ml/m^2		0.100	0.083
e' velocity, cm/s		−0.138	0.021
S' velocity, cm/s		−0.202	0.001
E/e'		0.013	0.833
|LV-GLS|, %		−0.257	<0.001
|LV-GCS|, %		−0.198	0.001
LV segmental longitudinal strain			
Base	Antero-septum	0.093	0.109
	Anterior	0.050	0.385
	Antero-lateral	0.073	0.207
	Infero-lateral	0.076	0.191
	Inferior	0.126	0.029
	Infero-septal	0.127	0.028
Mid LV	Antero-septum	0.183	0.001
	Anterior	0.081	0.164
	Antero-lateral	0.133	0.021
	Infero-lateral	0.058	0.316
	Inferior	0.270	<0.001
	Infero-septal	0.182	0.002
Apex	Septal	0.333	<0.001
	Anterior	0.236	<0.001
	Lateral	0.316	<0.001
	Inferior	0.271	<0.001

LVEDD, left ventricular end-diastolic dimension; LVESD, left ventricular end-systolic dimension; LVEF, left ventricular ejection fraction; LV, left ventricle; LA, left atrium; e', early diastolic mitral annular tissue velocity; S', systolic mitral annular tissue velocity; E/e', ratio of early diastolic mitral inflow velocity to early diastolic mitral annular tissue velocity; |LV-GLS|, absolute value of left ventricular global longitudinal strain; |LV-GCS|, absolute value of left ventricular global circumferential strain.

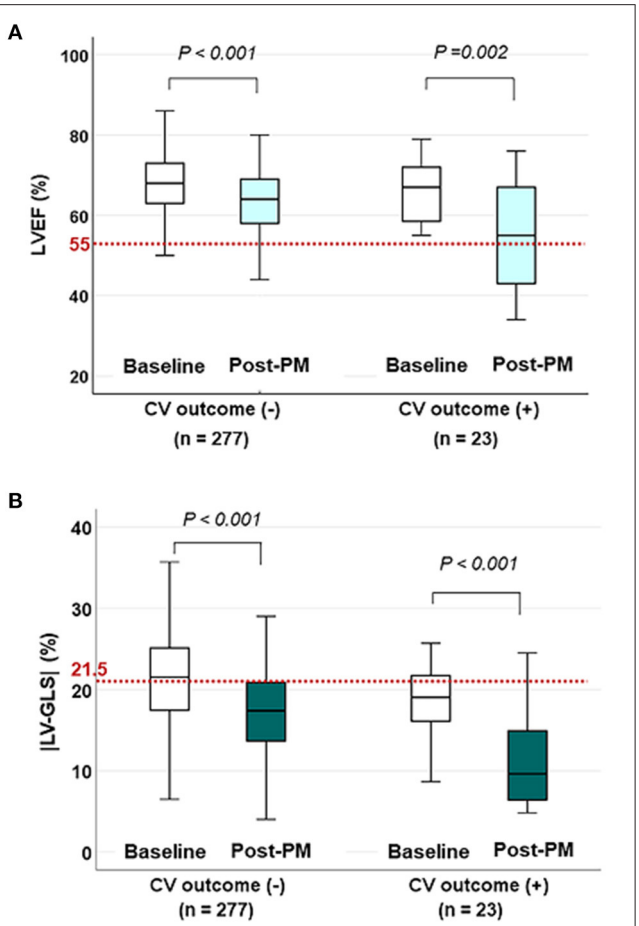

FIGURE 2 | The changes in LVEF and |LV-GLS| according to CV outcomes on baseline and post-PM echocardiogram. **(A)** LVEF decreased after PM implantation in both groups, but the mean values were within the normal range (red dotted line) even in patients with CV outcomes. **(B)** |LV-GLS| in patients with CV outcomes decreased more noticeably than in patients without CV outcomes under normal values (red dotted line). LVEF, left ventricular ejection fraction; CV, cardiovascular; |LV-GLS|, absolute value of left ventricular global longitudinal strain; PM, pacemaker.

occurrence of PMIC after PM implantation, but LVEF did not. In a previous study, Ahmed et al. showed changes in |LV-GLS| and LVEF after PM implantation in 55 patients. (22) 1 month after PM implantation, |LV-GLS| was significantly reduced from 16.3 ± 0.5 to 12.6 ± 0.9% in patients with PMIC compared to baseline. At 12 months of follow-up, |LV-GLS| impairment was reported as 11.9 ± 2.5%. This showed the sensitivity of LV-GLS in predicting the development of PMIC. However, the study included a small cohort of 55 patients, and the follow-up periods were relatively short for estimating CV outcomes. Moreover, LV-GLS was evaluated 1 month after PM implantation, and additional echocardiographic studies are required. On the other hand, the present study showed the predictive value of LV-GLS in the occurrence of PMIC, and this was assessed before PM implantation in a relatively large number of patients. In another study, Babu et al. demonstrated that 3D echocardiography with |LV-GLS| analysis played a role in predicting PMIC in a total of 36 patients (23). A decline in |LV-GLS| of 18.0% to 13.9% was noted at 6-months after PM implantation, whereas a decline in LVEF of 57.8% to 54.5% was noted after PM implantation. This study was conducted in a small population of 36 patients with short follow-up periods. Accordingly, the present study demonstrates the usefulness of LV-GLS for predicting PMIC occurrence and clinical outcome in patients with both baseline and post-PM echocardiography and sufficient regular clinical follow-up for an average of 44 months after post-PM echocardiography.

Pacing Percentage and LV Mechanical Dysfunction

It is well known that the incidence of heart failure in patients who underwent PM implantation is associated with RV pacing, and that a higher RV pacing percentage results in a higher incidence of CV events (24). In this study, it was confirmed that,

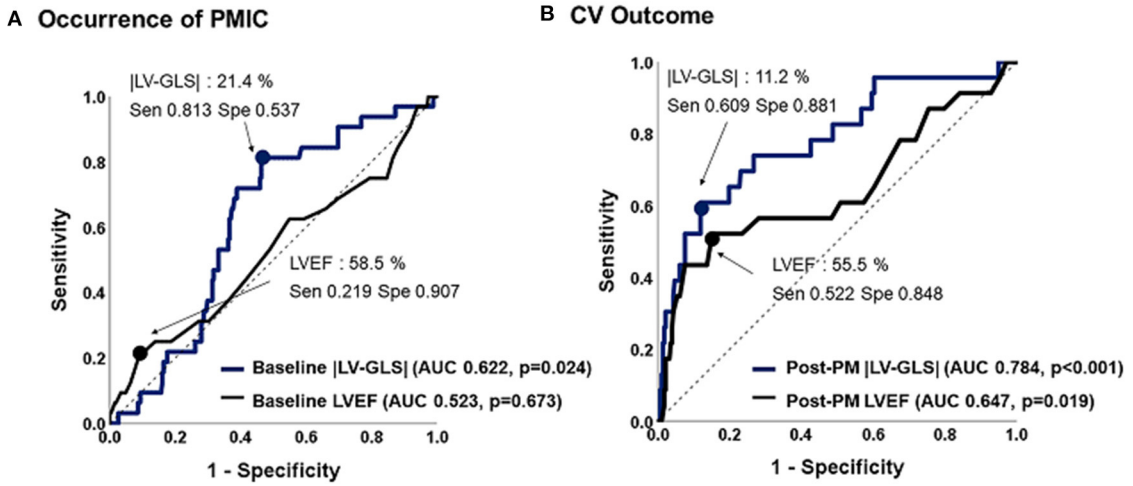

FIGURE 3 | Predictive values of |LV-GLS| and LVEF for occurrence of PMIC and CV outcome. **(A)** The |LV-GLS| on baseline echocardiogram revealed significant predictive value for occurrence of PMIC. **(B)** The |LV-GLS| on post-PM echocardiogram showed a better predictive value for CV outcomes than did LVEF. |LV-GLS|, absolute value of left ventricular global longitudinal strain; LVEF, left ventricular ejection fraction; PMIC, pacemaker-induced cardiomyopathy; PM, pacemaker; CV, cardiovascular.

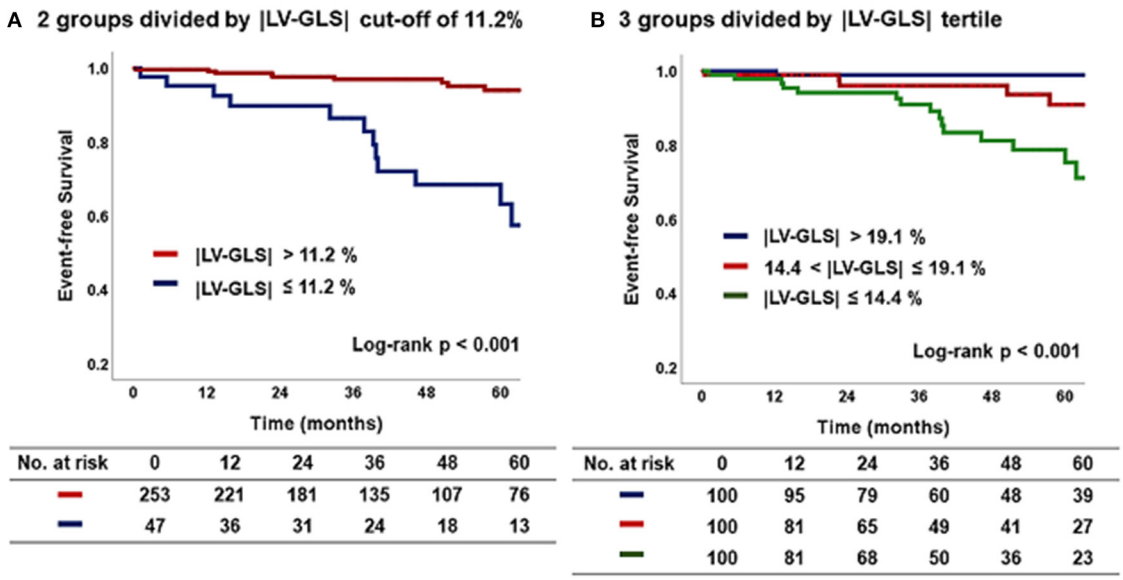

FIGURE 4 | Kaplan–Meier curve according to |LV-GLS| on post-PM echocardiogram. **(A)** The group of |LV-GLS| ≤ 11.2% revealed a significantly worse CV outcome than the other group (log-rank $p < 0.001$). **(B)** The lowest |LV-GLS| group revealed a significantly worse CV outcome than the others (log-rank $p < 0.001$). |LV-GLS|, absolute value of left ventricular global longitudinal strain; PM, pacemaker; CV, cardiovascular.

as RV pacing percentage increased, the global LV mechanical function evaluated by |LV-GLS| decreased, and it was more obvious when the analysis was performed divided by RV pacing site. Previous studies also tried to show the relationship between pacing percentage and LV-GLS; however, mainly due to the small number of study subjects, they failed to show a linear correlation (22, 25). Another strength of the present study is that it comprehensively shows LV regional mechanical dysfunction by pacing through segmental strain analysis. As pacing percentage increased, the absolute value of longitudinal strain in some specific segments decreased. The specific segments that were highly affected by pacing were those in the entire LV apex. The correlation weakened toward the mid-LV and base, but the absolute value of segmental strain in the inferior segment and infero-septal segment significantly decreased in proportion to pacing percentage. These results can be interpreted

TABLE 4 | Cox regression analysis for CV outcomes.

	Model 1		Model 2		Model 3	
	Hazard ratio [95% CI]	***P*-value**	**Hazard ratio [95% CI]**	***P*-value**	**Hazard ratio [95% CI]**	***P*-value**
|LV-GLS| > 19.1%	Reference		Reference		Reference	
14.4 < |LV-GLS| ≤ 19.1%	5.80 [0.68∼49.84]	0.109	4.06 [0.46∼35.66]	0.207	4.59 [0.52∼40.13]	0.169
|LV-GLS| ≤ 14.4%	14.8 [1.93∼112.70]	0.009	15.18 [1.96∼117.61]	0.009	13.97 [1.72∼113.39]	0.014

Model 1: Adjusted by age and sex.
Model 2: Adjusted by age, sex, CKD, and CAD.
Model 3: Adjusted by age, sex, CKD, CAD, LVEF, and LA volume index.
CI, confidence interval; CKD, chronic kidney disease; CAD, coronary artery disease; LVEF, left ventricular ejection fraction; LA, left atrium; |LV-GLS|, absolute value of left ventricular global circumferential strain.

based on the pathophysiology of PMIC. During RV pacing, conduction of an electrical wave passes through the myocardium, which is adjacent to the PM lead (6, 26). Therefore, there were significant decreases in strain in the regions close to the pacing area (27). This phenomenon results in dyssynchronous motion of LV. In patients with dyssynchronous motion due to higher RV pacing burden and subsequent lower LVEF, an upgrade from PM to cardiac resynchronization therapy might be considered to improve LV mechanical dysfunction and to treat heart failure (5). Considering the cut-off value of |LV-GLS| of post-PM implantation as 11.2%, patients with |LV-GLS| under 11.2% on post-PM implantation echocardiography are recommended to adjust the PM pacing parameters to reduce the pacing percentage or consider to converse to cardiac resynchronization therapy, with aggressive heart failure medication. In patients with |LV-GLS| in the gray zone between 11.2 to 20%, regular echocardiography follow-up to identify whether |LV-GLS| decreases under 11.2% and manage several risk factors regarding heart failure are required.

Limitations

This study has several limitations. First, this study was retrospectively designed and comprised patients who were followed up by regular visits. The interval of follow-up echocardiogram after PM implantation was not concordant in all patients. To minimize this limitation, the timing of follow-up echocardiogram was limited to between 6 months and 5 years after PM implantation to evaluate the predictability of future CV events of LV-GLS. Nevertheless, the population might be biased, and it is possible that the occurrence of clinical events was underestimated. Second, echocardiographic examinations of patients were not performed using the same equipment, which could have produced inconsistency of echocardiographic parameters, especially LV-GLS. However, we used vendor-independent software and tried to minimize the error of measurement by expert operators. Third, the |LV-GLS| value for predicting PMIC on the baseline echocardiogram before PM implantation was 21.4%, which was within the normal range. According to previous results of a head-to-head comparison of LV-GLS among vendors reported by the European Association of Cardiovascular Imaging/American Society of Echocardiography, the average |LV-GLS| values measured by TomTec software was 21.5%, trending higher than other software measures. (28). Also, there is a possibility that |LV-GLS| was high because of a compensatory increase in stroke volume due to bradycardia in some patients. As a result, we suggest that, if |LV-GLS| is lower than the normal reference value before PM implantation, close clinical and echocardiographic follow-up should be performed after PM implantation considering the risk of PMIC.

CONCLUSION

After PM implantation, there were significant regional and global changes in LV mechanical function. On post-PM echocardiogram, reduced |LV-GLS| rather than LVEF is associated with poor CV outcome. Assessments of LV-GLS by speckle-tracking echocardiography before and after PM implantation are beneficial for early detection of LV mechanical dysfunction and prediction of CV outcomes.

DATA AVAILABILITY STATEMENT

The original contributions presented in the study are included in the article/**Supplementary Material**, further inquiries can be directed to the corresponding author.

ETHICS STATEMENT

The studies involving human participants were reviewed and approved by Yonsei University Health System. Written informed consent for participation was not required for this study in accordance with the national legislation and the institutional requirements. Written informed consent was not obtained from the individual(s) for the publication of any potentially identifiable images or data included in this article.

AUTHOR CONTRIBUTIONS

D-YK and CS contributed to the concept and design of this study. D-YK, PL, JS, IC, G-RH, J-WH, and CS contributed to acquisition, analysis, and interpretation of the data. D-YK and CS contributed to drafting of the manuscript and statistical analysis. G-RH, J-WH, and CS contributed to revision and finalize the manuscript. All authors contributed to the article and approved the submitted version.

SUPPLEMENTARY MATERIAL

The Supplementary Material for this article can be found online at: https://www.frontiersin.org/articles/10.3389/fcvm.2021.705778/full#supplementary-material

Supplementary Table 1 | Multiple linear regression analysis for post-PM |LV-GLS| and |Apical septal strain|. |LV-GLS|, absolute value of left ventricular global longitudinal strain; |Apical septal strain|, absolute value of left ventricular apical septal strain; RV, right ventricle; HTN, hypertension; DM, diabetes mellitus.

Supplementary Figure 1 | Kaplan-Meier curve on 2 subgroups according to the RV pacing percentage divided by 50%. The subgroup with RV pacing under 50% had better event-free survival than those who were not (log rank p = 0.047). RV; right ventricle.

Supplementary Figure 2 | Kaplan-Meier curve on 2 subgroups according to the degree of |LV-GLS| change between baseline and post-PM echocardiogram. The subgroup with the |LV-GLS| reduction under 10% had better event-free survival than those who were not (log rank p = 0.035). |LV-GLS|; absolute value of left ventricular global longitudinal strain.

REFERENCES

1. Thackray SDR, Witte KKA, Nikitin NP, Clark AL, Kaye GC, Cleland JGF. The prevalence of heart failure and asymptomatic left ventricular systolic dysfunction in a typical regional pacemaker population. *Eur Heart J.* (2003) 24:1143–52. doi: 10.1016/S0195-668X(03)00199-4
2. Yu C-M, Chan JY-S, Zhang Q, Omar R, Yip GW-K, Hussin A, et al. Biventricular pacing in patients with bradycardia and normal ejection fraction. *N Engl J Med.* (2009) 361:2123–34. doi: 10.1056/NEJMoa0907555
3. Mumin G, Celiker C. Right ventricular apical and septal pacing: long term impacts on ventricular function. *Eur Hear J - Cardiovasc Imaging.* (2021) 22:432. doi: 10.1093/ehjci/jeaa356.367
4. Kiehl EL, Makki T, Kumar R, Gumber D, Kwon DH, Rickard JW, et al. Incidence and predictors of right ventricular pacing-induced cardiomyopathy in patients with complete atrioventricular block and preserved left ventricular systolic function. *Hear Rhythm.* (2016) 13:2272–8. doi: 10.1016/j.hrthm.2016.09.027
5. Cho SW, Gwag H. Bin, Hwang JK, Chun KJ, Park KM, On YK, Kim JS, Park SJ. Clinical features, predictors, and long-term prognosis of pacing-induced cardiomyopathy. *Eur J Heart Fail.* (2019) 21:643–51. doi: 10.1002/ejhf.1427
6. Shim CY. Pacing-induced alterations in left ventricular mechanical properties: effect of pacing sites. *J Cardiovasc Ultrasound.* (2011) 19:13. doi: 10.4250/jcu.2011.19.1.13
7. Tantengco MVT, Thomas RL, Karpawich PP. Left ventricular dysfunction after long-term right ventricular apical pacing in the young. *J Am Coll Cardiol.* (2001) 37:2093–100. doi: 10.1016/S0735-1097(01)01302-X
8. Ahmed M, Gorcsan J, Marek J, Ryo K, Haugaa K, Ludwig DR, et al. Right ventricular apical pacing-induced left ventricular dyssynchrony is associated with a subsequent decline in ejection fraction. *Hear Rhythm.* (2014) 11:602–8. doi: 10.1016/j.hrthm.2013.12.020
9. Özdemir K, Altunkaser BB, Daniş G, Özdemir A, Uluca Y, Tokaç M, et al. Effect of the isolated left bundle branch block on systolic and diastolic functions of left ventricle. *J Am Soc Echocardiogr.* (2001) 14:1075–9. doi: 10.1067/mje.2001.115655
10. Saito M, Negishi K, Eskandari M, Huynh Q, Hawson J, Moore A, et al. Association of left ventricular strain with 30-day mortality and readmission in patients with heart failure. *J Am Soc Echocardiogr.* (2015) 28:652–66. doi: 10.1016/j.echo.2015.02.007
11. Kalam K, Otahal P, Marwick TH. Prognostic implications of global LV dysfunction: A systematic review and meta-analysis of global longitudinal strain and ejection fraction. *Heart.* (2014) 100:1673–80. doi: 10.1136/heartjnl-2014-305538
12. Kim D, Shim CY, Cho YJ, Park S, Lee CJ, Park JH, et al. Continuous positive airway pressure therapy restores cardiac mechanical function in patients with severe obstructive sleep apnea: a randomized, sham-controlled study. *J Am Soc Echocardiogr.* (2019) 32:826–35. doi: 10.1016/j.echo.2019.03.020
13. Hwang IC, Cho GY, Yoon YE, Park JJ. Association between global longitudinal strain and cardiovascular events in patients with left bundle branch block assessed using two-dimensional speckle-tracking echocardiography. *J Am Soc Echocardiogr.* (2018) 31:52–63. doi: 10.1016/j.echo.2017.08.016
14. Khurshid S, Epstein AE, Verdino RJ, Lin D, Goldberg LR, Marchlinski FE, et al. Incidence and predictors of right ventricular pacing-induced cardiomyopathy. *Hear Rhythm.* (2014) 11:1619–25. doi: 10.1016/j.hrthm.2014.05.040
15. Lang RM, Badano LP, Mor-Avi V, Afilalo J, Armstrong A, Ernande L, et al. Recommendations for cardiac chamber quantification by echocardiography in adults: An update from the American society of echocardiography and the European association of cardiovascular imaging. *Eur Heart J Cardiovasc Imaging.* (2015) 16:233–71. doi: 10.1093/ehjci/jev014
16. Baumgartner H, Falk V, Bax JJ, De Bonis M, Hamm C, Holm PJ, et al. 2017 ESC/EACTS Guidelines for the management of valvular heart disease. *Eur Heart J.* (2017) 38:2739–86. doi: 10.1016/j.rec.2017.12.013
17. Risum N, Ali S, Olsen NT, Jons C, Khouri MG, Lauridsen TK, et al. Variability of global left ventricular deformation analysis using vendor dependent and independent two-dimensional speckle-tracking software in adults. *J Am Soc Echocardiogr.* (2012) 25:1195–203. doi: 10.1016/j.echo.2012.08.007
18. Voigt JU, Pedrizzetti G, Lysyansky P, Marwick TH, Houle H, Baumann R, et al. Definitions for a common standard for 2D speckle tracking echocardiography: consensus document of the EACVI/ASE/Industry Task Force to standardize deformation imaging. *Eur Heart J Cardiovasc Imaging.* (2015) 16:1–11. doi: 10.1093/ehjci/jeu184
19. Negishi K, Negishi T, Kurosawa K, Hristova K, Popescu BA, Vinereanu D, et al. Practical guidance in echocardiographic assessment of global longitudinal strain. *JACC Cardiovasc Imaging.* (2015) 8:489–92. doi: 10.1016/j.jcmg.2014.06.013
20. Uslan DZ, Tleyjeh IM, Baddour LM, Friedman PA, Jenkins SM, St Sauver JL, et al. Temporal trends in permanent pacemaker implantation: A population-based study. *Am Heart J.* (2008) 155:896–903. doi: 10.1016/j.ahj.2007.12.022
21. Seo J, Kim DY, Cho I, Hong GR, Ha JW, Shim CY. Prevalence, predictors, and prognosis of tricuspid regurgitation following permanent pacemaker implantation. *PLoS ONE.* (2020) 15:1–10. doi: 10.1371/journal.pone.0235230
22. Ahmed FZ, Motwani M, Cunnington C, Kwok CS, Fullwood C, Oceandy D, et al. One-month global longitudinal strain identifies patients who will develop pacing-induced left ventricular dysfunction over time: The pacing and ventricular dysfunction (PAVD) Study. *PLoS ONE.* (2017) 12:1–14. doi: 10.1371/journal.pone.0162072
23. Babu NMS, Srinath SC, Lahiri A, Chase D, John B, Roshan J. Three-dimensional echocardiography with left ventricular strain analyses helps earlier prediction of right ventricular pacing-induced cardiomyopathy. *J Saudi Hear Assoc.* (2018) 30:102–7. doi: 10.1016/j.jsha.2017.06.001
24. Sharma AD, Rizo-Patron C, Hallstrom AP, O'Neill GP, Rothbart S, Martins JB, et al. Percent right ventricular pacing predicts outcomes in the DAVID trial. *Hear Rhythm.* (2005) 2:830–4. doi: 10.1016/j.hrthm.2005.05.015
25. Tanaka H, Matsumoto K, Hiraishi M, Miyoshi T, Kaneko A, Tsuji T, et al. Multidirectional left ventricular performance detected with three-dimensional speckle-tracking strain in patients with chronic right ventricular pacing and preserved ejection fraction. *Eur Heart J Cardiovasc Imaging.* (2012) 13:849–56. doi: 10.1093/ehjci/jes056
26. Tops LF, Schalij MJ, Bax JJ. The effects of right ventricular apical pacing on ventricular function and dyssynchrony. Implications for therapy. *J Am Coll Cardiol.* (2009) 54:764–76. doi: 10.1016/j.jacc.2009.06.006

27. Prinzen FW, Hunter WC, Wyman BT, McVeigh ER. Mapping of regional myocardial strain and work during ventricular pacing: experimental study using magnetic resonance imaging tagging. *J Am Coll Cardiol.* (1999) 33:1735–42. doi: 10.1016/S0735-1097(99)00068-6
28. Farsalinos KE, Daraban AM, Ünlü S, Thomas JD, Badano LP, Voigt JU. Head-to-head comparison of global longitudinal strain measurements among nine different vendors: The EACVI/ASE inter-vendor comparison study. *J Am Soc Echocardiogr.* (2015) 28:1171–81. doi: 10.1016/j.echo.2015.06.011

Conflict of Interest: The authors declare that the research was conducted in the absence of any commercial or financial relationships that could be construed as a potential conflict of interest.

Publisher's Note: All claims expressed in this article are solely those of the authors and do not necessarily represent those of their affiliated organizations, or those of the publisher, the editors and the reviewers. Any product that may be evaluated in this article, or claim that may be made by its manufacturer, is not guaranteed or endorsed by the publisher.

frontiers in Cardiovascular Medicine

REVIEW
published: 17 August 2021
doi: 10.3389/fcvm.2021.703418

Novel Imaging and Genetic Risk Markers in Takotsubo Syndrome

Luca Arcari[1], Luca Rosario Limite[2], Carmen Adduci[3], Matteo Sclafani[3], Giacomo Tini[3], Francesca Palano[3], Pietro Cosentino[3], Ernesto Cristiano[3], Luca Cacciotti[1], Domitilla Russo[3], Speranza Rubattu[3,4], Massimo Volpe[3], Camillo Autore[3], Maria Beatrice Musumeci[3] and Pietro Francia[3]*

[1] Cardiology Unit, Mother Giuseppina Vannini Hospital, Rome, Italy, [2] Department of Cardiac Electrophysiology and Arrhythmology, IRCCS San Raffaele Scientific Institute, Milan, Italy, [3] Cardiology, Clinical and Molecular Medicine Department, Faculty of Medicine and Psychology, Sapienza University of Rome, Rome, Italy, [4] IRCCS Neuromed, Pozzilli, Italy

Takotsubo syndrome (TTS) is an increasingly recognized condition burdened by significant acute and long-term adverse events. The availability of novel techniques expanded the knowledge on TTS and allowed a more accurate risk-stratification, potentially guiding clinical management. The present review aims to summarize the recent advances in TTS prognostic evaluation with a specific focus on novel imaging and genetic markers. Parametric deformation analysis by speckle-tracking echocardiography, as well as tissue characterization by cardiac magnetic resonance imaging T1 and T2 mapping techniques, currently appear the most clinically valuable applications. Notwithstanding, computed tomography and nuclear imaging studies provided limited but promising data. A genetic predisposition to TTS has been hypothesized, though available evidence is still not sufficient. Although a genetic predisposition appears likely, further studies are needed to fully characterize the genetic background of TTS, in order to identify genetic markers that could assist in predicting disease recurrences and help in familial screening.

Keywords: takotsubo, cardiac magnetic resonance imaging, T1 mapping, T2 mapping, speckle tracking echocardiography, particle imaging velocimetry, genetic, prognosis

OPEN ACCESS

Edited by:
Giovanni Quarta,
Papa Giovanni XXIII Hospital, Italy

Reviewed by:
Riccardo Liga,
Pisana University Hospital, Italy
Ankush Gupta,
Military Hospital Jaipur, India

****Correspondence:***
Luca Arcari
luca_arcari@outlook.it

Specialty section:
This article was submitted to Cardiovascular Imaging, a section of the journal Frontiers in Cardiovascular Medicine

Received: *30 April 2021*
Accepted: *26 July 2021*
Published: *17 August 2021*

Citation:
Arcari L, Limite LR, Adduci C, Sclafani M, Tini G, Palano F, Cosentino P, Cristiano E, Cacciotti L, Russo D, Rubattu S, Volpe M, Autore C, Musumeci MB and Francia P (2021) Novel Imaging and Genetic Risk Markers in Takotsubo Syndrome. Front. Cardiovasc. Med. 8:703418. doi: 10.3389/fcvm.2021.703418

INTRODUCTION

Takotsubo syndrome (TTS) is an acute heart failure (HF) syndrome accounting for ∼1-2% of all suspected acute coronary syndromes, it is characterized by transient systolic dysfunction (1) and burdened by a significant rate of in-hospital and long-term mortality (2). Several diagnostic criteria have been proposed, all of which included the presence of transient left and/or right ventricular wall motion abnormalities, ECG changes and increased cardiac biomarkers with the absence of any identifiable culprit coronary artery disease (CAD) (1, 3, 4). In recent years, the clinical knowledge of TTS has progressively improved owing to growing awareness, increased reported prevalence (5), and the availability of a number of novel diagnostic tools and prognostic markers. The present review aims to summarize the recent advances in TTS risk stratification with a specific focus on novel imaging and genetic markers.

OUTCOME OF TAKOTSUBO SYNDROME

TTS was initially perceived as a benign condition (6, 7). This was likely due to the limited sample size of early population studies, which mostly included "classic" TTS patients and presentations (e.g., post-menopausal women experiencing an emotional stress). This subset of patients was indeed later recognized as being at lower risk of adverse outcomes (8, 9).

To date, multiple studies from several multicenter registries have led to a changing perspective and currently agree on considering TTS a not-entirely benign condition, burdened by both in-hospital and long-term mortality (2, 9–12). Several acute in-hospital complications of TTS have also been described, including acute HF, arrhythmias, and thromboembolic events (13, 14) (**Table 1**). The reported incidence of HF syndromes (including severe pulmonary edema and/or cardiogenic shock) ranges from 6 to 20% (15, 16). In these cases, TTS may even require inotropic or mechanical circulatory support (1). Also, life-threatening arrhythmias (complete atrioventricular block, ventricular arrhythmias, and cardiac arrest) may occur during the acute phase of TTS in up to 8% of the cases (17). Left ventricular (LV) thrombi secondary to apical akinesia have been reported in 2.5% of TTS patients and are associated with cardioembolic complications such as stroke or transient ischemic attacks (18).

Despite TTS is characterized by a substantial recovery of LV systolic function, studies with long-term follow-up have unraveled adverse outcomes, with rates of morbidity and mortality comparable to those experienced after an acute myocardial infarction (AMI). Stiermaier et al. reported a long-term mortality higher than in patients with ST-elevation AMI (19). In the SWEDEHEART registry, mid-term (median 25 months) mortality after TTS was similar to that of AMI (adjusted hazard ratio: 1.01, 95% CI 0.70–1.46, $p = 0.955$) (20). In the InterTAK registry, long-term rate of death from any cause was 5.6% per patient-year and that of major adverse cardiac and cerebrovascular events was 9.9% per patient-year, similar to that observed in a matched control-group of AMI patients (10). Likewise, the Italian TIN registry reported that TTS long-term mortality was comparable to a propensity score-matched cohort of AMI patients (21). Concordant data with comparable TTS mortality rates were reported by the GEIST (22) and RETAKO (23) registries.

Finally, the risk of TTS recurrence is low but persistent throughout the clinical history of TTS. This is a potentially life-threatening event, presenting even several years after the first occurrence (24). In this view, TTS should not be regarded as a benign disease, neither in the short- nor in the long-term (25). Accordingly, dedicated follow-up after the index event is strongly suggested (1).

Over the years, several studies have investigated the usefulness of diverse tools (particularly imaging) to better define risk stratification in TTS (**Table 2**).

TABLE 1 | A table summarizing the major acute complications of patients with TTS.

Acute complication	Frequency
Acute heart failure	12-45%
RV involvement	18-34%
LV outflow tract obstruction	10-25%
Mitral regurgitation	14-25%
Cardiogenic shock	6-20%
LV thrombus	2-8%
Ventricular arrhythmias	4-9%
In-hospital death	1-5%
Cardiac rupture	<1%

Rates taken from (1). RV, right ventricle; LV, left ventricular.

Imaging Markers

Echocardiography

In the acute phase of TTS, transthoracic echocardiography (TTE) is the cornerstone of risk stratification. Several features can be identified by standard TTE that are associated with a higher risk, including low LV ejection fraction (EF) (26, 27) and right ventricular (RV) involvement (2). Echocardiography might be helpful in identifying the ballooning pattern, although the negative prognostic value of apical ballooning as compared to atypical forms is still debated (28–31). Furthermore, TTE allows to identify acute complications of TTS that have been related to prognosis, such as LV outflow tract obstruction and functional mitral regurgitation (11, 32, 33).

Novel, advanced echocardiographic techniques may provide an accurate and sensitive detection of cardiac abnormalities during both the acute and the "recovery" phase of TTS. Speckle tracking-TTE (ST-TTE) provides parametric quantification of myocardial chambers deformation. In the acute phase of TTS, assessment of LV global longitudinal strain (GLS) by ST-TTE has an important prognostic value, being associated to worse outcomes including in-hospital death and major adverse cardiovascular events (34). Also RV assessment by ST-TTE can be useful, as RV-GLS outperform tricuspid annular plane systolic excursion in identifying RV dysfunction (35). Finally, left atrial deformation has been described as transiently impaired in the acute phase of TTS, suggesting a cardiac involvement extending beyond the visually assessed areas of abnormal ventricular wall motion, and its finding has been associated with a higher rate of in-hospital complications (36).

The added value of ST-TTE is even more evident after the acute event, as LVEF usually normalize, but functional LV abnormalities might persist (**Figure 1**). Indeed, within the first few months after TTS hospitalization, LV-GLS is impaired despite normalization of LVEF (37, 38), and a reduced LV-GLS at 3 months after TTS associated with both persistent elevation of natriuretic peptides and impaired physical exercise capacity (39). Furthermore, by means of ST-TTE, impaired LV systolic longitudinal function has been observed over 1 year after the acute event, questioning the common perception of TTS as a transient condition (40). However, larger long-term data of the prognostic usefulness of ST-TTE in TTS are currently lacking.

Echocardiographic particle imaging velocimetry (E-PIV) is an emerging technique for estimating intracardiac blood flow patterns (41, 42). To date, a single case report described E-PIV

TABLE 2 | A summary comparing the main diagnostic features and risk markers (established or emerging) of different imaging modalities.

Imaging modality	Diagnostic features	Established risk markers	Emerging risk markers
Echocardiography	- Transient circumferential wall motion abnormalities (except focal type)	- LV ejection fraction - RV involvement - LV outflow tract obstruction - Mitral regurgitation	- Atria and ventricles deformation analysis by speckle tracking
CMR	- Transient circumferential wall motion abnormalities (except focal type) - Increased native T1, T2 and ECV - Absence of LGE	- LV ejection fraction - RV involvement	- T1 and T2 mapping - Atria and ventricles deformation analysis by feature tracking - Brain activity by functional MR imaging
CT	- Absence of culprit CAD	- CAD	- pFAI
Nuclear imaging	–	–	- Reduced 123-I-MIBG uptake - Brain activation, amygdala activity (TTS recurrence)

CMR, cardiac magnetic resonance; CT, computed tomography; ECV, extra-cellular volume; LV, left ventricular; RV, right ventricle; CAD, coronary artery disease; pFAI, peri-coronary fat attenuation index.

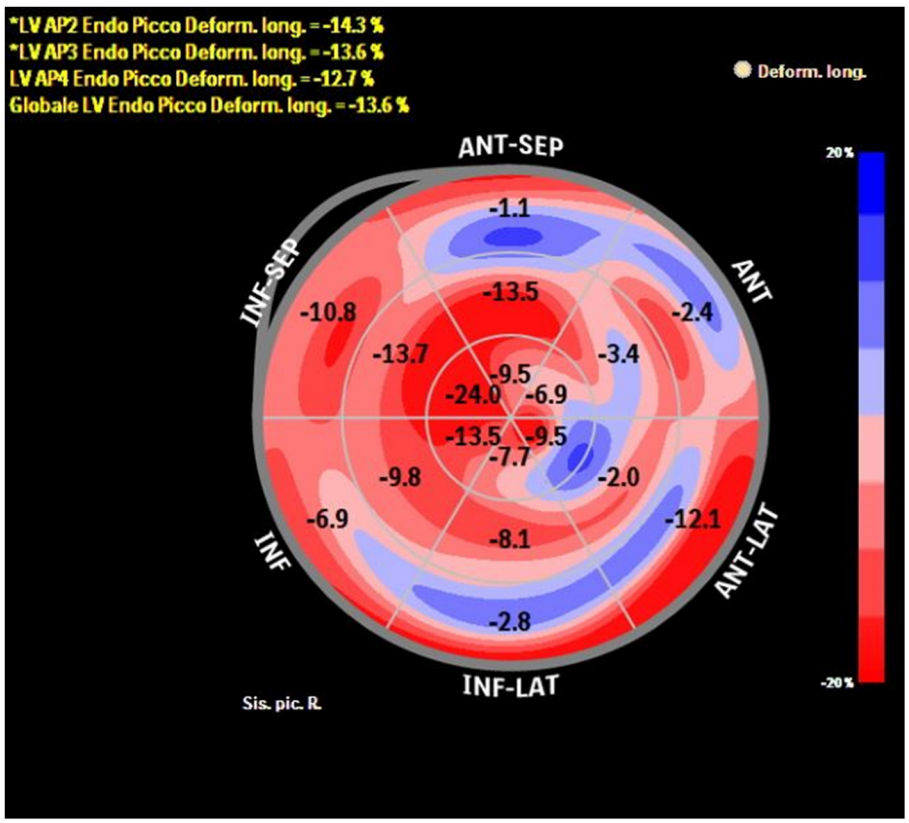

FIGURE 1 | Bull-eye depicting longitudinal strain of the LV by speckle tracking echocardiography in a patient with previous TTS at 1-month follow-up after the acute event. Despite complete recovery of LVEF, longitudinal systolic function is still impaired (global longitudinal strain −13.6%).

findings in TTS (**Figure 2**), in which a relatively preserved intra-ventricular pressure gradient and energy dissipation were observed when compared to usual findings in AMI patients (43). Since reduced energy dissipation is associated with poorer LV function (44), E-PIV findings in TTS needs to be clarified to ascertain whether the more physiologically vortex behavior is a common feature in this condition, and if this could have any relationship with outcomes.

Magnetic Resonance Imaging

Amongst cardiovascular imaging techniques, cardiac magnetic resonance (CMR) is the diagnostic gold standard for assessing cardiac volumes, function (**Figure 3**), and tissue characterization, allowing evaluation of edema, and replacement fibrosis (45).

Classic CMR appearance of TTS includes widespread myocardial edema in the absence of significant replacement

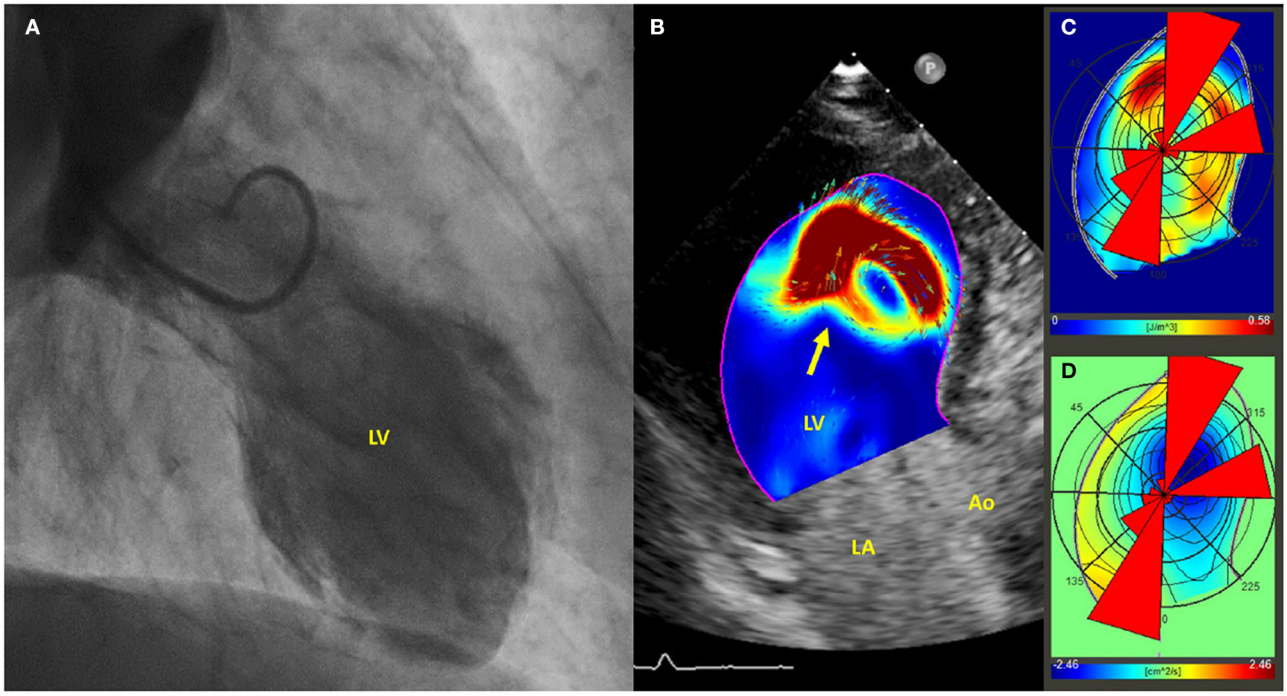

FIGURE 2 | (A) Left ventriculogram demonstrating apical ballooning of the left ventricle; **(B)** Echo-PIV analysis, revealing the presence of a single vortex, occupying the center of the left ventricle and non-interacting with others (arrow). **(C,D)** PIV derived polar histograms showing a relatively preserved base-apex flow direction. Adapted with permissions from Cimino et al. (43). Particle image velocimetry (PIV), left ventricle (LV), left atrium (LA), aorta (Ao).

fibrosis at late gadolinium enhancement (LGE) imaging, especially when strict criteria for identification are used (i.e., >5 standard deviation) (46). Notwithstanding this, variable rate of LGE detection have been described (47), and in some cases linked to worse prognosis (48). Hence, the presence of LGE should not be considered *per se* a CMR criteria to exclude TTS diagnosis, taking into account that bystander diseases conditioning the presence of replacement fibrosis might also be present (49), including coronary artery disease (50). Preforming a CMR examination is suggested in all suspected TTS patients (1), where its results might change the previously established diagnosis (51); however, taking into account the lower availability of CMR as compared to echocardiography, priority should be given to those atypical cases (such as patients who are males, with atypical ballooning patterns, suspected myocarditis or high cardiac troponin release) in which an alternative diagnosis is more likely (52). Focal TTS pattern represents an intriguing subset of atypical ballooning, in which segmental LV abnormalities more closely resemble those of AMI or myocarditis (30); in these cases, CMR imaging results (especially the presence of ischemic/non-ischemic LGE) must be carefully interpreted according to other clinical findings such as inflammatory biomarkers, red flags for myocarditis, occlusion of small coronary vessels, vasospasm, or coronary dissection. Notwithstanding, the boundary between TTS and other forms of MINOCA can sometimes be quite indistinct; in example, immune check-point inhibitor myocarditis might present with TTS-like transient myocardial dysfunction and absence of LGE at CMR imaging, making differential diagnosis a difficult task (53–56).

In summary, standard CMR techniques can be extremely useful to establish a TTS diagnosis against other forms of MINOCA, moreover, novel tools are emerging to grant quantitative analysis and more accurate prognostic information.

Feature-tracking CMR (FT-CMR) is a novel technique for evaluating cardiac chambers deformation in a similar fashion as ST-TTE does for echocardiography, though basic principles behind the two techniques are quite diverse (57). LV longitudinal, but not radial or circumferential, deformation analysis at FT-CMR aided differentiation between ballooning patterns and provided information regarding long-term outcome, outperforming evaluation of LVEF (58). Moreover, FT-CMR evaluation of LV rotational mechanics revealed transient dyssynchrony, more pronounced in the vulnerable subset of patients with stressful triggers, comorbidities and higher mortality risk (59). Acute phase left atrial functional impairment as assessed by FT-CMR is associated with long-term mortality, even when accounting for traditional cardiovascular risk factors and LVEF (60). This finding reiterates the view of TTS as causing global myocardium involvement, even beyond areas of visually assessed abnormal wall motion.

Recently developed CMR mapping sequences allow a parametric quantification of interstitial expansion in the myocardium, with signal intensity mainly depending on extracellular water (T2 mapping) as well as fibrosis and infiltration

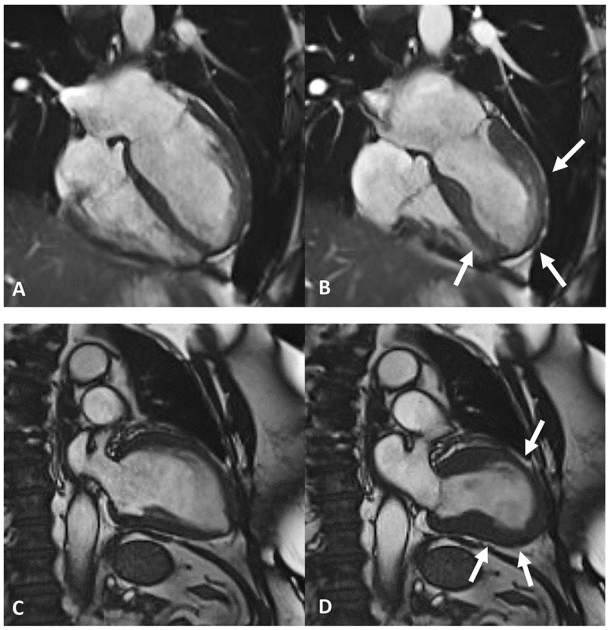

FIGURE 3 | Frames taken from cardiac magnetic resonance cine imaging. Top row, end-diastolic **(A)** and end-systolic **(B)** frames depict apical ballooning of the left ventricles (white arrows in **B**). Bottom row, end-diastolic **(C)** and end-systolic **(D)** frames depict mid-ventricular ballooning of the left ventricles (white arrows in **D**).

(native T1 and ECV). In TTS, marked increase of native T1 and T2 as well as ECV were observed in the acute phase (40, 61–63) (**Figure 4**). Interestingly, T2 shows direct correlation with native T1 and ECV (65), suggesting both a prominent role of extra-cellular myocardial edema in driving acute phase interstitial expansion (66), and a significant influence of myocardial edema on T1 mapping-derived measurements (both native T1 and ECV), as already demonstrated in multiple clinical settings (67, 68). Parametric edema quantification potentially retains prognostic value, since its presence and extent has been linked to both ECG abnormalities and potential TTS complications (69, 70). Higher T2 values within the first few days after the acute event were found in TTS patients with delayed recovery (62), as well as in those with lower LVEF at presentation. Notwithstanding, data on mortality are still lacking in this context, given the limited sample size of current CMR mapping studies in TTS.

In recovered TTS patients, native T1 has been described as persistently elevated when compared to that observed in a matched control group, even more than 1 year after the acute event (40). This finding was accompanied by impaired cardiac deformation (despite preserved LVEF), higher natriuretic peptide level and a persisting cardiac limitation observed on exercise testing at cardiopulmonary stress test, pointing toward subtle long-term non-transitory TTS related abnormalities. Moreover, magnetic resonance imaging including ultrasmall superparamagnetic particles of iron oxide enhancement showed signs of ongoing low-grade inflammation in the chronic phase (71). Further studies are needed to evaluate prognostic relevance of these persistent abnormalities.

Computed Tomography

Coronary computed tomography (CCT) is a non-invasive morphologic evaluation of the coronary tree, with an expanding role in the evaluation of patients with suspected coronary artery disease. In TTS presenting without ST-elevation at ECG, it can be reliably used in the acute phase to rule-out AMI (72, 73), also allowing a more accurate detection of coronary artery course abnormalities, such as myocardial bridging, quite common in TTS (73, 74). Some patients with TTS, especially those without an ST-elevation at presentation, with increased frailty and high comorbidity burden might benefit from CCT in order to avoid invasive procedures such as coronary angiography; in these cases, CCT can help confirming the diagnosis and providing a non-invasive assessment of bystander CAD that might be present even in TTS. Of note, this constitutes an important negative prognostic marker in TTS (50), whose identification can lead to significant changes in the therapeutic management such as more aggressive cholesterol treatment as well as long-term anti-aggregation.

When compared to matched control subjects, TTS patients were found to have increased peri-coronary fat attenuation index (pFAi), a measure associated with coronary artery inflammation (75). pFAi showed to be a risk factor for developing adverse cardiovascular events in the general population with suspected coronary artery disease (76). The easy evaluation of this measure from standard coronary computed tomography images makes it attractive to further investigate its potential association with outcome in TTS.

Nuclear Imaging

Single photon emission computed tomography (SPECT) with 201-thallium chloride has been used to investigate myocardial perfusion in TTS with conflicting results. Some studies reported a mild reduction of perfusion limited to the dis/akinetic segments in the acute phase, while others reported normal perfusion (77–80). Cardiac nuclear imaging was mostly used to investigate cardiac adrenergic function by SPECT with meta-iodobenzylguanidine (MIBG); a severe and persistent uptake defect was demonstrated in TTS patients, despite rapid normalization of myocardial perfusion, which suggested persistence of myocardial sympathetic dysfunction (81–84). Additionally, nuclear imaging may also investigate myocardial metabolism, and both SPECT using 123-I-β-methyl-iodophenyl pentadecanoic acid (which reflects fatty-acid metabolism) and positron emission tomography (PET) using 18-F-flourodeoxyglucose (which reflect glucose utilization) have shown persistently reduced metabolic activity in the impaired regions in TTS (80, 85–88).

However, up today, almost all nuclear imaging studies have been performed mainly for research purposes, while prognostic data are scarce. A recent study in a cohort of 90 TTS patients demonstrated that an extensive defect of 123-I-MIBG scintigraphy uptake appears to be associated with a higher rate of in-hospital complications (89). Patients

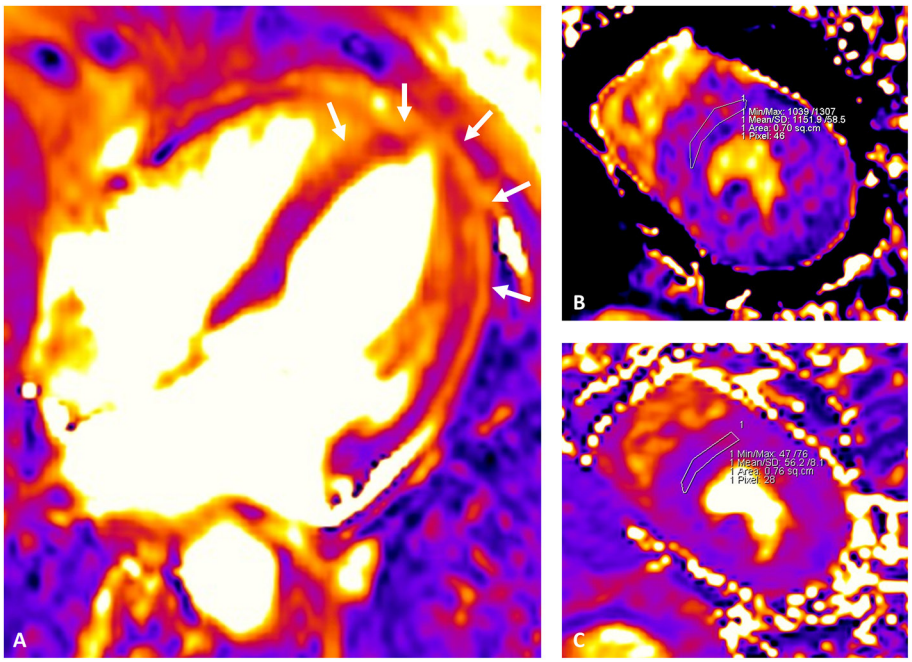

FIGURE 4 | Cardiac magnetic resonance mapping images depicting myocardial edema in the acute phase of TTS. Mid-apical circumferential edema of the left ventricle is visualized as areas of higher intensity from the T2 mapping image (white arrows in **A**). Parametric quantification of native T1 and T2 values is better performed from the mid short-axis view by drawing a conservative region of interest (ROI) within the interventricular septum. Native T1 (MOLLI) **(B)** and T2 **(C)** shows a parallel increase at 1,152 and 56 ms, respectively. Extra-cellular volume (ECV) fraction was calculated from native and post-contrast T1 mapping images (mid-slice, short-axis, interventricular septum ROI) and hematocrit level as described in the literature (64), resulting elevated at 31%. The examination was performed with a 1.5 T scanner (Siemens Aera, Erlangen, Germany); in-center upper reference of normality for the sequence and vendor used are as follow: native T1 995 ms; native T2 49 ms, ECV 26%.

with delayed improvement in LV function had significantly higher levels of catecholamine, higher washout rate in 123-I-MIBG and higher in-hospital complications. Consistently, it has been hypothesized that hyperactivation of autonomic nervous system and higher levels of norepinephrine may induce acute LV outflow obstruction and increased ventricular afterload, as well as elicit ventricular arrhythmias and subsequent sudden cardiac death (90, 91). Increased autonomic activity could also lead to delayed LV function recovery, which may be associated with complications due to heart failure (89). Hence, a severe defect of 123-I-MIBG scintigraphy uptake during the acute phase of TTS may identify patients at higher risk for in-hospital complications, while slower recovery of 123-I-MIBG uptake may identify those at a higher risk for TTS recurrence or for a worse long-term outcome.

Brain-Heart Axis

Both nuclear and non-nuclear imaging modalities have been used to investigate the brain-heart axis in TTS. The precise pathophysiological mechanisms of TTS are incompletely understood but there is considerable evidence that sympathetic stimulation is central to its pathogenesis (3), thus an underlying link between the brain and heart has long been proposed. Specifically, stress can activate the sympathetic nervous system and lead to a complex pathophysiologic cascade, including catecholamine toxicity, abnormal myocardial perfusion, myocardial stunning, and endothelial dysfunction (3).

The response to stressors is governed by an ensemble of neural structures, such as the limbic system (the amygdala, the cingulate gyrus, the hippocampus, the insula, etc.), the ventromedial prefrontal cortex and the brainstem. Recently, increasing interest has been directed toward the involvement of the brain–heart axis in in the pathophysiology of TTS. In 2014, Suzuki et al. first documented brain activation in three patients with TTS examining cerebral blood flow with single photon-emission computed tomography (SPECT). In the acute phase, the researchers observed a marked increase in brain activity in areas linked to abnormal stress-induced sympathetic arousal (brainstem, hippocampus, and basal ganglia). Furthermore, brain activation remained to some extent in the chronic phase, after full recovery of cardiac wall motion (92).

Later functional magnetic resonance imaging studies demonstrated structural alterations in the limbic networks of TTS patients during the acute (93) and chronic phases (94), while increased connectivity, in a network that included the left amygdala and the right insula, was shown after exposing patients with previous TTS to a local stress (cold) (95). Reduced functional connectivity in the limbic systems of a population of

TABLE 3 | Table summarizing studies on TTS genetic markers.

Protein name	SNP	Protein variation	Effect	Clinical outcomes
β1 adrenergic receptor	rs1801253	Arg389Gly	Gain of function	More frequently found in TTS patients No significant difference between TTS and healthy controls
β2 adrenergic receptor	rs1042714	Gln27Glu	Resistance to downregulation	More frequently found in healthy controls
Bcl2-associated athanogene 3 (BAG3)	rs8946	3' UTR	Altered cellular response to epinephrine	More frequently found in TTS patients
Estrogen receptor 1	rs2234693	–	unknown	Higher risk of TTS development in carriers

15 female patients with previous TTS compared to healthy age- and gender-matched controls (96).

All of these studies investigated brain alterations in TTS patients after the acute event.

The study by Radfar et al. is the first to assess cerebral activity prior to the onset of TTS. The amygdala activity using [18F] fluorodeoxyglucose positron emission tomography/computed tomography (18F-FDGPET/CT) was measured retrospectively in 104 patients who underwent clinical 18F-FDG-PET/CT imaging, including 41 who subsequently developed TTS and 63 matched controls. Patients with subsequent TTS had higher baseline amygdala activity and, among the patients who developed TTS, those with higher amygdala activity developed TTS about 2 years earlier compared with those with lower level of amygdala activity (97).

These neuroimaging findings demonstrate structural and functional alterations of stress-related brain networks in patients with TTS even before the acute event, suggesting long-lasting psychological stress. Chronically heightened stress-associated neural activity may hypothetically induce an individual to react to subsequent stressors with a more vigorous neurophysiological response, thus increasing TTS risk (97). Consequently "heart-brain axis" could represent a potential target to reduce TTS risk.

New neuroimaging techniques could be useful in identifying patients at high risk of TTS recurrence, suggesting a longer follow-up and the implementation of both pharmacological and non-pharmacological behavioral therapy (i.e., stress reduction).

However, additional randomized prospective trials and new interdisciplinary approaches are required to further investigate the role of the brain-heart axis in the pathogenesis and prognosis of TTS.

Genetic Markers

Table 3 summarizes the main results from studies on TTS genetic markers. Both familial (98, 99) and recurrent cases (24, 100) of TTS have been described, suggesting a possible influence of the genetic background in the pathogenesis of the syndrome. Single nucleotide polymorphisms (SNPs) belonging to both adrenergic pathway and estrogen receptors genes have been related to higher predisposition for developing TTS. One study reported the association between the Arg389Gly substitution within the adrenergic receptor B1 and TTS occurrence (101). However, these data were not confirmed by other reports (102–104). On the contrary, the Gln27Glu substitution within the adrenergic receptor B2 was observed more frequently in healthy controls than in TTS patients (101). SNPs linked to TTS involve the regulatory function of the anti-apoptotic protein Bcl-2-associated athanogene 3 gene, which likely contributes to myocyte stress resistance (105), and the rs2234693 within the estrogen receptor 1 gene which has been associated with higher risk of TTS occurrence (106). However, all mentioned studies are limited by a gene-target approach and an incomplete analysis of the whole adrenergic system pathway. Only a single study performed a whole-exome sequencing for genes related to catecholamines and adrenergic signaling in 28 TTS patients, and revealed no difference in the allelic frequencies between TTS patients and controls (107).

A relatively larger genome-wide association study reported findings from 96 TTS patients (108). Several promising candidate loci were identified, mostly linked to traits as psychiatric disorders, blood pressure, thyroid disease and cancer, further highlighting the role of comorbidities in the genesis of TTS (109).

In summary, current data on the genetic features of TTS only suggest a genetic etiology of this pathological condition. However, we are becoming aware that, whereas environmental triggers and concomitant comorbidities are pivotal in TTS development, the genetic heterogeneity and a potential polygenic predisposition may also play a contributory role mainly by determining the dysregulation of the adrenergic system. Larger cohorts are required for a better evaluation of the impact of genetic background on TTS occurrence and prognosis.

Clinical Perspective

Despite similar long-term outcomes, the nature of adverse events in AMI and TTS is different. Indeed, TTS is featured by mainly non-cardiovascular mortality (19, 21, 110–112), even during the acute phase characterized by different degrees of LV dysfunction (11). However, cardiovascular assessment still provides fundamental clinical and prognostic information in TTS, both in the short and in the long-term. Indeed, a higher cardiac involvement as detected by imaging modalities or cardiac biomarkers [especially natriuretic peptides, (113)] is associated with worse prognosis, even after recovery of left ventricular ejection fraction. In this view, the prognostic power of cardiac imaging in TTS should be interpreted as the ability of identifying both the cardiovascular consequences of TTS and those underlying pre-existing characteristics of vulnerable

phenotypes prone to heart failure. In this perspective, broader acute cardiac dysfunction or long-term abnormalities might just be a proxy of a wider comorbid state, which is actually the condition driving prognosis (114, 115). Advanced cardiac imaging might still provide reliable prognostic information (116) and should be considered, if available, in every patients with previous TTS even though appropriate therapies to improve outcome in these patients remain to be identified. Gaps in knowledge remain as to whether patients with previous TTS, recovered left ventricular ejection fraction, and persisting subtle cardiac abnormalities might benefit from specific therapies. Observational data indicate a lower long-term mortality in TTS patients treated with angiotensin-converting enzyme inhibitors (10). To this extent, a prospective ongoing trial is currently investigating the effect of N-Acetylcysteine and ramipril on edema resolution at CMR and longitudinal strain improvement in patients with acute TTS (117).

Genetic investigations, rather than cardiac imaging, may play an important role in risk stratification in the particular setting of the predisposition to TTS recurrence. However, where clinical implementation of genetic testing implies a multidisciplinary approach with genetic counseling and ethical considerations (118), currently available evidence still limits its applicability in the clinical field.

CONCLUSIONS

Patients with TTS may benefit from advanced cardiovascular imaging tools offering unique information to assist in short- and mid-term risk stratification, well beyond traditional assessment of left ventricular ejection fraction. Due to the limited robust evidence, genetic evaluation does not currently provide significant advantages in guiding the clinical management. Hopefully, future studies aimed at better characterizing the genetic background of TTS may identify useful markers that could assist in predicting disease recurrences and help in familial screening.

AUTHOR CONTRIBUTIONS

LA and LL designed the study. LA, LL, CA, MS, and GT drafted the manuscript. All authors provided relevant comments, revised the draft, and approved the final version of the manuscript.

REFERENCES

1. Lyon AR, Bossone E, Schneider B, Sechtem U, Citro R, Underwood SR, et al. Current state of knowledge on takotsubo syndrome: a Position Statement from the Taskforce on Takotsubo Syndrome of the Heart Failure Association of the European Society of Cardiology: current state of knowledge on Takotsubo syndrome. *Eur J Heart Fail.* (2016) 18:8–27. doi: 10.1002/ejhf.424
2. Santoro F, Núñez Gil IJ, Stiermaier T, El-Battrawy I, Guerra F, Novo G, et al. Assessment of the German and Italian Stress cardiomyopathy score for risk stratification for in-hospital complications in patients with Takotsubo syndrome. *JAMA Cardiol.* (2019) 4:892. doi: 10.1001/jamacardio.2019.2597
3. Ghadri J-R, Wittstein IS, Prasad A, Sharkey S, Dote K, Akashi YJ, et al. International expert consensus document on takotsubo syndrome (part i): clinical characteristics, diagnostic criteria, and pathophysiology. *Eur Heart J.* (2018) 39:2032–46. doi: 10.1093/eurheartj/ehy076
4. Dias A, Núñez Gil IJ, Santoro F, Madias JE, Pelliccia F, Brunetti ND, et al. Takotsubo syndrome: state-of-the-art review by an expert panel – Part 1. *Cardiovasc Revasc Med.* (2019) 20:70–9. doi: 10.1016/j.carrev.2018.11.015
5. Khera R, Light-McGroary K, Zahr F, Horwitz PA, Girotra S. Trends in hospitalization for takotsubo cardiomyopathy in the United States. *Am Heart J.* (2016) 172:53–63. doi: 10.1016/j.ahj.2015.10.022
6. Elesber AA, Prasad A, Lennon RJ, Wright RS, Lerman A, Rihal CS. Four-year recurrence rate and prognosis of the apical ballooning syndrome. *J Am Coll Cardiol.* (2007) 50:448–52. doi: 10.1016/j.jacc.2007.03.050
7. Cacciotti L, Passaseo I, Marazzi G, Camastra G, Campolongo G, Beni S, et al. Observational study on Takotsubo-like cardiomyopathy: clinical features, diagnosis, prognosis and follow-up. *BMJ Open.* (2012) 2:e001165. doi: 10.1136/bmjopen-2012-001165
8. Ghadri JR, Kato K, Cammann VL, Gili S, Jurisic S, Di Vece D, et al. Long-term prognosis of patients with takotsubo syndrome. *J Am Coll Cardiol.* (2018) 72:874–82. doi: 10.1016/j.jacc.2018.06.016
9. Núñez-Gil IJ, Almendro-Delia M, Andrés M, Sionis A, Martin A, Bastante T, et al. Secondary forms of Takotsubo cardiomyopathy: a whole different prognosis. *Eur Heart J Acute Cardiovasc Care.* (2016) 5:308–16. doi: 10.1177/2048872615589512
10. Templin C, Ghadri JR, Diekmann J, Napp LC, Bataiosu DR, Jaguszewski M, et al. Clinical features and outcomes of takotsubo (stress) cardiomyopathy. *N Engl J Med.* (2015) 373:929–38. doi: 10.1056/NEJMoa1406761
11. Almendro-Delia M, Núñez-Gil IJ, Lobo M, Andrés M, Vedia O, Sionis A, et al. Short- and long-term prognostic relevance of cardiogenic shock in takotsubo syndrome. *JACC Heart Fail.* (2018) 6:928–36. doi: 10.1016/j.jchf.2018.05.015
12. Santoro F, Ferraretti A, Ieva R, Musaico F, Fanelli M, Tarantino N, et al. Renal impairment and outcome in patients with takotsubo cardiomyopathy. *Am J Emerg Med.* (2016) 34:548–52. doi: 10.1016/j.ajem.2015.12.065
13. Santoro F, Mallardi A, Leopizzi A, Vitale E, Rawish E, Stiermaier T, et al. Current knowledge and future challenges in takotsubo syndrome: part 2-treatment and prognosis. *J Clin Med.* (2021) 10: doi: 10.3390/jcm10030468
14. Arcari L, Limite LR, Cacciotti L, Sclafani M, Russo D, Passaseo I, et al. Admission heart rate and in-hospital course of patients with Takotsubo syndrome. *Int J Cardiol.* (2018) 273:15–21. doi: 10.1016/j.ijcard.2018.07.145
15. Schneider B, Athanasiadis A, Schwab J, Pistner W, Gottwald U, Schoeller R, et al. Complications in the clinical course of tako-tsubo cardiomyopathy. *Int J Cardiol.* (2014) 176:199–205. doi: 10.1016/j.ijcard.2014.07.002
16. Sharkey SW, Windenburg DC, Lesser JR, Maron MS, Hauser RG, Lesser JN, et al. Natural history and expansive clinical profile of stress (tako-tsubo) cardiomyopathy. *J Am Coll Cardiol.* (2010) 55:333–41. doi: 10.1016/j.jacc.2009.08.057
17. El-Battrawy I, Santoro F, Stiermaier T, Möller C, Guastafierro F, Novo G, et al. Prevalence, management, and outcome of adverse rhythm disorders in takotsubo syndrome: insights from the international multicenter GEIST registry. *Heart Fail Rev.* (2020) 25:505–11. doi: 10.1007/s10741-019-09856-4
18. Santoro F, Stiermaier T, Tarantino N, De Gennaro L, Moeller C, Guastafierro F, et al. Left ventricular thrombi in takotsubo syndrome: incidence, predictors, and management: results from the GEIST (German Italian Stress Cardiomyopathy) registry. *J Am Heart Assoc.* (2017) 6:e006990. doi: 10.1161/JAHA.117.006990
19. Stiermaier T, Moeller C, Oehler K, Desch S, Graf T, Eitel C, et al. Long-term excess mortality in takotsubo cardiomyopathy: predictors, causes and clinical consequences. *Eur J Heart Fail.* (2016) 18:650–6. doi: 10.1002/ejhf.494
20. Redfors B, Vedad R, Angerås O, Råmunddal T, Petursson P, Haraldsson I, et al. Mortality in takotsubo syndrome is similar to mortality in myocardial infarction - a report from the SWEDEHEART registry. *Int J Cardiol.* (2015) 185:282–9. doi: 10.1016/j.ijcard.2015.03.162
21. Scudiero F, Arcari L, Cacciotti L, De Vito E, Marcucci R, Passaseo I, et al. Prognostic relevance of GRACE risk score in

Takotsubo syndrome. *Eur Heart J Acute Cardiovasc Care.* (2020) 9:721–8. doi: 10.1177/2048872619882363
22. Stiermaier T, Santoro F, El-Battrawy I, Möller C, Graf T, Novo G, et al. Prevalence and prognostic impact of diabetes in takotsubo syndrome: insights from the international, multicenter GEIST Registry. *Diabetes Care.* (2018) 41:1084–8. doi: 10.2337/dc17-2609
23. Martín-Demiguel I, Núñez-Gil IJ, Pérez-Castellanos A, Vedia O, Uribarri A, Durán-Cambra A, et al. Prevalence and significance of interatrial block in takotsubo syndrome (from the RETAKO Registry). *Am J Cardiol.* (2019) 123:2039–43. doi: 10.1016/j.amjcard.2019.03.028
24. Arcari L, Cacciotti L, Limite LR, Russo D, Sclafani M, Semeraro R, et al. Clinical characteristics of patients with takotsubo syndrome recurrence: an observational study with long-term follow-up. *Int J Cardiol.* (2021) 329:23–7. doi: 10.1016/j.ijcard.2020.12.047
25. Omerovic E. Takotsubo syndrome: not as benign as once believed. *Eur J Heart Fail.* (2016) 18:657–9. doi: 10.1002/ejhf.555
26. Arcari L, Musumeci MB, Stiermaier T, El-Battrawy I, Möller C, Guerra F, et al. Incidence, determinants and prognostic relevance of dyspnea at admission in patients with Takotsubo syndrome: results from the international multicenter GEIST registry. *Sci Rep.* (2020) 10:13603. doi: 10.1038/s41598-020-70445-9
27. Citro R, Radano I, Parodi G, Di Vece D, Zito C, Novo G, et al. Long-term outcome in patients with Takotsubo syndrome presenting with severely reduced left ventricular ejection fraction. *Eur J Heart Fail.* (2019) 21:781–9. doi: 10.1002/ejhf.1373
28. Stiermaier T, Möller C, Graf T, Eitel C, Desch S, Thiele H, et al. Prognostic usefulness of the ballooning pattern in patients with takotsubo cardiomyopathy. *Am J Cardiol.* (2016) 118:1737–41. doi: 10.1016/j.amjcard.2016.08.055
29. Ghadri JR, Cammann VL, Napp LC, Jurisic S, Diekmann J, Bataiosu DR, et al. Differences in the clinical profile and outcomes of typical and atypical takotsubo syndrome: data from the international takotsubo registry. *JAMA Cardiol.* (2016) 1:335. doi: 10.1001/jamacardio.2016.0225
30. Tini G, Limite LR, Arcari L, Cacciotti L, Russo D, Sclafani M, et al. A systematic review on focal takotsubo syndrome: a not-so-small matter. *Heart Fail Rev.* (2020). doi: 10.1007/s10741-020-09988-y. [Epub ahead of print].
31. Gaede L, Herchenbach A, Tröbs M, Marwan M, Achenbach S. Left ventricular contraction patterns in Takotsubo Syndrome and their correlation with long-term clinical outcome. *IJC Heart Vasc.* (2021) 32:100708. doi: 10.1016/j.ijcha.2020.100708
32. Citro R, Rigo F, Ciampi Q, D'Andrea A, Provenza G, Mirra M, et al. Echocardiographic assessment of regional left ventricular wall motion abnormalities in patients with tako-tsubo cardiomyopathy: comparison with anterior myocardial infarction. *Eur J Echocardiogr J Work Group Echocardiogr Eur Soc Cardiol.* (2011) 12:542–9. doi: 10.1093/ejechocard/jer059
33. Izumo M, Nalawadi S, Shiota M, Das J, Dohad S, Kuwahara E, et al. Mechanisms of acute mitral regurgitation in patients with takotsubo cardiomyopathy: an echocardiographic study. *Circ Cardiovasc Imaging.* (2011) 4:392–8. doi: 10.1161/CIRCIMAGING.110.962845
34. Dias A, Franco E, Rubio M, Bhalla V, Pressman GS, Amanullah S, et al. Usefulness of left ventricular strain analysis in patients with takotsubo syndrome during acute phase. *Echocardiogr Mt Kisco N.* (2018) 35:179–83. doi: 10.1111/echo.13762
35. Heggemann F, Hamm K, Brade J, Streitner F, Doesch C, Papavassiliu T, et al. Right ventricular function quantification in Takotsubo cardiomyopathy using two-dimensional strain echocardiography. *PLoS ONE.* (2014) 9:e103717. doi: 10.1371/journal.pone.0103717
36. Meimoun P, Stracchi V, Boulanger J, Martis S, Botoro T, Zemir H, et al. The left atrial function is transiently impaired in Tako-tsubo cardiomyopathy and associated to in-hospital complications: a prospective study using two-dimensional strain. *Int J Cardiovasc Imaging.* (2020) 36:299–307. doi: 10.1007/s10554-019-01722-6
37. Kim S-A, Jo S-H, Park K-H, Kim H-S, Han S-J, Park W-J. Functional recovery of regional myocardial deformation in patients with takotsubo cardiomyopathy. *J Cardiol.* (2017) 70:68–73. doi: 10.1016/j.jjcc.2016.09.006
38. Schwarz K, Ahearn T, Srinivasan J, Neil CJ, Scally C, Rudd A, et al. Alterations in cardiac deformation, timing of contraction and relaxation, and early myocardial fibrosis accompany the apparent recovery of acute stress-induced (takotsubo) cardiomyopathy: an end to the concept of transience. *J Am Soc Echocardiogr Off Publ Am Soc Echocardiogr.* (2017) 30:745–55. doi: 10.1016/j.echo.2017.03.016
39. Neil CJ, Nguyen TH, Singh K, Raman B, Stansborough J, Dawson D, et al. Relation of delayed recovery of myocardial function after takotsubo cardiomyopathy to subsequent quality of life. *Am J Cardiol.* (2015) 115:1085–9. doi: 10.1016/j.amjcard.2015.01.541
40. Scally C, Rudd A, Mezincescu A, Wilson H, Srivanasan J, Horgan G, et al. Persistent long-term structural, functional, and metabolic changes after stress-induced (takotsubo) cardiomyopathy. *Circulation.* (2018) 137:1039–48. doi: 10.1161/CIRCULATIONAHA.117.031841
41. Sengupta PP, Pedrizzetti G, Kilner PJ, Kheradvar A, Ebbers T, Tonti G, et al. Emerging trends in CV flow visualization. *JACC Cardiovasc Imaging.* (2012) 5:305–16. doi: 10.1016/j.jcmg.2012.01.003
42. Kheradvar A, Houle H, Pedrizzetti G, Tonti G, Belcik T, Ashraf M, et al. Echocardiographic particle image velocimetry: a novel technique for quantification of left ventricular blood vorticity pattern. *J Am Soc Echocardiogr Off Publ Am Soc Echocardiogr.* (2010) 23:86–94. doi: 10.1016/j.echo.2009.09.007
43. Cimino S, Arcari L, Filomena D, Agati L. In the eye of the storm: echocardiographic particle image velocimetry analysis in a patient with takotsubo syndrome. *Echocardiogr Mt Kisco N.* (2020) 37:1312–4. doi: 10.1111/echo.14776
44. Agati L, Cimino S, Tonti G, Cicogna F, Petronilli V, De Luca L, et al. Quantitative analysis of intraventricular blood flow dynamics by echocardiographic particle image velocimetry in patients with acute myocardial infarction at different stages of left ventricular dysfunction. *Eur Heart J Cardiovasc Imaging.* (2014) 15:1203–12. doi: 10.1093/ehjci/jeu106
45. Schulz-Menger J, Bluemke DA, Bremerich J, Flamm SD, Fogel MA, Friedrich MG, et al. Standardized image interpretation and post-processing in cardiovascular magnetic resonance - 2020 update : society for cardiovascular magnetic resonance (SCMR): board of trustees task force on standardized post-processing. *J Cardiovasc Magn Reson Off J Soc Cardiovasc Magn Reson.* (2020) 22:19. doi: 10.1186/s12968-020-00610-6
46. Eitel I, von Knobelsdorff-Brenkenhoff F, Bernhardt P, Carbone I, Muellerleile K, Aldrovandi A, et al. Clinical characteristics and cardiovascular magnetic resonance findings in stress (takotsubo) cardiomyopathy. *JAMA.* (2011) 306:277-86. doi: 10.1001/jama.2011.992
47. Gaikwad N, Butler T, Maxwell R, Shaw E, Strugnell WE, Chan J, et al. Late gadolinium enhancement does occur in Tako-tsubo cardiomyopathy - a quantitative cardiac magnetic resonance and speckle tracking strain study. *Int J Cardiol Heart Vasc.* (2016) 12:68–74. doi: 10.1016/j.ijcha.2016.07.009
48. Naruse Y, Sato A, Kasahara K, Makino K, Sano M, Takeuchi Y, et al. The clinical impact of late gadolinium enhancement in Takotsubo cardiomyopathy: serial analysis of cardiovascular magnetic resonance images. *J Cardiovasc Magn Reson Off J Soc Cardiovasc Magn Reson.* (2011) 13:67. doi: 10.1186/1532-429X-13-67
49. Gunasekara MY, Mezincescu AM, Dawson DK. An update on cardiac magnetic resonance imaging in takotsubo cardiomyopathy. *Curr Cardiovasc Imaging Rep.* (2020) 13:17. doi: 10.1007/s12410-020-09536-0
50. Napp LC, Cammann VL, Jaguszewski M, Szawan KA, Wischnewsky M, Gili S, et al. Coexistence and outcome of coronary artery disease in Takotsubo syndrome. *Eur Heart J.* (2020) 41:3255–68. doi: 10.1093/eurheartj/ehaa210
51. Pathik B, Raman B, Mohd Amin NH, Mahadavan D, Rajendran S, McGavigan AD, et al. Troponin-positive chest pain with unobstructed coronary arteries: incremental diagnostic value of cardiovascular magnetic resonance imaging. *Eur Heart J Cardiovasc Imaging.* (2016) 17:1146–52. doi: 10.1093/ehjci/jev289
52. Arcari L, Limite LR, Russo D, Sclafani M, Volpe M, Autore C, et al. P117Cardiac magnetic resonance imaging to solve the diagnostic dilemma in two cases of MINOCA: different sides of the same coin. *Eur Heart J Cardiovasc Imaging.* (2019) 20:jez110.015. doi: 10.1093/ehjci/jez110.015
53. Thavendiranathan P, Zhang L, Zafar A, Drobni ZD, Mahmood SS, Cabral M, et al. Myocardial T1 and T2 mapping by magnetic resonance in patients with immune checkpoint inhibitor–associated myocarditis. *J Am Coll Cardiol.* (2021) 77:1503–16. doi: 10.1016/j.jacc.2021.01.050

54. Escudier M, Cautela J, Malissen N, Ancedy Y, Orabona M, Pinto J, et al. Clinical features, management, and outcomes of immune checkpoint inhibitor–related cardiotoxicity. *Circulation.* (2017) 136:2085–7. doi: 10.1161/CIRCULATIONAHA.117.030571
55. Camastra G, Arcari L, Ciolina F, Danti M, Cacciotti L. Cardiac magnetic resonance imaging of transient myocardial dysfunction in a patient treated with checkpoint-targeted immunotherapy. *Eur J Cancer.* (2021) 144:389–91. doi: 10.1016/j.ejca.2020.11.026
56. Spallarossa P, Sarocchi M, Tini G, Arboscello E, Toma M, Ameri P, et al. How to monitor cardiac complications of immune checkpoint inhibitor therapy. *Front Pharmacol.* (2020) 11:972. doi: 10.3389/fphar.2020.00972
57. Pedrizzetti G, Claus P, Kilner PJ, Nagel E. Principles of cardiovascular magnetic resonance feature tracking and echocardiographic speckle tracking for informed clinical use. *J Cardiovasc Magn Reson Off J Soc Cardiovasc Magn Reson.* (2016) 18:51. doi: 10.1186/s12968-016-0269-7
58. Stiermaier T, Lange T, Chiribiri A, Möller C, Graf T, Villnow C, et al. Left ventricular myocardial deformation in Takotsubo syndrome: a cardiovascular magnetic resonance myocardial feature tracking study. *Eur Radiol.* (2018) 28:5160–70. doi: 10.1007/s00330-018-5475-2
59. Backhaus SJ, Stiermaier T, Lange T, Chiribiri A, Lamata P, Uhlig J, et al. Temporal changes within mechanical dyssynchrony and rotational mechanics in Takotsubo syndrome: a cardiovascular magnetic resonance imaging study. *Int J Cardiol.* (2018) 273:256–62. doi: 10.1016/j.ijcard.2018.04.088
60. Backhaus SJ, Stiermaier T, Lange T, Chiribiri A, Uhlig J, Freund A, et al. Atrial mechanics and their prognostic impact in Takotsubo syndrome: a cardiovascular magnetic resonance imaging study. *Eur Heart J Cardiovasc Imaging.* (2019) 20:1059–69. doi: 10.1093/ehjci/jey219
61. Dabir D, Luetkens J, Kuetting DLR, Feisst A, Isaak A, Schild HH, et al. Cardiac magnetic resonance including parametric mapping in acute Takotsubo syndrome: preliminary findings. *Eur J Radiol.* (2019) 113:217–24. doi: 10.1016/j.ejrad.2019.02.026
62. Aikawa Y, Noguchi T, Morita Y, Tateishi E, Kono A, Miura H, et al. Clinical impact of native T1 mapping for detecting myocardial impairment in takotsubo cardiomyopathy. *Eur Heart J Cardiovasc Imaging.* (2019) 20:1147–55. doi: 10.1093/ehjci/jez034
63. Vermes E, Berradja N, Saab I, Genet T, Bertrand P, Pucheux J, et al. Cardiac magnetic resonance for assessment of cardiac involvement in Takotsubo syndrome: do we still need contrast administration? *Int J Cardiol.* (2020) 308:93–5. doi: 10.1016/j.ijcard.2020.03.039
64. Haaf P, Garg P, Messroghli DR, Broadbent DA, Greenwood JP, Plein S. Cardiac T1 mapping and extracellular volume (ECV) in clinical practice: a comprehensive review. *J Cardiovasc Magn Reson.* (2017) 18:89. doi: 10.1186/s12968-016-0308-4
65. Vermes E, Bertrand P, Saab I, Berradja N. Response to "cardiac magnetic resonance in takotsubo syndrome: welcome to mapping, but long live late gadolinium enhancement." *Int J Cardiol.* (2020) 319:36. doi: 10.1016/j.ijcard.2020.06.056
66. Arcari L, Cacciotti L, Camastra G, Ciolina F, Danti M, Sbarbati S, et al. Cardiac magnetic resonance in Takotsubo syndrome: welcome to mapping, but long live late gadolinium enhancement. *Int J Cardiol.* (2020) 319:150. doi: 10.1016/j.ijcard.2020.05.046
67. Child N, Suna G, Dabir D, Yap M-L, Rogers T, Kathirgamanathan M, et al. Comparison of MOLLI, shMOLLLI, and SASHA in discrimination between health and disease and relationship with histologically derived collagen volume fraction. *Eur Heart J Cardiovasc Imaging.* (2018) 19:768–76. doi: 10.1093/ehjci/jex309
68. Arcari L, Hinojar R, Engel J, Freiwald T, Platschek S, Zainal H, et al. Native T1 and T2 provide distinctive signatures in hypertrophic cardiac conditions - comparison of uremic, hypertensive and hypertrophic cardiomyopathy. *Int J Cardiol.* (2020) 306:102–8. doi: 10.1016/j.ijcard.2020.03.002
69. Migliore F, Zorzi A, Marra MP, Basso C, Corbetti F, De Lazzari M, et al. Myocardial edema underlies dynamic T-wave inversion (Wellens' ECG pattern) in patients with reversible left ventricular dysfunction. *Heart Rhythm.* (2011) 8:1629–34. doi: 10.1016/j.hrthm.2011.04.035
70. Brunetti ND, D'Arienzo G, Sai R, Pellegrino PL, Ziccardi L, Santoro F, et al. Delayed ventricular pacing failure and correlations between pacing thresholds, left ventricular ejection fraction, and QTc values in a male with Takotsubo cardiomyopathy. *Clin Cardiol.* (2018) 41:1487–90. doi: 10.1002/clc.23082
71. Scally C, Abbas H, Ahearn T, Srinivasan J, Mezincescu A, Rudd A, et al. Myocardial and systemic inflammation in acute stress-induced (takotsubo) cardiomyopathy. *Circulation.* (2019) 139:1581–92. doi: 10.1161/CIRCULATIONAHA.118.037975
72. Ghadri J-R, Wittstein IS, Prasad A, Sharkey S, Dote K, Akashi YJ, et al. International expert consensus document on takotsubo syndrome (part ii): diagnostic workup, outcome, and management. *Eur Heart J.* (2018) 39:2047–62. doi: 10.1093/eurheartj/ehy077
73. Dias A, Núñez Gil IJ, Santoro F, Madias JE, Pelliccia F, Brunetti ND, et al. Takotsubo syndrome: state-of-the-art review by an expert panel – Part 2. *Cardiovasc Revasc Med.* (2019) 20:153–66. doi: 10.1016/j.carrev.2018.11.016
74. Arcari L, Limite LR, Cacciotti L, Alonzo A, Musumeci MB, Passaseo I, et al. Tortuosity, recurrent segments, and bridging of the epicardial coronary arteries in patients with the takotsubo syndrome. *Am J Cardiol.* (2017) 119:243–8. doi: 10.1016/j.amjcard.2016.09.055
75. Gaibazzi N, Martini C, Botti A, Pinazzi A, Bottazzi B, Palumbo AA. Coronary inflammation by computed tomography pericoronary fat attenuation in MINOCA and Tako-Tsubo Syndrome. *J Am Heart Assoc.* (2019) 8:e013235. doi: 10.1161/JAHA.119.013235
76. Oikonomou EK, Marwan M, Desai MY, Mancio J, Alashi A, Hutt Centeno E, et al. Non-invasive detection of coronary inflammation using computed tomography and prediction of residual cardiovascular risk (the CRISP CT study): a post-hoc analysis of prospective outcome data. *Lancet Lond Engl.* (2018) 392:929–39. doi: 10.1016/S0140-6736(18)31114-0
77. Ito K, Sugihara H, Kawasaki T, Yuba T, Doue T, Tanabe T, et al. Assessment of ampulla (Takotsubo) cardiomyopathy with coronary angiography, two-dimensional echocardiography and 99mTc-tetrofosmin myocardial single photon emission computed tomography. *Ann Nucl Med.* (2001) 15:351–5. doi: 10.1007/BF02988242
78. Abe Y, Kondo M, Matsuoka R, Araki M, Dohyama K, Tanio H. Assessment of clinical features in transient left ventricular apical ballooning. *J Am Coll Cardiol.* (2003) 41:737–42. doi: 10.1016/S0735-1097(02)02925-X
79. Ghadri JR, Dougoud S, Maier W, Kaufmann PA, Gaemperli O, Prasad A, et al. A PET/CT-follow-up imaging study to differentiate takotsubo cardiomyopathy from acute myocardial infarction. *Int J Cardiovasc Imaging.* (2014) 30:207–9. doi: 10.1007/s10554-013-0311-x
80. Cimarelli S, Imperiale A, Ben-Sellem D, Rischner J, Detour J, Morel O, et al. Nuclear medicine imaging of takotsubo cardiomyopathy: typical form and midventricular ballooning syndrome. *J Nucl Cardiol Off Publ Am Soc Nucl Cardiol.* (2008) 15:137–41. doi: 10.1007/BF02976903
81. Owa M, Aizawa K, Urasawa N, Ichinose H, Yamamoto K, Karasawa K, et al. Emotional stress-induced "ampulla cardiomyopathy": discrepancy between the metabolic and sympathetic innervation imaging performed during the recovery course. *Jpn Circ J.* (2001) 65:349–52. doi: 10.1253/jcj.65.349
82. Cimarelli S, Sauer F, Morel O, Ohlmann P, Constantinesco A, Imperiale A. Transient left ventricular dysfunction syndrome: patho-physiological bases through nuclear medicine imaging. *Int J Cardiol.* (2010) 144:212–8. doi: 10.1016/j.ijcard.2009.04.025
83. Verberne HJ, van der Heijden DJ, van Eck-Smit BLF, Somsen GA. Persisting myocardial sympathetic dysfunction in takotsubo cardiomyopathy. *J Nucl Cardiol Off Publ Am Soc Nucl Cardiol.* (2009) 16:321–4. doi: 10.1007/s12350-008-9017-1
84. Sestini S, Pestelli F, Leoncini M, Bellandi F, Mazzeo C, Mansi L, et al. The natural history of takotsubo syndrome: a two-year follow-up study with myocardial sympathetic and perfusion G-SPECT imaging. *Eur J Nucl Med Mol Imaging.* (2017) 44:267–83. doi: 10.1007/s00259-016-3575-2
85. Bybee KA, Murphy J, Prasad A, Wright RS, Lerman A, Rihal CS, et al. Acute impairment of regional myocardial glucose uptake in the apical ballooning (takotsubo) syndrome. *J Nucl Cardiol Off Publ Am Soc Nucl Cardiol.* (2006) 13:244–50. doi: 10.1007/BF02971249
86. Obunai K, Misra D, Van Tosh A, Bergmann SR. Metabolic evidence of myocardial stunning in takotsubo cardiomyopathy: a positron emission tomography study. *J Nucl Cardiol Off Publ Am Soc Nucl Cardiol.* (2005) 12:742–4. doi: 10.1016/j.nuclcard.2005.06.087
87. Yoshida T, Hibino T, Kako N, Murai S, Oguri M, Kato K, et al. A pathophysiologic study of tako-tsubo cardiomyopathy with F-18

fluorodeoxyglucose positron emission tomography. *Eur Heart J.* (2007) 28:2598–604. doi: 10.1093/eurheartj/ehm401
88. Christensen TE, Bang LE, Holmvang L, Ghotbi AA, Lassen ML, Andersen F, et al. Cardiac ^{99}mTc sestamibi SPECT and ^{18}F FDG PET as viability markers in Takotsubo cardiomyopathy. *Int J Cardiovasc Imaging.* (2014) 30:1407–16. doi: 10.1007/s10554-014-0453-5
89. Matsuura T, Ueno M, Iwanaga Y, Miyazaki S. Importance of sympathetic nervous system activity during left ventricular functional recovery and its association with in-hospital complications in Takotsubo syndrome. *Heart Vessels.* (2019) 34:1317–24. doi: 10.1007/s00380-019-01359-4
90. Fallavollita JA, Heavey BM, Luisi AJ, Michalek SM, Baldwa S, Mashtare TL, et al. Regional myocardial sympathetic denervation predicts the risk of sudden cardiac arrest in ischemic cardiomyopathy. *J Am Coll Cardiol.* (2014) 63:141–9. doi: 10.1016/j.jacc.2013.07.096
91. Malhotra S, Fernandez SF, Fallavollita JA, Canty JM. Prognostic significance of imaging myocardial sympathetic innervation. *Curr Cardiol Rep.* (2015) 17:62. doi: 10.1007/s11886-015-0613-9
92. Suzuki H, Matsumoto Y, Kaneta T, Sugimura K, Takahashi J, Fukumoto Y, et al. Evidence for brain activation in patients with takotsubo cardiomyopathy. *Circ J Off J Jpn Circ Soc.* (2014) 78:256–8. doi: 10.1253/circj.CJ-13-1276
93. Dichtl W, Tuovinen N, Barbieri F, Adukauskaite A, Senoner T, Rubatscher A, et al. Functional neuroimaging in the acute phase of Takotsubo syndrome: volumetric and functional changes of the right insular cortex. *Clin Res Cardiol.* (2020) 109:1107–13. doi: 10.1007/s00392-020-01602-3
94. Hiestand T, Hänggi J, Klein C, Topka MS, Jaguszewski M, Ghadri JR, et al. Takotsubo syndrome associated with structural brain alterations of the limbic system. *J Am Coll Cardiol.* (2018) 71:809–11. doi: 10.1016/j.jacc.2017.12.022
95. Silva AR, Magalhães R, Arantes C, Moreira PS, Rodrigues M, Marques P, et al. Brain functional connectivity is altered in patients with Takotsubo Syndrome. *Sci Rep.* (2019) 9:4187. doi: 10.1038/s41598-019-40695-3
96. Templin C, Hänggi J, Klein C, Topka MS, Hiestand T, Levinson RA, et al. Altered limbic and autonomic processing supports brain-heart axis in Takotsubo syndrome. *Eur Heart J.* (2019) 40:1183–7. doi: 10.1093/eurheartj/ehz068
97. Radfar A, Abohashem S, Osborne MT, Wang Y, Dar T, Hassan MZO, et al. Stress-associated neurobiological activity associates with the risk for and timing of subsequent Takotsubo syndrome. *Eur Heart J.* (2021) 42:1898–1908. doi: 10.1093/eurheartj/ehab029
98. Kumar G, Holmes DR, Prasad A. "Familial" apical ballooning syndrome (Takotsubo cardiomyopathy). *Int J Cardiol.* (2010) 144:444–5. doi: 10.1016/j.ijcard.2009.03.078
99. Musumeci B, Saponaro A, Pagannone E, Proietti G, Mastromarino V, Conti E, et al. Simultaneous Takotsubo syndrome in two sisters. *Int J Cardiol.* (2013) 165:e49-50. doi: 10.1016/j.ijcard.2012.11.016
100. Gogas BD, Antoniadis AG, Zacharoulis AA, Kolokathis F, Lekakis J, Kremastinos DT. Recurrent apical ballooning syndrome "The masquerading acute cardiac syndrome." *Int J Cardiol.* (2011) 150:e17-9. doi: 10.1016/j.ijcard.2009.07.038
101. Vriz O, Minisini R, Citro R, Guerra V, Zito C, De Luca G, et al. Analysis of beta1 and beta2-adrenergic receptors polymorphism in patients with apical ballooning cardiomyopathy. *Acta Cardiol.* (2011) 66:787–90. doi: 10.1080/AC.66.6.2136964
102. Figtree GA, Bagnall RD, Abdulla I, Buchholz S, Galougahi KK, Yan W, et al. No association of G-protein-coupled receptor kinase 5 or β-adrenergic receptor polymorphisms with Takotsubo cardiomyopathy in a large Australian cohort. *Eur J Heart Fail.* (2013) 15:730–3. doi: 10.1093/eurjhf/hft040
103. Sharkey SW, Maron BJ, Nelson P, Parpart M, Maron MS, Bristow MR. Adrenergic receptor polymorphisms in patients with stress (tako-tsubo) cardiomyopathy. *J Cardiol.* (2009) 53:53–7. doi: 10.1016/j.jjcc.2008.08.006
104. Mattsson E, Saliba-Gustafsson P, Ehrenborg E, Tornvall P. Lack of genetic susceptibility in takotsubo cardiomyopathy: a case-control study. *BMC Med Genet.* (2018) 19:39. doi: 10.1186/s12881-018-0544-6
105. d'Avenia M, Citro R, De Marco M, Veronese A, Rosati A, Visone R, et al. A novel miR-371a-5p-mediated pathway, leading to BAG3 upregulation in cardiomyocytes in response to epinephrine, is lost in Takotsubo cardiomyopathy. *Cell Death Dis.* (2015) 6:e1948. doi: 10.1038/cddis.2015.280
106. Pizzino G, Bitto A, Crea P, Khandheria B, Vriz O, Carerj S, et al. Takotsubo syndrome and estrogen receptor genes: partners in crime? *J Cardiovasc Med Hagerstown Md.* (2017) 18:268–76. doi: 10.2459/JCM.0000000000000500
107. Goodloe AH, Evans JM, Middha S, Prasad A, Olson TM. Characterizing genetic variation of adrenergic signalling pathways in Takotsubo (stress) cardiomyopathy exomes. *Eur J Heart Fail.* (2014) 16:942–9. doi: 10.1002/ejhf.145
108. Eitel I, Moeller C, Munz M, Stiermaier T, Meitinger T, Thiele H, et al. Genome-wide association study in takotsubo syndrome - preliminary results and future directions. *Int J Cardiol.* (2017) 236:335–9. doi: 10.1016/j.ijcard.2017.01.093
109. Pelliccia F, Parodi G, Greco C, Antoniucci D, Brenner R, Bossone E, et al. Comorbidities frequency in Takotsubo syndrome: an international collaborative systematic review including 1109 patients. *Am J Med.* (2015) 128:654.e11–9. doi: 10.1016/j.amjmed.2015.01.016
110. Looi J-L, Lee M, Webster MWI, To ACY, Kerr AJ. Postdischarge outcome after Takotsubo syndrome compared with patients post-ACS and those without prior CVD: ANZACS-QI 19. *Open Heart.* (2018) 5:e000918. doi: 10.1136/openhrt-2018-000918
111. Vriz O, Brosolo G, Martina S, Pertoldi F, Citro R, Mos L, et al. In-hospital and long-term mortality in Takotsubo cardiomyopathy: a community hospital experience. *J Community Hosp Intern Med Perspect.* (2016) 6:31082. doi: 10.3402/jchimp.v6.31082
112. Kim H, Senecal C, Lewis B, Prasad A, Rajiv G, Lerman LO, et al. Natural history and predictors of mortality of patients with Takotsubo syndrome. *Int J Cardiol.* (2018) 267:22–7. doi: 10.1016/j.ijcard.2018.04.139
113. Stiermaier T, Santoro F, Graf T, Guastafierro F, Tarantino N, De Gennaro L, et al. Prognostic value of N-Terminal Pro-B-Type Natriuretic Peptide in Takotsubo syndrome. *Clin Res Cardiol.* (2018) 107:597–606. doi: 10.1007/s00392-018-1227-1
114. Limite LR, Arcari L, Cacciotti L, Russo D, Musumeci MB. Cardiogenic shock in takotsubo syndrome: a clue to unravel what hides behind the curtain? *JACC Heart Fail.* (2019) 7:175–6. doi: 10.1016/j.jchf.2018.11.003
115. Rosa GM, Tini G, Porto I. Takotsubo syndrome: lonely hearts. *Pol Arch Intern Med.* (2020) 130:6–7. doi: 10.20452/pamw.15166
116. Dastidar AG, Baritussio A, De Garate E, Drobni Z, Biglino G, Singhal P, et al. Prognostic role of CMR and conventional risk factors in myocardial infarction with nonobstructed coronary arteries. *JACC Cardiovasc Imaging.* (2019) 12:1973–82. doi: 10.1016/j.jcmg.2018.12.023
117. Ong GJ, Nguyen TH, Stansborough J, Surikow S, Mahadavan G, Worthley M, et al. The N-AcetylCysteine and RAMipril in Takotsubo Syndrome Trial (NACRAM): rationale and design of a randomised controlled trial of sequential N-Acetylcysteine and ramipril for the management of Takotsubo Syndrome. *Contemp Clin Trials.* (2020) 90:105894. doi: 10.1016/j.cct.2019.105894
118. Girolami F, Frisso G, Benelli M, Crotti L, Iascone M, Mango R, et al. Contemporary genetic testing in inherited cardiac disease: tools, ethical issues, and clinical applications. *J Cardiovasc Med.* (2018) 19:1–11. doi: 10.2459/JCM.0000000000000589

Conflict of Interest: The authors declare that the research was conducted in the absence of any commercial or financial relationships that could be construed as a potential conflict of interest.

Publisher's Note: All claims expressed in this article are solely those of the authors and do not necessarily represent those of their affiliated organizations, or those of the publisher, the editors and the reviewers. Any product that may be evaluated in this article, or claim that may be made by its manufacturer, is not guaranteed or endorsed by the publisher.

frontiers in Cardiovascular Medicine

REVIEW
published: 14 September 2021
doi: 10.3389/fcvm.2021.709124

The Potential Role of Cardiac CT in the Evaluation of Patients With Known or Suspected Cardiomyopathy: From Traditional Indications to Novel Clinical Applications

Edoardo Conte[1,2], *Saima Mushtaq*[1], *Giuseppe Muscogiuri*[1], *Alberto Formenti*[1], *Andrea Annoni*[1], *Elisabetta Mancini*[1], *Francesca Ricci*[1], *Eleonora Melotti*[1], *Carlo Gigante*[1], *Zanotto Lorenza*[1], *Marco Guglielmo*[1], *Andrea Baggiano*[1,2], *Riccardo Maragna*[1], *Carlo Maria Giacari*[1], *Corrado Carbucicchio*[1], *Valentina Catto*[1], *Mauro Pepi*[1], *Daniele Andreini*[1,3] *and Gianluca Pontone*[1]*

[1] *Centro Cardiologico Monzino, Istituto di Ricerca e Cura a Carattere Scientifico (IRCCS), Milan, Italy,* [2] *Department of Biomedical Science for Health, University of Milan, Milan, Italy,* [3] *Department of Clinical Sciences and Community Health, Cardiovascular Section, University of Milan, Milan, Italy*

OPEN ACCESS

Edited by:
Giovanni Quarta,
Papa Giovanni XXIII Hospital, Italy

Reviewed by:
Filippo Cademartiri,
IRCCS SDN, Italy
Maria Concetta Pastore,
Università del Piemonte Orientale, Italy

***Correspondence:**
Gianluca Pontone
gianluca.pontone@ccfm.it

Specialty section:
This article was submitted to Cardiovascular Imaging, a section of the journal Frontiers in Cardiovascular Medicine

Received: *13 May 2021*
Accepted: *05 August 2021*
Published: *14 September 2021*

Citation:
Conte E, Mushtaq S, Muscogiuri G, Formenti A, Annoni A, Mancini E, Ricci F, Melotti E, Gigante C, Lorenza Z, Guglielmo M, Baggiano A, Maragna R, Giacari CM, Carbucicchio C, Catto V, Pepi M, Andreini D and Pontone G (2021) The Potential Role of Cardiac CT in the Evaluation of Patients With Known or Suspected Cardiomyopathy: From Traditional Indications to Novel Clinical Applications. Front. Cardiovasc. Med. 8:709124. doi: 10.3389/fcvm.2021.709124

After 15 years from its advent in the clinical field, coronary computed tomography (CCTA) is now widely considered as the best first-step test in patients with low-to-moderate pre-test probability of coronary artery disease. Technological innovation was of pivotal importance for the extensive clinical and scientific interest in CCTA. Recently, the advent of last generation wide-coverage CT scans paved the way for new clinical applications of this technique beyond coronary arteries anatomy evaluation. More precisely, both biventricular volume and systolic function quantification and myocardial fibrosis identification appeared to be feasible with last generation CT. In the present review we would focus on potential applications of cardiac computed tomography (CCT), beyond CCTA, for a comprehensive assessment patients with newly diagnosed cardiomyopathy, from technical requirements to novel clinical applications.

Keywords: cardiac computed tomographic imaging, cardiomyopathies, myocardial fibrosis, multimodality imaging, cardiac imaging and diagnostics

INTRODUCTION

Multimodality imaging has recently gained a pivotal role in the management of cardiovascular disease, and the diagnostic work-up of cardiomyopathies, in order to define the different phenotypes, was deeply influenced by the recent introduction of advanced cardiovascular imaging modalities, such as cardiac magnetic resonance (CMR) (1). Even if transthoracic echocardiography (TTE) remains the first step test thanks to its wide availability, it could be limited by the low-image quality and by the lack of tissue characterization. On the contrary, CMR enables reproducible evaluation of biventricular volumes and systolic function together with non-invasive tissue characterization providing pivotal diagnostic insights, especially when TTE is negative for structural heart disease (SHD). In this regard, Andreini et al. in a population of 946 patients with ventricular arrhythmias without pathological findings at TEE identified 241 patients (25.5%) with

SHD at CMR (2). These findings have deep clinical consequences because, beyond the accurate identification of structural heart abnormalities, tissue characterization by CMR, thanks to the identification of myocardial fibrosis at late-gadolinium enhancement (LGE) images, is associated with worse cardiovascular prognosis (3, 4). These data support the growing role that CMR gained in recent clinical guidelines for the diagnosis and management of cardiomyopathies (5) and the recent introduction of T1 and T2 mapping techniques may further expand its clinical application (6). However, clinical use of CMR could be limited by resource availability and by some conditions that represent relative or absolute contraindications (7). Moreover, image quality could be affected by metallic elements and cardiac arrhythmias, limiting CMR application in a specific clinical setting; last but not least, claustrophobia may limit access to the CMR environment for some subjects.

In the DANAMI-3-DEFER CMR substudy (8), 181 of 990 eligible patients (18.2%) were excluded from the study due to claustrophobia or contraindication to CMR. Taking into consideration the importance of non-invasive tissue characterization for an up-to-date diagnosis and management of cardiomyopathies, cardiac CT (CCT) recently emerged as a potential alternative to CMR for both the biventricular function evaluation and myocardial fibrosis identification, beyond the well-validated and accepted role for the non-invasive evaluation of coronary anatomy.

The present review will focus on potential applications of CCT for a comprehensive assessment of patients with newly diagnosed cardiomyopathy, from the well-validated evaluation of coronary anatomy to novel potential clinical applications.

THE CLINICAL INDICATION OF CCT IN THE MANAGEMENT OF CARDIOMYOPATHIES

Coronary Anatomy Evaluation

In the diagnostic pathway of dilated cardiomyopathy (DCM) of unknown etiology, the identification of patients with ischemic heart disease (IHD) is pivotal (9). Despite invasive coronary angiography (ICA) is still considered in patients with DCM and intermediate-to-high pretest probability of coronary artery disease (CAD) (10), CCT could be a reasonable alternative to rule out ischemic etiology when revascularization is not expected. Recently, an emerging role of coronary computed tomography angiography for preprocedural planning in those with IHD before percutaneous coronary revascularization was showed (11). Among patients with heart failure (HF) and reduced ejection fraction (HFrEF), the very high diagnostic accuracy of CCT vs. ICA for the identification of severe coronary stenosis was described, even with old generation CT (12) (**Figure 1**). A possible explanation of the excellent diagnostic accuracy reported is that these patients usually have an optimal heart rate as medical therapy, for HF contemplates a target heart rate < 65 bpm; moreover, severe systolic dysfunction is associated with reduced cardiac and coronary motion, further improving the quality of the image. For these reasons, a consensus document from the European Society of Cardiology (ESC) published in 2019 suggested CCT as a highly valuable tool to exclude significant CAD in patients with newly diagnosed DCM (13). Similarly, ESC Guidelines on chronic coronary syndrome suggested CCT as an alternative to ICA in patients with newly diagnosed reduction of ejection fraction to establish the presence and extent of CAD and evaluate clinical indication to myocardial revascularization (13).

Cardiac Vein Anatomy Evaluation

In 2012, Malagò et al. reported optimal imaging quality focused on cardiac vein anatomy evaluation in a consecutive cohort of patients (301 subjects) who previously underwent CCT for coronary anatomy evaluation and were retrospectively evaluated for cardiac vein mapping (14). Of interest, the authors reported an elevated variability of cardiac vein anatomy evaluated using CCT in patients with HFrEF, mostly involving the posterolateral and marginal left ventricular vein that are commonly used for cardiac resynchronization therapy (CRT). In this regard, Pontone et al. described the potential use of a dedicated acquisition protocol for cardiac vein anatomy evaluation with CT reporting an improved evaluability of a cardiac vein, especially in those with HFrEF of ischemic origin (15). In the clinical setting of patients with HFrEF, accurate characterization of cardiac vein anatomy could be of clinical interest for appropriate selection of patients with favorable anatomy before left ventricle (LV) electro-catheter implantation for CRT (16). Nowadays, after several pieces of evidence of accuracy and feasibility, non-invasive coronary vein mapping with CCT prior to placement of biventricular pacemaker is supported by clinical guidelines and consensus paper (17) (**Figure 2**).

Take-home message:

- *Cardiac computed tomography is indicated in patients with DCM of unknown etiology to rule out IHD as an alternative to ICA*
- *Cardiac computed tomography for coronary anatomy evaluation provides concomitant cardiac vein mapping in patients with HFrEF*

AN EMERGING APPLICATION OF CCT

Biventricular Volumes and Systolic Function

Besides the well-validated and widely recognized role of CCT as a non-invasive tool for coronary anatomy evaluation, clinical and research interest is focusing on the potential application of CCT for a comprehensive cardiac assessment.

In 2004, Juergens et al. reported a very early experience of left ventricular volumes and systolic function evaluation with 4-slices CT compared with CMR in 30 subjects showing a good correlation between the two techniques (18). Similarly, in 2006, Sugeng et al. reported that 16-slices CCT scan provides highly reproducible measurements, especially if compared with three-dimensional echocardiography, with mild but significant overestimation of volumes and underestimation of ejection fraction when compared with CMR (19). Then, the advent in the clinical field of 64-slices CT enables concomitant right and left ventricular volumes quantification, and several reports

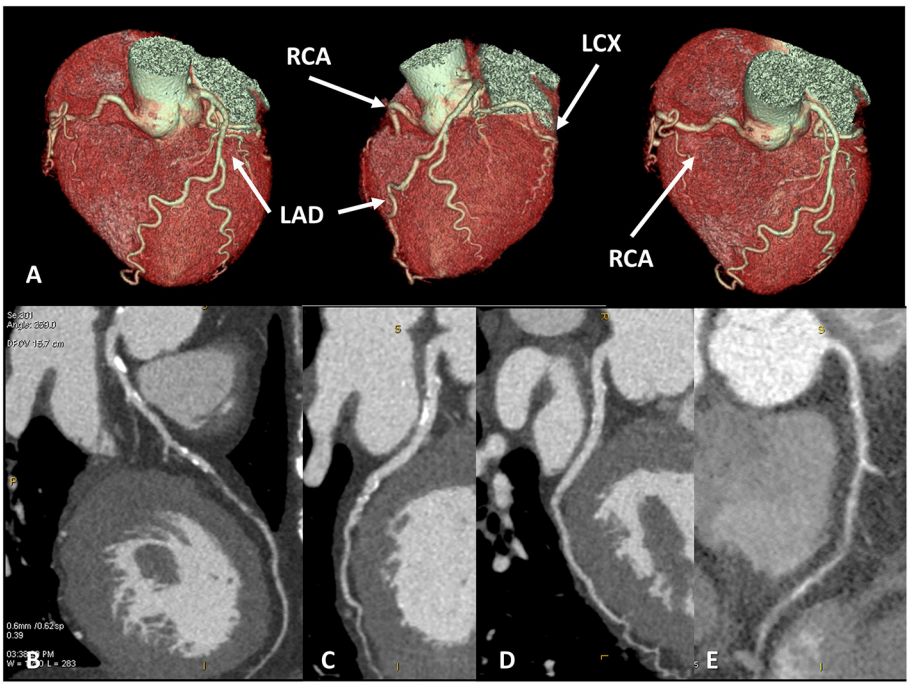

FIGURE 1 | Coronary artery anatomy evaluation. A case example of 65 years old female patients with newly diagnosed severe reduction of left ventricular ejection fraction (<30%), symptomatic for dyspnea. Cardiac CT was performed with optimal image quality **(A)**. A severe multivessel coronary artery disease was found with a subocclusive lesion on mid-left anterior descendent artery **(B)**, significative lesion on left-circumflex artery **(C)**, no significative lesion on the marginal branch and subocclusive disease on right coronary artery **(D,E)**.

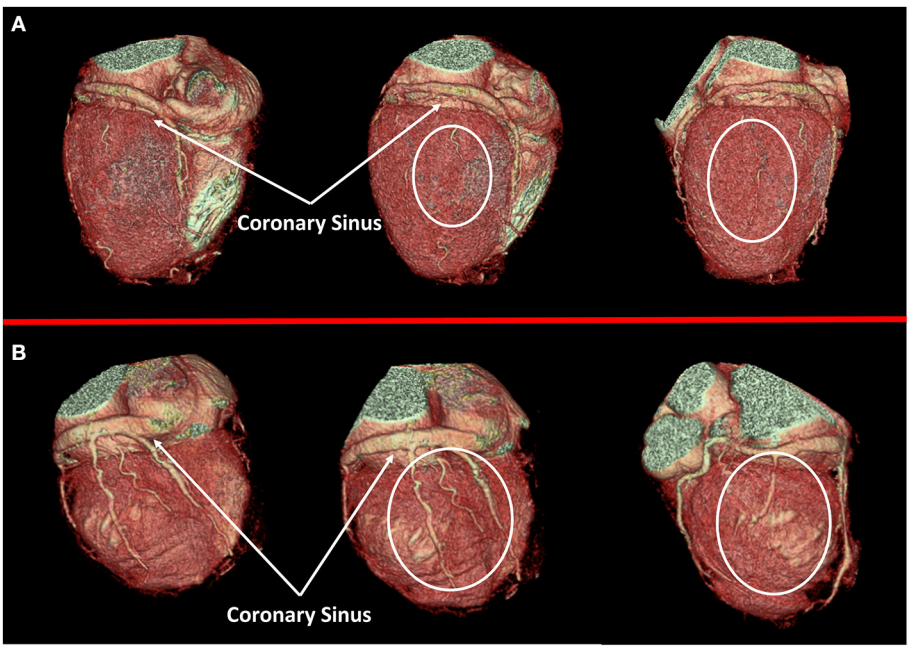

FIGURE 2 | Cardiac veins anatomy evaluation. In **(A)** a case of dilated cardiomyopathy (DCM) without favorable cardiac vein anatomy for cardiac resynchronization therapy (CRT) implantation is represented; a white circle highlights the absence of adequate cardiac vein on a posterolateral wall. On the contrary, a case of optimal cardiac vein anatomy for CRT implantation is reported in **(B)**.

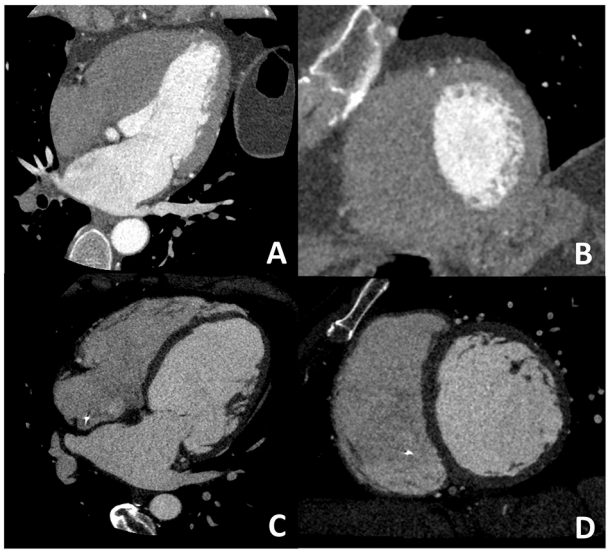

FIGURE 3 | Dedicated cardiac CT (CCT) scan protocol for the comprehensive evaluation in DCM patients. In **(A,B)** a cardiac CT dedicated to coronary anatomy evaluation is shown; it is well evident how it is not possible to correctly identify the right ventricular border of the interventricular septum. In **(C,D)** a CT with dedicated acquisition protocol for biventricular volume and function in which all four chambers are opacified by contrast medium enabling correct right ventricular border identification. These examples highlight the need for a dedicated acquisition protocol for most of the non-coronary cardiac CT findings.

provided evidence of the feasibility and accuracy of CT vs. CMR (20–28). A potential explanation of these discrepancies between imaging modalities could be the different respiratory phases at which images are acquired. In 2012, a meta-analysis and systematic review including 12 studies, assessing CCT-based ejection fraction obtained with 64-slices CT or dual-source CT compared with CMR or TTE (29), reported excellent concordance between CCT and MRI, especially when dual-source CCT is used; thanks to its higher temporal resolution.

Despite several reports on the feasibility and accuracy of CCT for biventricular systolic function evaluation, its clinical application is limited mainly due to the elevated radiation dose up to 18–20 mSv with old-generation CT scans (30, 31). Indeed, in order to quantify ejection fraction, the entire cardiac cycle should be acquired for correct identification of end-diastolic/end-systolic phases; moreover, for the identification of the right ventricular endocardial border, a higher dose of iodinated contrast is needed to obtain a balanced contrast opacification between left and right ventricular (**Figure 3**).

Recently, the myocardial strain has been proposed as a promising tool for the evaluation of left and right ventricular function, especially in patients with HF and preserved ejection fraction (HFpEF). Even if echocardiography remains the most used technique for myocardial global and regional strain evaluation, both cardiac MRI (32) and, more recently, cardiac CT (33) resulted to provide accurate global strain evaluation, thanks to its volumetric data acquisition. Of interest in 2021, a study including 50 patients undergoing both CCT and CMR demonstrated very good accuracy of CCT vs. CMR in the evaluation of global myocardial strain with feature strain technique providing a true three-dimensional evaluation of all myocardial points in all the cardiac phases and in all directions (34).

In summary, despite promising results, the clinical use of CCT for biventricular volume and function is still a matter of debate especially because the need for dedicated acquisition protocol has the following three main consequences: (1) elevated radiation dose; (2) higher dose of contrast medium is usually administered for biventricular balanced contrast opacification during the entire images acquisition; (3) a *post hoc* analysis for biventricular volume and systolic function is not feasible if CT scan acquisition was focused on coronary anatomy evaluation. All these points are now limiting the clinical use of CCT for the evaluation of biventricular function. However, the promising role of CCT for the evaluation of biventricular function is confirmed by the inclusion of this technique as a potential alternative to CMR in several consensus documents on cardiomyopathies (35, 36).

Recently, the advent in the clinical field of new generation CT scans, from dual-source scanners to wide detectors enabling the entire heart volume to be covered in one beat, represents an interesting opportunity to overcome previous limitations of CCT. Moreover, new generation CT scans are characterized by a reduction in gantry rotation time that is associated with increase temporal resolution improving end-systolic/end-diastolic phase identification (**Figure 4**).

Results from the E PLURIBUS study (37) will soon provide important insight on this topic. The study is aiming to verify the feasibility and accuracy of single-step evaluation of biventricular volume and function, myocardial fibrosis (vs. CMR), and coronary and vein anatomy using the last generation CT scanner with a 16-cm wide detector enabling the entire cardiac volume to be acquired in a single R-R cycle; this would provide a reduction in radiation dose and contrast medium needed to obtain biventricular homogenous contrast opacification.

Myocardial Tissue Characterization

Beyond myocardial function evaluation, myocardial fibrosis identification is widely considered to have a significant prognostic value. In 2016, a meta-analysis including 19 studies and 2,850 patients for a total of 423 arrhythmic events (38) supported the prognostic value of LGE in patients with severe reduction of ejection fraction, irrespective of the ischemic or non-ischemic nature; these data support the role of LGE for better identification of patients who may merit implantable cardioverter defibrillator (ICD) implantation. These data have been recently confirmed by the DERIVATE registry including more than 1,500 non-ischemic DCM in which a composite clinical and CMR-based risk score provides incremental prognostic value beyond the standard of care evaluation for major adverse arrhythmic cardiac events (39). Of interest, AHA/ACC 2020 guidelines on diagnosis and treatment of hypertrophic cardiomyopathy (HCM) included LGE presence and extension

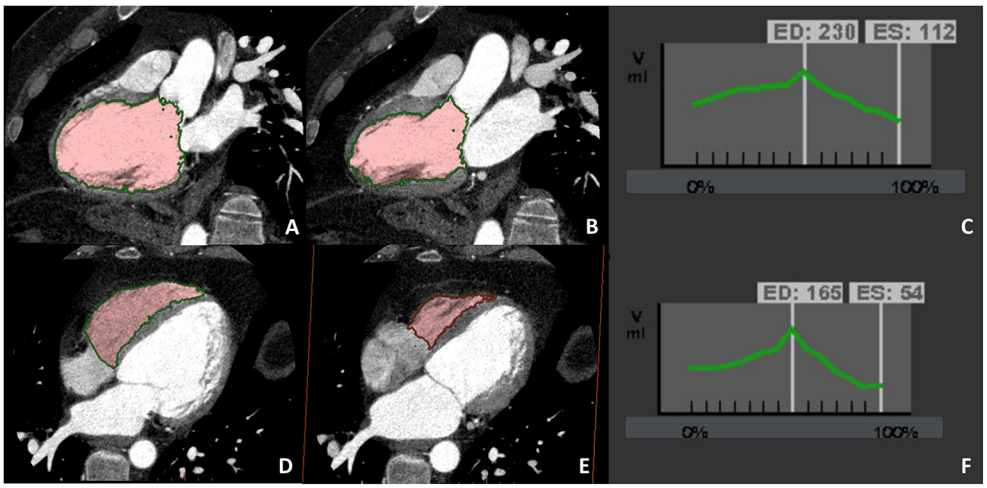

FIGURE 4 | A case example of patients in which biventricular volume and function have been evaluated at CCT due to cardiac magnetic resonance (CMR) contraindication (claustrophobia). Biventricular balanced opacification enabled to correctly quantify both the left (panel **A–C**) and right (panel **D–F**) ventricular ejection fraction (LVEF 49%, RVEF 68%). Images were acquired during the entire cardiac cycle and the radiation dose needed for this evaluation was 7.5 mSv, heightening one of the main limitations to the routine clinical use of CCT for left ventricular evaluation.

among parameters that should be evaluated when considering ICD implantation for primary prevention (35). In the same document, CCT is proposed as an alternative technique for an appropriate definition of LV structure including myocardial tissue characterization. These clinical recommendations are supported by some reports highlighting the capability of CCT to adequately assess myocardial structure (40). It is of the utmost importance to recognize that even CCT images acquired for coronary anatomy evaluation are suitable for myocardial thickness quantification and the identification of myocardial fat infiltration (41–43). To observe and describe these non-coronary but cardiac findings is mandatory, even if a definite diagnosis should be performed with CMR when feasible.

On the contrary, the recently described capability of CCT to identify the presence of myocardial fibrosis needs a dedicated acquisition protocol (**Figure 5**). The pathophysiological basis of myocardial fibrosis identification by contrast CCT is the same as CMR taking into consideration that pharmacokinetic properties of iodinated contrast medium are similar to gadolinium (44). The acquisition protocol for the delayed enhancement imaging in CT is nowadays based on two key rules: (1) the administration of larger amounts of iodinated contrast medium (at least 1.5 ml/kg) when compared to the dose needed for coronary anatomy evaluation and (2) the acquisition of CT images with ECG gating after 8–10 min postcontrast administration.

One of the first reports of exploring the assessment of myocardial viability was described in a small experimental study involving 17 animals (10 dogs and 7 pigs) in which an accurate identification and quantification of myocardial fibrosis by CT vs. postmortem autopsy evaluation was demonstrated (45).

In 2005, a first-in-human study enrolled 28 consecutive patients with a previous history of myocardial infarction who underwent both CMR and CCT with late CT scan for myocardial fibrosis evaluation (46); using 16-slice CT, authors reported

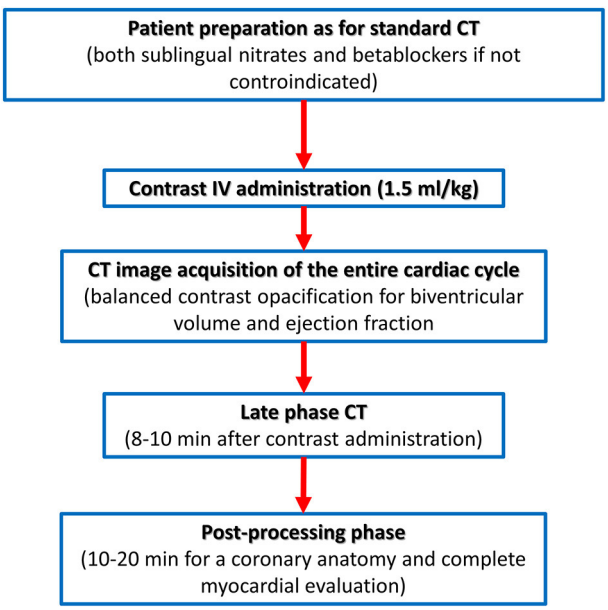

FIGURE 5 | Computed tomography acquisition protocol dedicated to biventricular myocardial function and tissue characterization.

an excellent agreement of myocardial infarction (MI) size for late-phase CCT and CMR with 415 myocardial segments (92.63%) on 448 assessed showing concordant results between the two techniques.

In 2008, le Polain de Waroux et al. enrolled 71 consecutive patients with new-onset of left ventricular dysfunction (LVD) who underwent ICA, CMR, and CCT with myocardial fibrosis evaluation (47); on a per-patient basis, CCT for both the coronary

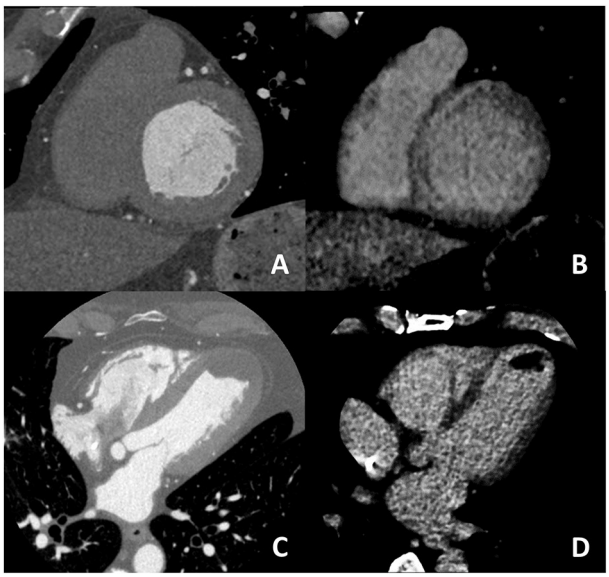

FIGURE 6 | In **(A,B)** an example of non-ischemic fibrosis on the interventricular septum is shown; more specifically, in **(A)** angiographic phase CT is presented with corresponding late CT acquisition well demonstrating non-ischemic mid-wall myocardial fibrosis in **(B)**. In **(C,D)** a case of ischemic cardiomyopathy is presented; an apical left ventricular thrombus is evident both at first pass CT **(C)** and at late phase CT **(D)** from which the ischemic subendocardial fibrosis could be evidenced.

anatomy and myocardial fibrosis assessment had an excellent agreement ($k = 0.89$; $P = 0.001$) with ICA and CMR for etiological classification of LVD. For what concern myocardial fibrosis identification only two patients had false-negative results at CCT vs. CMR, possibly caused by the poor image quality and low signal-to-noise ratio. However, an overall very good accuracy ($k = 0.88$, $p < 0.001$) for the identification of fibrosis by CCT was reported.

For what concern non-ischemic fibrosis, a validation study was performed in 2014 including 24 patients with hypertrophic phenotype who underwent both CCT and CMR for myocardial fibrosis evaluation (**Figure 6**). On a per-patient basis, CCT had a 100% sensitivity for myocardial fibrosis vs. CMR and mean myocardial scar area resulted of 2.2 ± 1.4 cm^2 in CCT vs. 2.9 ± 2.4 cm^2 in CMR; of interest, authors reported that the relative intensity ratio between normal remote myocardium and area of myocardial fibrosis in CT was 1.8 ± 0.3 (48). Similar promising results have been recently reported in a consecutive cohort of patients with sarcoidosis evaluated with both CCT and CMR (49). For optimal evaluation of myocardial fibrosis at late CT scan, dedicated post-processing analysis is needed, as previously described (50). More precisely, an 8–10 mm thickness in short-axis LV view should be obtained and narrow window and level settings (W300, L150) are suggested (**Figure 5**).

Despite promising results, myocardial fibrosis evaluation by CCT remains limited by low signal-to-noise ratio and by the need for a high dose of contrast medium. Technological advances are needed to overcome these limitations. One of the most promising novelties in this field is the use of dual-energy CT that appeared to enable myocardial fibrosis identification with reduced contrast amount. Dual-energy CT (both with dual-source CT or with single-source CT and rapid kVp switching) technology permits contemporary use of different tube potential enabling tissue characterization with extracellular volume (ECV) estimation that is considered a myocardial fibrosis equivalent when evaluation with CMR. More precisely, in 2020, Ohta et al. reported that strong correlations were seen between CT-ECV and MR-ECV at postcontrast CT images in 23 patients (51). Similarly, in 2019 Kumar et al. (52) reported that multi-energy CT in 21 subjects, when compared with a single-energy approach, better discriminate the presence or absence of myocardial fibrosis severity when compared with CMR, with correct classification rates of 89 and 71%, respectively; similarly, the multi energy CT better discriminates normal from elevated ECV, with a correct classification in 89% of patients vs. correct distinction of normal vs. elevated ECV in only 70% using single energy CT. Recently, radiomics models with an artificial intelligence approach achieved a good diagnostic accuracy (AUC: 0.78, 95% CI: 0.75–0.81) on a per-segment basis for the identification of myocardial fibrosis with CCR vs. MRI (53). Even if promising, these novel approaches need further studies before being proposed for clinical use.

Take-home messages:

- *Biventricular volume and systolic function analysis are feasible and accurate with CCT.*
- *Myocardial fibrosis assessment is feasible with CT, even if a low contrast-to-noise ratio limits diagnostic accuracy vs. CMR.*
- *For both the myocardial fibrosis and biventricular function assessment with CT, dedicate acquisition protocol is needed with an increase in radiation dose and iodinated contrast amount administration, limiting their clinical use to those patients with CMR contraindication.*
- *In the next future, technological advances may further expand the clinical application of non-coronary CCT evaluation.*

TECHNICAL CONSIDERATION FOR A COMPREHENSIVE APPROACH

As previously outlined, a dedicated acquisition protocol for comprehensive evaluation of myocardial fibrosis and biventricular volumes and function is needed; it is important to underline that coronary anatomy analysis is feasible using the same imaging dataset. More precisely, biventricular volumes and function are evaluated using imaging acquired at the first pass contrast angiographic phase, the same used for coronary evaluation. What differs from traditional CCTA is the total volume of contrast needed (at least 1.5 ml/kg for function and fibrosis vs. <1 ml/kg for coronary anatomy) and the need for biventricular opacification, that may cause, in rare cases, artifacts on the mid-portion of the right coronary artery. On the other side, the need for contrast medium bolus for optimal angiographic evaluation of coronary vessels has been indicated as a potential cause to mild, but significative, overestimation of right ventricular end-diastolic volume (RVEDV); to reduce

discrepancies vs. CMR in RVEDV quantification, contrast injection at lower infusion rate has been proposed, but this approach would make coronary stenosis not evaluable. Overall, high priority should be given to coronary anatomy evaluation as this is the most important and validated CCT application.

For what concerns myocardial fibrosis evaluation, the late post-contrast acquisition is needed without a significative increase in radiation dose. It should be underlined that, especially in patients with DCM, where a higher dose of contrast medium is needed to evaluate coronary anatomy, adding a late post-contrast scan could be proposed on a regular basis; on the contrary, this is not true for biventricular volumes and function evaluation for which the need of entire cardiac cycle acquisition is associated with a significative increase in radiation dose.

Finally, it should be underlined that all these advanced uses of cardiac CT are strictly dependent on the availability of the last generation CT; indeed, 64-slice CT technology is suboptimal especially for biventricular volumes and function analysis and is associated with very high radiation dose (up to 1,820 mSv), prohibitive especially when serial evaluation at follow-up is needed.

EMERGING CLINICAL APPLICATION IN SPECIFIC SETTINGS

Hypertrophic Cardiomyopathy

Several clinical fields may benefit from a wider application of CCT beyond coronary anatomy evaluation, even if extensive supporting data are still to come. The unique capability of CCT to evaluate both coronary and myocardial anatomy may support its use in the evaluation of patients with HCM. In this setting, beyond the analysis of myocardial thickness and fibrosis, CCT may provide an accurate evaluation of the concomitant presence of coronary artery disease; more precisely, in a previous study including 60 patients with HCM (54), CCT provided a 100% sensitivity, a 94.4% specificity, a 92.3% positive predictive value, and a 100% negative predictive value for the identification of significative coronary stenosis when compared with ICA. Moreover, CCT may enable accurate evaluation of myocardial bridges, whose prevalence among patients with HCM is not negligible, and up to 40% according to previous reports (54). Previous studies suggested that myocardial bridges among patients with HCM are longer and deeper when compared to a control group of patients (55); thus, accurate evaluation of coronary anatomy is of utmost importance in these patients. Moreover, in those with clinical indications to myomectomy preprocedural planning with CCT may provide important insight on septum anatomy for a safer and more effective procedure, as previously suggested (56). Moreover, CCT may provide an accurate evaluation of right ventricular wall thickness with identification of wall hypertrophy that could be missed at TEE.

Arrhythmogenic Cardiomyopathy

Accurate analysis of the right ventricle is of the utmost importance in patients with suspected arrhythmogenic cardiomyopathy (AC); even if validated cut-offs for AC diagnosis are still missing, the presence of right ventricular bulging and/or right ventricular dilation or systolic dysfunction could be identified with CCT. However, it should be underlined that previous reports suggested a mild, but significative, overestimation of right ventricular diastolic volume with CT vs. CMR (31), possibly because of the different phases of the respiratory cycle at which images are obtained in the two techniques and/or to the contrast medium bolus that is administered during CT images acquisition. Of interest, the recent data correlated right ventricle wall tissues heterogeneity identified at CT with abnormal findings at invasive electroanatomical mapping (EAM), proposing CT as a potential tool for accurate identification of patients with AC vs. those with right ventricular dilation due to adaptive remodeling (i.e., athletes) (57).

Preprocedural Planning of Ventricular Arrhythmias Ablation

For what concerns myocardial tissue analysis, one of the most promising clinical applications of CCT is the evaluation of anatomical substrate in patients with unstable ventricular arrhythmias and possible indications to transcatheter ablation. In this setting, identification of myocardial arrhythmic substrate by CMR has been demonstrated to improve procedural outcome (58); unfortunately, CMR could sometimes be of difficult feasibility due to both the presence of unstable heart rhythm (with safety issues of potential patients in an MRI environment) and previous implanted electronic device (i.e., intern defibrillator). A recently published state-of-the-art paper well-summarized clinical indication and acquisition protocol for CCT in this specific clinical setting (59); the most interesting feature is the possibility to import CCT data during invasive electrophysiological mapping providing live guidance based on anatomical substrate and possibly avoid ICA. More precisely, CCT enables concomitant myocardial tissue characterization (myocardial fibrosis) and analysis of coronary anatomy, excluding severe coronary stenosis as the cause of arrhythmic storm; both these information can be imported during the invasive electrophysiological procedure for live visualization and guidance. Moreover, a detailed analysis of the anatomy at the access site for the epicardial approach could be performed for optimal preprocedural planning. Esposito et al. reported that CCT with late scan acquisition was able to detect myocardial scars responsible for pathological low-amplitude voltages at invasive electroanatomic mapping with high sensitivity and very high negative predictive values (76 and 95%, respectively), regardless of substrate etiology and ICD presence (60).

Apart from this advanced application, CCT should be considered in clinical practice for biventricular volume and function analysis and myocardial fibrosis identification when CMR is contraindicated and TTE is inconclusive. This approach is supported by guidelines and consensus documents previously published (9, 17, 35, 36, 61).

TABLE 1 | Main pro/cons features of CCT compared with other imaging modalities according to different clinical settings.

	Transthoracic echocardiography		Cardiac MRI		Cardiac CT	
	Pro	**Cons**	**Pro**	**Cons**	**Pro**	**Cons**
All settings	Wide availability	Tissue characterization is not feasible	Well-validated tissue characterization	Dedicated environment may represent contraindication	Non-invasive evaluation of coronary anatomy	Radiation dose, especially if serial evaluation needed at follow-up
DCM	Well-validated prognostic role of ejection fraction in this setting	Apical thrombus could be missed	Enable differential diagnosis among non-ischemic etiologies (i.e., myocarditis)	Diastolic function evaluation is not feasible	Biventricular function analysis and coronary anatomy evaluation is feasible at the same time	Higher dose of contrast medium is needed due to chamber dilation
HCM	Enable dynamic evaluation of hemodynamic features (LVOT obstruction)	Apical hypertrophy could be missed	Myocardial fibrosis identification has well-validated prognostic role	Hemodynamic evaluation is not feasible	Identification of myocardial bridging and coronary artery disease	Hemodynamic evaluation is not feasible
ARVC	Comprehensive evaluation of right ventricular hemodynamic pattern	Right ventricular evaluation could be suboptimal in some cases	Accurate analysis of right ventricular kinesis, volumes and function	Accurate evaluation of right ventricular could be difficult due to frequent ventricular arrhythmias	Enable exclusion of other causes of right ventricular dilation	Possible over-estimation of right ventricular end-diastolic volume

LIMITATION OF NOVEL CLINICAL APPLICATION OF CCT

Despite promising results from CCT, nowadays, CMR remains the gold standard for biventricular volume and function quantification and for myocardial tissue characterization, as several technical reasons limit CCT clinical application for non-coronary evaluation. First, the temporal resolution of CCT is lower when compared with CMR. Second, CCT analysis is associated with non-negligible radiation dose (at least 5–6 mVs for a complete examination including coronary anatomy, biventricular volumes/function, and myocardial fibrosis); this is of particular concern in young patients who may undergo serial CCT during follow-up and for which cumulative radiation dose would result to be prohibitive. Moreover, the diagnostic accuracy of CCT for myocardial fibrosis evaluation is lower when compared to CMR due to a lower signal-to-noise ratio.

These limitations could be overcome in the future if further technological advances, especially in the field of artificial intelligence, should be applied in clinical practice (62).

CONCLUSION

When CMR is contraindicated and TTE results to be inconclusive, CCT may be considered in clinical practice as an alternative to CMR during diagnostic evaluation of patients with cardiomyopathies (**Table 1**). Adequate CT technology (preferable more than a 64-slice scanner) and a dedicated acquisition protocol are needed for biventricular function assessment and myocardial fibrosis evaluation. Of note, non-coronary but cardiac findings should be always carefully assessed, as myocardial hypertrophy and fat infiltration are often well evident even if CCT is focused on coronary anatomy.

AUTHOR CONTRIBUTIONS

EC and SM wrote the first draft of the manuscript. GM, AF, AA, EMe, and FR performed literature research and data evaluation. EMa, CG, ZL, MG, AB, RM, and CMG performed manuscript and figure editing and revision. CC, VC, MP, DA, and GP provided expert revision and supervision. All authors contributed to the article and approved the submitted version.

FUNDING

Centro Cardiologico Monzino will cover publication fees.

REFERENCES

1. Rapezzi C, Arbustini E, Caforio AL, Charron P, Gimeno-Blanes J, Heliö T, et al. Diagnostic work-up in cardiomyopathies: bridging the gap between clinical phenotypes and final diagnosis. A position statement from the ESC Working Group on Myocardial and Pericardial Diseases. *Eur Heart J.* (2013) 34:1448–58. doi: 10.1093/eurheartj/ehs397
2. Andreini D, Dello Russo A, Pontone G, Mushtaq S, Conte E, Perchinunno M, et al. CMR for identifying the substrate of ventricular arrhythmia in patients with normal echocardiography. *JACC*

Cardiovasc Imaging. (2020) 13(Pt. 1):410–21. doi: 10.1016/j.jcmg.2019.04.023
3. Grigoratos C, Todiere G, Barison A, Aquaro GD. The role of MRI in prognostic stratification of cardiomyopathies. *Curr Cardiol Rep.* (2020) 22:61. doi: 10.1007/s11886-020-01311-3
4. Pontone G, Guaricci AI, Andreini D, Solbiati A, Guglielmo M, Mushtaq S, et al. Prognostic benefit of cardiac magnetic resonance over transthoracic echocardiography for the assessment of ischemic and nonischemic dilated cardiomyopathy patients referred for the evaluation of primary prevention implantable cardioverter-defibrillator therapy. *Circ Cardiovasc Imaging.* (2016) 9:e004956. doi: 10.1016/S0735-1097(16)31683-7
5. von Knobelsdorff-Brenkenhoff F, Schulz-Menger J. Role of cardiovascular magnetic resonance in the guidelines of the European Society of Cardiology. *J Cardiovasc Magn Reson.* (2016) 18:6. doi: 10.1186/s12968-016-0225-6
6. Baggiano A, Boldrini M, Martinez-Naharro A, Kotecha T, Petrie A, Rezk T, et al. Noncontrast magnetic resonance for the diagnosis of cardiac amyloidosis. *JACC Cardiovasc Imaging.* (2020) 13(Pt.1):69–80. doi: 10.1016/j.jcmg.2019.03.026
7. Barison A, Baritussio A, Cipriani A, De Lazzari M, Aquaro GD, Guaricci AI, et al. Cardiovascular magnetic resonance: what clinicians should know about safety and contraindications. *Int J Cardiol.* (2021) 331:322–8. doi: 10.1016/j.ijcard.2021.02.003
8. Lønborg J, Engstrøm T, Ahtarovski KA, Nepper-Christensen L, Helqvist S, Vejlstrup N, et al. Myocardial damage in patients with deferred stenting after STEMI: a DANAMI-3-DEFER substudy. *J Am Coll Cardiol.* (2017) 69:2794–804. doi: 10.1016/j.jacc.2017.03.601
9. Donal E, Delgado V, Bucciarelli-Ducci C, Galli E, Haugaa KH, Charron P, et al. Multimodality imaging in the diagnosis, risk stratification, and management of patients with dilated cardiomyopathies: an expert consensus document from the European Association of Cardiovascular Imaging. *Eur Heart J Cardiovasc Imaging.* (2019) 20:1075–93. doi: 10.1093/ehjci/jez178
10. Ponikowski P, Voors AA, Anker SD, Bueno H, Cleland JGF, Coats AJS, et al. 2016 ESC Guidelines for the diagnosis treatment of acute chronic heart failure: the Task Force for the diagnosis treatment of acute chronic heart failure of the European Society of Cardiology (ESC)Developed with the special contribution of the Heart Failure Association (HFA) of the ESC. *Eur Heart J.* (2016) 37:2129–200. doi: 10.1093/eurheartj/ehw128
11. Wolff G, Dimitroulis D, Andreotti F, Kolodziejczak M, Jung C, Scicchitano P, et al. Survival benefits of invasive versus conservative strategies in heart failure in patients with reduced ejection fraction and coronary artery disease: a meta-analysis. *Circ Heart Fail.* (2017) 10:e003255. doi: 10.1161/CIRCHEARTFAILURE.116.003255
12. Andreini D, Pontone G, Pepi M, Ballerini G, Bartorelli AL, Magini A, et al. Diagnostic accuracy of multidetector computed tomography coronary angiography in patients with dilated cardiomyopathy. *J Am Coll Cardiol.* (2007) 49:2044–50. doi: 10.1016/j.jacc.2007.01.086
13. Knuuti J, Wijns W, Saraste A, Capodanno D, Barbato E, Funck-Brentano C, et al. 2019 ESC Guidelines for the diagnosis and management of chronic coronary syndromes. *Eur Heart J.* (2020) 41:407–77. doi: 10.1093/eurheartj/ehz425
14. Malagò R, Pezzato A, Barbiani C, Sala G, Zamboni GA, Tavella D, et al. Non invasive cardiac vein mapping: role of multislice CT coronary angiography. *Eur J Radiol.* (2012) 81:3262–9. doi: 10.1016/j.ejrad.2012.03.007
15. Pontone G, Andreini D, Cortinovis S, Mushtaq S, Bertella E, Annoni A, et al. Imaging of cardiac venous system in patients with dilated cardiomyopathy by 64-slice computed tomography: comparison between non-ischemic and ischemic etiology. *Int J Cardiol.* (2010) 144:340–3. doi: 10.1016/j.ijcard.2009.03.043
16. Giraldi F, Cattadori G, Roberto M, Carbucicchio C, Pepi M, Ballerini G, et al. Long-term effectiveness of cardiac resynchronization therapy in heart failure patients with unfavorable cardiac veins anatomy comparison of surgical versus hemodynamic procedure. *J Am Coll Cardiol.* (2011) 58:483–90. doi: 10.1016/j.jacc.2011.02.065
17. Andreini D, Martuscelli E, Guaricci AI, Carrabba N, Magnoni M, Tedeschi C, et al. Clinical recommendations on Cardiac-CT in 2015: a position paper of the Working Group on Cardiac-CT and Nuclear Cardiology of the Italian Society of Cardiology. *J Cardiovasc Med.* (2016) 17:73–84. doi: 10.2459/JCM.0000000000000318
18. Juergens KU, Grude M, Maintz D, Fallenberg EM, Wichter T, Heindel W, et al. Multi-detector row CT of left ventricular function with dedicated analysis software versus MR imaging: initial experience. *Radiology.* (2004) 230:403–10. doi: 10.1148/radiol.2302030042
19. Sugeng L, Mor-Avi V, Weinert L, Niel J, Ebner C, Steringer-Mascherbauer R, et al. Quantitative assessment of left ventricular size and function: side-by-side comparison of real-time three-dimensional echocardiography and computed tomography with magnetic resonance reference. *Circulation.* (2006) 114:654–61. doi: 10.1161/CIRCULATIONAHA.106.626143
20. Abbara S, Chowa JWB, Pena AJ, Cury RC, Hoffmann U, Nieman K, et al. Assessment of left ventricular function with 16- and 64-slice multi-detector computed tomography. *Eur J Radiol.* (2008) 67:481–6. doi: 10.1016/j.ejrad.2007.07.022
21. Bansal D, Singh RM, Sarkar M, Sureddi R, Mcbreen KC, Griffis T, et al. Assessment of left ventricular function: comparison of cardiac multidetector-row computed tomography with two-dimension standard echocardiography for assessment of left ventricular function. *Int J Cardiovasc Imaging.* (2008) 24:317–25. doi: 10.1007/s10554-007-9252-6
22. Heuschmid M, Rothfuss JK, Schroeder S, Fenchel M, Stauder N, Burgstahler C, et al. Assessment of left ventricular myocardial function using 16-slice multidetector-row computed tomography: comparison with magnetic resonance imaging and echocardiography. *Eur Radiol.* (2006) 16:551–9. doi: 10.1007/s00330-005-0015-2
23. Krishnam MS, Tomasian A, Iv MI, Ruehm SG, Saleh R, Panknin C, et al. Left ventricular ejection fraction using 64-slice CT coronary angiography and new evaluation software: initial experience. *Br J Radiol.* (2008) 81:450–5. doi: 10.1259/bjr/54748900
24. Busch S, Johnson TR, Wintersperger BJ, Minaifar N, Bhargava A, Rist C, et al. Quantitative assessment of left ventricular function with dual-source CT in comparison to cardiac magnetic resonance imaging: initial findings. *Eur Radiol.* (2008) 18:570–5. doi: 10.1007/s00330-007-0767-y
25. Brodoefel H, Reimann A, Klumpp B, Fenchel M, Heuschmid M, Burgstahler C, et al. Sixty-four-slice CT in the assessment of global and regional left ventricular function: comparison with MRI in a porcine model of acute and subacute myocardial infarction. *Eur Radiol.* (2007) 17:2948–56. doi: 10.1007/s00330-007-0673-3
26. Caudron J, Fares J, Vivier PH, Lefebvre V, Petitjean C, Dacher JN. Diagnostic accuracy and variability of three semi-quantitative methods for assessing right ventricular systolic function from cardiac MRI in patients with acquired heart disease. *Eur Radiol.* (2011) 21:2111–20. doi: 10.1007/s00330-011-2152-0
27. Guo YK, Gao HL, Zhang XC, Wang QL, Yang ZG, Ma ES. Accuracy and reproducibility of assessing right ventricular function with 64-section multidetector row CT Comparison with magnetic resonance imaging. *Int J Cardiol.* (2010) 139:254–62. doi: 10.1016/j.ijcard.2008.10.031
28. Plumhans C, Mühlenbruch G, Rapaee A, Sim KH, Seyfarth T, Günther RW, et al. Assessment of global right ventricular function on 64-MDCT compared with MRI. *AJR Am J Roentgenol.* (2008) 190:1358–61. doi: 10.2214/AJR.07.3022
29. Asferg C, Usinger L, Kristensen TS, Abdulla J. Accuracy of multi-slice computed tomography for measurement of left ventricular ejection fraction compared with cardiac magnetic resonance imaging and two-dimensional transthoracic echocardiography: a systematic review and meta-analysis. *Eur J Radiol.* (2012) 81:e757–62. doi: 10.1016/j.ejrad.2012.02.002
30. Lin FY, Devereux RB, Roman MJ, Meng J, Jow VM, Jacobs A, et al. Cardiac chamber volumes, function, and mass as determined by 64-multidetector row computed tomography: mean values among healthy adults free of hypertension and obesity. *JACC Cardiovasc Imaging.* (2008) 1:782–6. doi: 10.1016/j.jcmg.2008.04.015

31. Maffei E, Messalli G, Martini C, Nieman K, Catalano O, Rossi A, et al. Left and right ventricle assessment with Cardiac CT: validation study vs. Cardiac MR. *Eur Radiol.* (2012) 22:1041–9. doi: 10.1007/s00330-011-2345-6
32. T. Chitiboi, L. Axel, Magnetic resonance imaging of myocardial strain: a review of current approaches. *J Magn Reson Imaging.* (2017) 46:1263–80. doi: 10.1002/jmri.25718
33. McVeigh ER, Pourmorteza A, Guttman M, Sandfort V, Contijoch F, Budhiraja S, et al. Regional myocardial strain measurements from 4DCT in patients with normal LV function. *J Cardiovasc Comput Tomogr.* (2018) 12:372–8. doi: 10.1016/j.jcct.2018.05.002
34. Wang R, Fang Z, Wang H, Schoepf UJ, Emrich T, Giovagnoli D, et al. Quantitative analysis of three-dimensional left ventricular global strain using coronary computed tomography angiography in patients with heart failure: comparison with 3T cardiac MR. *Eur J Radiol.* (2021) 135:109485. doi: 10.1016/j.ejrad.2020.109485
35. Ommen SR, Mital S, Burke MA, Day SM, Deswal A, Elliott P, et al. 2020 AHA/ACC Guideline for the diagnosis and treatment of patients with hypertrophic cardiomyopathy: a report of the American College of Cardiology/American Heart Association Joint Committee on clinical practice guidelines. *J Am Coll Cardiol.* (2020) 76:e159–240. doi: 10.1016/j.jacc.2020.08.045
36. Te Riele ASJM, Tandri H, Sanborn DM, Bluemke DA. Noninvasive multimodality imaging in ARVD/C. *JACC Cardiovasc Imaging.* (2015) 8:597–611. doi: 10.1016/j.jcmg.2015.02.007
37. Andreini D, Conte E, Mushtaq S, Pontone G, Guglielmo M, Baggiano A, et al. Rationale and design of the EPLURIBUS Study (Evidence for a comPrehensive evaLUation of left ventRicle dysfnctIon By a whole-heart coverage cardiac compUted tomography Scanner). *J Cardiovasc Med.* (2020) 21:812–19. doi: 10.2459/JCM.0000000000001051
38. Disertori M, Rigoni M, Pace N, Casolo G, Masè M, Gonzini L, et al. Myocardial fibrosis assessment by LGE is a powerful predictor of ventricular tachyarrhythmias in ischemic and nonischemic LV dysfunction: a meta-analysis. *JACC Cardiovasc Imaging.* (2016) 9:1046–55. doi: 10.1016/j.jcmg.2016.01.033
39. Guaricci AI, Masci PG, Muscogiuri G, Guglielmo M, Baggiano A, Fusini L, et al. CarDiac magnEtic resonance for prophylactic implantable-cardioverter defibrillAtor ThErapy in non-ischaemic dilated CardioMyopathy: an international Registry. *Europace.* (2021) 23:1072–83. doi: 10.1093/europace/euaa401
40. Choi AD, Abbara S, Branch KR, Feuchtner GM, Ghoshhajra B, Nieman K, et al. Society of Cardiovascular Computed Tomography guidance for use of cardiac computed tomography amidst the COVID-19 pandemic Endorsed by the American College of Cardiology. *J Cardiovasc Comput Tomogr.* (2020) 4:101–4. doi: 10.1016/j.jcct.2020.03.002
41. Conte E, Mushtaq S, Pontone G, Casella M, Russo AD, Pepi M, et al. Left-dominant arrhythmogenic cardiomyopathy diagnosed at cardiac CT. *J Cardiovasc Comput Tomogr.* (2020) 14:e7–8. doi: 10.1016/j.jcct.2018.09.004
42. Nassar M, Arow Z, Monakier D, Zusman O, Shafir G, Kornowski R, et al. Effect of intramural course of coronary arteries assessed by computed tomography angiography in patients with hypertrophic cardiomyopathy. *Am J Cardiol.* (2019) 124:1279–85. doi: 10.1016/j.amjcard.2019.07.024
43. Sommariva E, Brambilla S, Carbucicchio C, Gambini E, Meraviglia V, Dello Russo A, et al. Cardiac mesenchymal stromal cells are a source of adipocytes in arrhythmogenic cardiomyopathy. *Eur Heart J.* (2016) 37:1835–46. doi: 10.1093/eurheartj/ehv579
44. Mendoza DD, Joshi SB, Weissman G, Taylor AJ, Weigold WG. Viability imaging by cardiac computed tomography. *J Cardiovasc Comput Tomogr.* (2010) 4:83–91. doi: 10.1016/j.jcct.2010.01.019
45. Lardo AC, Cordeiro MA, Silva C, Amado LC, George RT, Saliaris AP, et al. Contrast-enhanced multidetector computed tomography viability imaging after myocardial infarction: characterization of myocyte death, microvascular obstruction, and chronic scar. *Circulation.* (2006) 113:394–404. doi: 10.1161/CIRCULATIONAHA.105.521450
46. Mahnken AH, Koos R, Katoh M, Wildberger JE, Spuentrup E, Buecker A, et al. Assessment of myocardial viability in reperfused acute myocardial infarction using 16-slice computed tomography in comparison to magnetic resonance imaging. *J Am Coll Cardiol.* (2005) 45:2042–7. doi: 10.1016/j.jacc.2005.03.035
47. le Polain de Waroux JB, Pouleur AC, Goffinet C, Pasquet A, Vanoverschelde JL, Gerber BL. Combined coronary and late-enhanced multidetector-computed tomography for delineation of the etiology of left ventricular dysfunction: comparison with coronary angiography and contrast-enhanced cardiac magnetic resonance imaging. *Eur Heart J.* (2008) 29:2544–51. doi: 10.1093/eurheartj/ehn381
48. Langer C, Lutz M, Eden M, Lüdde M, Hohnhorst M, Gierloff C, et al. Hypertrophic cardiomyopathy in cardiac CT: a validation study on the detection of intramyocardial fibrosis in consecutive patients. *Int J Cardiovasc Imaging.* (2014) 30:659–67. doi: 10.1007/s10554-013-0358-8
49. Aikawa T, Oyama-Manabe N, Naya M, Ohira H, Sugimoto A, Tsujino I, et al. Delayed contrast-enhanced computed tomography in patients with known or suspected cardiac sarcoidosis: a feasibility study. *Eur Radiol.* (2017) 27:4054–63. doi: 10.1007/s00330-017-4824-x
50. Bettencourt N, Ferreira ND, Leite D, Carvalho M, Ferreira WDS, Schuster A, et al. CAD detection in patients with intermediate-high pre-test probability: low-dose CT delayed enhancement detects ischemic myocardial scar with moderate accuracy but does not improve performance of a stress-rest CT perfusion protocol. *JACC Cardiovasc Imaging.* (2013) 6:1062–71. doi: 10.1016/j.jcmg.2013.04.013
51. Ohta Y, Kishimoto J, Kitao S, Yunaga H, Mukai-Yatagai N, Fujii S, et al. Investigation of myocardial extracellular volume fraction in heart failure patients using iodine map with rapid-kV switching dual-energy CT: segmental comparison with MRI T1 mapping. *J Cardiovasc Comput Tomogr.* (2020) 14:349–55. doi: 10.1016/j.jcct.2019.12.032
52. Kumar V, Harfi TT, He X, McCarthy B, Cardona A, Simonetti OP, et al. Estimation of myocardial fibrosis in humans with dual energy CT. *J Cardiovasc Comput Tomogr.* (2019) 13:315–18. doi: 10.1016/j.jcct.2018.12.004
53. Qin L, Chen C, Gu S, Zhou M, Xu Z, Ge Y, et al. A radiomic approach to predict myocardial fibrosis on coronary CT angiography in hypertrophic cardiomyopathy. *Int J Cardiol.* (2021) 337:113–18. doi: 10.1016/j.ijcard.2021.04.060
54. Zhao L, Ma X, Ge H, Zhang C, Wang Z, Teraoka K, et al. Diagnostic performance of computed tomography for detection of concomitant coronary disease in hypertrophic cardiomyopathy. *Eur Radiol.* (2015) 25:767–75. doi: 10.1007/s00330-014-3465-6
55. Shariat M, Thavendiranathan P, Nguyen E, Wintersperger B, Paul N, Rakowski H, et al. Utility of coronary CT angiography in outpatients with hypertrophic cardiomyopathy presenting with angina symptoms. *J Cardiovasc Comput Tomogr.* (2014) 8:429–37. doi: 10.1016/j.jcct.2014.09.007
56. Takayama H, Yu SN, Sorabella R, Leb J, Pulerwitz TC, Cooper C, et al. Virtual septal myectomy for preoperative planning in hypertrophic cardiomyopathy. *J Thorac Cardiovasc Surg.* (2019) 158:455–63. doi: 10.1016/j.jtcvs.2018.10.138
57. Venlet J, Tao Q, de Graaf MA, Glashan CA, de Riva Silva M, van der Geest RJ, et al. RV tissue heterogeneity on CT: a novel tool to identify the VT substrate in ARVC. *JACC Clin Electrophysiol.* (2020) 6:1073–85. doi: 10.1016/j.jacep.2020.04.029
58. Muser D, Nucifora G, Castro SA, Enriquez A, Chahal CAA, Magnani S, et al. Myocardial substrate characterization by CMR T1 mapping in patients with NICM and no LGE undergoing catheter ablation of VT. *JACC Clin Electrophysiol.* (2021) 7:831–40. doi: 10.1016/j.jacep.2020.10.002
59. Conte E, Mushtaq S, Carbucicchio C, Piperno G, Catto V, Mancini ME, et al. State of the art paper: cardiovascular CT for planning ventricular tachycardia ablation procedures. *J Cardiovasc Comput Tomogr.* (2021) 15(5):394–402. doi: 10.1016/j.jcct.2021.01.002
60. Esposito A, Palmisano A, Antunes S, Maccabelli G, Colantoni C, Rancoita PMV, et al. Cardiac CT with delayed enhancement in the characterization of ventricular tachycardia structural substrate: relationship between CT-segmented scar and electro-anatomic mapping. *JACC Cardiovasc Imaging.* (2016) 9:822–32. doi: 10.1016/j.jcmg.2015.10.024

61. Haugaa KH, Basso C, Badano LP, Bucciarelli-Ducci C, Cardim N, Gaemperli O, et al. Comprehensive multi-modality imaging approach in arrhythmogenic cardiomyopathy-an expert consensus document of the European Association of Cardiovascular Imaging. *Eur Heart J Cardiovasc Imaging*. (2017) 18:237–53. doi: 10.1093/ehjci/jew229
62. Collet C, Onuma Y, Miyazaki Y, Morel MA, Serruys PW. Integration of non-invasive functional assessments with anatomical risk stratification in complex coronary artery disease: the non-invasive functional SYNTAX score. *Cardiovasc Diagn Ther*. (2017) 7:151–8. doi: 10.21037/cdt.2017.03.19

Conflict of Interest: The authors declare that the research was conducted in the absence of any commercial or financial relationships that could be construed as a potential conflict of interest.

Publisher's Note: All claims expressed in this article are solely those of the authors and do not necessarily represent those of their affiliated organizations, or those of the publisher, the editors and the reviewers. Any product that may be evaluated in this article, or claim that may be made by its manufacturer, is not guaranteed or endorsed by the publisher.

frontiers in Cardiovascular Medicine

SYSTEMATIC REVIEW
published: 18 October 2021
doi: 10.3389/fcvm.2021.702560

Facts and Gaps in Exercise Influence on Arrhythmogenic Cardiomyopathy: New Insights From a Meta-Analysis Approach

Julia Martínez-Solé[1†], *María Sabater-Molina*[2,3,4†], *Aitana Braza-Boïls*[4,5‡], *Juan J. Santos-Mateo*[6‡], *Pilar Molina*[5,7], *Luis Martínez-Dolz*[1,4], *Juan R. Gimeno*[3,4,6] *and Esther Zorio*[1,4,5*]

[1] Cardiology Department, Hospital Universitario y Politécnico La Fe, Valencia, Spain, [2] Laboratorio de Cardiogenética, Unidad de Cardiopatías Familiares, Instituto Murciano de Investigación Biosanitaria (IMIB-Arrixaca), Murcia, Spain, [3] Unidad CSUR (Centros, Servicios y Unidades de Referencia) en Cardiopatías Familiares, Hospital Universitario Virgen de la Arrixaca, Murcia, Spain, [4] CIBERCV, Center for Biomedical Network Research on Cardiovascular Diseases, Madrid, Spain, [5] Unidad de Cardiopatías Familiares, Muerte Súbita y Mecanismos de Enfermedad (CaFaMuSMe), Instituto de Investigación Sanitaria La Fe, Valencia, Spain, [6] Cardiology Department, Hospital Universitario Virgen de la Arrixaca, Murcia, Spain, [7] Instituto de Medicina Legal y Ciencias Forenses de Valencia, Histology Unit, Universitat de València, Valencia, Spain

OPEN ACCESS

Edited by:
Fabrizio Ricci,
University of Studies G. D'Annunzio Chieti and Pescara, Italy

Reviewed by:
Franz Gerald Greil,
University of Texas Southwestern Medical Center, United States
Maria Aurora Morales,
National Research Council (CNR), Italy

***Correspondence:**
Esther Zorio
zorio_est@gva.es

[†]*These authors share first authorship*

[‡]*These authors share second authorship*

Specialty section:
This article was submitted to Cardiovascular Imaging, a section of the journal Frontiers in Cardiovascular Medicine

Received: *29 April 2021*
Accepted: *09 September 2021*
Published: *18 October 2021*

Citation:
Martínez-Solé J, Sabater-Molina M, Braza-Boïls A, Santos-Mateo JJ, Molina P, Martínez-Dolz L, Gimeno JR and Zorio E (2021) Facts and Gaps in Exercise Influence on Arrhythmogenic Cardiomyopathy: New Insights From a Meta-Analysis Approach. Front. Cardiovasc. Med. 8:702560. doi: 10.3389/fcvm.2021.702560

Arrhythmogenic cardiomyopathy (ACM) is a genetic cardiac condition characterized by fibrofatty myocardial replacement, either at the right ventricle, at the left ventricle, or with biventricular involvement. Ventricular arrhythmias and heart failure represent its main clinical features. Exercise benefits on mental and physical health are worldwide recognized. However, patients with ACM appear to be an exception. A thorough review of the literature was performed in PubMed searching for original papers with the terms "ARVC AND sports/exercise" and "sudden cardiac death AND sports/exercise." Additional papers were then identified through other sources and incorporated to the list. All of them had to be based on animal models or clinical series. Information was structured in a regular format, although some data were not available in some papers. A total of 34 papers were selected and processed regarding sports-related sudden cardiac death, pre-clinical models of ACM and sport, and clinical series of ACM patients engaged in sports activities. Eligible papers were identified to obtain pooled data in order to build representative figures showing the global incidence of the most important causes of sudden cardiac death in sports and the global estimates of life-threatening arrhythmic events in ACM patients engaged in sports. Tables and figures illustrate their major characteristics. The scarce points of controversy were discussed in the text. Fundamental concepts were summarized in three main issues: sports may accelerate ACM phenotype with either structural and/or arrhythmic features, restriction may soften the progression, and these rules also apply to phenotype-negative mutation carriers. Additionally, remaining gaps in the current knowledge were also highlighted, namely, the applicability of those fundamental concepts to non-classical ACM phenotypes since left dominant ACM or non-plakophillin-2 genotypes were absent or very poorly

represented in the available studies. Hopefully, future research endeavors will provide solid evidence about the safest exercise dose for each patient from a personalized medicine perspective, taking into account a big batch of genetic, epigenetic, and epidemiological variables, for instance, in order to assist clinicians to provide a final tailored recommendation.

Keywords: sports, exercise, arrhythmogenic cardiomyopathy, disease progression, risk factors

INTRODUCTION

The classical definition of arrhythmogenic cardiomyopathy (ACM) refers to a rare genetic disease resulting in myocardial loss and fibrofatty substitution of the ventricular myocardium, involving either right, left, or both ventricles (1, 2) and often presenting inflammatory infiltrates (1) (**Figure 1**). However, in the last years a broader definition of the disease has been proposed to include under this umbrella term also other acquired and genetic pathological entities which share a primary myocardial involvement and a clinical presentation with arrhythmias such as myocarditis, sarcoidosis, amyloidosis, sarcomeric, and mitochondrial defects (3). From now onward, this review is focused only on the original definition of ACM whose reported incidence is 1:5,000 in general population (3).

The genetic basis of ACM has been widely expanded since the initial identification of mutations in the genes encoding desmosomal proteins, and currently other disease-causing non-desmosomal genes have also been recognized (1). Mutations in some genes are prone to present with classical forms of the disease and profound structural and electrical alterations arising from the right ventricle while mutations in other genes tend to involve the left ventricle either in isolation or as the main feature of the disease (**Table 1**) (1, 3–7). Mutations can be identified in 50% of the probands, and the family screening often confirms an incomplete penetrance and a variable expression of the disease. Thus, other factors are thought to play a relevant role as modulators to explain these clinical findings, including epigenetics, virus, sexual hormones, and sports (3). Importantly, gene elusive patients should not be reassessed as having a non-genetic disease since not all ACM genes are known so far and/or certain types of mutation might not be detected with the technology routinely employed (i.e., big rearrangements could be missed by conventional NGS sequencing without copy number variation analyses).

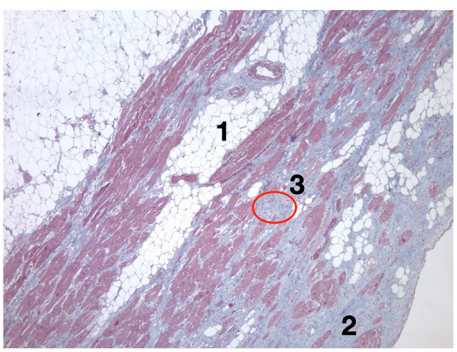

FIGURE 1 | Histological view of the left ventricle of a heart with biventricular arrhythmogenic cardiomyopathy due to the TMEM43 S358L mutation. This patient suffered a sudden cardiac death while practicing sports. The histological hallmarks that define the disease are shown, such as myocardial loss due to fatty infiltration (1) and fibrosis (2); additionally, lymphocytic infiltrates can be observed (3). TMEM43, transmembrane protein 43.

Mutations in ACM mostly involve desmosomal genes and affect the composition of the intercalated disk. Structural remodeling at the intercalated disks yields subsequent electrical remodeling at the neighboring gap junctions and sodium channels and, furthermore, modifications in nuclear signaling and transcriptional activity mediated by Wnt and Hippo pathways (8, 9). The final myocardial substitution by fibrofatty tissue (**Figure 1**) provides the macroscopic anatomical substrate for the ventricular arrhythmias that characterize the disease, but also, at a subcellular scenario, the abovementioned gap junction and sodium current remodeling promote patchy slow conduction areas and re-entrant circuits for ventricular arrhythmias (3).

Exercise and sports practice confer beneficial effects on such a wide variety of organs that their recommendation in general population remains out of debate (10). Despite this compelling evidence, in the last years extensive data have been published to support an adverse influence on patients with ACM. Thus, clinical guidelines have accordingly been released to restrict sports recommendations in this population (**Table 2**) (11), yet a low-intensity exercise is recommended to these patients. A practical advice could be to avoid exercise levels that hamper maintaining a conversation (13).

Exercise testing is usually included in the routine study protocol triggered by the suspicion of ACM ever since it was recommended in the original Task Force criteria for probands and family members. These consensus documents considered left bundle branch ventricular arrhythmias recorded at different tests (including exercise testing) as a minor criterion for probands and as one of the four additional criteria besides being a first-degree relative for family members (14). A challenging paper demonstrated that exercise testing could unmask depolarization and repolarization abnormalities as well as ventricular arrhythmia in mutation carriers, irrespective of the fulfillment of Task Force criteria and the symptomatic state, suggesting a potential use of this test to prescribe exercise in case it could be validated in that scenario (15). Against this hypothesis, another interesting work compared the arrhythmogenicity response during the isoproterenol and

TABLE 1 | List of arrhythmogenic cardiomyopathy-causing genes and the main characteristics of their phenotype.

Gene name	Gene symbol	Gene location	RV involvement	Biventricular involvement	LV involvement	% In probands*
Plakoglobin	JUP	17q21.2	Yes	Yes	No	0–1
Desmoplakin	DSP	6p24.3	No	Yes	Yes	3–15
Plakophillin-2	PKP2	12p11.21	Yes	Yes	No	20–46
Desmoglein-2	DSG2	18q12.1	Yes	Yes	Yes	3–20
Desmocollin-2	DSC2	18q12.1	Yes	Yes	No	1–8
Transforming growth factor beta-3	TGFB3	14q24.3	Yes	No	No	?
Transmembrane protein 43	TMEM43	3p25.1	Yes	Yes	No	0–2
Titin	TTN	2q31.2	Yes	Yes	Yes	0–10
Desmin	DES	2q35	No	Yes	Yes	0–2
Filamin C	FLNC	7q32.1	No	No	Yes	3
Lamin A/C	LMNA	1q22	No	Yes	Yes	0–4
Phospholamban	PLN	6q22.31	No	Yes	Yes	0–1
Alpha-3 catenin	CTNNA3	10q21.3	Yes	Yes	No	0–2
Cadherin-2	CDH2	18q12.1	Yes	Yes	No	0–2
Sodium voltage-gated channel, alpha subunit 5	SCN5A	3p22.2	Yes	Yes	Yes	2
RNA-binding motiv protein 20	RBM20	10q25.2	No	No	Yes	1
LIM domain binding 3	LDB3	10q23.2	Yes	No	No	?
Tight junction protein 1	TJP1	15q13.1	Yes	Yes	No	<5%

**Except in specific geographical regions, where it could be much higher. Modified from (1, 3–7). ?: unknown.*

TABLE 2 | Modified exercise recommendations for patients with arrhythmogenic cardiomyopathy included in the European Society of Cardiology guidelines.

ESC 2020 exercise recommendation	Class of recommendation	Level of evidence
Participation in 150 min of low-intensity exercise per week should be considered for all individuals.	IIa	C
Participation in low- to moderate-intensity recreational exercise/sports*, if desired, may be considered for individuals with no history of cardiac arrest/VA, unexplained syncope, minimal structural cardiac abnormalities, <500 PVCs/24 h, and no evidence of exercise-induced VAs. *This category includes bowling, cricket, curling, golf, riflery, and yoga.	IIb	C
Participation in high-intensity recreational exercise/sports or any competitive sports is not recommended in individuals with ACM, including those who are gene positive but phenotype negative.	III	B

Low-intensity, light exercise: below the aerobic threshold, <40% of maximum oxygen consumption, <55% of maximum heart rate, <40% of heart rate reserve, rate of perceived exertion scale 10-11. Moderate-intensity exercise: between the aerobic and the anaerobic thresholds, 40–69% of maximum oxygen consumption, 55–74% of maximum heart rate, 40–69% of heart rate reserve, rate of perceived exertion scale 12-13. VA, ventricular arrhythmias; PVC, pre-mature ventricular contraction; ACM, arrhythmogenic cardiomyopathy (11, 12).

the exercise test in 37 ACM patients and underlined the frequent and falsely reassuring reduction or abolishment of baseline ventricular arrhythmia during the exercise testing (16). Only one paper has assessed the safety and usefulness of cardiopulmonary exercise testing in 38 ACM patients, concluding that it is safe and that the ventilatory efficiency may predict heart transplantation-free survival (17). However, no studies have been carried out focused on the role of exercise and cardiopulmonary exercise testing to prescribe exercise in ACM patients engaged in sports and followed during a suitable period of time. Additionally, one may acknowledge that it is hard to extrapolate the ideal timely situation of these tests performed in a hospital setting with a random training session in which hydration, blood volume, electrolytes, acid–base balance, and catecholamine levels can widely vary and transiently increase the baseline electrical instability in ACM patients necessary to trigger ventricular arrhythmias during sports. Thus, no specific recommendation can be given regarding this issue and the authors strongly advise to adhere the current guidelines (**Table 2**) designed on the exercise dose without considering the result of any type of exercise testing and based on the body of evidence discussed in the following sections.

From a mechanistic point of view, the pressure overload produced by physical exertion may cause a stronger wall stress and more severe myocardial damage at the right ventricle than at the left ventricle (3, 13, 18). Thus, as long as no other factor played any other role, a more deleterious effect on ACM with right ventricular involvement might be expected than in left dominant forms. Damage may include abnormal signaling promoting apoptosis, fibrosis, and adipogenic and inflammatory cascades (13). The last one might be exaggerated in trained patients with ACM or mutation carriers since prolonged periods of intensive physical training can additionally depress immunity and promote inflammation as well (19).

Herein we present a review of the published evidence regarding exercise and sports practice in ACM patients, highlighting the remaining gaps to be addressed in the future.

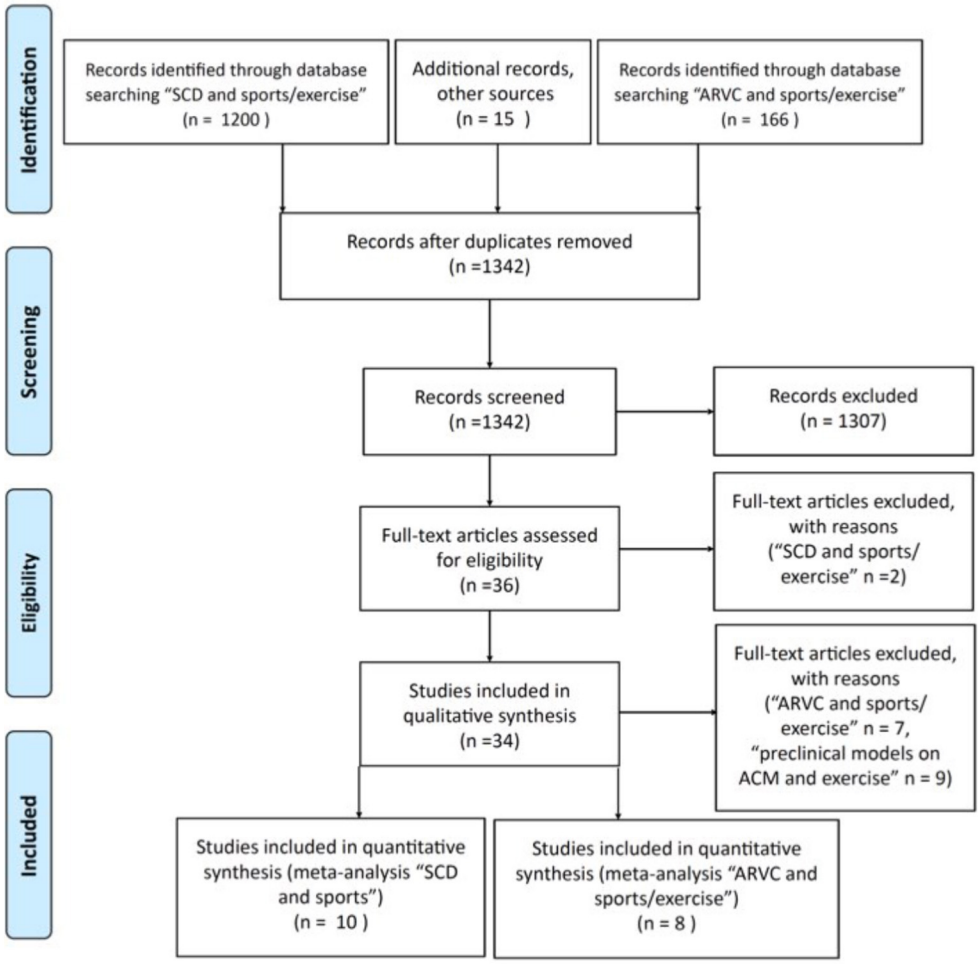

FIGURE 2 | PRISMA flowchart for the identification of papers to obtained pooled data on the causes of sports-related sudden cardiac deaths and on the estimates of life-threatening arrhythmic events in ACM patients engaged in sports. SCD, sudden cardiac death; ARVC, arrhythmogenic cardiomyopathy.

METHODS

A thorough review of the literature was performed in PubMed by searching papers with the terms "sudden cardiac death (SCD) AND sports/exercise" and "ARVC AND sports/exercise" between 2002 and February 2021 and in English language (**Figure 2**). This search yielded 1,366 papers, and 15 additional papers were then identified through other searches and/or cited by reviews. Duplicates were eliminated and records screened yielding 36 original papers assessed for eligibility. The information given in these papers was structured in a regular format and presented in Tables, although some data were not available in some papers. We next excluded two papers from the search "SCD AND sports/exercise" because data from SCD cases could not be differentiated from those from cases surviving from sudden cardiac arrests ($n = 1$) and because the same research group had published another selected paper with a bigger sample size which included the excluded paper ($n = 1$). At this point of the PRISMA flowchart, some other studies were excluded for quantitative analyses because relevant numerical data were missing but nonetheless were considered suitable for full-text qualitative synthesis and structured in descriptive Tables dealing with preclinical models on ACM and exercise ($n = 9$) and "ARVC AND sports/exercise" ($n = 7$). The final quantitative synthesis to analyze the global prevalence of the different causes of sports-related SCD and the quantitative synthesis to estimate the life-threatening arrhythmic events (LAEs) in ACM athletes were performed as follows. Proportions for each diagnosis as the cause of death in sports-related SCD series were extracted from each of the 10 selected studies, and their 95% confidence intervals (CIs) were calculated. Annual LAE rates of ACM athletes were calculated for each of the eight selected studies, and CIs were calculated by using the Poisson distribution. Standardized (5-year) rates of LAE were presented in forest plot graphs, and odds ratio calculations were obtained with a meta-analysis dedicated software [Review Manager (RevMan) 5.4. Copenhagen:

The Nordic Cochrane Center, The Cochrane Collaboration, 2020]. Three main sections were prepared, namely, observational studies regarding ACM in sports-triggered sudden cardiac death, preclinical ACM models, and exercise and clinical series analyzing the effect of exercise on ACM. Finally, an additional fourth section supporting the possibility of strenuous exercise as stand-alone cause of ACM was added to the present manuscript.

OBSERVATIONAL STUDIES: ACM IN SPORTS-TRIGGERED SUDDEN CARDIAC DEATH

The causes underlying a heart arrest or an SCD of someone practicing sports have focused the attention of researchers. Published papers have tried to shed some light on the causes of sports-related SCD from a wide range of settings and based on a variable percentage of forensic studies. They have underlined that ACM represents a not negligible cause of death in this scenario, accounting for roughly 0–28% of the autopsied cases (20–29). The fact that in non-autopsy-based studies ACM is sometimes not even mentioned highlights the difficulties in getting a firm diagnosis when cardiac pathology is missing, as it often happens both in SCD and in sudden cardiac arrest reports (29, 30). Moreover, the pathological overlap of ACM, myocarditis, and idiopathic left ventricular fibrosis allows to speculate that some of the cases with those diagnoses should further increase the real percentage of ACM as the cause of death in case a molecular autopsy confirmed this hypothesis. **Supplementary Table 1** summarizes the main papers reporting the cause of death in sports-related SCD series. As expected, the percentage of SCD attributable to coronary artery disease (CAD) increases paralleling the age of the recruited victims, with a maximal prevalence (63%) in the Spanish study by Morentin et al. ($n = 288$) which also reported male predominance and the highest mean age (44 ± 14 years old) of the reviewed series (28). For unknown reasons, even though Spain is considered a country with low prevalence of CAD, its 63% CAD prevalence (28) is double as much as that observed in the Danish series reported by Risgaard et al., with a similar age (41 ± 10 years old) and also with male predominance but with a remarkably smaller sample size ($N = 44$).

Pooled data obtained from papers in **Supplementary Table 1** are shown in **Figure 3** with the global estimates of the prevalence of CAD, hypertrophic cardiomyopathy, ACM, and sudden arrhythmic death syndrome in these series. Our data show that CAD and hypertrophic cardiomyopathy should be considered the leader causes of sports-related SCD, although in the youngest subsets of victims inherited cardiac conditions such as hypertrophic cardiomyopathy, ACM, and sudden arrhythmic death syndrome clearly prevail (20, 21, 24, 27). Right after CAD and hypertrophic cardiomyopathy, sudden arrhythmic death syndrome represents the third global cause of death in sports-related SCD. As cardiogenetic knowledge and resources continue to grow, more molecular autopsies will be hopefully performed and thus specifically ascribe these deaths to certain syndromes such as long QT syndrome, Brugada syndrome, and catecholaminergic polymorphic ventricular tachycardia. Taking into account the prevalence in general population of hypertrophic cardiomyopathy and ACM (1:500 vs. 1:5,000, respectively) and our global estimates for them in sports-related SCD series (roughly 20 and 10%, respectively), another important remark is that the risk for developing a sports-related SCD in ACM patients is five-fold that of patients with hypertrophic cardiomyopathy. In keeping with these data, in 72% of 66 ACM cases recruited after a sudden cardiac death or a sudden cardiac arrest, events occurred on exertion (31). Although the genetic background of the geographical area in which the studies were performed and the implementation of pre-participation screening may have influenced the final outcomes, it appears clear that ACM is overrepresented in sports-triggered sudden cardiac death.

PRECLINICAL ACM MODELS AND EXERCISE

Animal models provide a useful setting to test hypotheses that cannot easily be tested in *in vitro* cultures, such as the global effect of exercise in an organism in terms of development of both arrhythmic and structural burden. **Table 3** updates the major findings of the effect of exercise in several animal models of ACM. Additionally, a paper based on cell cultures assuming stress shear as a subrogate of exercise has been incorporated.

In summary, trained heterozygous transgenic mice suffered adverse cardiac remodeling. All in all, experiments with plakoglobin, plakophillin-2, and desmoplakin transgenic animals revealed a pro-arrhythmic remodeling with an impaired cardiac electrical conduction and an altered expression of Ca2+-handling-related proteins, with controversial results with respect to development of structural abnormalities in this scenario, as summarized in **Table 3**. The great differences in the selected genetic background, the study protocols, and their endpoints foreclose precise comparisons between these studies and/or data processing to obtain pooled data with meta-analysis strategies. Slowed conduction was probably the consequence of the C×43 dyslocalization and reduced sodium current (33, 36) and the substrate for ventricular arrhythmias and increased inducibility (32–34, 39). Additionally, exercise-triggered development of fibrosis, apoptosis, chamber enlargement, and systolic dysfunction was reported by some authors (32, 33, 36–38) but not by others (39). Interestingly, pretreatment with preload-reducing therapy (furosemide and nitrates) softened the ACM phenotype after exercise, in terms of both structural and electrical abnormalities (33). Moreover, similar results to these were observed with intervention to downregulate the canonical Wnt pathway by inhibiting GSK3b with SB216763, either in sedentary and exercised mutant mice (38) or in cell cultures exposed to shear stress (35). Thus, in keeping with the current pathophysiology of ACM, down-expression of the Wnt pathway does play a key role in ACM development under exercise and wall stress conditions, which challenges the desmosome integrity and the electrical stability.

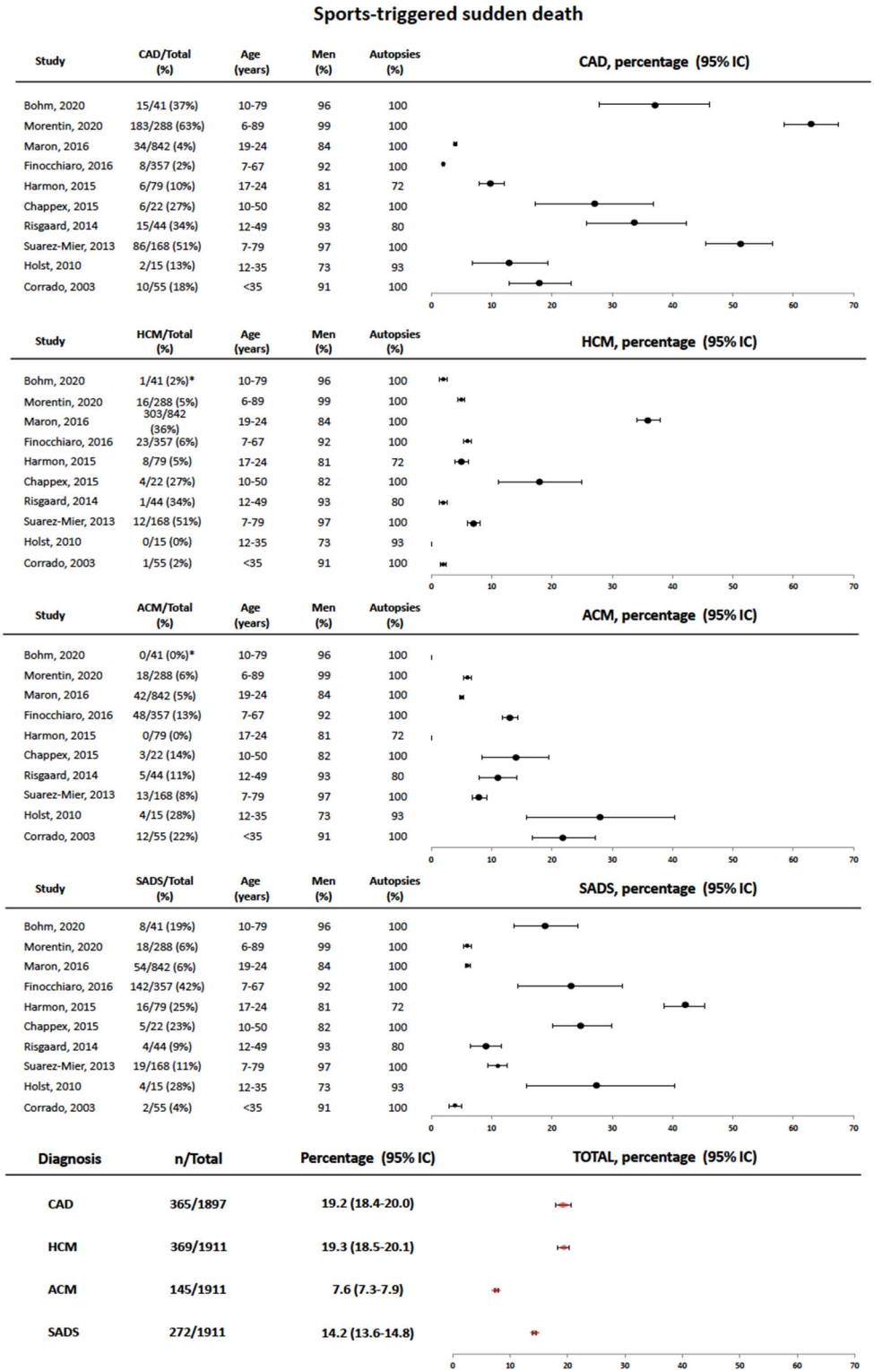

FIGURE 3 | Forest plot showing pooled data of the causes of sports-triggered sudden cardiac death in different series referenced in the text. At the bottom, total estimates are provided for each diagnosis. SCD, sudden cardiac death; CAD, coronary artery disease; SADS, sudden arrhythmic death syndrome; HCM, hypertrophic cardiomyopathy; ACM, arrhythmogenic cardiomyopathy. *The causes of death can be only retrieved form the 41 cases of sports-related sudden death cases with autopsy.

TABLE 3 | Pre-clinical ACM models to test the effect of exercise on the phenotype.

	Type of model	Age of the mice	Exercise protocol details	Results
Kirchhof et al. (32)	Heterozygous plakoglobin-deficient mice (PG–/+) vs. WT	10 months old	Swimming endurance protocol, 8 weeks	PG–/+ mice exhibited structural and arrhythmic ACM features. Isolated, perfused PG–/+ hearts had spontaneous VT of RV origin and prolonged RV conduction times compared with WT hearts. Endurance training accelerated abnormalities in PG–/+ mice. RV histology and electron microscopy were normal in affected animals.
Fabritz et al. (33)	Heterozygous plakoglobin-deficient mice (PG–/+) vs. WT	10 months old	Swimming endurance protocol, 7 weeks Mice were randomized to a load-reducing therapy (furosemide and nitrates) or placebo	Therapy prevented training-induced RV enlargement in PG–/+ mice. Untreated PG–/+ hearts had reduced RV longitudinal conduction velocity, more spontaneous macro re-entrant VTs than treated and WT and lower concentration of phosphorylated C×43 than WT, especially in those with VTs. PG–/+ hearts showed reduced myocardial plakoglobin concentration, whereas b-catenin and N-cadherin concentration was not changed.
Lyon et al. (34)	Homozygous desmoplakin-deficient mice (DSP–/–) vs. WT	4 months old	Running on a treadmill, 5 days of acclimatization and 1 session of at least 45 min or until exhaustion, then, mice received a high (2 mg/kg) or low (0.5 mg/kg) epinephrine dose	Increased PVCs were observed in DSP–/– mice when exposed to exercise and epinephrine. Interestingly, high doses of epinephrine in combination with exercise could also induce sudden cardiac death in DSP–/– mice that was not observed in littermate controls.
Hariharan et al. (35)	Cell cultures expressing mutant plakoglobin (JUP) or plakophillin-2 (PKP2) vs. knockdown cell cultures vs. WT cell cultures	-	Cell–cell adhesion assays, immunoblotting, atomic force microscopy, immunofluorescence, TUNEL assay and shear flow experiments (to simulate strenuous exercise) were performed	Mutant cells showed no differences, while knockdown cultures showed weakened cell–cell adhesions. Upon shear stress, mutant cultures failed to increase the amount of immunoreactive signal for plakoglobin or N-cadherin, as observed in WT. In contrast to WT, apoptosis was increased in cells expressing mutant JUP, both in resting conditions and also in response to shear stress. Abnormal responses to shear stress associated with mutant JUP or PKP2 could be reversed by SB216763 (SB2), a GSK3b inhibitor.
Cruz et al. (36)	Heterozygous PKP2 R735X mice (PKP2–/+), obtained with AAV9 technology	AAV9 injection at 4–6 weeks old Exercise 2 weeks later	Swimming endurance protocol, 8 weeks	CMR at 10-months post-infection detected an overt RV ACM phenotype and histologically C×43 dyslocalization in trained PKP2–/+ mice but not in their sedentary littermates.
Martherus et al. (37)	Heterozygous mice for the human desmoplakin gene carrying DSP R2834H vs. WT	4 months old	Running on a treadmill, 12 weeks	DSP R2834H mice displayed structural features of RV ACM with normal LV and endurance exercise accelerated ACM pathogenesis paralleling a perturbed AKT1 and GSK3-β signaling pathways.
Chelko et al. (38)	Homozygous DSG2 and heterozygous JUP mutant mice vs. WT	3 months old.	Graded exercise training (swimming) since week 5 until 12. Since week 3 some mice started treatment with SB216763 (SB2)	SB2 prevents myocyte injury and cardiac dysfunction *in vivo* in two murine models of ACM at baseline and in response to exercise (in terms of LVEF, survival, and normalization of intercalated disk distribution or in terms of ventricular ectopy and myocardial fibrosis/inflammation reduction, respectively).
van Opbergen (39)	Heterozygous plakophillin-2-deficient mice (PKP2–/+) vs. WT	4 months old	Running on a treadmill, 4 weeks	In PKP2–/+ mice, protein levels of Ca2+ -handling proteins were reduced compared to WT. Trained PKP2–/+ showed a pro-arrhythmic remodeling with RV lateral connexin43 expression, RV conduction slowing, and a higher susceptibility toward arrhythmias.
Cheedipudi (40)	Heterozygous desmoplakin-deficient mice (DSP–/+) vs. WT	6 months old	Running in a treadmill, 12 weeks	A differential gene expression was observed in DSP–/+ vs. WT mice, including upregulated genes inhibitors of the canonical Wnt pathway. Exercise restored transcript levels of 2/3rd of the differentially expressed genes. The changes were associated with reduced myocardial apoptosis and eccentric cardiac hypertrophy without changes in cardiac function and arrhythmias.

WT, wild type; Cx43, Connexin43; GSK3-β, glycogen synthase kinase 3-β; AKT1, protein kinase B; LV, left ventricular; RV, right ventricular; CMR, cardiac magnetic resonance imaging.

In contrast, only one paper supported a somehow beneficial effect of exercise on ACM. Indeed, it showed a restoration of the abnormal baseline expression pattern in the left ventricular myocardium of DSP-mutant mice upon exercise, so that it reduced myocardial apoptosis and induced eccentric cardiac hypertrophy without affecting cardiac function or arrhythmia

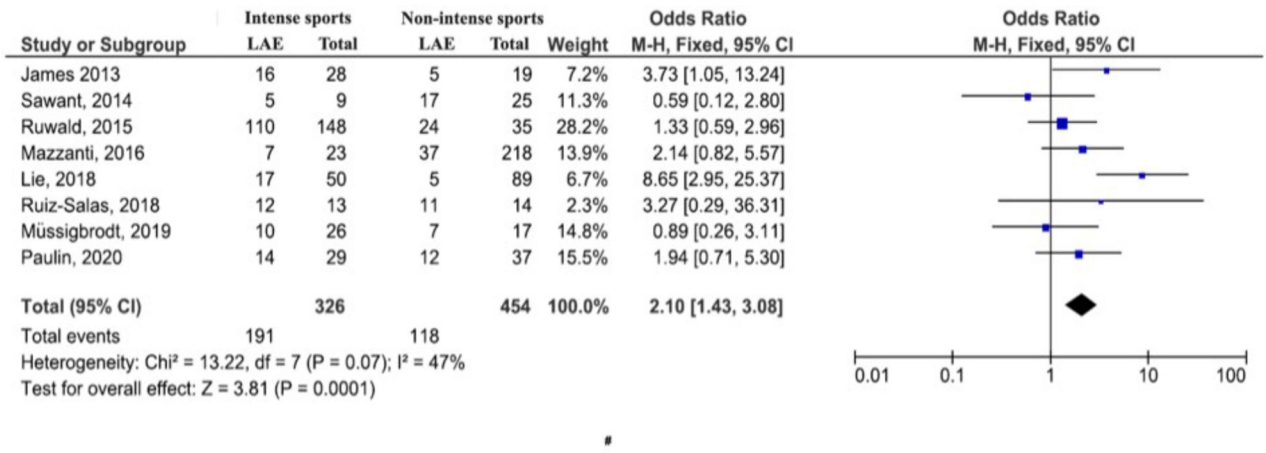

#

Reference	LAE/Total (%)	Age	Men (%)	Sports class	LAE before (%)	PKP2/DSP[&] (%)	TFC2010 (+) (%)	ALVC (%)
James, 2013	39/87 (45%)	44±18	53	B,A	30,0	87/3	64	NA
Sawant, 2014	28/43 (65%)	43±14*	65*	B,A	72,0	0/0*	100	NA
Ruwald, 2015	79/108 (73%)	41 *	56	B,A	69,0	NA	87	NA
Mazzanti, 2016	47/267 (18%)	38±18 *	58 *	A	0,0	NA	100	NA
Lie, 2018	18/117 (15%)	40±17	50	B	0,0	74/2	100	17
Ruiz-Salas, 2018	21/36 (58%)	45±18	78	B,A	83,0	53/8	53	8
Müssigbrodt, 2019^	15/23 (65%)	53±14	68	B,A	100,0	NA	100	NA
Paulin, 2020^^	30/80 (38%)	37 *	40	B	0,0	0/0 #	NA	NA

FIGURE 4 | Forest plot represents standardized (5-year) rate of life-threatening arrhythmic events (LAE) and 95% CI from eight selected studies referenced in the text. Odds ratios for intense vs. non-intense exercise were calculated per study. Pooled data represented in the bottom black diamond (Review Manager 5.4). Bottom table summarizes relevant extracted demographic and clinical data from the eight selected articles. N, number; Y, years; FU, follow-up; TFC2010, Definite Task Force Criteria for arrhythmogenic right ventricular cardiomyopathy; ALVC, arrhythmogenic left ventricular cardiomyopathy; ∧VT ablation series, ∧∧ICD series, primary prophylaxis. Sports class: sports classification depending on physical activity before (B)/after (A) recruitment. [&]Data referred to the total sample size referred at the second column, even though some patients may not have had genetic studies performed and, if done, others may not have mutation identified. *Figure approximated from the data given in the paper. #All carriers of the mutation TMEM43 S358L. NA, not available.

susceptibility (40) with a similar protocol to that used in another study also on DSP-mutant mice which yielded opposite results (37). Maybe the slight differences in the age of the animals, the details of the exercise treadmill protocol, or the different DSP mutations (deletion vs. missense) could account for part of these discrepancies which, anyhow, lay out of the scope of this review and could be clarified with future studies assessing this issue.

CLINICAL SERIES ANALYZING THE EFFECT OF EXERCISE ON ACM

In line with the previous sections of this manuscript regarding the causes of sports-associated SCD and the results on exercised ACM animal models, also clinicians have gathered a valuable piece of evidence by analyzing clinical series of ACM patients engaged in sports. Shown in **Supplementary Table 2** is a list of observational studies which have reported outcomes in clinical series.

Taken all together, a definite deleterious effect of exercise on the structural and the arrhythmic phenotype of ACM has been proved. Some studies focus their interest on sports training defined in terms of intensity and duration (either competitive or recreational), but others broaden the analysis to physical activity in general. Some interesting series have helped to define the specific risk of physical activity in mutation carriers not exhibiting an overt ACM phenotype, concluding that exercise also promotes disease progression in this scenario (41, 42). Others have assessed the effect of exercise restriction to find out an improvement in outcomes (43, 44) regardless of the previous level of training (45). Although more exercise causes more electrical and/or structural progression (41, 43, 46–48), the intensity rather than the duration of the exercise performed seems to play a more determinant role. Indeed, intensity rather than duration is strongly linked to adverse prognosis (49, 50) and, furthermore, its reduction more effectively improves the arrhythmic burden (44). Also in the scenario of ACM patients with ablation for ventricular tachycardia, exercise activity was an independent risk factor for future LAEs (51, 52). Aiming to give a quantitative recommendation to patients, several authors suggested that <2.5 h per week and <6 METS both in probands and relatives (50) or <650 MET-Hr/years (metabolic equivalent hours obtained from multiplying METs by duration)

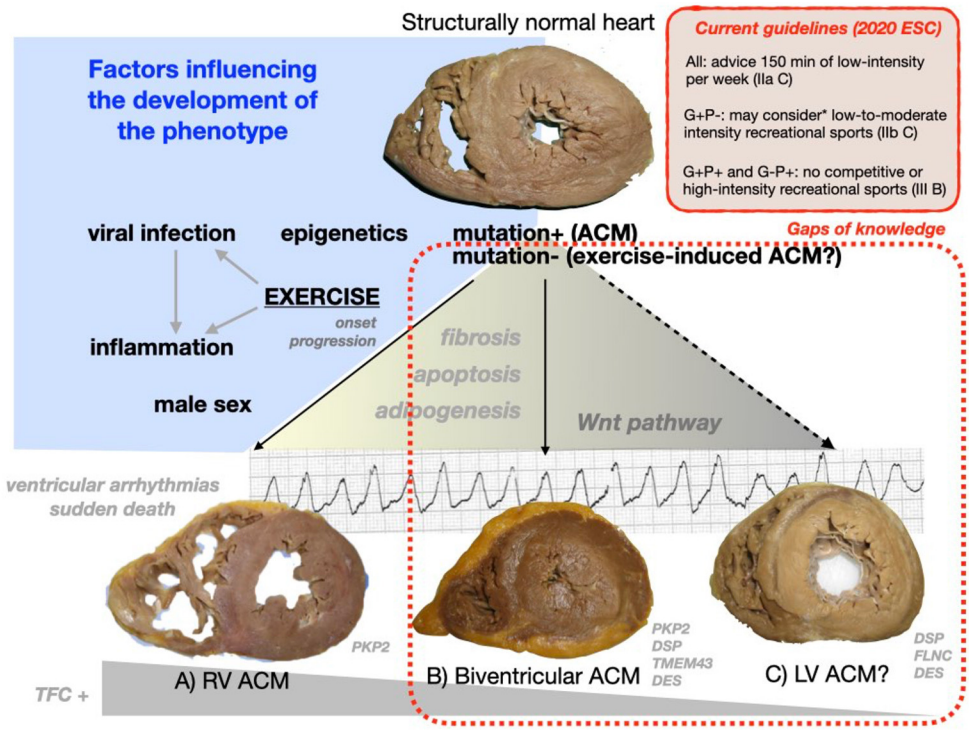

FIGURE 5 | Central figure. The progression of a structurally normal heart harboring a mutation or without any genetic hit to an ACM phenotype involving just the right ventricle **(A)**, both ventricles **(B)** or the left ventricle in isolation **(C)**. **(A–C)** Were obtained at autopsies of patients with ACM and sports-triggered sudden cardiac death. Different factors may modulate this transition yielding structural and arrhythmic features through the Wnt pathway dysregulation (as presented in **Table 3**). The rate of patients fulfilling TFC 2010 and the specific mutated genes underlying may widely differ among ACM phenotypes A–C. The most important genotype–phenotype associations based on the authors clinical and forensic experience are shown at the bottom of this figure (further information on this topic is provided in **Table 1**). *Only applicable to low risk patients with no history of cardiac arrest/ventricular arrhythmias, unexplained syncope, minimal structural cardiac abnormalities, <500 PVCs/24 h, and no evidence of exercise-induced complex ventricular arrhythmias (11). ACM, arrhythmogenic cardiomyopathy; ESC, European Society of Cardiology; G, genotype; P, phenotype; TFC, Task Force Criteria 2010; LV, left ventricular; RV, right ventricular; PKP2, plakophillin-2; DSP, desmoplakin; DSG2, desmoglein-2; DES, desmin; TMEM43, transmembrane protein 43; FLNC, filamin C; PVCs, premature ventricular complexes.

in relatives (49) could be safe and healthy. Accordingly, a precise recommendation has been introduced in current guidelines (**Table 2**). From an ambiguous qualitative perspective, one paper highlighted that recreational but not competitive sports may be safe in ACM patients since their practice does not aggravate prognosis in comparison to inactive patients (53). However, reports on LAEs triggered by recreational sports in ACM patients (54) and the wide range of the intensity of recreational sports hamper the extrapolation of this result to everyday practice so that sports quantification in terms of intensity and duration is preferred over a recreational vs. competitive sports classification. Finally, the hypothesis of the interaction of environmental and genetic factors on the final ACM phenotype remarkably gathers strength in this scenario. Indeed, the more weight of the environment (sports), the least influence of genetics and, vice versa; highly lethal mutations entail such a poor prognosis that there is little room left for environmental influence on the final phenotype. Thus, patients with a negative genetic result appear to have the greatest influence of sports on their structural and electric ACM phenotype (42), whereas in carriers of the dangerous TMEM43 S358L mutation, the impact of exercise on prognosis fades out by increasing the threshold up to 9 MET-Hr/day (3,285 MET-Hr/year) in order to find significant differences in LAEs (55).

Suitable papers from **Supplementary Table 2** were further processed to integrate all those series in a meta-analysis with stronger evidence. First, we acknowledge certain limitations in data collection derived from the great differences observed in the design of the studies. There were also differences in assessing the sport performed, sometimes before recruitment, others before and after, and occasionally only the sport performed after enrollment was used to classify patients. As observed in **Figure 4**, our pooled data confirm that ACM patients engaged in high-intensity sports activities have a significant two-fold increase in the risk of developing LAE when compared to ACM patients who report lower physical activity habits (OR 2.1, 95% CI 1.43–3.8). Unfortunately, we have not been able to compare the age of the LAEs in both groups, but, as observed in some of the reviewed papers, it was significantly younger in the sports-engaged ACM patients. Our meta-analysis approach to evaluate the risk of LAE in ACM patients depending on their sports practice is brand new and provides strong and compelling evidence to reassure the need of sports restriction in this scenario. Furthermore, our

systematic review of all these papers has allowed us to highlight that the vast majority of patients exhibited a classical phenotype (definite Task Force Criteria 2010), that the representation of patients harboring non-PKP2 mutations was really small, and that the percentage of patients with left ventricular involvement remains widely unknown. Thus, clinicians should be aware that little evidence now support any exercise recommendation out of the clinical profile of the papers herein reviewed.

STRENUOUS EXERCISE AS STAND-ALONE CAUSE OF ACM

Strenuous exercise may induce cardiac adaptation in the so-called athlete heart. Further maladaptive remodeling may lead to develop features resembling ACM at one or both ventricles.

Endurance athletes are exposed to myocardial damage as a direct consequence of their high-level training with a subsequent rise in blood BNP, CK-MB, troponin-T, and troponin-I (56). Additionally, athletes exhibit an increased risk of right ventricular remodeling and ventricular arrhythmias typically arising from the right ventricle, yielding a variable percentage of individuals fulfilling ACM Task Force Criteria 2010, up to 59% definite and 30% borderline/possible by some authors (57) or 57% borderline/possible in other series (58). However, these athletes have been proved to have a lower than expected rate of mutation-positive studies (13% in athletes vs. 50% reported in papers concerning ACM in general) (59). Thus, the so-called exercise-induced ACM was proposed to explain the occasional development of a phenotype identical to classical ACM in endurance athletes (mostly cyclists) (56), sometimes with subepicardial right ventricular outflow tract scar as substrate for fast ventricular tachycardia (60), which was then reproduced in a mouse model (61). The incidence of such a cardiac behavior is rare, around 1/1,000 at risk individuals but suspected to be as high as 1/100 in top elite athletes (56). Remarkably, the continuum between sports-triggered right ventricular remodeling and an ACM phenotype, the low incidence of exercise-induced ACM, and the limitation of the yield of the genetic studies (see introduction) preclude an accurate definition of the outcomes of this entity. Thus, current guidelines on sports recommendations (11) do not make any distinction between genetic and suspected exercise-induced ACM in terms of exercise restriction once an overt ACM phenotype is present. Among the clinical series reviewed on the topic "ACM and sports/exercise," two of them specifically focused on outcomes in gene elusive individuals (41, 46). As previously commented, this group might include both genetic ACM with negative genetic results and sports-induced ACM. **Supplementary Table 2** includes a brief summary of these papers showing that, in comparison to gene-positive individuals, gene-negative patients need to train harder to develop the ACM phenotype (41) and that sports restriction reduced ventricular arrhythmias in them more often than in gene-positive patients (46).

Finally, also the left ventricle can suffer some sort of exercise-triggered damage identified as non-ischemic subepicardial scars mimicking those observed in left dominant ACM patients, healed myocarditis, or even Fabry disease. Indeed, myocardial fibrosis detected by late gadolinium enhancement resonance imaging has been reported to occur in up to 50% of asymptomatic athletes and veteran triathletes, mostly at meso/epicardial inferolateral left ventricular walls, mostly in men, and associated with higher blood pressure, myocardial mass, and longer cumulative distances (62–65). A cycling race distance of >1,880 km completed during competition had the highest accuracy to predict late gadolinium enhancement (63). On the contrary, other clinical series did not find any late gadolinium enhancement in endurance athletes (58) so that the real prevalence of this feature unfortunately remains widely unknown.

CONCLUSIONS

Arrhythmogenic cardiomyopathy accounts for roughly 10% of all sports-related SCDs which implies a five-fold risk of suffering an SCD in comparison to that of patients with hypertrophic cardiomyopathy based on sports-related SCD series. The young age of the athletes and certain specific geographical regions may profoundly increase these estimates. Despite the beneficial effect of exercise in general population, physical activity promotes the onset and aggravates the structural and electrical features of ACM both in preclinical models and in clinical series. The very few exceptions of papers reporting conflicting results may account for differences in the design of the studies. Our pooled data based on previously published studies confirm that high-intensity sport is associated with a two-fold increase in the risk of LAE. The promising preclinical data which support a beneficial effect of drug intervention to lower preload may open avenues in the future to partially mitigate the negative impact of sports on ACM patients who, despite international recommendations, decide to maintain their high-intensity physical activities. Already reported evidence shows that the intensity rather than duration of exercise is responsible for this negative effect. Moreover, sports restriction seems to partially improve the phenotype but does not completely blur the risk of structural progression and arrhythmic events in previously trained athletes, so that the decision to implant an ICD should remain independent of their degree of sport engagement. Physical exercise at <6 METS and <2.5 h (150 min) per week could be safe for both ACM patients and mutation carriers.

Remarkably, the knowledge herein reviewed suffer from some challenging limitations (knowledge and gaps are showed in **Figure 5**).

First, evidence has been gathered in preclinical and clinical series with *classical* ACM phenotypes often *requiring a definite* Task Force Criteria 2010 at recruitment and with a high percentage of *plakophillin-2* mutations. The clinical characterization of left ventricular involvement was incomplete in most of the available papers and the presence of mutations in genes typically associated with left ventricular phenotype is rare (**Supplementary Table 2**). Therefore, the global effect of physical activity and the threshold for a safe exercise recommendation in left ventricular ACM and in carriers of non-plakophillin-2 mutations (such as desmoplakin or desmin) have not been yet specifically addressed.

Second, although it has been suggested that *strength exercise* (predominantly static) might be safer for ACM patients than sports with a high dynamic demand, it has not been specifically studied and proved so far. Sports with a low dynamic and static component include bowling, cricket, curling, golf, riflery, and yoga.

Furthermore, to *what extent endurance exercise may induce* a right ventricular or left ventricular ACM phenotypes itself or if some sort of genetic background needs to be present remains unknown.

Future research endeavors may hopefully fill in these gaps soon (**Figure 2**). Personalized medicine will probably take into account a wide range of genetic, epigenetic, and epidemiological variables, to accurately assist clinicians willing to recommend a safe exercise-practice to ACM patients.

DATA AVAILABILITY STATEMENT

Publicly available datasets were analyzed in this study. This data can be found here: we have reviewed the available papers on sports and arrhythmogenic cardiomyopathy to show the evidence in a systematic approach to the readers. No original dataset have been used for this article.

AUTHOR CONTRIBUTIONS

JM-S and JS-M reviewed the papers regarding the effect of sport on ACM in clinical series, prepared **Supplementary Table 2**, and edited the manuscript. PM and EZ performed the Pubmed search, reviewed the papers regarding the sports-triggered SCD, prepared **Supplementary Table 1**, selected the pictures included in **Figures 1**, **5** from her personal archive, and edited the manuscript. JG, MS-M, and AB-B reviewed the papers regarding the pre-clinical evidence of sports on ACM, prepared the **Table 3**, and edited the manuscript. LM-D reviewed the current knowledge about the genetic background of ACM, prepared **Tables 1**, **2**, and edited the manuscript. JG and EZ prepared the data from the papers to perform the meta-analyses. JG and MS-M performed the statistical analyses. MS-M built the Forest plots and draw the **Figures 3**, **4**. EZ conceived the review manuscript, supervised the tables, figures, wrote, and edited the manuscript. All authors contributed to the article and approved the submitted version.

FUNDING

This work was in part supported by grants from Instituto de Salud Carlos III and FEDER Union Europea, Una forma de hacer Europa (PI18/01582, PI18/01231).

SUPPLEMENTARY MATERIAL

The Supplementary Material for this article can be found online at: https://www.frontiersin.org/articles/10.3389/fcvm.2021.702560/full#supplementary-material

REFERENCES

1. Elliott PM, Anastasakis A, Asimaki A, Basso C, Bauce B, Brooke MA, et al. Definition and treatment of arrhythmogenic cardiomyopathy: an updated expert panel report. *Eur J Heart Fail.* (2019) 21:955–64. doi: 10.1002/ejhf.1534
2. Corrado D, Marra MP, Zorzi A, Beffagna G, Cipriani A, De Lazzari M, et al. Diagnosis of arrhythmogenic cardiomyopathy: the Padua criteria. *Int J Cardiol.* (2020) 319:106–14. doi: 10.1016/j.ijcard.2020.06.005
3. Bennett RG, Haqqani HM, Berruezo A, Della Bella P, Marchlinski FE, Hsu CJ, et al. Arrhythmogenic cardiomyopathy in 2018-2019: ARVC/ALVC or both? *Heart Lung Circ.* (2019) 28:164–77. doi: 10.1016/j.hlc.2018.10.013
4. Towbin JA, McKenna WJ, Abrams DJ, Ackerman MJ, Calkins H, Darrieux FC, et al. (2019). 2019 HRS expert consensus statement on evaluation, risk stratification, and management of arrhythmogenic cardiomyopathy. *Heart Rhythm*. 16:e301–72. doi: 10.1016/j.hrthm.2019.05.007
5. Lopez-Ayala JM, Ortiz-Genga M, Gomez-Milanes I, Lopez-Cuenca D, Ruiz-Espejo F, Sanchez-Munoz JJ, et al. A mutation in the Z-line Cypher/ZASP protein is associated with arrhythmogenic right ventricular cardiomyopathy. *Clin Gen.* (2015) 88:172–6. doi: 10.1111/cge.12458
6. Fedida J, Fressart V, Charron P, Surget E, Hery T, Richard P, et al. Contribution of exome sequencing for genetic diagnostic in arrhythmogenic right ventricular cardiomyopathy/dysplasia. *PLoS ONE.* (2017) 12:e0181840. doi: 10.1371/journal.pone.0181840
7. De Bortoli M, Postma AV, Poloni G, Calore M, Minervini G, Mazzotti E, et al. Whole-exome sequencing identifies pathogenic variants in TJP1 gene associated with arrhythmogenic cardiomyopathy. *Circ Genom Precision Med.* (2018) 11:e002123. doi: 10.1161/CIRCGEN.118.002123
8. Chen SN, Gurha P, Lombardi R, Ruggiero A, Willerson JT, Marian AJ. The hippo pathway is activated and is a causal mechanism for adipogenesis in arrhythmogenic cardiomyopathy. *Circ Res.* (2014) 114:454–68. doi: 10.1161/CIRCRESAHA.114.302810
9. Garcia-Gras E, Lombardi R, Giocondo MJ, Willerson JT, Schneider MD, Khoury DS, et al. Suppression of canonical Wnt/β-catenin signaling by nuclear plakoglobin recapitulates phenotype of arrhythmogenic right ventricular cardiomyopathy. *J Clin Investig.* (2006) 116:2012–21. doi: 10.1172/JCI27751
10. Sharma S, Merghani A, Mont L. Exercise and the heart: the good, the bad, the ugly. *Eur Heart J.* (2015) 36:1445–53. doi: 10.1093/eurheartj/ehv090
11. Pelliccia A, Sharma S, Gati S, Bäck M, Börjesson M, Caselli S, et al. 2020 ESC Guidelines on sports cardiology and exercise in patients with cardiovascular disease: the Task Force on sports cardiology and exercise in patients with cardiovascular disease of the European Society of Cardiology (ESC). *Eur Heart J.* (2021) 42:17–96. doi: 10.1093/eurheartj/ehaa605
12. De Innocentiis C, Ricci F, Khanji MY, Aung N, Tana C, Verrengia E, et al. Athlete's heart: diagnostic challenges and future perspectives sports medicine. *Sports Med.* (2018) 48:2463–77. doi: 10.1007/s40279-018-0985-2
13. Prior D, La Gerche A. Exercise and arrhythmogenic right ventricular cardiomyopathy. *Heart Lung Circ.* (2020) 29:547–55. doi: 10.1016/j.hlc.2019.12.007
14. Marcus FI, McKenna WJ, Sherrill D, Basso C, Bauce B, Bluemke DA, et al. Diagnosis of arrhythmogenic right ventricular cardiomyopathy/dysplasia: proposed modification of the Task Force Criteria. *Eur Heart J.* (2010) 31:806–14. doi: 10.1093/eurheartj/ehq025
15. Perrin MJ, Angaran P, Laksman Z, Zhang H, Porepa LF, Rutberg J, et al. Exercise testing in asymptomatic gene carriers exposes a latent electrical substrate of arrhythmogenic right ventricular cardiomyopathy. *J Am Coll Cardiol.* (2013) 62:1772–9. doi: 10.1016/j.jacc.2013.04.084
16. Denis A, Sacher F, Derval N, Martin R, Lim HS, Pambrun T, et al. Arrhythmogenic response to isoproterenol testing vs. exercise testing in arrhythmogenic right ventricular cardiomyopathy patients. *Europace.* (2018) 20:f30–6. doi: 10.1093/europace/euy007

17. Scheel PJ III, Florido R, Hsu S, Murray B, Tichnell C, James CA. Safety NA, and utility of cardiopulmonary exercise testing in arrhythmogenic right ventricular cardiomyopathy/dysplasia. *J Am Heart Assoc*. (2020) 9:e013695. doi: 10.1161/JAHA.119.013695
18. La Gerche A, Rakhit DJ, Claessen G. Exercise and the right ventricle: a potential Achilles' heel. *Cardiovasc Res*. (2017) 113:1499–508. doi: 10.1093/cvr/cvx156
19. Simpson RJ, Kunz H, Agha N, Graff R. Exercise and the regulation of immune functions. *Prog Mol Biol Transl Sci*. (2015) 135:355–80. doi: 10.1016/bs.pmbts.2015.08.001
20. Corrado D, Basso C, Rizzoli G, Schiavon M, Thiene G. Does sports activity enhance the risk of sudden death in adolescents and young adults? *J Am Coll Cardiol*. (2003) 42:1959–63. doi: 10.1016/j.jacc.2003.03.002
21. Holst AG, Winkel BG, Theilade J, Kristensen IB, Thomsen JL, Ottesen GL, et al. Incidence and etiology of sports-related sudden cardiac death in Denmark-implications for preparticipation screening. *Heart Rhythm*. (2010) 7:1365–71. doi: 10.1016/j.hrthm.2010.05.021
22. Suárez-Mier MP, Aguilera B, Mosquera RM, Sánchez-de-León MS. Pathology of sudden death during recreational sports in Spain. *Foren Sci Int*. (2013) 226:188–96. doi: 10.1016/j.forsciint.2013.01.016
23. Risgaard B, Winkel BG, Jabbari R, Glinge C, Ingemann-Hansen O, Thomsen JL, et al. Sports-related sudden cardiac death in a competitive and a noncompetitive athlete population aged 12 to 49 years: data from an unselected nationwide study in Denmark. *Heart Rhythm*. (2014) 11:1673–81. doi: 10.1016/j.hrthm.2014.05.026
24. Harmon KG, Asif IM, Maleszewski JJ, Owens DS, Prutkin JM, Salerno JC, et al. Incidence, cause, and comparative frequency of sudden cardiac death in national collegiate athletic association athletes: a decade in review. *Circulation*. (2015) 132:10–9. doi: 10.1161/CIRCULATIONAHA.115.015431
25. Chappex N, Schlaepfer J, Fellmann F, Bhuiyan ZA, Wilhelm M, Michaud K. Sudden cardiac death among general population and sport related population in forensic experience. *J Foren Legal Med*. (2015) 35:62–8. doi: 10.1016/j.jflm.2015.07.004
26. Finocchiaro G, Papadakis M, Robertus JL, Dhutia H, Steriotis AK, Tome M, et al. Etiology of sudden death in sports: insights from a united kingdom regional registry. *J Am Coll Cardiol*. (2016) 67:2108–15. doi: 10.1016/j.jacc.2016.02.062
27. Maron BJ, Haas TS, Ahluwalia A, Murphy CJ, Garberich RF. Demographics and epidemiology of sudden deaths in young competitive athletes: from the United States National Registry. *Am J Med*. (2016) 129:1170–7. doi: 10.1016/j.amjmed.2016.02.031
28. Morentin B, Suárez-Mier MP, Monzó A, Ballesteros J, Molina P, Lucena J. Sports-related sudden cardiac death in Spain. A multicenter, population-based, forensic study of 288 cases. *Revista Española Cardiol*. (2021) 74:225–32. doi: 10.1016/j.rec.2020.05.044
29. Bohm P, Scharhag J, Egger F, Tischer KH, Niederseer D, Schmied C, et al. Sports-Related sudden cardiac arrest in Germany. *Can J Cardiol*. (2021) 37:105–12. doi: 10.1016/j.cjca.2020.03.021
30. Landry CH, Allan KS, Connelly KA, Cunningham K, Morrison LJ, Dorian P. Sudden cardiac arrest during participation in competitive sports. *N Engl J Med*. (2017) 377:1943–53. doi: 10.1056/NEJMoa1615710
31. Gupta R, Tichnell C, Murray B, Rizzo S, Te Riele A, Tandri H, et al. Comparison of features of fatal versus nonfatal cardiac arrest in patients with arrhythmogenic right ventricular dysplasia/cardiomyopathy. *Am J Cardiol*. (2017) 120:111–7. doi: 10.1016/j.amjcard.2017.03.251
32. Kirchhof P, Fabritz L, Zwiener M, Witt H, Schäfers M, Zellerhoff S, et al. Age- and training-dependent development of arrhythmogenic right ventricular cardiomyopathy in heterozygous plakoglobin-deficient mice. *Circulation*. (2006) 114:1799–806. doi: 10.1161/CIRCULATIONAHA.106.624502
33. Fabritz L, Hoogendijk MG, Scicluna BP, Van Amersfoorth SC, Fortmueller L, Wolf S, et al. Load-reducing therapy prevents development of arrhythmogenic right ventricular cardiomyopathy in plakoglobin-deficient mice. *J Am Coll Cardiol*. (2011) 57:740–50. doi: 10.1016/j.jacc.2010.09.046
34. Lyon RC, Mezzano V, Wright AT, Pfeiffer E, Chuang J, Banares K, et al. Connexin defects underlie arrhythmogenic right ventricular cardiomyopathy in a novel mouse model. *Hum Mol Genet*. (2014) 23:1134–50. doi: 10.1093/hmg/ddt508
35. Hariharan V, Asimaki A, Michaelson JE, Plovie E, MacRae CA, Saffitz JE, et al. Arrhythmogenic right ventricular cardiomyopathy mutations alter shear response without changes in cell-cell adhesion. *Cardiovasc Res*. (2014) 104:280–9. doi: 10.1093/cvr/cvu212
36. Cruz FM, Sanz-Rosa D, Roche-Molina M, García-Prieto J, García-Ruiz JM, Pizarro G, et al. Exercise triggers ARVC phenotype in mice expressing a disease-causing mutated version of human plakophilin-2. *J Am Coll Cardiol*. (2015) 65:1438–50. doi: 10.1016/j.jacc.2015.01.045
37. Martherus R, Jain R, Takagi K, Mendsaikhan U, Turdi S, Osinska H, et al. Accelerated cardiac remodeling in desmoplakin transgenic mice in response to endurance exercise is associated with perturbed Wnt/β-catenin signaling. *Am J Physiol Heart Circ Physiol*. (2016) 310:H174–87. doi: 10.1152/ajpheart.00295.2015
38. Chelko SP, Asimaki A, Andersen P, Bedja D, Amat-Alarcon N, DeMazumder D, et al. Central role for GSK3β in the pathogenesis of arrhythmogenic cardiomyopathy. *JCI Insight*. (2016) 1:85923. doi: 10.1172/jci.insight.85923
39. van Opbergen CJ, Noorman M, Pfenniger A, Copier JS, Vermij SH, Li Z, et al. Plakophilin-2 haploinsufficiency causes calcium handling deficits and modulates the cardiac response towards stress. *Int J Mol Sci*. (2019) 20:4076. doi: 10.3390/ijms20174076
40. Cheedipudi SM, Hu J, Fan S, Yuan P, Karmouch J, Czernuszewicz G, et al. Exercise restores dysregulated gene expression in a mouse model of arrhythmogenic cardiomyopathy. *Cardiovasc Res*. (2020) 116:1199–213. doi: 10.1093/cvr/cvz199
41. Saberniak J, Hasselberg NE, Borgquist R, Platonov PG, Sarvari SI, Smith HJ, et al. Vigorous physical activity impairs myocardial function in patients with arrhythmogenic right ventricular cardiomyopathy and in mutation positive family members. *Eur J Heart Fail*. (2014) 16:1337–44. doi: 10.1002/ejhf.181
42. Sawant AC, Bhonsale A, te Riele AS, Tichnell C, Murray B, Russell SD, et al. Exercise has a disproportionate role in the pathogenesis of arrhythmogenic right ventricular dysplasia/cardiomyopathy in patients without desmosomal mutations. *J Am Heart Assoc*. (2014) 3:e001471. doi: 10.1161/JAHA.114.001471
43. James CA, Bhonsale A, Tichnell C, Murray B, Russell SD, Tandri H, et al. Exercise increases age-related penetrance and arrhythmic risk in arrhythmogenic right ventricular dysplasia/cardiomyopathy-associated desmosomal mutation carriers. *J Am Coll Cardiol*. (2013) 62:1290–7. doi: 10.1016/j.jacc.2013.06.033
44. Wang W, Orgeron G, Tichnell C, Murray B, Crosson J, Monfredi O, et al. Impact of exercise restriction on arrhythmic risk among patients with arrhythmogenic right ventricular cardiomyopathy. *J Am Heart Assoc*. (2018) 7:e008843. doi: 10.1161/JAHA.118.008843
45. Müssigbrodt A, Czimbalmos C, Stauber A, Bertagnolli L, Bode K, Dagres N, et al. Effect of exercise on outcome after ventricular tachycardia ablation in arrhythmogenic right ventricular dysplasia/cardiomyopathy. *Int J Sports Med*. (2019) 40:657–62. doi: 10.1055/a-0962-1325
46. Ruiz Salas A, Barrera Cordero A, Navarro-Arce I, Jiménez Navarro M, García Pinilla JM, Cabrera Bueno F, et al. Impact of dynamic physical exercise on high-risk definite arrhythmogenic right ventricular cardiomyopathy. *J Cardiovasc Electrophysiol*. (2018) 29:1523–9. doi: 10.1111/jce.13704
47. Lie ØH, Rootwelt-Norberg C, Dejgaard LA, Leren IS, Stokke MK, Edvardsen T, et al. Prediction of life-threatening ventricular arrhythmia in patients with arrhythmogenic cardiomyopathy: a primary prevention cohort study. *JACC Cardiovasc Imag*. (2018) 11:1377–86. doi: 10.1016/j.jcmg.2018.05.017
48. Costa S, Gasperetti A, Medeiros-Domingo A, Akdis D, Brunckhorst C, Saguner AM, et al. Familial arrhythmogenic cardiomyopathy: clinical determinants of phenotype discordance and the impact of endurance sports. *J Clin Med*. (2020) 9:3781. doi: 10.3390/jcm9113781
49. Sawant AC, Te Riele AS, Tichnell C, Murray B, Bhonsale A, Tandri H, et al. Safety of American Heart Association-recommended minimum exercise for desmosomal mutation carriers. *Heart Rhythm*. (2016) 13:199–207. doi: 10.1016/j.hrthm.2015.08.035
50. Lie ØH, Dejgaard LA, Saberniak J, Rootwelt C, Stokke MK, Edvardsen T, et al. Harmful effects of exercise intensity and exercise duration in patients with arrhythmogenic cardiomyopathy. *JACC Clin Electrophysiol*. (2018) 4:744–53. doi: 10.1016/j.jacep.2018.01.010
51. Mazzanti A, Ng K, Faragli A, Maragna R, Chiodaroli E, Orphanou N, et al. Arrhythmogenic right ventricular cardiomyopathy: clinical course

and predictors of arrhythmic risk. *J Am Coll Cardiol.* (2016) 68:2540–50. doi: 10.1016/j.jacc.2016.09.951
52. Lin CY, Chung FP, Kuo L, Lin YJ, Chang SL, Lo LW, et al. Characteristics of recurrent ventricular tachyarrhythmia after catheter ablation in patients with arrhythmogenic right ventricular cardiomyopathy. *J Cardiovasc Electrophysiol.* (2019) 30:582–92. doi: 10.1111/jce.13853
53. Ruwald AC, Marcus F, Estes NM III, Link M, McNitt S, Polonsky B, et al. Association of competitive and recreational sport participation with cardiac events in patients with arrhythmogenic right ventricular cardiomyopathy: results from the North American multidisciplinary study of arrhythmogenic right ventricular cardiomyopathy. *Eur Heart J.* (2015) 36:1735–43. doi: 10.1093/eurheartj/ehv110
54. Catto V, Dessanai MA, Sommariva E, Tondo C, Dello Russo A. S-ICD is effective in preventing sudden death in arrhythmogenic cardiomyopathy athletes during exercise. *Pacing Clin Electrophysiol.* (2019) 42:1269–72. doi: 10.1111/pace.13702
55. Paulin FL, Hodgkinson KA, MacLaughlan S, Stuckless SN, Templeton C, Shah S, et al. Exercise and arrhythmic risk in TMEM43 p. *S358L* arrhythmogenic right ventricular cardiomyopathy. *Heart Rhythm.* (2020) 17:1159–66. doi: 10.1016/j.hrthm.2020.02.028
56. Heidbuchel H, Prior DL, La Gerche A. Ventricular arrhythmias associated with long-term endurance sports: what is the evidence? *Br J Sports Med.* (2012) 46(Suppl. 1):i44–50. doi: 10.1136/bjsports-2012-091162
57. Heidbüchel H, Hoogsteen J, Fagard R, Vanhees L, Ector, MJ, Ector H, et al. High prevalence of right ventricular involvementin endurance athletes with ventricular arrhythmias: role of an electrophysiologic study in risk stratification. *Eur Heart J.* (2003) 24:1473–80. doi: 10.1016/S0195-668X(03)00282-3
58. Zaidi A, Sheikh N, Jongman JK, Gati S, Panoulas VF, Carr-White G, et al. Clinical differentiation between physiological remodeling and arrhythmogenic right ventricular cardiomyopathy in athletes with marked electrocardiographic repolarization anomalies. *J Am Coll Cardiol.* (2015) 65:2702–11. doi: 10.1016/j.jacc.2015.04.035
59. La Gerche A, Robberecht C, Kuiperi C, Nuyens D, Willems R, De Ravel T, et al. Lower than expected desmosomal gene mutation prevalence in endurance athletes with complex ventricular arrhythmias of right ventricular origin. *Heart.* (2010) 96:1268–74. doi: 10.1136/hrt.2009.189621
60. Venlet J, Piers SR, Jongbloed JD, Androulakis AF, Naruse Y, den Uijl DW, et al. Isolated subepicardial right ventricular outflow tract scar in athletes with ventricular tachycardia. *J Am Coll Cardiol.* (2017) 69:497–507. doi: 10.1016/j.jacc.2016.11.041
61. Benito B, Gay-Jordi G, Serrano-Mollar A, Guasch E, Shi Y, Tardif JC, et al. Cardiac arrhythmogenic remodeling in a rat model of long-term intensive exercise training. *Circulation.* (2011) 123:13–22. doi: 10.1161/CIRCULATIONAHA.110.938282
62. Pujadas S, Doñate M, Li CH, Merchan S, Cabanillas A, Alomar X, et al. Myocardial remodelling and tissue characterisation by cardiovascular magnetic resonance (CMR) in endurance athletes. *BMJ Open Sport Exerc Med.* (2018) 4:e000422. doi: 10.1136/bmjsem-2018-000422
63. Tahir E, Starekova J, Muellerleile K, von Stritzky A, Münch J, Avanesov M, et al. Myocardial fibrosis in competitive triathletes detected by contrast-enhanced CMR correlates with exercise-induced hypertension and competition history. *JACC Cardiovasc Imag.* (2018) 11:1260–70. doi: 10.1016/j.jcmg.2017.09.016
64. Wilson M, O'Hanlon R, Prasad S, Deighan A, Macmillan P, Oxborough D, et al. Diverse patterns of myocardial fibrosis in lifelong, veteran endurance athletes. *J Appl Physiol.* (2011) 110:1622–6. doi: 10.1152/japplphysiol.01280.2010
65. McDiarmid AK, Swoboda PP, Erhayiem B, Lancaster RE, Lyall GK, Broadbent DA, et al. Athletic cardiac adaptation in males is a consequence of elevated myocyte mass. *Circ Cardiovasc Imag.* (2016) 9:e003579. doi: 10.1161/CIRCIMAGING.115.003579

Conflict of Interest: The authors declare that the research was conducted in the absence of any commercial or financial relationships that could be construed as a potential conflict of interest.

frontiers in Cardiovascular Medicine

ORIGINAL RESEARCH
published: 15 November 2021
doi: 10.3389/fcvm.2021.748003

Layer-Specific Global Longitudinal Strain Predicts Arrhythmic Risk in Arrhythmogenic Cardiomyopathy

Diego Segura-Rodríguez[1,2], Francisco José Bermúdez-Jiménez[2,3,4], Lorena González-Camacho[3], Eduardo Moreno Escobar[1,2], Rocío García-Orta[2,3], Juan Emilio Alcalá-López[2,3], Alicia Bautista Pavés[1,2], José Manuel Oyonarte-Ramírez[2,3], Silvia López-Fernández[2,3], Miguel Álvarez[2,3], Luis Tercedor[2,3] and Juan Jiménez-Jáimez[2,3]*

[1] Cardiology Department, Hospital Universitario San Cecilio, Granada, Spain, [2] Instituto de Investigación Biosanitaria ibs.GRANADA, Granada, Spain, [3] Cardiology Department, Hospital Universitario Virgen de las Nieves, Granada, Spain, [4] Centro Nacional de Investigaciones Cardiovasculares, CNIC, Instituto de Salud Carlos III, Madrid, Spain

OPEN ACCESS

Edited by:
Juan R. Gimeno,
Hospital Universitario Virgen de la Arrixaca, Spain

Reviewed by:
Adelina Doltra,
Hospital Clínic de Barcelona, Spain
Pedro Grilo Diogo,
Centro Hospitalar Universitário de São João (CHUSJ), Portugal

***Correspondence:**
Francisco José Bermúdez-Jiménez
bermudezfrancisco23y@gmail.com

Specialty section:
This article was submitted to Cardiovascular Imaging, a section of the journal Frontiers in Cardiovascular Medicine

Received: 27 July 2021
Accepted: 15 October 2021
Published: 15 November 2021

Citation:
Segura-Rodríguez D, Bermúdez-Jiménez FJ, González-Camacho L, Moreno Escobar E, García-Orta R, Alcalá-López JE, Bautista Pavés A, Oyonarte-Ramírez JM, López-Fernández S, Álvarez M, Tercedor L and Jiménez-Jáimez J (2021) Layer-Specific Global Longitudinal Strain Predicts Arrhythmic Risk in Arrhythmogenic Cardiomyopathy. Front. Cardiovasc. Med. 8:748003. doi: 10.3389/fcvm.2021.748003

Background: Arrhythmogenic cardiomyopathy (AC) is a life-threatening disease which predispose to malignant arrhythmias and sudden cardiac death (SCD) in the early stages of the disease. Risk stratification relies on the electrical, genetic, and imaging data. Our study aimed to investigate how myocardial deformation parameters may identify the subjects at risk of known predictors of major ventricular arrhythmias.

Methods: A cohort of 45 subjects with definite or borderline diagnosis of AC was characterized using the advanced transthoracic echocardiography (TTE) and cardiac magnetic resonance (CMR) and divided into the groups according to the potential arrhythmic risk markers, such as non-sustained ventricular tachycardia (NSVT), late gadolinium enhancement (LGE), and genetic status. Layer-specific global longitudinal strain (GLS) by TTE 2D speckle tracking was compared in patients with and without these arrhythmic risk markers.

Results: In this study, 23 (51.1%) patients were men with mean age of 43 ± 16 years. Next-generation sequencing identified a potential pathogenic mutation in 39 (86.7%) patients. Thirty-nine patients presented LGE (73.3%), mostly located at the subepicardial-to-mesocardial layers. A layer-specific-GLS analysis showed worse GLS values at the epicardial and mesocardial layers in the subjects with NSVT and LGE. The epicardial GLS values of −15.4 and −16.1% were the best cut-off values for identifying the individuals with NSVT and LGE, respectively, regardless of left ventricular ejection fraction (LVEF).

Conclusions: The layer-specific GLS assessment identified the subjects with high-risk arrhythmic features in AC, such as NSVT and LGE. An epicardial GLS may emerge as a potential instrument for detecting the subjects at risk of SCD in AC.

Keywords: sudden cardiac death (SCD), late gadolinium enhanced, non-sustained ventricular tachycardia, arrhythmogenic cardiomyopathy (ACM), global longitudinal strain

INTRODUCTION

Arrhythmogenic cardiomyopathy (AC) is a genetically determined myocardial disease characterized by the progressive fibro-fatty myocardial replacement leading to heart failure and life-threatening arrhythmias in the early stages of the disease (1). It is a clinically heterogeneous disease due to its incomplete penetrance and variable expression. Therefore, there is no single gold standard for the diagnosis of AC and the diagnostic process is considered challenging. The diagnosis of AC is currently made on the consensus based revised 2010 Task Force criteria (TFC) (2), and updated in 2019 with the Padua criteria for left sided forms (3). The imaging criteria underlines the importance of cardiac imaging in AC with a great influence of cardiac magnetic resonance imaging (CMR). The detection of a regional wall motion abnormality is required to score a major or minor criterion regardless of the outflow tract dilatation or systolic dysfunction. Moreover, the presence and location of late gadolinium enhancement (LGE) on CMR are reported as the predictive markers of ventricular arrhythmias and sudden cardiac death (SCD) (4, 5).

Through the post-mortem studies, it is established that fibrofatty replacement begins at the epicardium level with progressive extension to mesocardial layers (6). This fibrofatty involvement can be assessed non-invasively by using CMR through the LGE sequences allowing not only detection of scars, but also evaluate the location, extension, and distribution, which helps arrhythmic risk stratification and facilitates the selection of susceptible individuals at risk of developing malignant events (7).

Despite the CMR advances, an echocardiography remains a non-invasive, relatively inexpensive, widely available first-line diagnostic tool. The recent developments in echocardiography, as tissue imaging deformation (TID) mainly assessed by the speckle-tracking technology, may increase the performance of conventional echocardiography. Ejection fraction (EF) is a well-known classic echocardiographic parameter which describes the capacity of the ventricle to oust a determined volume, which is a global systolic parameter and usually remains preserved when either the few segments are affected or at early stages of the disease (8). However, TID allows the regional wall performance analysis and detecting incipient pathological changes when the traditional echocardiography measures (i.e., volumes and EF) are still normal. Myocardial strain has proved as a wide clinical utility throughout numerous cardiovascular areas: cardio-oncology, ischemic cardiomyopathy, valvular heart disease, and several non-ischemic cardiomyopathies, such as amyloidosis (9–12). The TID usefulness remains not only on its capability to detect the subclinical damage, but also to guide the medical and interventional treatment as well as to stratify the short- and long-term prognosis (13–15). Furthermore, the growing TID evidence has emerged in AC, demonstrating the diagnostic and prognostic value which may guide decision-making for arrhythmic primary prevention (16, 17).

Since arrhythmic events and SCD may occur in the absence of a definite diagnosis, there is a need to identify new tools to facilitate the earliest diagnosis and risk stratification. Some authors have attempted to assess the value of speckle-tracking strain in the early diagnosis and disease progression of AC (18). However, there is lack of information on the arrhythmic prognostic value of speckle-tracking strain. This study aimed to evaluate the association of TID with the major SCD risk factors as non-sustained ventricular arrhythmia, fibrous scar on CMR, or genetic background.

METHODS

Study Population and Clinical Evaluation

We retrospectively recruited 45 subjects with definite or borderline diagnosis of AC, based on 2010 TFC, who underwent transthoracic echocardiography and CMR (2). The patients were evaluated between 2007 and 2020 at the Inherited Cardiomyopathies Unit of two tertiary hospitals. The study was approved by the Institutional Review Board and the Local Ethics Committee, and all the participants signed the informed consent. We excluded all the patients with permanent pacemaker pacing, ischemic heart disease, more than mild valvular involvement (stenosis/regurgitation), and poorly controlled hypertension.

The clinical assessment comprised exhaustive evaluation of medical history, family history of SCD or cardiomyopathy, 12-lead electrocardiogram, basic laboratory test, and genetic testing. In addition, 24-h Holter monitoring, echocardiography, and CMR were obtained within 6 months for each patient. We thoroughly assessed the medical history for arrhythmic events: (a) non-sustained ventricular (NSVT) tachycardia defined as $\geq$3 consecutive premature complexes with a heart rate of $>$120 beats/min lasting $<$30 s, and (b) a composite of (1) ventricular tachycardia/ventricular fibrillation (VT/VF) defined as the presence of a ventricular rhythm at a rate $>$120 beats/min that lasts longer than 30 s, (2) the incidence aborted cardiac arrest due to VF which is reversed by the successful resuscitation maneuvers, and (3) the incidence of an appropriate implantable cardioverter-defibrillator (ICD) shock when they occurred in response to VT or VF.

The peripheral blood samples for the genetic analysis were obtained from the probands or the deceased index case, as applicable. A next-generation sequencing (NGS) gene panel containing 21 genes (previously associated with the development of arrhythmogenic cardiomyopathy) was applied (**Supplementary Material**). The pathogenicity of the identified variants was classified according to the current guidelines of the American College of Medical Genetics and Genomics (ACMG) (19). After a potential disease-causing variant was identified in the index patient, the genetic and clinical cascade were conducted. The subjects were classified according to the genetic test results as the desmosomal mutations carriers, non-desmosomal carriers, and negative/unknown mutations carriers.

Cardiovascular Imaging Analysis

The echocardiography and CMR imaging acquisition, interpretation and analysis were performed by the two experienced, independent, and blinded imaging specialists. The acquisition protocols and post-processing are described in the **Supplementary Material**.

Echocardiography

Transthoracic echocardiography acquisition was performed using Vivid 9 system (GE® Healthcare, Hørten, Norway). The size of chamber, quantifications, and severity partition cut-offs of left ventricular (LV) dysfunction were measured according to the current guidelines (20). We used an 18-segment model to analyze the regional wall motion abnormalities (RWMA) and deformation assessment. The images were acquired at 65 frames per second and processed offline using Echo-PAC software GE® (GE®, Hørten, Norway).

The strain analyses were performed using a dedicated software (EchoPac strain package for analysis, GE® Healthcare, Hørten, Norway), tracing endocardial border, and adjusting region of interest avoiding pericardium. We obtained the global longitudinal strain (GLS) by using a 2D speckle-tracking method (21). We evaluated: layer-specific GLS, regional longitudinal strain, and mechanical dispersion from the analysis of the SD (MD_{SD}) and range between maximum and minimum time value (MD_{delta}) of the time to reach peak negative strain. The GLS-specific and mechanical dispersion values were analyzed according to the references values (22–24). We calculated the ratio of endocardial GLS to epicardial GLS (Endo-Epi GLS ratio) using the endocardial GLS/epicardial GLS for the assessment of the strain gradient, as previously described (23). Twenty patients were randomly selected for analyzing interobserver variability by another observer blinded to the results of the first reader, assessing the GLS at each myocardial layer (GLS_{epi}, GLS_{meso}, and GLS_{endo}).

CMR Study

All the patients underwent a CMR evaluation. The LV and right ventricular (RV) function were categorized according to the current guidelines (25). We considered the presence of LV involvement when any of the following conditions were present: LV RWMA, LV wall thinning, left ventricular ejection fraction (LVEF) <50%, or LGE with non-ischemic pattern. On the other hand, right ventricular (RV) involvement was considered according to TFC (2). The LGE sequences were qualitatively assessed (presence, location, and layer-distribution) according to an 18-segment model.

Finally, the patients were classified on the basis of RV and/or LV involvement as follows: lone RV (isolated RV involvement), biventricular, LV dominant (isolated LV involvement), and negative CMR (absence of any CMR signs).

Statistical Analysis

The qualitative variables were described using the absolute frequencies and percentages. The continuous variables were expressed as mean and SD, or median, when applicable. The normality of the data was tested with Shapiro–Wilk test.

A comparative analysis between the groups was performed using Pearson's chi-square test or Fisher's exact test for the qualitative variables. Intergroup comparisons for the quantitative variables were made using Student's *t*-test or Mann–Whitney *U*-test when indicated. For quantitative comparison among the three groups, an ANOVA test or Kruskal–Wallis were performed. Interobserver variability was evaluated using the intraclass correlation coefficient (ICC) for layer-specific GLS analysis. The receiver operating characteristics (ROC) curves were used to define the GLS cut-offs able to predict the NSVT and LGE. A value $p < 0.05$ was considered statistically significant. The data were processed using the SPSS Statistics 25 software (IBM®, Armonk, NY, USA).

RESULTS

The baseline clinical characteristics are summarized in **Table 1**. We included 37 Caucasian patients with a definite and eight patients with a borderline diagnosis of AC (mean age 43 ± 16 years and 51% were men), belonging to the 19 families, who had previously undergone a TTE and CMR. Overall, a high prevalence of family history of SCD was found (39; 86.7%). Twenty-four patients (53.3%) had cardiac symptoms at first evaluation, mainly dyspnea (10; 22.2%) and palpitations (7; 15.6%). The asymptomatic patients were diagnosed primarily by family cascade screening. In 37 patients, we found a pathogenic or likely a pathogenic variant (**Figure 1** and **Supplementary Table 1**). During 24 h Holter monitoring or 12-lead ECG, we identified 16 patients (35.5%) presenting NSVT. The incidence of NSVT was not significantly associated with LVEF (51.9 ± 8.3 vs. 47.7 ± 10.7%; $p = 0.15$) or indexed LV end-diastolic volumes (55.5 ± 15 vs. 58.8 ± 17 ml/m^2; $p = 0.497$).

Twelve patients (26.6%) had experienced the composite outcome of VT/VF with five individuals receiving an appropriate ICD shock.

An echocardiographic analysis revealed that nearly half of the patients (23; 51.1%) showed an impaired LVEF (mean 42.9 ± 5.9%), with 69.6% of the patients presenting with mildly reduced, 26.1% moderately reduced, and 4.3% severely reduced LVEF. In addition, majority of the patients had no RV systolic dysfunction [mean tricuspid annular plane systolic excursion (TAPSE) 20.1 ± 4 mm]. Overall, the structural evaluation showed a normal LV end-diastolic volume (LVEDV 104.9 ± 28.9 ml and indexed LVEDV 56.7 ± 15.6 ml/m^2). Moreover, 31 patients presented regional RWMA at evaluation, mainly located at basal (23; 51.1%) and mid inferolateral (24; 53.3%) segments and mid lateral segments (23; 51.1%). In all the individuals, it was feasible to evaluate regional and GLS according to each myocardial layer. The GLS analysis results are shown in **Supplementary Table 2**. The mechanical dispersion parameters were MD_{SD} 51.3 ± 18 ms and MD_{delta} 174.2 ± 61.5 ms, being higher values than the normal ranges in the healthy population (24).

Regarding the AC appearance on CMR, a nearly exclusive LV involvement was the most frequent AC phenotype (42.2%), with 15 (33.3%) presenting a biventricular (BV) affection, and 5 (11.1%) a predominant RV involvement. The LV and RV ejection fraction (RVEF) distributions are displayed at **Supplementary Figures 1, 2**. The mean LVEF and RVEF values were 51.7 ± 10.2 and 50.9 ± 10.1%, respectively. With respect to LGE, 33 (73.3%) patients presented LGE with non-ischemic pattern. Distribution of LGE was identified as biventricular in 18 patients (54.5%), lone LV in 10 subjects (30.3%), and lone RV in five cases (15.2%). LV-LGE was predominantly

TABLE 1 | The baseline characteristics.

	Overall (45)	VT/VF (-) (33)	VT/VF (+) (12)	*p*-value
Sex (male) *n*, (%)	23 (51.1)	12 (36.4)	11 (91.1)	0.001
Age (years), mean ± SD	43.13 ± 16.5	41.3 ± 17.8	48.3 ± 11.6	0.21
Body mass index, kg/m^2	26.8 ± 4.1	27.2 ± 4.4	25.8 ± 3.4	0.31
Body surface area, m^2	1.8 ± 0.2	1.83 ± 0.2	1.96 ± 0.21	0.08
Hypertension *n*, (%)	2 (4.4)	2 (6.1)	0 (0)	1
Dyslipidaemia *n*, (%)	2 (4.4)	1 (3)	1 (8.3)	0.46
Type 2 diabetes *n*, (%)	1 (2.2)	1 (3)	0 (0)	1
Tobacco use				0.66
Active smoking *n*, (%)	4 (8.9)	3 (9.1)	1 (8.3)	
Former smoking *n*, (%)	2 (4.4)	2 (6.1)	0 (0)	
Family history SCD, *n* (%)	39 (86.7)	33 (100)	6 (50)	<0.001
Asymptomatic, *n* (%)	21 (46.7)	20 (60.6)	1 (8.3)	0.002
Symptoms, *n* (%)	24 (53.3)			<0.001
Dyspnoea	10 (22.2)	8 (24.2)	2 (16.7)	
Chest pain	2 (4.4)	2 (6.1)	0 (0)	
Palpitations	7 (15.6)	1 (3)	6 (50)	
Syncope	3 (6.7)	2 (6.1)	1 (8.3)	
Aborted SCD	2 (4.4)	0 (0)	2 (16.7)	
NYHA class I *n*, (%)	34 (75.6)	24 (72.7)	10 (83.3)	0.021
NYHA class II *n*, (%)	9 (20)	9 (27.3)	0 (0)	
NYHA class III *n*, (%)	2 (4.4)	0 (0)	2 (16.7)	
Abnormal ECG *n*, (%)	34 (75.6)	23 (69.7)	11 (91.7)	0.24
Atrial fibrillation *n*, (%)	4 (8.9)	2 (6.1)	2 (16.7)	0.28
Paroxysmal	2 (4.4)	1 (50)	1 (50)	
Persistent	1 (2.2)	0	1 (50)	
Permanent	1 (2.2)	1 (50)	0	
Genetic testing *n*, (%)				<0.001
Desmosomal mutation	15 (33.3)	11 (33.3)	4 (16.7)	
Non-desmosomal mutation	24 (53.3)	22 (66.7)	2 (16.7)	
Unknown	6 (13.3)	0	6 (50)	
Phenotype,[†] *n* (%)				0.022
RV	5 (11.1)	2 (6.1)	3 (25)	
LV	19 (42.2)	17 (51.1)	1 (8.3)	
BV	15 (33.3)	9 (27.3)	7 (58.3)	
Silent	6 (13.3)	5 (15.2)	1 (8.3)	
NSVT *n*, (%)	16 (35.6)	7 (21.2)	9 75)	0.002
ICD *n*, (%)	23 (51.1)	13 (39.4)	10 (83.3)	0.001
Primary prevention *n*, (%)	14 (60)	12 (92.3)	2 (20)	
Secondary prevention *n*, (%)	9 (40)	1 (7.7)	8 (80)	
ICD shocks *n*, (%)	7 (15)	2 (6.1)	5 (41.7)	0.011
Appropriate *n*, (%)	5 (71.4)	0 (0)	5 100	
Inappropriate *n*, (%)	2 (28.6)	2 (100)	0 (0)	
LGE presence *n*, (%)	33 (73.3)	23 (69.7)	10 (83.3)	0.46
LGE phenotype *n*, (%)				0.297
RV:	10 (22.2)	8 (24.2)	2 (16.7)	
LV:	5 (11.1)	2 (6.1)	3 (25)	
BV:	18 (40)	13 (39.4)	5 (41.7)	

CMR, cardiac magnetic resonance; Cardiac SCD, sudden cardiac death; RV, right ventricle; LGE, late gadolinium enhancement; LV, Left Ventricle; BV, Biventricular; ICD, Implantable cardioverter defibrillator.

[†]Based on the regional wall motion abnormalities and late gadolinium enhancement.

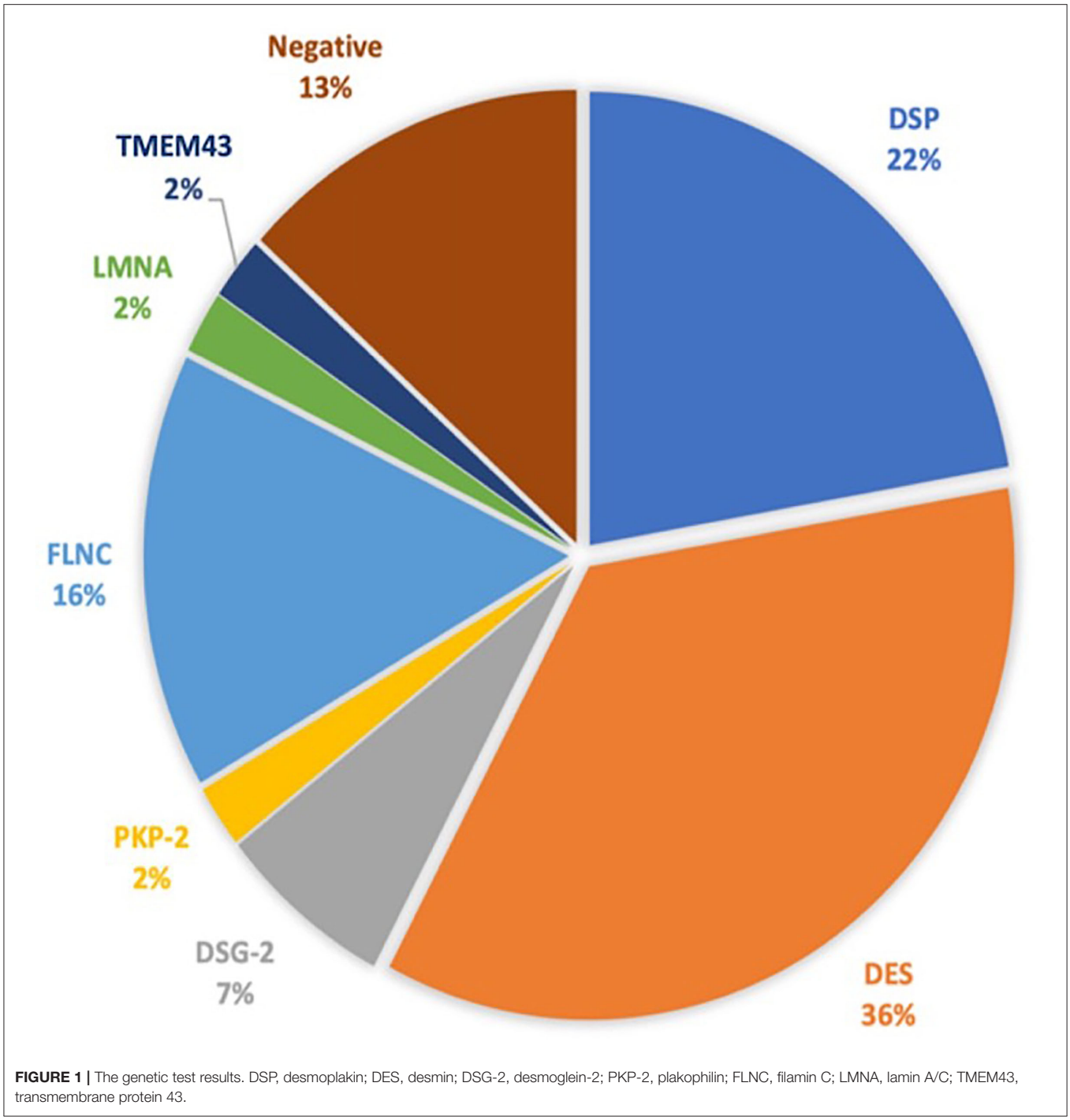

FIGURE 1 | The genetic test results. DSP, desmoplakin; DES, desmin; DSG-2, desmoglein-2; PKP-2, plakophilin; FLNC, filamin C; LMNA, lamin A/C; TMEM43, transmembrane protein 43.

located at the subepicardial-to-mesocardial layer ($n = 27$; 96.4%) and only one patient had focal patchy transmural LGE at the interventricular septum. None of the patients had subendocardial LGE involvement. In addition, LV-LGE was predominantly located at the lateral/inferolateral wall in 27 individuals (96.4%), with an extended circumferential pattern in 19 (70.37%) of these patients.

Among the patients who experienced VT/VF during follow-up, the BV phenotype was the most frequently encountered (7, 58.3%), followed by the exclusive RV (3, 25%) and LV phenotype (1, 8.3%).

GLS and Major Arrhythmic Events

The layer-specific GLS comparing the patients with and without previous VT/VF [VT/VF (+) vs. VT/VF (–)] showed in the epicardial GLS values differences (-14.4 ± 2.2 vs. -16.1 ± 3.1%; $p = 0.09$), with no differences at either mesocardial or endocardial GLS analysis.

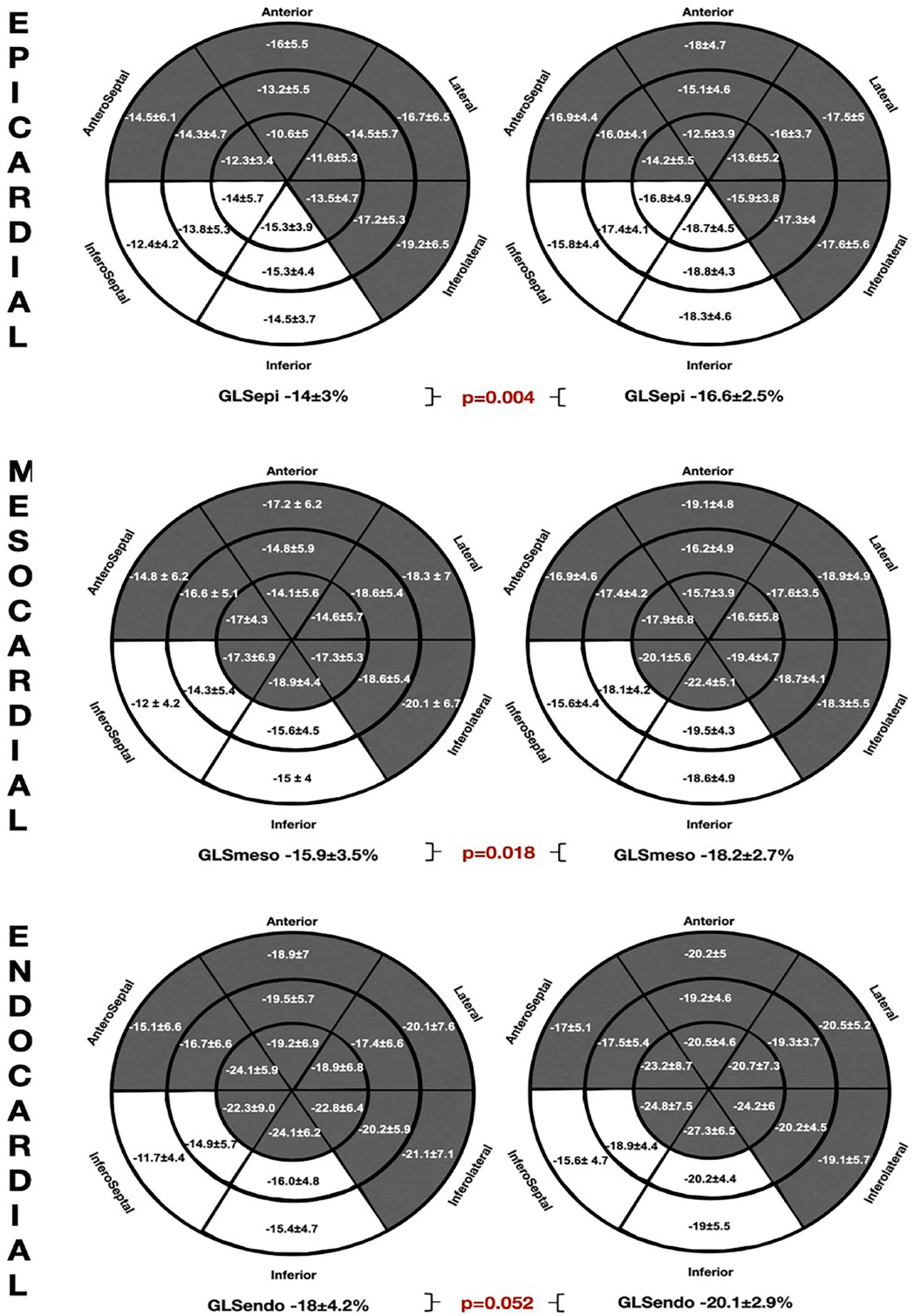

FIGURE 2 | The comparative global and regional layer-specific GLS analysis global between the NVST (+) and NSVT (–) groups represented in the left ventricular (LV) 18-segment models according to each myocardial layer. White areas remark significant differences in regional longitudinal strain between the groups. GLS, global longitudinal strain; NSVT, non-sustained ventricular tachycardia.

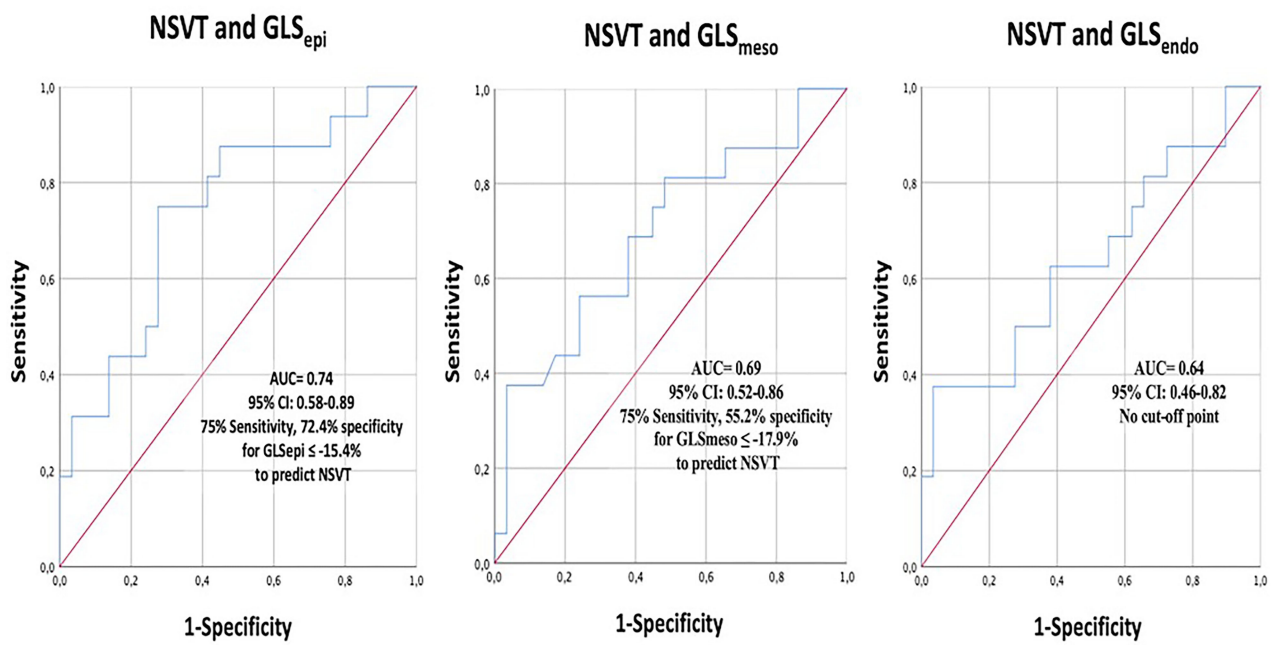

FIGURE 3 | The receiver operating characteristics (ROC) curve analysis of layer-specific GLS to predict NSVT. GLS, global longitudinal strain; NSVT, non-sustained ventricular tachycardia.

Strain Association With Arrhythmic Risk Markers

GLS and NSVT

The comparative regional and GLS analysis according to myocardial layer between the patients with history of NSVT [NSVT(+)] and without NSVT [NSVT(−)] is shown in **Figure 2**. The LV layer-specific GLS analysis showed poorer LV-GLS values in the NSVT(+) group at the mesocardial and epicardial layers. However, no significant differences were found between the groups when comparing GLS at the endocardial myocardial layer. Similarly, the mechanical dispersion parameters were not different in both the groups [MD_{SD}: NSVT (+) 53.6 ± 15.6 ms vs. NSVT (−) 50 ± 19.3 ms; $p = 0.434$ and MD_{delta}: NSVT (+) 185.6 ± 66.8 ms vs. NSVT (−) 167.9 ± 58.6 ms; $p = 0.448$].

Furthermore, the regional longitudinal strain at the inferoseptal and inferior basal-to-mid segments were consistently impaired within all the myocardial layers in the NSVT (+) group when compared with the NSVT (−) group. In addition, the Endo-Epi GLS ratio showed a tendency to the lower values in the NSVT (+) group (1.2 ± 0.1 vs. 1.3 ± 0.1; $p = 0.06$).

In **Figure 3**, the ROC curves analysis of the layer GLS analysis to predict the presence of NSVT is represented. The best area under the curve (AUC) was 0.739 (95% *CI* 0.585–0.893) for GLS_{epi} with the best cut-off value −15.41%, giving a sensitivity of 75% and specificity of 72.4%.

GLS and LGE

The comparative analysis between the layer-specific GLS and LGE presence (LGE+ vs. LGE−) is exposed at **Figure 4**. We found significant differences in GLS according to the LGE presence, specifically at the mesocardial and the epicardial layers. Conversely, there were no significant alterations in the endocardial layer GLS between the groups of patients with and without LGE. In addition, the Endo-Epi GLS ratio was lower in the LGE (+) group (1.3 ± 0.1 vs. 1.2 ± 0.06; $p = 0.035$).

As observed in the NSVT (+) group, the patients presenting LGE showed worse GLS values in the inferior and inferoseptal segments throughout all the myocardial layers. However, no significant differences were found on the mechanical dispersion parameters [MD_{delta}: LGE (+) 52.2 ± 16.3 ms vs. LGE (−) 48.7 ± 22.7 ms; $p = 0.57$ and MD_{delta}: LGE (+) 176.3 ± 57.1 ms vs. LGE (−) 168.5 ± 74.9 ms $p = 0.36$].

Figure 5 depicts the ROC curves analysis of the layer GLS analysis to predict the presence of LGE. The best AUC was 0.75 (95% *CI* 0.0.57–0.9) for GLS_{epi} with the best cut-off value −16.1%, giving a sensitivity of 72.7% and specificity of 75%.

GLS and Genetics

We did not find significant differences in the GLS, dispersion parameters, or regional longitudinal strain analysis between the different genetic background (**Supplementary Tables 3–5**). Likewise, no significant differences were detected regarding the mechanical dispersion parameters (MD_{SD}: desmosomal 52.2

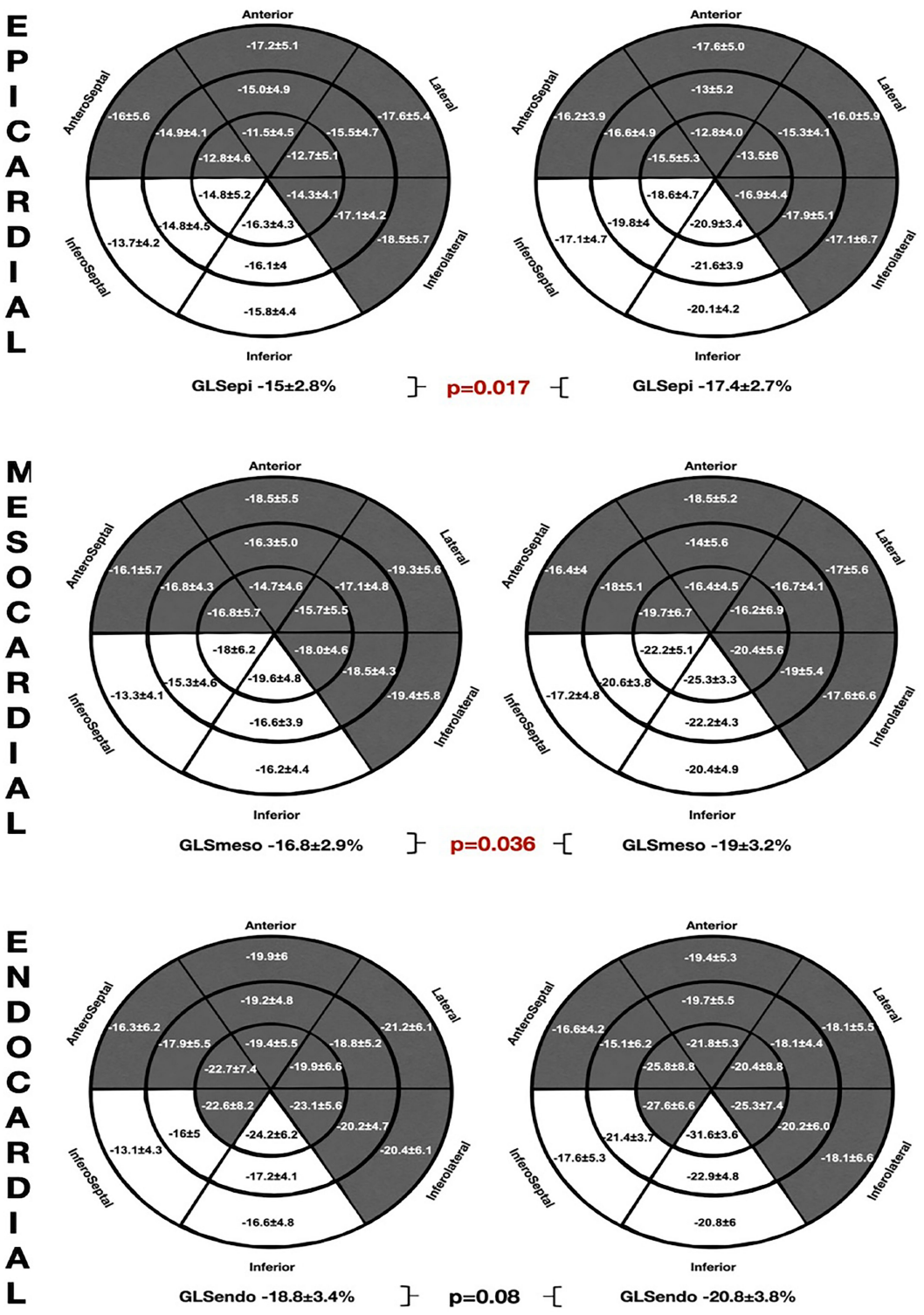

FIGURE 4 | The comparative global and regional layer-specific GLS analysis global between the LGE (+) and LGE (–) groups represented in the LV 18-segment models according to each myocardial layer. White areas remark significant differences in regional longitudinal strain between the groups. GLS, global longitudinal strain; LGE, late gadolinium enhancement.

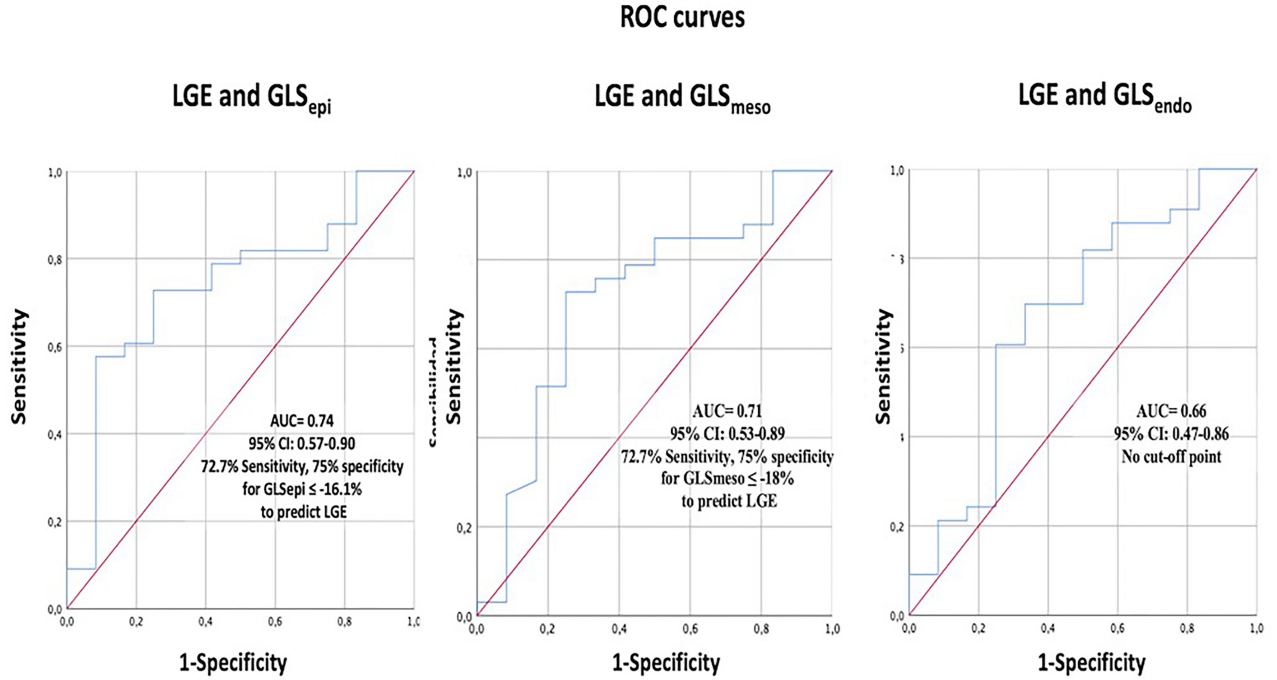

FIGURE 5 | The ROC curve analysis of layer-specific GLS to predict the presence of LGE. GLS, global longitudinal strain; LGE, Late gadolinium enhancement.

± 14.6 ms vs. non-desmosomal 50 ± 21.4 ms vs. unknown mutations 53.9 ± 11.6 ms; $p = 0.89$, MD_{delta}: desmosomal 165.9 ± 37 ms vs. non-desmosomal 170.2 ± 68.2 ms vs. unknown mutations 211 ± 78.4 ms; $p = 0.41$) or Endo-Epi GLS ratio (desmosomal 1.3 ± 0.1 vs. non-desmosomal 1.2 ± 0.1 vs. unknown mutations $p = 0.17$).

Interobserver Analysis

An interobserver analysis showed excellent agreement between the observers with ICC 0.93 (95% *CI*, 0.80–0.97) for GLSepi, 0.93 (95% *CI*, 0.83–0.97) for GLSmeso and 0.87 (95% *CI*, 0.72–0.95) for GLSendo.

DISCUSSION

Arrhythmic risk stratification in AC remains a matter of debate and can be challenging, particularly in the early stages of the disease. LVEF is a poor predictor with a remarkable incidence of SCD in the patients with preserved or mildly impaired systolic function, particularly in the certain genotypes, such as *FLNC*, *LMNA*, *TMEM43*, or *DES* (26–29). New stratification tools are needed, and advanced cardiac imaging is gaining relevance in this field. Our work is the first to correlate the LV regional layer-specific GLS analysis with the traditionally accepted arrhythmic risk factors of ventricular arrhythmias in AC, such as NSVT, LGE, or genetic status. Our results seem promising as we were able to detect, in a small cohort of the patients with AC, significant TID disturbances that were associated with the presence of classical SCD risk factors, such as the presence of LGE or NSVT.

In general, LVEF remains one of the cornerstones during the decision-making process to select the high-risk patients who may benefit from the ICD implantation for primary prevention (19, 20). However, the LVEF loses discriminative capability in the setting of AC, as ventricular arrhythmias (VAs) or SCD might happen during the so-called electrical phase in the subjects with no evident macroscopic structural changes and normal LVEF. Therefore, it is mandatory to detect more sensitive parameters capable of detecting the pathological changes in the vulnerable phase before LVEF impairment. The present study aimed to go beyond the LVEF and standard average GLS, performing a layer-specific analysis to detect the subjects with the stablished arrhythmic risk markers. Several studies have shown that greater GLS (more positive) and LV mechanical dispersion might be the markers of ventricular arrhythmias but to date have not been included in the solid predictive models (16).

Nonetheless, NSVT and LGE are the well-recognized risk factors for arrhythmic risk. NSVT is classically included in the prediction models algorithms for VAs in AC (30–33). More recently, the LGE has shown remarkable prognostic value in AC showing that LV involvement and LV dominant phenotype are the independent factors of major events (34). Hence, searching these elements during the patient evaluation is of upmost relevance. In this sense, our study has shown that especially epicardial GLS had a good association for detecting the subjects with NSVT or LGE, pointing the best cut-off at ∼-16 to −15%. Adding epicardial GLS to the routinely echocardiographic assessment may increase the sensitive capability to detect the subjects potentially at risk of VAs and therefore, of SCD.

The previous studies have shown that LV dominant AC presents a typical subepicardial-to-mesocardial LGE distribution, with a specific distribution at the inferolateral and lateral walls with circumferential extension (ring-like patterns) (35). Majority of our cohort of patients had subepicardial-to-mesocardial LV-LGE distribution and only one subject had patchy mesocardial fibrosis located at the interventricular septum. A good correlation observed, not only between the LGE and impaired GLS, but also in the distribution of the segments, reinforcing the potential of speckle-tracking TTE as a useful tool to detect the individuals with early involvement and as an arrhythmic risk predictor.

It has been previously described that the endocardial GLS is higher than epicardial GLS in the normal subjects with a Endo-Epi GLS ratio of ∼1.3 (36). This might be explained by the differences in wall stress (more stress in the endocardial fibers during diastole making them larger than epicardial fibers) or changes in coronary perfusion (37, 38). Nevertheless, this Endo-Epi GLS gradient is likely accentuated when the progressive fibrosis accumulation occurs in the epicardial layers which is the central pathophysiology of AC. Indeed, lateral LV epicardium is affected before endocardium in AC (18). In our cohort, only at the epicardial and mesocardial level, the differences were observed between the patients at higher and lower arrhythmic risk, as defined by the presence of arrhythmic risk markers.

Despite of the potential clinical usefulness of TID by *speckle tracking*, it is mandatory to always check the tracking results visually and defining a good region of interest tracing (excluding pericardium and blood pool). When performed by expertise personnel, GLS has shown higher accuracy than the conventional diagnostic echocardiographic parameters, providing both the higher sensitivity and specificity to detect AC (39, 40).

However, due to the small sample size of this study, assumption in the terms of prognosis needs to be evaluated in larger prospective studies, taking into account major events, such as ventricular fibrillation, sustained ventricular tachycardia, or sudden cardiac death. In this regard, the integrating parameters, such as family history, LGE, arrhythmic burden, and genetics and potentially, the layer-specific GLS, such as epicardial GLS may increase the predictive capability to select the high-risk individuals who may benefit for the ICD implantation.

LIMITATIONS

These data should be interpreted with caution due to the small sample size. In addition, the retrospective and cross-sectional design nature of this study does not allow inferences in the terms of prognosis. Hence, the VT events were included only through either Holter monitoring or 12-lead ECG which may have lower yield when compared with the monitoring using an implanted cardiac device. Furthermore, we are aware of the inherent limitations in ejection fraction, GLS, and LGE interpretation. Definition of region of interest in the speckle-tracking analysis is of utmost importance as it requires accurate tracing to avoid pericardial inclusion which may cause differential bias (21). The values of longitudinal strain may vary depending on age, sex, and vendor specific software, so that these values may not be applicable in a different population. Since major arrhythmic events were not used as the primary endpoint because there were few in such relatively rare pathology, future prospective, larger, and multicenter studies are needed to evaluate the predictive capacity of GLS to detect individuals at risk of malignant arrhythmic events need to be confirmed in a prospective study.

CONCLUSION

The layer-specific GLS assessment identified the subjects with high-risk arrhythmic markers, such as NSVT and LGE presence. An epicardial GLS analysis showed the best of the ability for detecting the subjects with the arrhythmic risk factors. The larger prospective studies may correlate layer-specific GLS evaluation with the malignant arrhythmic events and its prognostic role.

DATA AVAILABILITY STATEMENT

The raw data supporting the conclusions of this article will be made available by the authors, without undue reservation.

ETHICS STATEMENT

The studies involving human participants were reviewed and approved by Comité Ético de Investigación Clínica (CEI) de la provincia de Granada. The patients/participants provided their written informed consent to participate in this study.

AUTHOR CONTRIBUTIONS

DS-R: conceptualization, methodology, statistical analysis, investigation, writing the original draft, images elaboration, and coordination. FB-J and JJ-J: conceptualization, methodology, supervision, writing-review and editing, and clinical perspectives. LG-C, EM, RG-O, JO-R, and AB: validation, clinical evaluation, and image acquisition. JA-L and SL-F: imaging interpretation and analysis. MÁ and LT: clinical perspectives and discussion. All authors reviewed and approved the final manuscript.

ACKNOWLEDGMENTS

The authors wish to thank to the patients and families from our Inherited Cardiomyopathies Units for their kindness and willingness to participate in this study. These results are from Dr. Segura-Rodríguez's PhD program.

SUPPLEMENTARY MATERIAL

The Supplementary Material for this article can be found online at: https://www.frontiersin.org/articles/10.3389/fcvm.2021.748003/full#supplementary-material

REFERENCES

1. Corrado D, Basso C, Judge DP. Arrhythmogenic Cardiomyopathy. *Circ Res.* (2017) 121:784–802. doi: 10.1161/CIRCRESAHA.117.309345
2. Marcus FI, McKenna WJ, Sherrill D, Basso C, Bauce B, Bluemke DA, et al. Diagnosis of arrhythmogenic right ventricular cardiomyopathy/dysplasia: proposed modification of the Task Force Criteria. *Eur Heart J.* (2010) 31:806–14. doi: 10.1093/eurheartj/ehq025
3. Corrado D, Perazzolo Marra M, Zorzi A, Beffagna G, Cipriani A, Lazzari MD, et al. Diagnosis of arrhythmogenic cardiomyopathy: the Padua criteria. *Int J Cardiol.* (2020) 319:106–14. doi: 10.1016/j.ijcard.2020.06.005
4. Neilan TG, Farhad H, Mayrhofer T, Shah RV, Dodson JA, Abbasi SA, et al. Late gadolinium enhancement among survivors of sudden cardiac arrest. *JACC Cardiovasc Imaging.* (2015) 8:414–23. doi: 10.1016/j.jcmg.2014.11.017
5. Marra MP, Leoni L, Bauce B, Corbetti F, Zorzi A, Migliore F, et al. Imaging study of ventricular scar in arrhythmogenic right ventricular cardiomyopathy: comparison of 3D standard electroanatomical voltage mapping and contrast-enhanced cardiac magnetic resonance. *Circ Arrhythm Electrophysiol.* (2012) 5:91–100. doi: 10.1161/CIRCEP.111.964635
6. Corrado D, Basso C, Thiene G, McKenna WJ, Davies MJ, Fontaliran F, et al. Spectrum of clinicopathologic manifestations of arrhythmogenic right ventricular cardiomyopathy/dysplasia: a multicenter study. *J Am Coll Cardiol.* (1997) 30:1512–20. doi: 10.1016/S0735-1097(97)00332-X
7. Feliu E, Moscicki R, Carrillo L, García-Fernández A, Martínez Martínez JG, Ruiz-Nodar JM. Importance of cardiac magnetic resonance findings in the diagnosis of left dominant arrythmogenic cardiomyopathy. *Rev Esp Cardiol.* (2020) 73:885–92. doi: 10.1016/j.rec.2019.12.004
8. Kalam K, Otahal P, Marwick TH. Prognostic implications of global LV dysfunction: a systematic review and meta-analysis of global longitudinal strain and ejection fraction. *Heart.* (2014) 100:1673–80. doi: 10.1136/heartjnl-2014-305538
9. Ali MT, Yucel E, Bouras S, Wang L, Fei H-W, Halpern EF, et al. Myocardial strain is associated with adverse clinical cardiac events in patients treated with anthracyclines. *J Am Soc Echocardiogr.* (2016) 29:522–7.e3. doi: 10.1016/j.echo.2016.02.018
10. Haugaa KH, Smedsrud MK, Steen T, Kongsgaard E, Loennechen JP, Skjaerpe T, et al. Mechanical dispersion assessed by myocardial strain in patients after myocardial infarction for risk prediction of ventricular arrhythmia. *JACC Cardiovasc Imaging.* (2010) 3:247–56. doi: 10.1016/j.jcmg.2009.11.012
11. Kim HM, Cho G-Y, Hwang I-C, Choi H-M, Park J-B, Yoon YE, et al. Myocardial strain in prediction of outcomes after surgery for severe mitral regurgitation. *JACC Cardiovasc Imaging.* (2018) 11:1235–44. doi: 10.1016/j.jcmg.2018.03.016
12. Phelan D, Collier P, Thavendiranathan P, Popović ZB, Hanna M, Plana JC, et al. Relative apical sparing of longitudinal strain using two-dimensional speckle-tracking echocardiography is both sensitive and specific for the diagnosis of cardiac amyloidosis. *Heart.* (2012) 98:1442–8. doi: 10.1136/heartjnl-2012-302353
13. Zamorano JL, Lancellotti P, Rodriguez Muñoz D, Aboyans V, Asteggiano R, Galderisi M, et al. 2016 ESC Position Paper on cancer treatments and cardiovascular toxicity developed under the auspices of the ESC Committee for Practice Guidelines: the Task Force for cancer treatments and cardiovascular toxicity of the European Society of Cardiology (ESC). *Eur Heart J.* (2016) 37:2768–801. doi: 10.1093/eurheartj/ehw211
14. Alexandre J, Cautela J, Ederhy S, Damaj GL, Salem J-E, Barlesi F, et al. Cardiovascular toxicity related to cancer treatment: a pragmatic approach to the American and European Cardio-Oncology Guidelines. *J Am Heart Assoc.* (2020) 9:e018403. doi: 10.1161/JAHA.120.018403
15. Delgado-Montero A, Tayal B, Goda A, Ryo K, Marek JJ, Sugahara M, et al. Additive prognostic value of echocardiographic global longitudinal and global circumferential strain to electrocardiographic criteria in patients with heart failure undergoing cardiac resynchronization therapy. *Circ Cardiovasc Imaging.* (2016) 9:e004241. doi: 10.1161/CIRCIMAGING.115.004241
16. Lie ØH, Rootwelt-Norberg C, Dejgaard LA, Leren IS, Stokke MK, Edvardsen T, et al. Prediction of life-threatening ventricular arrhythmia in patients with arrhythmogenic cardiomyopathy: a primary prevention cohort study. *JACC Cardiovasc Imaging.* (2018) 11:1377–86. doi: 10.1016/j.jcmg.2018.05.017
17. Kirkels FP, Lie ØH, Cramer MJ, Chivulescu M, Rootwelt-Norberg C, Asselbergs FW, et al. Right ventricular functional abnormalities in arrhythmogenic cardiomyopathy: association with life-threatening ventricular arrhythmias. *JACC Cardiovasc Imaging.* (2021) 14:900–10. doi: 10.1016/j.jcmg.2020.12.028
18. Réant P, Hauer AD, Castelletti S, Pantazis A, Rosmini S, Cheang MH, et al. Epicardial myocardial strain abnormalities may identify the earliest stages of arrhythmogenic cardiomyopathy. *Int J Cardiovasc Imaging.* (2016) 32:593–601. doi: 10.1007/s10554-015-0813-9
19. Richards S, Aziz N, Bale S, Bick D, Das S, Gastier-Foster J, et al. Standards and guidelines for the interpretation of sequence variants: a joint consensus recommendation of the American College of Medical Genetics and Genomics and the Association for Molecular Pathology. *Genet Med.* (2015) 17:405–23. doi: 10.1038/gim.2015.30
20. Lang RM, Badano LP, Mor-Avi V, Afilalo J, Armstrong A, Ernande L, et al. Recommendations for cardiac chamber quantification by echocardiography in adults: an update from the American Society of Echocardiography and the European Association of Cardiovascular Imaging. *J Am Soc Echocardiogr.* (2015) 28:1–39.e14. doi: 10.1016/j.echo.2014.10.003
21. Voigt J-U, Pedrizzetti G, Lysyansky P, Marwick TH, Houle H, Baumann R, et al. Definitions for a common standard for 2D speckle tracking echocardiography: consensus document of the EACVI/ASE/Industry Task Force to standardize deformation imaging. *Eur Heart J Cardiovasc Imaging.* (2015) 16:1–11. doi: 10.1093/ehjci/jeu184
22. Sugimoto T, Dulgheru R, Bernard A, Ilardi F, Contu L, Addetia K, et al. Echocardiographic reference ranges for normal left ventricular 2D strain: results from the EACVI NORRE study. *Eur Heart J Cardiovasc Imaging.* (2017) 18:833–40. doi: 10.1093/ehjci/jex140
23. Tsugu T, Postolache A, Dulgheru R, Sugimoto T, Tridetti J, Nguyen Trung M-L, et al. Echocardiographic reference ranges for normal left ventricular layer-specific strain: results from the EACVI NORRE study. *Eur Heart J Cardiovasc Imaging.* (2020) 21:896–905. doi: 10.1093/ehjci/jeaa050
24. Rodríguez-Zanella H, Haugaa K, Boccalini F, Secco E, Edvardsen T, Badano LP, et al. Physiological determinants of left ventricular mechanical dispersion: a 2-dimensional speckle tracking echocardiographic study in healthy volunteers. *JACC Cardiovasc Imaging.* (2018) 11:650–1. doi: 10.1016/j.jcmg.2017.06.015
25. Petersen SE, Khanji MY, Plein S, Lancellotti P, Bucciarelli-Ducci C. European Association of Cardiovascular Imaging expert consensus paper: a comprehensive review of cardiovascular magnetic resonance normal values of cardiac chamber size and aortic root in adults and recommendations for grading severity. *Eur Heart J Cardiovasc Imaging.* (2019) 20:1321–31. doi: 10.1093/ehjci/jez232
26. Ortiz-Genga MF, Cuenca S, Dal Ferro M, Zorio E, Salgado-Aranda R, Climent V, et al. Truncating FLNC mutations are associated with high-risk dilated and arrhythmogenic cardiomyopathies. *J Am Coll Cardiol.* (2016) 68:2440–51. doi: 10.1016/j.jacc.2016.09.927
27. van Rijsingen IAW, Arbustini E, Elliott PM, Mogensen J, Hermans-van Ast JF, van der Kooi AJ, et al. Risk factors for malignant ventricular arrhythmias in lamin a/c mutation carriers a European cohort study. *J Am Coll Cardiol.* (2012) 59:493–500. doi: 10.1016/j.jacc.2011.08.078
28. Hodgkinson KA, Connors SP, Merner N, Haywood A, Young T-L, McKenna WJ, et al. The natural history of a genetic subtype of arrhythmogenic right ventricular cardiomyopathy caused by a pS358L mutation in TMEM43. *Clin Genet.* (2013) 83:321–31. doi: 10.1111/j.1399-0004.2012.01919.x
29. Bermúdez-Jiménez FJ, Carriel V, Brodehl A, Alaminos M, Campos A, Schirmer I, et al. Novel desmin mutation pGlu401Asp impairs filament formation, disrupts cell membrane integrity, and causes severe arrhythmogenic left ventricular cardiomyopathy/dysplasia. *Circulation.* (2018) 137:1595–610. doi: 10.1161/CIRCULATIONAHA.117.028719
30. Corrado D, Wichter T, Link MS, Hauer RNW, Marchlinski FE, Anastasakis A, et al. Treatment of arrhythmogenic right ventricular cardiomyopathy/dysplasia: an international task force consensus statement. *Circulation.* (2015) 132:441–53. doi: 10.1161/CIRCULATIONAHA.115.017944
31. Cadrin-Tourigny J, Bosman LP, Wang W, Tadros R, Bhonsale A, Bourfiss M, et al. Sudden cardiac death prediction in arrhythmogenic right

ventricular cardiomyopathy: a multinational collaboration. *Circ Arrhythmia Electrophysiol.* (2021) 14:8509. doi: 10.1161/CIRCEP.120.008509
32. Cadrin-Tourigny J, Bosman LP, Nozza A, Wang W, Tadros R, Bhonsale A, et al. A new prediction model for ventricular arrhythmias in arrhythmogenic right ventricular cardiomyopathy. *Eur Heart J.* (2019) 40:1850–8. doi: 10.1093/eurheartj/ehz103
33. Orgeron GM, te Riele A, Tichnell C, Wang W, Murray B, Bhonsale A, et al. Performance of the 2015 international task force consensus statement risk stratification algorithm for implantable cardioverter-defibrillator placement in arrhythmogenic right ventricular dysplasia/cardiomyopathy. *Circulation.* (2018) 11:e005593. doi: 10.1161/CIRCEP.117.005593
34. Aquaro GD, De Luca A, Cappelletto C, Raimondi F, Bianco F, Botto N, et al. Prognostic value of magnetic resonance phenotype in patients with arrhythmogenic right ventricular cardiomyopathy. *J Am Coll Cardiol.* (2020) 75:2753–65. doi: 10.1016/j.jacc.2020.04.023
35. Segura-Rodríguez D, Bermúdez-Jiménez FJ, Carriel V, López-Fernández S, González-Molina M, Oyonarte Ramírez JM, et al. Myocardial fibrosis in arrhythmogenic cardiomyopathy: a genotype-phenotype correlation study. *Eur Heart J Cardiovasc Imaging.* (2020) 21:378–86. doi: 10.1093/ehjci/jez277
36. Nagata Y, Wu VC-C, Otsuji Y, Takeuchi M. Normal range of myocardial layer-specific strain using two-dimensional speckle tracking echocardiography. *PLoS ONE.* (2017) 12:e0180584. doi: 10.1371/journal.pone.0180584
37. Büchi M, Hess OM, Murakami T, Krayenbuehl HP. Left ventricular wall stress distribution in chronic pressure and volume overload: effect of normal and depressed contractility on regional stress-velocity relations. *Basic Res Cardiol.* (1990) 85:367–83. doi: 10.1007/BF01907129
38. Kuwada Y, Takenaka K. Transmural heterogeneity of the left ventricular wall: subendocardial layer and subepicardial layer. *J Cardiol.* (2000) 35:205–18.
39. Teske AJ, Cox MG, De Boeck BW, Doevendans PA, Hauer RN, Cramer MJ. Echocardiographic tissue deformation imaging quantifies abnormal regional right ventricular function in arrhythmogenic right ventricular dysplasia/cardiomyopathy. *J Am Soc Echocardiogr.* (2009) 22:920–7. doi: 10.1016/j.echo.2009.05.014
40. Vitarelli A, Cortes Morichetti M, Capotosto L, De Cicco V, Ricci S, Caranci F, et al. Utility of strain echocardiography at rest and after stress testing in arrhythmogenic right ventricular dysplasia. *Am J Cardiol.* (2013) 111:1344–50. doi: 10.1016/j.amjcard.2013.01.279

Conflict of Interest: The authors declare that the research was conducted in the absence of any commercial or financial relationships that could be construed as a potential conflict of interest.

Publisher's Note: All claims expressed in this article are solely those of the authors and do not necessarily represent those of their affiliated organizations, or those of the publisher, the editors and the reviewers. Any product that may be evaluated in this article, or claim that may be made by its manufacturer, is not guaranteed or endorsed by the publisher.

frontiers in Cardiovascular Medicine

REVIEW
published: 07 December 2021
doi: 10.3389/fcvm.2021.746321

Histopathological Features and Protein Markers of Arrhythmogenic Cardiomyopathy

*Carlos Bueno-Beti and Angeliki Asimaki**

Molecular and Clinical Sciences Research Institute, St. George's University of London, London, United Kingdom

Arrhythmogenic cardiomyopathy (ACM) is a heritable heart muscle disease characterized by syncope, palpitations, ventricular arrhythmias and sudden cardiac death (SCD) especially in young individuals. It is estimated to affect 1:5,000 individuals in the general population, with >60% of patients bearing one or more mutations in genes coding for desmosomal proteins. Desmosomes are intercellular adhesion junctions, which in cardiac myocytes reside within the intercalated disks (IDs), the areas of mechanical and electrical cell-cell coupling. Histologically, ACM is characterized by fibrofatty replacement of cardiac myocytes predominantly in the right ventricular free wall though left ventricular and biventricular forms have also been described. The disease is characterized by age-related progression, vast phenotypic manifestation and incomplete penetrance, making proband diagnosis and risk stratification of family members particularly challenging. Key protein redistribution at the IDs may represent a specific diagnostic marker but its applicability is still limited by the need for a myocardial sample. Specific markers of ACM in surrogate tissues, such as the blood and the buccal epithelium, may represent a non-invasive, safe and inexpensive alternative for diagnosis and cascade screening. In this review, we shall cover the most relevant biomarkers so far reported and discuss their potential impact on the diagnosis, prognosis and management of ACM.

Keywords: arrhythmogenic cardiomyopathy, sudden cardiac death, desmosomes, intercalated disk, histopathology, protein markers, buccal cells, plasma auto-antibodies

OPEN ACCESS

Edited by:
Nuno Cardim,
Hospital da Luz Lisboa, Portugal

Reviewed by:
Francisco José Bermúdez-Jiménez,
Hospital Universitario Virgen de las Nieves, Spain
Gaetano Thiene,
University of Padua, Italy

****Correspondence:***
Angeliki Asimaki
aasimaki@sgul.ac.uk

Specialty section:
This article was submitted to Cardiovascular Imaging, a section of the journal Frontiers in Cardiovascular Medicine

Received: *23 July 2021*
Accepted: *17 November 2021*
Published: *07 December 2021*

Citation:
Bueno-Beti C and Asimaki A (2021) Histopathological Features and Protein Markers of Arrhythmogenic Cardiomyopathy. Front. Cardiovasc. Med. 8:746321. doi: 10.3389/fcvm.2021.746321

INTRODUCTION

Demographics

Current experts in the field estimate that ACM affects 1:5,000 individuals in the general population although regional differences exist (1). SCD is often the first manifestation of ACM, and the diagnosis is missed at autopsy, particularly if this is not performed by an expert cardiac pathologist. The disease is also frequently missed clinically, owing to its vast phenotypic manifestation, age-related progression, incomplete penetrance and overlap with other disease entities (1). In a large cohort of ACM patients, the mean age at first evaluation was 36 ± 14 years with a median age of cardiac arrest of 25 years (1). Accounting for up to 20% of the cases, ACM is one of the leading causes of SCD in the young (2) and it is responsible between 4.7 and 27% of SCD in athletes (3–5). The incidence and severity of ACM is higher in men than in women (male/female ratio 2.7:1) (6–8). The pathophysiology behind this difference could be attributed to a direct effect of sex hormones on the disease phenotype or to differences in the amount and intensity of exercise between genders (9, 10).

Clinical Presentation, Progression, and Diagnosis

The most common clinical manifestations of ACM are syncope, palpitations and SCD caused by ventricular arrhythmias. In the natural history of the classical right ventricular (RV) disease, four different stages have been documented (11). In the first phase (so-called pre-clinical or concealed), patients are at risk of SCD, especially during strenuous exertion, even if structural abnormalities are very subtle or totally absent. The second phase is characterized by an overt electrical disorder with ECG abnormalities such as inverted T-waves and arrhythmias with left bundle branch block morphology. Structural abnormalities are discernible by conventional imaging but restricted to the RV. In the third phase, the extension of the disease through the RV results in isolated right heart failure. Localized involvement of the left ventricle (LV) may occur at this stage but the function of the left heart is still preserved. In the final phase, LV involvement leads to end-stage heart failure with biventricular involvement (11). It seems plausible that during the early stages of the disease, arrhythmias may arise entirely in the context of molecular and subcellular abnormalities. Conversely, at later stages, tissue scarring and fibrofatty replacement of healthy myocardium appears to be responsible for the generation of the arrhythmogenic substrate.

New cardiac imaging techniques and genotype-phenotype correlations identified patients with biventricular and left-dominant form of the disease (11, 12). The most common presentation of these forms are ventricular arrhythmias with right-bundle-branch-block morphology indicating a LV origin and ECG abnormalities such as low QSR voltages in the limb leads and negative T-waves in the lateral or inferolateral leads. LV systolic function is normal or mildly reduced with mild or no dilatation (13). In the left-dominant ACM structural remodeling is found earlier and predominantly in the LV affecting the posterolateral region of LV free wall and, less commonly, the septum (14). Structural remodeling of the LV is most likely responsible for the generation of the arrhythmogenic substrate. In fact, in a recent study, the presence of fat infiltration in the subepicardial posterolateral region of the LV determined by cardiac magnetic resonance supports the diagnosis of left-dominant form of the disease and rules out myocarditis, a known phenocopy of ACM (15).

ACM is a complex disease, and its phenotype is determined by the presence of abnormal electrical and structural substrates. Its diagnosis can be challenging and requires evidence of all structural, functional, and electrophysiological abnormalities. Accordingly, the International Task Force (ITF) criteria for the clinical diagnosis of ACM were proposed for the first time in 1994 (16) and updated in 2010 (17). These include major and minor criteria from six different categories including: repolarization/depolarization abnormalities, arrhythmias, morphological alterations, functional changes, histopathological changes, and family history/genetic findings. Definite ACM diagnosis requires fulfillment of two major criteria, one major and two minor criteria or four minor criteria from different categories. These criteria, however, were more tailored to recognizing the "classical," RV form of the disease. To improve the diagnosis of left-sided phenotypes, a revision of the 2010 ITF criteria (18) and the introduction of new diagnostic criteria regarding tissue characterization and ventricular arrhythmia features have recently been suggested, resulting in a new set of criteria, The Padua Criteria (13).

Several diseases may mimic ACM making its diagnosis even more challenging. Early phases of ACM are often misdiagnosed as idiopathic right ventricular outflow tract (RVOT) tachycardia (19) or Brugada syndrome (20). In the more advanced biventricular form of the disease, ACM is indistinguishable from dilated cardiomyopathy (DCM) (21). In some instances, patients with cardiac sarcoidosis present with clinical manifestations highly reminiscent of ACM and differential diagnosis is achieved only by the presence of non-caseating granulomas or other sarcoid features not seen in ACM. Other diseases that mimic ACM are myocarditis and pulmonary hypertension (21).

Genetics

On the Greek island of Naxos, *Protonotarios* and colleagues first described a syndromic form of ACM characterized by cardiomyopathy, wooly hair and palmoplantar keratoderma (PPK). The syndrome, named Naxos disease, was inherited in an autosomal recessive manner and was fully penetrant by adolescence (22). In the year 2000, genetic linkage analysis identified a homozygous deletion in the *JUP* gene (*PG*; encoding for plakoglobin) as the cause of Naxos disease (23). Almost at the same time, *Carvajal-Huerta* and colleagues reported a homozygous truncating mutation in the *DSP* gene (encoding for desmoplakin) as causative of Carvajal Syndrome; a similar disease, characterized by biventricular cardiomyopathy, wooly hair, and PPK (24). Mutations following an autosomal dominant inheritance pattern have also been described for JUP and DSP genes (25, 26). Both plakoglobin and desmoplakin are integral proteins of the desmosome, a specialized adhesion protein complex located at intercellular junctions. In tissues subjected to increased mechanical stress, such as the heart and the epidermis, desmosomes are responsible for maintaining tissue integrity by serving as a mechanical link between the intermediate filaments of two adjacent cells (23, 24).

Genetic studies of other components of the cardiac desmosome in ACM patients led to the discovery of missense and truncating mutations in further desmosomal genes, specifically those coding for: plakophilin 2 (*PKP2*) (27), desmoglein-2 (*DSG2*) (28–30) and desmocollin-2 (*DSC2*) (31–33). Today it

Abbreviations: ACM, Arrhythmogenic Cardiomyopathy; APC, Adenomatous Polyposis Coli; CDH2, Cadherin 2; CTNNA3, Catenin-α3; Cx43, Connexin 43; DCM, Dilated Cardiomyopathy; DCS2, Desmocollin-2; DES, Desmin; DSG2, Desmoglein-2; DSP, Desmoplakin; ECG, Electrocardiogram; EMB, Endomyocardial Biopsies; FLNC, Filamin C; GSK3β, Glycogen Synthase Kinase 3β; HCM, Hypertrophic Cardiomyopathy; ICM, Ischaemic Cardiomyopathy; ID, Intercalated Disk; iPSC-CMs, Induced Pluripotent Stem Cell-derived Cardiomyocytes; ITF, International Task Force; LV, Left Ventricle; PG, Plakoglobin; PKP, Palmoplantar Keratoderma; PKP1, Plakophilin-1; PKP2, Plakophilin 2; PLN, Phospholamban; RV, Right Ventricle; RVOT, Right Ventricular Outflow Tract; SAP97, Synapse-Associated Protein 97; SCD, Sudden Cardiac Death; SCN5A, Cardiac Sodium Channel Nav1. 5; TGFB3, Transforming Growth Factor-β3; TMEM43, Transmembrane protein 43; TTN, Titin.

is estimated that >60% of ACM patients are bearing one or more mutations in these 5 genes; *PKP2* being the most highly mutated (1, 34). Most commonly, desmosomal mutations follow an autosomal dominant pattern of inheritance with age-related, incomplete penetrance and variable expressivity, although autosomal recessive patterns of inheritance have also been observed such as in Naxos disease and Carvajal Syndrome. The occurrence of ACM patients harboring multiple mutations (compound or digenic heterozygosity) is common and increases the risk of arrhythmias and SCD (1, 10, 35). Importantly, genetic studies to identify an underlying mutation in a proband diagnosed with ACM can aid cascade screening. Mutation-carrying relatives have an earlier onset of symptoms, increased risk of arrhythmias and a 6-fold increased risk of ACM diagnosis compared to relatives without a mutation (36).

Historically, ACM caused by desmosomal mutations has largely been associated to the classical RV variant of the disease. However, exceptions to this general trend have been observed. Patients carrying mutations in PKP2 gene often present LV involvement at advanced stages of the disease while mutations in DSG2 and DSC are often associated to biventricular forms of ACM. Mutations in DSP (37, 38) and more recently in DSG2 (39) genes have been associated to left-dominant forms of the disease.

At the IDs, the desmosomes, together with the adherens and gap junctions, control the electrical and mechanical coupling of cardiomyocytes (40). The tight structural and functional interaction between these macromolecular structures stimulated the search for gene mutations in other constituents of the IDs leading to the discovery of mutations in the adherens junction genes coding for Cadherin 2 (*CDH2*) (41–43) and catenin-α3 (*CTNNA3*) (44).

Mutations in non-desmosomal genes are increasingly recognized and are usually associated with more severe presentation and left-dominant or biventricular forms of ACM. Some of these mutations are in genes encoding for proteins of the cytoskeleton. Patients with mutations in desmin (DES) (45) and filamin C (FLNC) (46) genes have been found to present circumferential pattern of subepicardial late gadolinium enhancement and fibrosis in the LV that was associated with higher risk of SCD (47). Another gene coding for cytoskeleton proteins commonly mutated is titin (TTN) (48). Of note is the fully penetrant mutation (p.S358L) in transmembrane protein 43 (TMEM43) gene responsible for the most aggressive heterozygous form of ACM (type V). Mutation carriers show increased incidence of SCD that is higher in males and common LV involvement (49). Other implicated genes in ACM code for calcium handling proteins such as phospholamban (PLN) (50). Patients carrying the mutation PLN-p.Arg14del present late gadolinium enhancement in the LV posterolateral wall and LV dysfunction. Finally, rare ACM-causing mutations have been identified in the genes coding for the major subunit of the cardiac sodium channel nav1.5 (*SCN5A*) (51) and the profibrotic cytokine transforming growth factor-β3 (*TGFB3*) (52). The frequency of non-desmosomal mutations tends to be very low in large cohorts of ACM patients. However, some of these are found in higher frequencies in specific regions. For instance, the R14del mutation in the *PLN* gene has a very high frequency in the Netherlands due to a founder effect (50, 53). A summary of all genes implicated in ACM pathogenesis can be found in **Table 1**. Although ACM is a genetically determined cardiomyopathy its relatively late onset, around the second and the fourth decades of life, is still poorly understood and it is believed to be associated with chronic, accumulated stress to the heart. Pathogenic mutations in the genes presented in **Table 1** predispose to ACM and environmental factors such as exercise (9, 55, 56) and male gender (57, 58) modulate disease onset and progression.

Very recently an evidence-based re-evaluation of all reported ACM genes by using the semiquantitative Clinical Genome Resource framework revealed that only 8 of the aforementioned genes (*PKP2, DSP, DSG2, DSC2, JUP/PG, TMEM43, PLN*, and *DES*) had definitive or moderate evidence for ACM (59). Moreover, these genes account for virtually all (97.4%) pathogenic/likely pathogenic ACM variants in Clinvar. Accordingly, the authors recommend that only pathogenic/likely pathogenic alterations in these 8 genes should yield a major criterion for ACM diagnosis (59).

This is crucial, as incomplete/misleading information of the genetics underlying the pathogenesis of ACM can increase the risk of misdiagnosis. Currently, molecular genetic testing is indicated to identify a pathogenic or likely pathogenic mutation in a proband fulfilling the diagnostic criteria for ACM (60). If a mutation is found in the proband, mutation-specific genetic testing is then applied to family members to identify individuals carrying the mutation(s) and thus guide their management accordingly (18).

HISTOPATHOLOGICAL FEATURES AND PROTEIN MARKERS

Gross Histological Features

The histological hallmark of ACM is regarded to be the fibrofatty replacement of myocardial tissue associated with ventricular atrophy (2, 6). The pathological changes in the heart start in the epicardium spreading to the endocardium to eventually become transmural in more advanced stages of the disease, mainly affecting the RV free wall. Within the RV, the most common areas affected are the inflow tract, the outflow tract and the apex, collectively known as the triangle of dysplasia (**Figure 1A**) (6). The endocardial trabeculated muscles of the RV and the septum are generally spared of histopathological changes. Aneurysms, if present, are commonly located in the inflow and outflow tract of the RV. In an autopsy series of classical right-sided cases of ACM, alterations in the LV were found in 76% of the hearts.

Genotype-phenotype correlations and the use of contrast-enhancement cardiac magnetic resonance to evidence fibrofatty replacement in the LV have uncovered biventricular and left-dominant forms of the disease (11, 12). In the left dominant form of ACM, pathohistological structural remodeling can be observed originating in the epicardium and progressing toward the endocardium, to finally become transmural with localized or extensive wall thinning in the most severe presentation

TABLE 1 | Genes associated with ACM.

Localization/ function	Gene symbol	Protein	Estimated frequency (%)	Mode of inheritance	Overlapping diseases	Affected ventricle	References
Desmosome	*PKP2*	Plakophilin 2	46	AD	BrS	RV, biventricular	(1, 30)
	DSP	Desmoplakin	14	AD, AR (Carvajal Syndrome)	DCM	LV, biventricular	(26, 30)
	DSG2	Desmoglein 2	10	AD	DCM	RV, biventricular	(28, 30)
	DSC2	Desmocollin 2	9	AD, AR (no skin manifestation)	–	RV, biventricular	(30)
	JUP	Plakoglobin	0.4	AD, AR (Naxos disease)	–	RV, biventricular	(1, 30)
Area Composita	*CTNNA3*	Catenin-α3	2.6	AD	–	RV, biventricular	(44)
	CDH2	Cadherin 2	1.2	AD	–	RV, biventricular	(41)
Cytoskeleton	*DES*	Desmin	Rare	AD	DCM, HCM	LV, biventricular	(45)
	FLNC	Filamin C	Rare	AD	DCM	LV	(46)
	TMEM43	transmembrane protein 43	Rare	AD	–	RV, biventricular	(54)
	TTN	Titin	Rare	AD	DCM, HCM	RV, LV, biventricular	(48)
Ion transport	*SCN5A*	Nav1.5	Rare	AD	BrS, LQTS	LV, biventricular	(51)
	PLN	Phospholamban	Rare	AD	DCM	LV, biventricular	(50)
Cytokine	*TGFB3*	Transforming growth factor-ß3	Rare	AD	–	RV	(52)

AD, autosomal dominant; AR, autosomal recessive; BrS, Brugada Syndrome; DCM, dilated cardiomyopathy; HCM, hypertrophic cardiomyopathy; LQTS, Long QT syndrome; LV, left ventricle; Nav1.5, α-subunit of the cardiac sodium channel complex; RV, right ventricle.

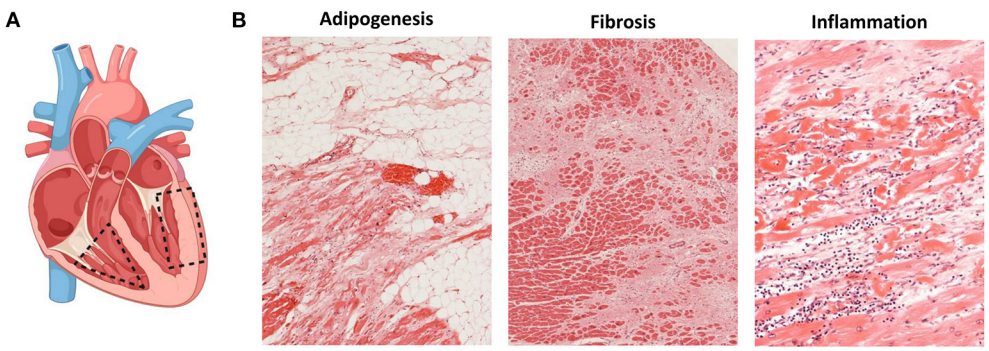

FIGURE 1 | Histopathological changes in ACM. **(A)** Most affected heart regions in ACM. In the right ventricle, structural changes mostly affect areas of the inflow tract, the outflow tract and the apex known as the triangle of dysplasia (dashed triangle). When the left ventricle is affected, structural changes are observed in the inferior and inferolateral walls (dashed rectangle); created with BioRender.com. **(B)** Histopathological changes observed in ACM namely adipogenesis (left), fibrosis (middle) and presence of inflammatory infiltrates (right).

of the disease. The fibrofatty replacement is mostly located in the subepicardial inferolateral LV free wall (11, 12, 14). In a large cohort of SCD victims due to ACM, isolated LV disease was observed in 17% whereas biventricular involvement was observed in 70% of the cases. In this cohort, the most common areas of the LV presenting fibrofatty replacement were the posterobasal (68%) and anterolateral walls (58%) (61). Similarly to the classical ACM, structural remodeling of

the LV is most likely responsible for the generation of the arrhythmogenic substrate.

The isolated infiltration of epicardial adipocytes is not enough to diagnose ACM as it can be a normal finding in elderly and obese individuals. It must be accompanied by myocyte degeneration and fibrotic replacement (**Figure 1B**) (62). The current ITF criteria now establish a residual number of cardiomyocytes at <60% by morphometric analysis coupled with fibrous replacement as a major histological criterion (17). The histopathological characterization of fibrofatty replacement of the healthy myocardium can be made either in full hearts (post-mortem or following cardiac transplantation) or in cardiac biopsy samples (17).

The presence of inflammatory infiltrates is another common feature of ACM and it has been reported in up to 75% of hearts at autopsy (**Figure 1B**) (63). Such infiltrates consist of concentrations of mononuclear cells (lymphocytes and macrophages) around necrotic or injured cardiomyocytes and can be found both in the ventricular walls and the septum (64). The presence of inflammatory infiltrates is indicative of ongoing myocardial damage suggesting a pathological role for inflammation and/or myocarditis in ACM (64). It is not clear yet, however, if the infiltrates accumulate in the heart as a response to myocyte damage of if those cells themselves promote myocyte injury, fibrofatty replacement and arrhythmias through immune mechanisms. Noteworthily, the activation of the major inflammatory pathway NFκB was recently reported as a driver of key features of ACM in several experimental models (65).

Similar to the clinical, natural history of the disease, there are also four histological stages characterizing ACM progression (66). The concealed phase is characterized by minimal or no histological changes. The second phase is characterized by minor histological alterations confined to the RV. The third phase is characterized by extensive RV remodeling with severe dilatation but preserved LV structure/function. Finally, extensive remodeling of both ventricles is evident in advanced disease (67).

Endomyocardial Biopsies

Given the severe, extended histological changes observed in explanted hearts of ACM patients (**Figure 1B**) the frequency of false negative results obtained on endomyocardial biopsies (EMBs) is surprising. This can be explained by the natural course of the disease, its patchy nature as well as technical limitations of the sampling process. Since the disease progresses from the epicardium to the endocardium, samples obtained from the endocardium of patients with early/mild forms of the disease may be totally devoid of the aforementioned pathological features (62). Moreover, EMBs tend to be taken from the interventricular septum, generally spared of the histopathological changes of ACM. To determine what area of the heart is more informative for the diagnosis of ACM, Basso et al. analyzed simulated biopsies obtained from various locations of explanted hearts (62). With a specificity of 95% and sensitivity of 80%, the main diagnostic parameter was the amount of residual myocardium (<59%) with the presence of fat (>22%) and fibrous tissue (>31%). The diagnostic yield varied across the different regions of the heart with the "triangle of dysplasia" being the most informative region and the septum and the LV the least (62). Noteworthily, however, sampling the RV free wall comes with an increased risk of ventricular perforation and tamponade (68).

The diagnostic yield of EMBs can be improved by the use of electroanatomic voltage mapping as areas showing low voltage have been associated with myocyte degeneration and fibrofatty replacement. In one study, electroanatomic voltage mapping-guided EBM was diagnostic of ACM in 81% of the cases rendering a high diagnostic sensitivity (69). In another case series, the approach allowed for the accurate differential diagnosis of myocarditis, a known phenocopy of ACM (70). In a very recent study, electroanatomic voltage mapping-guided EMB improved the 2010 ITF criteria diagnostic yield by upgrading one-third of the patients at risk to definite ACM with negligible complications. This study supports the notion that electroanatomic voltage mapping-guided EMB may still be a safe and useful tool for the diagnosis of ACM (71).

Nevertheless, EMB is still considered an invasive procedure with associated risks that has a low diagnostic yield. Nowadays, it is rarely performed in the initial diagnosis of the disease. It is indicated in cases of non-familial ACM for differential diagnosis of phenocopies (72), specifically in probands with sporadic ACM and negative gene testing to exclude sarcoidosis, myocarditis, or other heart muscle disorders (13). Post-mortem and explanted hearts do not have any of these limitations and should be meticulously examined by expert cardiac pathologists whenever possible (73). Immunohistochemical examination of protein markers of ACM in heart samples or surrogate tissues may provide added diagnostic value and are reviewed in the next section.

Protein Markers in Heart Tissue

The discovery of the first ACM-causative genes, has helped the scientific community uncover some of the mechanisms driving the pathophysiology of the disease. As a result, key molecular players were identified, which can be used in the future as therapeutic targets and/or specific molecular markers of the disease. In this section we will cover the protein markers in heart tissue samples reported so far that can potentially help the diagnosis and risk stratification of ACM.

Human myocardial samples obtained at autopsy or following transplantation are most commonly used in the search of specific protein markers. Due to the associated risk of RV perforation and tamponade, the studies on EMBs have been more limited. Following the discovery of the causative gene for Naxos disease (23), the most logical candidate to investigate first was plakoglobin. In 2004 Kaplan et al. showed for the first time that even if the mutated plakoglobin was expressed in the hearts of Naxos disease patients it failed to reach the IDs where the protein executes its structural roles (74). The re-distribution of plakoglobin was accompanied by gap junction remodeling as evidenced by decreased immunoreactive signal for Connexin 43 (*Cx43*; the major ventricular gap junction protein) at the IDs and smaller/fewer gap junctions connecting ventricular myocytes in both RV and LV samples. The expression of other desmosomal proteins at the IDs of patients with Naxos disease was normal (74). In a patient with Carvajal Syndrome, similar findings were

reported. In this case, it was desmoplakin, being the mutated protein, that failed to localize at the IDs (75). Gap junction remodeling was also observed in this syndrome. Interestingly, the localization of plakoglobin at the ID was also prevented, even if it was not itself mutated (75). This observation revealed for the first time, that a mutation in a gene coding for a given protein can affect the localization of further, interacting proteins, even if they are not themselves affected by genetic alterations.

These findings were validated in larger cohorts of patients with a definite diagnosis of ACM and dominantly inherited mutations in the *DSP, DSC2, PKP2*, or *DSG2* genes. Most patients showed a marked reduction in immunoreactive signal for plakoglobin at the ID, which was not confined to areas of the RV showing pathological changes but was also present in areas of the LV and septum that appeared structurally normal (**Figure 2**). This observation suggested that even an EMB sample obtained from the right side of the septum would show this diagnostic change hence reducing the number of false negatives and risk associated with this technique. Other desmosomal proteins showed variable patterns of distribution confirming that mutations in a single protein can affect the localization of other non-mutated partners. Plakoglobin redistribution from the ID to the cytosolic pool was shown to be specific for ACM as this change was not observed in heart samples of patients with documented hypertrophic cardiomyopathy (HCM), DCM or ischemic cardiomyopathy (ICM) (76). It is important to highlight that in order to bring up differences in PG junctional distribution between control and ACM myocardial samples a broad range of antibody dilutions need to be tested. The endpoint is to achieve a binary result up to the point where you detect signal or no signal at the intercalated disks of the cardiomyocytes. By removing the necessity of image quantification, we reduce the subjectivity in the interpretation of the results while increasing the reproducibility of the technique across laboratories (77).

Cx43 expression was diffusely reduced throughout the heart in all ACM samples analyzed in this cohort but was not specific of ACM. Reduced Cx43 expression at the IDs has been observed in end-stage HCM, DCM, and ICM, being more apparent in areas with substantial structural remodeling (78, 79). However, in ACM, gap junction remodeling seems to occur diffusely in early stages of the disease in areas of the heart with minimal or no structural remodeling, potentially playing a primary role in the highly arrhythmogenic nature of this disease (76). How mutations in desmosomal proteins can impact on the stability and function of the gap junctions it is poorly understood. More recently, the molecular mechanism behind gap junction remodeling in ACM has been uncovered by using a murine model of desmosomal ACM. Specifically, it has been shown that DSP maintains the integrity of the gap junctions by inhibiting Connexin 43 lysosomal degradation (80). Despite its specificity among the cardiomyopathies, however, plakoglobin redistribution could not discriminate ACM from sarcoidosis and giant cell myocarditis (81). Plakoglobin labeling is an additional test but on its own it is not conclusive for the diagnosis of ACM. For this reason, is has not been added to the ITF criteria as of now.

Furthermore, EMB samples obtained from two patients with subclinical ACM bearing *DSP* variants showed loss of ID immunoreactive signal for desmoplakin but not for plakoglobin (82). Notably, *DSP* variants have been increasingly linked to biventricular or left-dominant ACM. In fact, a recent report, suggested that patients bearing pathogenic *DSP* variants manifest with a disease distinct from ACM or DCM, termed desmoplakin cardiomyopathy (37, 38).

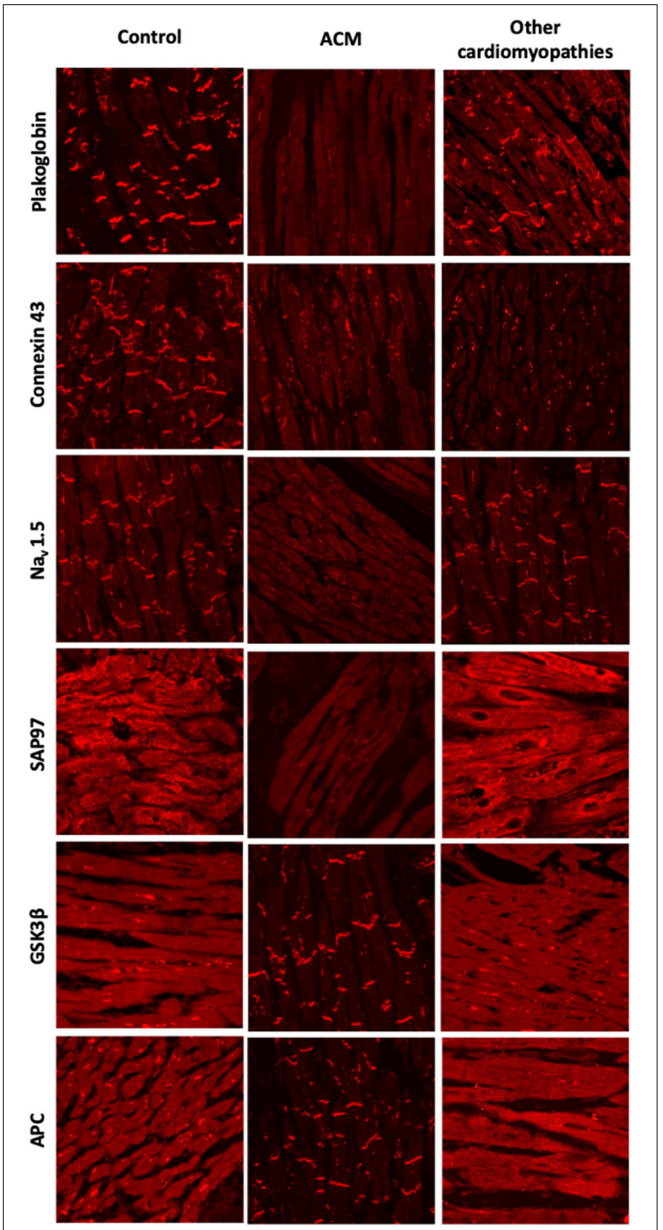

FIGURE 2 | Protein re-distribution in the hearts of ACM patients. Representative confocal immunofluorescence images showing loss of junctional signal for PG, Cx43, and Nav1.5 in ACM myocardium compared to controls. Additionally, both sarcomeric and junctional signal for SAP97 is lost while GSK3β and APC translocate to the junctions. Myocardium from patients with other forms of cardiomyopathy show normal distribution of PG, Nav1.5, GSK3β and APC. Gap junction remodeling is, however, evident and ID signal for SAP97 is also lost, though its sarcomeric distribution is preserved.

Reduced densities of the cardiac I_{Na} current and the inward rectifying K^+ current I_{K1} have been reported in different experimental models of ACM (83–85). Moreover, induced pluripotent stem cell-derived cardiomyocytes (iPSC-CMs) from a patient bearing a mutation in *PKP2* showed reduced I_{Na} (86) and abnormal Ca^{+2} dynamics (87). There is also direct evidence of reduced ID immunoreactive signal for Nav1.5 in patients with ACM (77). These electrophysiological alterations together with gap junctional remodeling could be responsible for the highly arrhythmogenic nature of ACM at its early stages. One possible explanation for these observations is that mutations in desmosomal proteins could alter the complex interactions that take place within the ID between the mechanical, electrical and gap junction components. However, both Nav1.5 and Kir2.1 (the major protein responsible for the I_{K1} current) have SIV motifs binding to the PDZ domains of the synapse-associated protein 97 (SAP97). SAP97 silencing seems to regulate Nav1.5 and the stoichiometry of Nav1.5 and Kir2.1 at the ID (88, 89). Also, SAP97 together with the ion channel proteins traffic as a multiprotein complex, suggesting a role for abnormal protein trafficking in ACM. Decreased immunoreactive signal for SAP97 was observed at the IDs in the myocardium of patients with ACM as well as two *in vitro* models of the disease (85). Sarcomeric signal for SAP97 was retained in the myocardium of patients with HCM, DCM or ICM although concentrated ID signal was also lost. Accordingly, loss of immunoreactive signal from both sarcomeric and junctional pools appears to be a specific feature of ACM (**Figure 2**) (85).

A drug screening study in a transgenic zebrafish model of ACM revealed that one compound, SB216763, a specific inhibitor of glycogen synthase kinase 3β (GSK3β), prevented all disease endpoints in this experimental model (85). Moreover, in two transgenic mouse models of ACM, SB216763 was able to prevent all clinical and subcellular disease features (90). In agreement with the work led by professor Saffitz, more recently Padrón-Barthe et al. have recapitulated these results in another *in vitro* (iPS) and *in vivo* (transgenic mouse) experimental models of non-desmosomal type 5 ACM caused by the expression of TMEM43 p.S358L mutation (91). In the healthy myocardium, GSK3β and its binding partner adenomatous polyposis coli (APC) show a diffuse cytoplasmic localization. In sharp contrast, in ACM myocardium, the proteins strongly localize at the IDs. GSK3β and APC redistribution from the cytosol to the ID was specific for ACM as it was not observed in other forms of heart disease including HCM, DCM, ICM, or cardiac sarcoidosis (**Figure 2**) (85).

Protein redistribution in the hearts of ACM patients occurs diffusely throughout the myocardium, preceding gross histopathologic changes. EMBs from the right side of the septum would thus show this diagnostic change, increasing the diagnostic yield of this technique. Not all the protein changes presented in this section are specific to ACM. Their combination, however, may represent an unequivocal molecular signature for the disease. Redistribution of plakoglobin, Cx43, Nav1.5, and SAP97 from the ID to the cytoplasm in conjunction with a shift of GSK3β and APC from the cytosol to the ID appears to be the most consistent finding in the myocardium of most ACM patients analyzed to date (**Figure 2**). More recently, it has been found that in non-desmosomal ACM caused by the PLN p.Arg14del mutation, key protein distribution in the heart differs to that exhibited by classical, desmosomal ACM (92). This indicates that additional genetic variants may contribute to the phenotypical heterogeneity of ACM.

Highly informative as this "molecular signature" may be, its use is still limited by the implicit need for a heart sample. As mentioned above, EMBs are invasive and risky, tend to be used as a "last resort" and could not be used to screen potentially healthy family members of ACM patients. This limitation would be bypassed if similar diagnostic information could be obtained from surrogate tissues expressing desmosomal proteins such as the hair follicles or the skin, particularly the buccal epithelium; a specialized form of skin that does not require a full thickness biopsy procedure to be sampled. Some groups have explored this idea and their findings are covered in the next section.

Protein Markers in Buccal Mucosa Cells

The buccal mucosa consists of non-keratinized stratified squamous epithelium where cells adhere to one another through different types of junctional structures. Of these structures, desmosomes are the ones connecting the keratin intermediate filaments of adjacent cells creating a 3D array within the entire epithelium (93). The protein makeup of a desmosome is very similar between the buccal mucosa and the heart. Buccal cells can be obtained easily and safely through a non-invasive procedure and therefore they would represent the ideal surrogate tissue to study protein redistribution in ACM patients and unaffected family members at a relatively low cost.

Accordingly, the localization of plakoglobin, desmoplakin, plakophilin-1 (*PKP1*; an isoform of PKP2 expressed in the upper epithelia) and Cx43 was investigated in the buccal mucosa of 39 patients with a definite clinical diagnosis of ACM bearing desmosomal gene mutations. Protein localization was also investigated in 15 family members of the aforementioned probands, who were bearing ACM-causing variants without showing clinical evidence of disease. Buccal smears from 40 individuals with no family history or clinical evidence of heart disease served as negative controls. Cells from 7 individuals with other forms of cardiomyopathy were used to test the specificity of the findings (94). Immunoreactive signal for plakoglobin and Cx43 was reduced in the buccal mucosa of the majority of ACM patients when compared to healthy controls and individuals with other forms of heart disease. Interestingly, junctional signal for these proteins was also decreased in the majority of family members carrying mutated alleles without showing evidence of heart disease, suggesting that redistribution of desmosomal proteins does not necessarily correlate with clinical expression of the disease.

Another interesting finding in this study was the link between the reduced junctional localization of specific desmosomal proteins in the buccal mucosa cells and the mutant gene of interest. Signal for desmoplakin was reduced in buccal mucosa cells from patients bearing mutations in *DSP, DSC2*, or *DSG2* but not patients bearing mutations in *PKP2*. Similarly, signal for PKP1 was reduced in buccal mucosa cells from patients bearing

mutations in *PKP2* but not those with mutations in *DSP, DSC2*, or *DSG2* (**Figure 3**). This association becomes even more interesting if one considers that PKP1 and PKP2 are expressed by different genes, located on different chromosomes. Yet, they appear to share common regulatory mechanisms where a mutation in one isoform expressed in one tissue, can affect the localization of a different isoform, expressed in a different tissue. Importantly, when buccal mucosa cells of ACM patients were cultured *in vitro* and exposed to SB216763, abnormal protein distribution for plakoglobin and Cx43 was reversed (94). Similarly to what was observed in myocardial tissue samples, in buccal mucosa cells obtained from healthy subjects, there was strong junctional signal for SAP97 and diffuse cytosolic signal for GSK3β and APC. Conversely, buccal cells obtained from ACM subjected showed loss of junctional signal for SAP97 and strong membrane signal for GSK3β and APC. These findings were consistent in all ACM cases regardless of the underlying desmosomal mutation causing the disease (**Figure 3**).

DCM patients carrying a frameshift mutation in the *FLNC* gene, show normal expression for plakoglobin and reduced expression for DSP, Cx43, and SAP97 in their buccal cells, indicating a partial overlap of the pathological cellular phenotype between desmosomal and non-desmosomal ACM (95). More recently, the initial observation of reduced plakoglobin expression in the buccal mucosa of ACM patients carrying a desmosomal mutation was confirmed in another patient cohort from the Netherlands (96). However, buccal mucosa cells from ACM patients carrying the R14del mutation in *PLN* showed normal plakoglobin expression, pointing at distinct pathological mechanisms (96).

Despite the non-cardiac origin of buccal mucosa cells, they show similar pathologic protein distribution to that exhibited by cardiac myocytes. Buccal mucosa cells could as well represent a new *in vitro* model to study disease mechanisms and aid drug screening for ACM in general and in personalized medicine to monitor the patient's response to a specific treatment. Confirmatory studies in larger cohorts of ACM patients and family members are still needed to validate the buccal mucosa as a source of meaningful information for the diagnosis and risk stratification in ACM.

Autoantibodies

Antibodies against self-antigens (autoantibodies) are often detected in the plasma of patients with inflammatory diseases such as myocarditis and pemphigus. Due to the complexity of inflammatory diseases, however, the contribution of autoantibodies to disease progression in these conditions is incompletely known. Recently, a few studies showed the potential of autoantibodies in the diagnosis of ACM. Chatterjee et al. evaluated the presence of antibodies against cardiac desmosomal cadherin proteins in the sera of a small cohort of patients with ACM. They identified autoantibodies against DSG2 in the sera of all the patients with ACM, regardless of the genetic background, while the autoantibodies were absent in virtually all the control subjects. The level of anti-DSG2 antibodies correlated with disease burden and caused gap junction dysfunction (97). Whether this marker is specific for the diagnosis of ACM is still to be proven in larger cohorts and in known phenocopies of the disease such as sarcoidosis. The potential of the autoantibodies in detecting subclinical disease

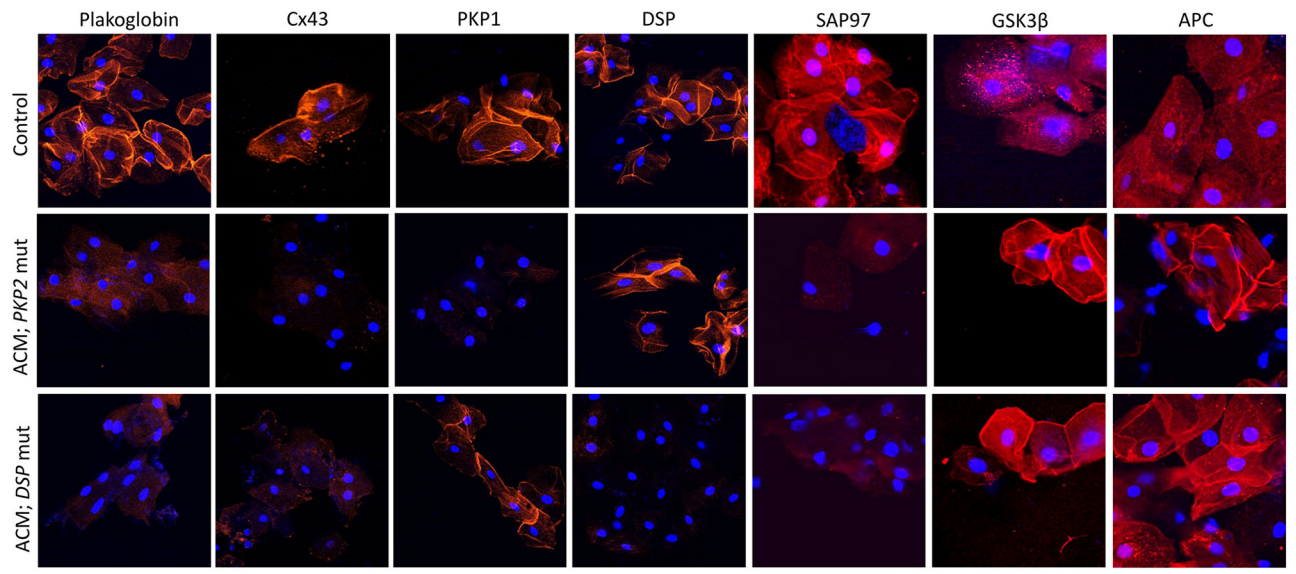

FIGURE 3 | Protein re-distribution in buccal mucosa cells from ACM patients. Representative confocal immunofluorescence images showing loss of PG, Cx43 and SAP97 membrane signal in buccal cells from ACM patients bearing a mutation in *PKP2* or *DSP* compared to control subjects. Conversely, signal for GSK3β and APC shifts from cytosolic to junctional pools. The patient bearing a mutation in *PKP2* shows loss of PKP1 signal but not DSP while the patient bearing a mutation in *DSP* shows loss of DSP signal but not PKP1. Immunoreactive signal of PG, Cx43, PKP1, DSP, SAP97, GSK3β and APC in red; nuclei were counterstained with DAPI in blue.

in mutation carriers should as well be explored. Caforio et al. found anti-heart antibodies and anti-ID antibodies at a higher frequency in ACM probands, affected relatives and healthy relatives when compared to non-inflammatory cardiac disease, ICM or healthy subjects, providing evidence of autoimmunity in the course of ACM (98). More recently, a combination of four autoantibodies against α-cardiac actin, α-skeletal actin, keratin, and Cx43 has been proposed as a highly sensitive and specific biomarker for Brugada syndrome, irrespective of the underlying genetic cause. These autoantibodies were absent in sera samples from patients with ACM, HCM or DCM (99). Although these findings may have diagnostic potential, extensive confirmatory studies are necessary before autoantibodies can be adopted as a novel diagnostic tool for ACM (100).

CONCLUSIONS

ACM is a complex and progressive disease. SCD may occur in the early stages of the disease in the absence of pathologic structural changes making diagnosis and risk stratification quite challenging. Hearts of SCD victims should be examined by expert cardiac pathologists as a definite post-mortem diagnosis of ACM can greatly aid cascade screening and management of surviving family members. Obtaining EMB samples from patients with equivocal diagnoses is an invasive and risky procedure, and the histological analysis of such samples has a low diagnostic yield. Analysis of localization of key protein markers in the heart can greatly improve the diagnostic yield. However, the utility of this approach is greatly limited by the need for a heart sample. The identification of surrogate tissues mimicking the pathological changes of the heart such the buccal mucosa and the presence of specific autoantibodies in the blood samples of patients with ACM may transform the diagnosis, prognosis, and management of the disease as well as the screening of the patient's relatives that may be at risk of fatal arrhythmias or SCD. More research is needed before these protein markers can be adopted as diagnostic tools for ACM. We are confident, however, that one of these approaches, or a combination of them, will improve the detection, risk stratification and management of ACM reducing the burden of SCD.

AUTHOR CONTRIBUTIONS

CB-B prepared the manuscript draft. AA reviewed and approved the draft for submission. All authors contributed to the article and approved the submitted version.

FUNDING

AA was supported by the Rosetrees Foundation Trust corn seed fund (M689), the British Heart Foundation project grant (PG/18/27/33616) and the Wellcome Trust project grant (208460/Z/17/Z). CB-B was supported by the British Heart Foundation project grant (PG/18/27/33616).

REFERENCES

1. Groeneweg JA, Bhonsale A, James CA, te Riele AS, Dooijes D, Tichnell C, et al. Clinical presentation, long-term follow-up, and outcomes of 1001 arrhythmogenic right ventricular dysplasia/cardiomyopathy patients and family members. *Circ Cardiovasc Genet.* (2015) 8:437–46. doi: 10.1161/CIRCGENETICS.114.001003
2. Thiene G, Nava A, Corrado D, Rossi L, Pennelli N. Right ventricular cardiomyopathy and sudden death in young people. *N Engl J Med.* (1988) 318:129–33. doi: 10.1056/NEJM198801213180301
3. Finocchiaro G, Papadakis M, Robertus J-L, Dhutia H, Steriotis AK, Tome M, et al. Etiology of sudden death in sports insights from a United Kingdom regional registry. *J Am Coll Cardiol.* (2016) 67:2108–15. doi: 10.1016/j.jacc.2016.02.062
4. Wasfy MM, Hutter AM, Weiner RB. Sudden cardiac death in athletes. *Methodist Debakey Cardiovasc J.* (2016) 12:76–80. doi: 10.14797/mdcj-12-2-76
5. D'Ascenzi F, Valentini F, Pistoresi S, Frascaro F, Piu P, Cavigli L, et al. Causes of sudden cardiac death in young athletes and non-athletes: systematic review and meta-analysis sudden cardiac death in the young. *Trends Cardiovas Med.* (2021) doi: 10.1016/j.tcm.2021.06.001. [Epub ahead of print].
6. Marcus FI, Fontaine GH, Guiraudon G, Frank R, Laurenceau JL, Malergue C, et al. Right ventricular dysplasia: a report of 24 adult cases. *Circulation.* (1982) 65:384–98. doi: 10.1161/01.CIR.65.2.384
7. Hulot J-S, Jouven X, Empana J-P, Frank R, Fontaine G. Natural history and risk stratification of arrhythmogenic right ventricular dysplasia/cardiomyopathy. *Circulation.* (2004) 110:1879–84. doi: 10.1161/01.CIR.0000143375.93288.82
8. Choudhary N, Tompkins C, Polonsky B, McNitt S, Calkins H, Mark Estes NA III, et al. Clinical presentation and outcomes by sex in arrhythmogenic right ventricular cardiomyopathy: findings from the North American ARVC registry. *J Cardiovasc Electr.* (2016) 27:555–62. doi: 10.1111/jce.12947
9. James CA, Bhonsale A, Tichnell C, Murray B, Russell SD, Tandri H, et al. Exercise increases age-related penetrance and arrhythmic risk in arrhythmogenic right ventricular dysplasia/cardiomyopathy–associated desmosomal mutation carriers. *J Am Coll Cardiol.* (2013) 62:1290–7. doi: 10.1016/j.jacc.2013.06.033
10. Rigato I, Bauce B, Rampazzo A, Zorzi A, Pilichou K, Mazzotti E, et al. Compound and digenic heterozygosity predicts lifetime arrhythmic outcome and sudden cardiac death in desmosomal gene–related arrhythmogenic right ventricular cardiomyopathy. *Circ Cardiovasc Genet.* (2013) 6:533–42. doi: 10.1161/CIRCGENETICS.113.000288
11. Sen-Chowdhry S, Syrris P, Ward D, Asimaki A, Sevdalis E, McKenna WJ. Clinical and genetic characterization of families with arrhythmogenic right ventricular dysplasia/cardiomyopathy provides novel insights into patterns of disease expression. *Circulation.* (2007) 115:1710–20. doi: 10.1161/CIRCULATIONAHA.106.660241
12. Sen-Chowdhry S, Syrris P, Prasad SK, Hughes SE, Merrifield R, Ward D, et al. Left-dominant arrhythmogenic cardiomyopathy an under-recognized clinical entity. *J Am Coll Cardiol.* (2008) 52:2175–87. doi: 10.1016/j.jacc.2008.09.019
13. Corrado D, Marra Perazzolo M, Zorzi A, Beffagna G, Cipriani A, Lazzari MD, et al. Diagnosis of arrhythmogenic cardiomyopathy: the Padua criteria. *Int J Cardiol.* (2020) 319:106–14. doi: 10.1016/j.ijcard.2020.06.005
14. Lazzari MD, Zorzi A, Cipriani A, Susana A, Mastella G, Rizzo A, et al. Relationship between electrocardiographic findings and cardiac magnetic resonance phenotypes in arrhythmogenic cardiomyopathy. *J Am Heart Assoc.* (2018) 7:e009855. doi: 10.1161/JAHA.118.009855
15. Andreini D, Conte E, Casella M, Mushtaq S, Pontone G, Russo AD, et al. Cardiac magnetic resonance features of left dominant arrhythmogenic cardiomyopathy: differential diagnosis with myocarditis. *Int J Cardiovasc Imaging.* (2021) 1–9. doi: 10.1007/s10554-021-02408-8. [Epub ahead of print].

16. McKenna WJ, Thiene G, Nava A, Fontaliran F, Blomstrom-Lundqvist C, Fontaine G, et al. Diagnosis of arrhythmogenic right ventricular dysplasia/cardiomyopathy. Task Force of the Working Group Myocardial and Pericardial Disease of the European Society of Cardiology and of the Scientific Council on Cardiomyopathies of the International Society and Federation of Cardiology. *Br Heart J.* (1994) 71:215–8. doi: 10.1136/hrt.71.3.215
17. Marcus FI, McKenna WJ, Sherrill D, Basso C, Bauce B, Bluemke DA, et al. Diagnosis of arrhythmogenic right ventricular cardiomyopathy/dysplasia: proposed modification of the Task Force Criteria. *Eur Heart J.* (2010) 31:806–14. doi: 10.1093/eurheartj/ehq025
18. Corrado D, van Tintelen PJ, McKenna WJ, Hauer RNW, Anastastakis A, Asimaki A, et al. Arrhythmogenic right ventricular cardiomyopathy: evaluation of the current diagnostic criteria and differential diagnosis. *Eur Heart J.* (2019) 41:1414–29. doi: 10.1093/eurheartj/ehz669
19. Ren L, Liu Z, Jia Y, Fang P, Pu J, Zhang S. Electrocardiographic difference between ventricular arrhythmias from the right ventricular outflow tract and idiopathic right ventricular arrhythmias. *Pacing Clin Electrophysiol.* (2014) 37:1658–64. doi: 10.1111/pace.12463
20. Agullo-Pascual E, Cerrone M, Delmar M. Arrhythmogenic cardiomyopathy and Brugada syndrome: diseases of the connexome. *Febs Lett.* (2014) 588:1322–30. doi: 10.1016/j.febslet.2014.02.008
21. Ellinor PT, MacRae CA, Thierfelder L. Arrhythmogenic right ventricular cardiomyopathy. *Heart Fail Clin.* (2010) 6:161–77. doi: 10.1016/j.hfc.2009.12.003
22. Protonotarios N, Tsatsopoulou A, Patsourakos P, Alexopoulos D, Gezerlis P, Simitsis S, et al. Cardiac abnormalities in familial palmoplantar keratosis. *Brit Heart J.* (1986) 56:321. doi: 10.1136/hrt.56.4.321
23. McKoy G, Protonotarios N, Crosby A, Tsatsopoulou A, Anastasakis A, Coonar A, et al. Identification of a deletion in plakoglobin in arrhythmogenic right ventricular cardiomyopathy with palmoplantar keratoderma and woolly hair (Naxos disease). *Lancet.* (2000) 355:2119–24. doi: 10.1016/S0140-6736(00)02379-5
24. Norgett EE, Hatsell SJ, Carvajal-Huerta L, Cabezas J-CR, Common J, Purkis PE, et al. Recessive mutation in desmoplakin disrupts desmoplakin–intermediate filament interactions and causes dilated cardiomyopathy, woolly hair and keratoderma. *Hum Mol Genet.* (2000) 9:2761–6. doi: 10.1093/hmg/9.18.2761
25. Asimaki A, Syrris P, Wichter T, Matthias P, Saffitz JE, McKenna WJ. A novel dominant mutation in plakoglobin causes arrhythmogenic right ventricular cardiomyopathy. *Am J Hum Genet.* (2007) 81:964–73. doi: 10.1086/521633
26. Rampazzo A, Nava A, Malacrida S, Beffagna G, Bauce B, Rossi V, et al. Mutation in human desmoplakin domain binding to plakoglobin causes a dominant form of arrhythmogenic right ventricular cardiomyopathy. *Am J Hum Genet.* (2002) 71:1200–6. doi: 10.1086/344208
27. Gerull B, Heuser A, Wichter T, Paul M, Basson CT, McDermott DA, et al. Mutations in the desmosomal protein plakophilin-2 are common in arrhythmogenic right ventricular cardiomyopathy. *Nat Genet.* (2004) 36:1162–4. doi: 10.1038/ng1461
28. Pilichou K, Nava A, Basso C, Beffagna G, Bauce B, Lorenzon A, et al. Mutations in desmoglein-2 gene are associated with arrhythmogenic right ventricular cardiomyopathy. *Circulation.* (2006) 113:1171–9. doi: 10.1161/CIRCULATIONAHA.105.583674
29. Gehmlich K, Asimaki A, Cahill TJ, Ehler E, Syrris P, Zachara E, et al. Novel missense mutations in exon 15 of desmoglein-2: role of the intracellular cadherin segment in arrhythmogenic right ventricular cardiomyopathy? *Heart Rhythm.* (2010) 7:1446–53. doi: 10.1016/j.hrthm.2010.08.007
30. Xu Z, Zhu W, Wang C, Huang L, Zhou Q, Hu J, et al. Genotype-phenotype relationship in patients with arrhythmogenic right ventricular cardiomyopathy caused by desmosomal gene mutations: A systematic review and meta-analysis. *Sci Rep.* (2017) 7:41387. doi: 10.1038/srep41387
31. Syrris P, Ward D, Evans A, Asimaki A, Gandjbakhch E, Sen-Chowdhry S, et al. Arrhythmogenic right ventricular dysplasia/cardiomyopathy associated with mutations in the desmosomal gene desmocollin-2. *Am J Hum Genet.* (2006) 79:978–84. doi: 10.1086/509122
32. Heuser A, Plovie ER, Ellinor PT, Grossmann KS, Shin JT, Wichter T, et al. Mutant desmocollin-2 causes arrhythmogenic right ventricular cardiomyopathy. *Am J Hum Genet.* (2006) 79:1081–8. doi: 10.1086/509044
33. Beffagna G, Bortoli MD, Nava A, Salamon M, Lorenzon A, Zaccolo M, et al. Missense mutations in Desmocollin-2 N-terminus, associated with arrhythmogenic right ventricular cardiomyopathy, affect intracellular localization of desmocollin-2 *in vitro*. *BMC Med Genet.* (2007) 8:65–5. doi: 10.1186/1471-2350-8-65
34. den Haan AD, Tan BY, Zikusoka MN, Lladó LI, Jain R, Daly A, et al. Comprehensive desmosome mutation analysis in North Americans with arrhythmogenic right ventricular dysplasia/cardiomyopathy. *Circ Cardiovasc Genet.* (2009) 2:428–35. doi: 10.1161/CIRCGENETICS.109.858217
35. Xu T, Yang Z, Vatta M, Rampazzo A, Beffagna G, Pilichou K, et al. Compound and digenic heterozygosity contributes to arrhythmogenic right ventricular cardiomyopathy. *J Am Coll Cardiol.* (2010) 55:587–97. doi: 10.1016/j.jacc.2009.11.020
36. Cox MGPJ, van der Zwaag PA, van der Werf C, van der Smagt JJ, Noorman M, Bhuiyan ZA, et al. Arrhythmogenic right ventricular dysplasia/cardiomyopathy. *Circulation.* (2011) 123:2690–700. doi: 10.1161/CIRCULATIONAHA.110.988287
37. Smith ED, Lakdawala NK, Papoutsidakis N, Aubert G, Mazzanti A, McCanta AC, et al. Desmoplakin cardiomyopathy, a fibrotic and inflammatory form of cardiomyopathy distinct from typical dilated or arrhythmogenic right ventricular cardiomyopathy. *Circulation.* (2020) 141:1872–84. doi: 10.1161/CIRCULATIONAHA.119.044934
38. Wang W, Murray B, Tichnell C, Gilotra NA, Zimmerman SL, Gasperetti A, et al. Clinical characteristics and risk stratification of desmoplakin cardiomyopathy. *Ep Europace.* (2021) euab183. doi: 10.1093/europace/euab183. [Epub ahead of print].
39. Lao N, Laiq Z, Courson J, Al-Quthami A. Left-dominant arrhythmogenic cardiomyopathy: an association with desmoglein-2 gene mutation—a case report. *Eur Hear J Case Rep.* (2021) 5:ytab213. doi: 10.1093/ehjcr/ytab213
40. Moncayo-Arlandi J, Brugada R. Unmasking the molecular link between arrhythmogenic cardiomyopathy and Brugada syndrome. *Nat Rev Cardiol.* (2017) 14:744–56. doi: 10.1038/nrcardio.2017.103
41. Ghidoni A, Elliott PM, Syrris P, Calkins H, James CA, Judge DP, et al. Cadherin 2-related arrhythmogenic cardiomyopathy: prevalence and clinical features. *Circ Genom Precis Med.* (2021) 14:e003097 doi: 10.1161/CIRCGEN.120.003097
42. Mayosi BM, Fish M, Shaboodien G, Mastantuono E, Kraus S, Wieland T, et al. Identification of Cadherin 2 (CDH2) mutations in arrhythmogenic right ventricular cardiomyopathy. *Circ Cardiovasc Genet.* (2017) 10:e001605. doi: 10.1161/CIRCGENETICS.116.001605
43. Turkowski KL, Tester DJ, Bos JM, Haugaa KH, Ackerman MJ. Whole exome sequencing with genomic triangulation implicates CDH2-encoded N-cadherin as a novel pathogenic substrate for arrhythmogenic cardiomyopathy. *Congenit Heart Dis.* (2017) 12:226–35. doi: 10.1111/chd.12462
44. van Hengel J, Calore M, Bauce B, Dazzo E, Mazzotti E, Bortoli MD, et al. Mutations in the area composita protein αT-catenin are associated with arrhythmogenic right ventricular cardiomyopathy. *Eur Heart J.* (2013) 34:201–10. doi: 10.1093/eurheartj/ehs373
45. Bermúdez-Jiménez FJ, Carriel V, Brodehl A, Alaminos M, Campos A, Schirmer I, et al. Novel desmin mutation p.Glu401Asp impairs filament formation, disrupts cell membrane integrity, and causes severe arrhythmogenic left ventricular cardiomyopathy/dysplasia. *Circulation.* (2018) 137:1595–610. doi: 10.1161/CIRCULATIONAHA.117.028719
46. Ortiz-Genga MF, Cuenca S, Ferro MD, Zorio E, Salgado-Aranda R, Climent V, et al. Truncating FLNC mutations are associated with high-risk dilated and arrhythmogenic cardiomyopathies. *J Am Coll Cardiol.* (2016) 68:2440–51. doi: 10.1016/j.jacc.2016.09.927
47. Segura-Rodríguez D, Bermúdez-Jiménez FJ, Carriel V, López-Fernández S, González-Molina M, Ramírez JMO, et al. Myocardial fibrosis in arrhythmogenic cardiomyopathy: a genotype–phenotype correlation study. *Eur Hear J Cardiovasc Imaging.* (2019) 21:378–86. doi: 10.1093/ehjci/jez277
48. Taylor M, Graw S, Sinagra G, Barnes C, Slavov D, Brun F, et al. Genetic variation in titin in arrhythmogenic right ventricular cardiomyopathy–overlap syndromes. *Circulation.* (2011) 124:876–85. doi: 10.1161/CIRCULATIONAHA.110.005405

49. Dominguez F, Zorio E, Jimenez-Jaimez J, Salguero-Bodes R, Zwart R, Gonzalez-Lopez E, et al. Clinical characteristics and determinants of the phenotype in TMEM43 arrhythmogenic right ventricular cardiomyopathy type 5. *Heart Rhythm.* (2020) 17:945–54. doi: 10.1016/j.hrthm.2020.01.035
50. Heijden JF van der, Hassink RJ. The phospholamban p.Arg14del founder mutation in Dutch patients with arrhythmogenic cardiomyopathy. *Neth Heart J.* (2013) 21:284–5. doi: 10.1007/s12471-013-0413-z
51. te Riele ASJM, Agullo-Pascual E, James CA, Leo-Macias A, Cerrone M, Zhang M, et al. Multilevel analyses of SCN5A mutations in arrhythmogenic right ventricular dysplasia/cardiomyopathy suggest non-canonical mechanisms for disease pathogenesis. *Cardiovasc Res.* (2017) 113:102–11. doi: 10.1093/cvr/cvw234
52. Beffagna G, Occhi G, Nava A, Vitiello L, Ditadi A, Basso C, et al. Regulatory mutations in transforming growth factor-β3 gene cause arrhythmogenic right ventricular cardiomyopathy type 1. *Cardiovasc Res.* (2005) 65:366–73. doi: 10.1016/j.cardiores.2004.10.005
53. Zwaag PA, Rijsingen IAW, Asimaki A, Jongbloed JDH, Veldhuisen DJ, Wiesfeld ACP, et al. Phospholamban R14del mutation in patients diagnosed with dilated cardiomyopathy or arrhythmogenic right ventricular cardiomyopathy: evidence supporting the concept of arrhythmogenic cardiomyopathy. *Eur J Heart Fail.* (2012) 14:1199–207. doi: 10.1093/eurjhf/hfs119
54. Merner ND, Hodgkinson KA, Haywood AFM, Connors S, French VM, Drenckhahn J-D, et al. Arrhythmogenic right ventricular cardiomyopathy type 5 is a fully penetrant, lethal arrhythmic disorder caused by a missense mutation in the TMEM43 gene. *Am J Hum Genetics*. (2008) 82:809–21. doi: 10.1016/j.ajhg.2008.01.010
55. Buja G, Nava A, Daliento L, Scognamiglio R, Miorelli M, Canciani B, et al. Right ventricular cardiomyopathy in identical and nonidentical young twins. *Am Heart J.* (1993) 126:1187–93. doi: 10.1016/0002-8703(93)90673-W
56. Wlodarska EK, Konka M, Zaleska T, Ploski R, Cedro K, Pucilowska B, et al. Arrhythmogenic right ventricular cardiomyopathy in two pairs of monozygotic twins. *Int J Cardiol.* (2005) 105:126–33. doi: 10.1016/j.ijcard.2004.11.016
57. Akdis D, Saguner AM, Shah K, Wei C, Medeiros-Domingo A, von Eckardstein A, et al. Sex hormones affect outcome in arrhythmogenic right ventricular cardiomyopathy/dysplasia: from a stem cell derived cardiomyocyte-based model to clinical biomarkers of disease outcome. *Eur Heart J.* (2017) 38:1498–508. doi: 10.1093/eurheartj/ehx011
58. Boese AC, Kim SC, Yin K-J, Lee J-P, Hamblin MH. Sex differences in vascular physiology and pathophysiology: estrogen and androgen signaling in health and disease. *Am J Physiol Heart C.* (2017) 313:H524–45. doi: 10.1152/ajpheart.00217.2016
59. James CA, Jongbloed JDH, Hershberger RE, Morales A, Judge DP, Syrris P, et al. An international evidence based reappraisal of genes associated with arrhythmogenic right ventricular cardiomyopathy (ARVC) using the ClinGen framework. *Circ Genom Precis Med.* (2021) 14:273-84. doi: 10.1161/CIRCGEN.120.003273
60. Ackerman MJ, Priori SG, Willems S, Berul C, Brugada R, Calkins H, et al. HRS/EHRA expert consensus statement on the state of genetic testing for the channelopathies and cardiomyopathies this document was developed as a partnership between the Heart Rhythm Society (HRS) and the European Heart Rhythm Association (EHRA). *Heart Rhythm.* (2011) 8:1308–39. doi: 10.1016/j.hrthm.2011.05.020
61. Miles C, Finocchiaro G, Papadakis M, Gray B, Westaby J, Ensam B, et al. Sudden death and left ventricular involvement in arrhythmogenic cardiomyopathy. *Circulation.* 139:1786–97. doi: 10.1161/CIRCULATIONAHA.118.037230
62. Basso C, Ronco F, Marcus F, Abudureheman A, Rizzo S, Frigo AC, et al. Quantitative assessment of endomyocardial biopsy in arrhythmogenic right ventricular cardiomyopathy/dysplasia: an *in vitro* validation of diagnostic criteria. *Eur Heart J.* (2008) 29:2760–71. doi: 10.1093/eurheartj/ehn415
63. Corrado D, Basso C, Thiene G, McKenna WJ, Davies MJ, Fontaliran F, et al. Spectrum of clinicopathologic manifestations of arrhythmogenic right ventricular cardiomyopathy/dysplasia: a multicenter study. *J Am Coll Cardiol.* (1997) 30:1512–20. doi: 10.1016/S0735-1097(97)00332-X
64. Basso C, Thiene G, Corrado D, Angelini A, Nava A, Valente M. Arrhythmogenic right ventricular cardiomyopathy: dysplasia, dystrophy, or myocarditis? *Circulation.* (1996) 94:983–91. doi: 10.1161/01.CIR.94.5.983
65. Chelko SP, Asimaki A, Lowenthal J, Bueno-Beti C, Bedja D, Scalco A, et al. Therapeutic modulation of the immune response in arrhythmogenic cardiomyopathy. *Circulation.* (2019) 140:1491–505. doi: 10.1161/CIRCULATIONAHA.119.040676
66. van der Voorn SM, te Riele ASJM, Basso C, Calkins H, Remme CA, van Veen TAB. Arrhythmogenic cardiomyopathy: pathogenesis, pro-arrhythmic remodelling, and novel approaches for risk stratification and therapy. *Cardiovasc Res.* (2020) 116:1571–84. doi: 10.1093/cvr/cvaa084
67. Basso C, Corrado D, Marcus FI, Nava A, Thiene G. Arrhythmogenic right ventricular cardiomyopathy. *Lancet.* (2009) 373:1289–300. doi: 10.1016/S0140-6736(09)60256-7
68. Sen-Chowdhry S, Morgan RD, Chambers JC, McKenna WJ. Arrhythmogenic cardiomyopathy: etiology, diagnosis, and treatment. *Annu Rev Med.* (2010) 61:233–53. doi: 10.1146/annurev.med.052208.130419
69. Avella A, D'Amati G, Pappalardo A, Re F, Silenzi PF, Laurenzi F, et al. Diagnostic value of endomyocardial biopsy guided by electroanatomic voltage mapping in arrhythmogenic right ventricular cardiomyopathy/dysplasia. *J Cardiovasc Electr.* (2008) 19:1127–34. doi: 10.1111/j.1540-8167.2008.01228.x
70. Pieroni M, Russo AD, Marzo F, Pelargonio G, Casella M, Bellocci F, et al. High prevalence of myocarditis mimicking arrhythmogenic right ventricular cardiomyopathy differential diagnosis by electroanatomic mapping-guided endomyocardial biopsy. *J Am Coll Cardiol.* (2009) 53:681–9. doi: 10.1016/j.jacc.2008.11.017
71. Casella M, Bergonti M, Russo AD, Maragna R, Gasperetti A, Compagnucci P, et al. Endomyocardial biopsy: the forgotten piece in the arrhythmogenic cardiomyopathy puzzle. *J Am Heart Assoc.* (2021) 10:e021370. doi: 10.1161/JAHA.121.021370
72. Corrado D, Link MS, Calkins H. Arrhythmogenic right ventricular cardiomyopathy. *N Engl J Med.* (2017) 376:61–72. doi: 10.1056/NEJMra1509267
73. Towbin JA, McKenna WJ, Abrams DJ, Ackerman MJ, Calkins H, Darrieux FCC, et al. 2019 HRS expert consensus statement on evaluation, risk stratification, and management of arrhythmogenic cardiomyopathy. *Heart Rhythm.* (2019) 16:e301–72. doi: 10.1016/j.hrthm.2019.05.007
74. Kaplan SR, Gard JJ, Protonotarios N, Tsatsopoulou A, Spiliopoulou C, Anastasakis A, et al. Remodeling of myocyte gap junctions in arrhythmogenic right ventricular cardiomyopathy due to a deletion in plakoglobin (Naxos disease). *Heart Rhythm.* (2004) 1:3–11. doi: 10.1016/j.hrthm.2004.01.001
75. Kaplan SR, Gard JJ, Carvajal-Huerta L, Ruiz-Cabezas JC, Thiene G, Saffitz JE. Structural and molecular pathology of the heart in Carvajal syndrome. *Cardiovasc Pathol.* (2004) 13:26–32. doi: 10.1016/S1054-8807(03)00107-8
76. Asimaki A, Tandri H, Huang H, Halushka MK, Gautam S, Basso C, et al. A new diagnostic test for arrhythmogenic right ventricular cardiomyopathy. *N Engl J Med.* (2009) 360:1075–84. doi: 10.1056/NEJMoa0808138
77. Noorman M, Hakim S, Kessler E, Groeneweg JA, Cox MGPJ, Asimaki A, et al. Remodeling of the cardiac sodium channel, connexin43, and plakoglobin at the intercalated disk in patients with arrhythmogenic cardiomyopathy. *Heart Rhythm.* (2013) 10:412–9. doi: 10.1016/j.hrthm.2012.11.018
78. Nattel S, Maguy A, Bouter SL, Yeh Y-H. Arrhythmogenic ion-channel remodeling in the heart: heart failure, myocardial infarction, and atrial fibrillation. *Physiol Rev.* (2007) 87:425–56. doi: 10.1152/physrev.00014.2006
79. Peters NS, Green CR, Poole-Wilson PA, Severs NJ. Reduced content of connexin43 gap junctions in ventricular myocardium from hypertrophied and ischemic human hearts. *Circulation.* (1993) 88:864–75. doi: 10.1161/01.CIR.88.3.864
80. Kam CY, Dubash AD, Magistrati E, Polo S, Satchell KJF, Sheikh F, et al. Desmoplakin maintains gap junctions by inhibiting Ras/MAPK and lysosomal degradation of connexin-43. *J Cell Biol.* (2018) 217:3219–35. doi: 10.1083/jcb.201710161
81. Asimaki A, Tandri H, Duffy ER, Winterfield JR, Mackey-Bojack S, Picken MM, et al. Altered desmosomal proteins in granulomatous myocarditis and potential pathogenic links to arrhythmogenic right

ventricular cardiomyopathy. *Circ Arrhyth Electrophysiol.* (2011) 4:743–52. doi: 10.1161/CIRCEP.111.964890
82. Rosset S, Domingo AM, Asimaki A, Graf D, Metzger J, Schwitter J, et al. Reduced Desmoplakin immunofluorescence signal in arrhythmogenic cardiomyopathy with epicardial right ventricular outflow tract tachycardia. *Hear Case Rep.* (2018) 5:57–62. doi: 10.1016/j.hrcr.2018.06.013
83. Sato PY, Musa H, Coombs W, Guerrero-Serna G, Patiño GA, Taffet SM, et al. Loss of plakophilin-2 expression leads to decreased sodium current and slower conduction velocity in cultured cardiac myocytes. *Circ Res.* (2009) 105:523–6. doi: 10.1161/CIRCRESAHA.109.201418
84. Cerrone M, Noorman M, Lin X, Chkourko H, Liang F-X, van der Nagel R, et al. Sodium current deficit and arrhythmogenesis in a murine model of plakophilin-2 haploinsufficiency. *Cardiovasc Res.* (2012) 95:460–8. doi: 10.1093/cvr/cvs218
85. Asimaki A, Kapoor S, Plovie E, Arndt AK, Adams E, Liu Z, et al. Identification of a new modulator of the intercalated disc in a zebrafish model of arrhythmogenic cardiomyopathy. *Sci Transl Med.* (2014) 6:240ra74. doi: 10.1126/scitranslmed.3008008
86. Cerrone M, Lin X, Zhang M, Agullo-Pascual E, Pfenniger A, Gusky HC, et al. Missense mutations in plakophilin-2 cause sodium current deficit and associate with a brugada syndrome phenotype. *Circulation.* (2014) 129:1092–103. doi: 10.1161/CIRCULATIONAHA.113.003077
87. Kim C, Wong J, Wen J, Wang S, Wang C, Spiering S, et al. Studying arrhythmogenic right ventricular dysplasia with patient-specific iPSCs. *Nature.* (2013) 494:105–10. doi: 10.1038/nature11799
88. Milstein ML, Musa H, Balbuena DP, Anumonwo JMB, Auerbach DS, Furspan PB, et al. Dynamic reciprocity of sodium and potassium channel expression in a macromolecular complex controls cardiac excitability and arrhythmia. *Proc Natl Acad Sci USA.* (2012) 109:E2134–43. doi: 10.1073/pnas.1109370109
89. Petitprez S, Zmoos A-F, Ogrodnik J, Balse E, Raad N, El-Haou S, et al. SAP97 and dystrophin macromolecular complexes determine two pools of cardiac sodium channels Nav1.5 in cardiomyocytes. *Circ Res.* (2011) 108:294–304. doi: 10.1161/CIRCRESAHA.110.228312
90. Chelko SP, Asimaki A, Andersen P, Bedja D, Amat-Alarcon N, DeMazumder D, et al. Central role for GSK3β in the pathogenesis of arrhythmogenic cardiomyopathy. *Jci Insight.* (2016) 1:e85923. doi: 10.1172/jci.insight.85923
91. Padrón-Barthe L, Villalba-Orero M, Gómez-Salinero JM, Domínguez F, Román M, Larrasa-Alonso J, et al. Severe cardiac dysfunction and death caused by ARVC type 5 is improved by inhibition of GSK3β. *Circulation.* (2019) 140:1188–204. doi: 10.1161/CIRCULATIONAHA.119.040366
92. te Rijdt WP, Asimaki A, Jongbloed JDH, Hoorntje ET, Lazzarini E, van Zwaag PA, et al. Distinct molecular signature of phospholamban p.Arg14del arrhythmogenic cardiomyopathy. *Cardiovasc Pathol.* (2019) 40:2–6. doi: 10.1016/j.carpath.2018.12.006
93. Presland RB, Dale BA. Epithelial structural proteins of the skin and oral cavity: function in health and disease. *Crit Rev Oral Biol M.* (2000) 11:383–408. doi: 10.1177/10454411000110040101
94. Asimaki A, Protonotarios A, James CA, Chelko SP, Tichnell C, Murray B, et al. Characterizing the molecular pathology of arrhythmogenic cardiomyopathy in patient buccal mucosa cells. *Circ Arrhyth Electrophysiol.* (2016) 9:e003688. doi: 10.1161/CIRCEP.115.003688
95. Begay RL, Graw SL, Sinagra G, Asimaki A, Rowland TJ, Slavov DB, et al. Filamin C truncation mutations are associated with arrhythmogenic dilated cardiomyopathy and changes in the cell–cell adhesion structures. *JACC Clin Electrophysiol.* (2018) 4:504–14. doi: 10.1016/j.jacep.2017.12.003
96. Voorn SVD, Driessen H, Lint FV, Bourfiss M, Mirzad F, Onsri LE, et al. Buccal mucosa cells as a diagnostic tool in patients with arrhythmogenic cardiomyopathy. *Ep Europace.* (2021) 23:euab116.114. doi: 10.1093/europace/euab116.035
97. Chatterjee D, Fatah M, Akdis D, Spears DA, Koopmann TT, Mittal K, et al. An autoantibody identifies arrhythmogenic right ventricular cardiomyopathy and participates in its pathogenesis. *Eur Heart J.* (2018) 39:3932–44. doi: 10.1093/eurheartj/ehy567
98. Caforio ALP, Re F, Avella A, Marcolongo R, Baratta P, Seguso M, et al. Evidence from family studies for autoimmunity in arrhythmogenic right ventricular cardiomyopathy. *Circulation.* (2020) 141:1238–48. doi: 10.1161/CIRCULATIONAHA.119.043931
99. Chatterjee D, Pieroni M, Fatah M, Charpentier F, Cunningham KS, Spears DA, et al. An autoantibody profile detects Brugada syndrome and identifies abnormally expressed myocardial proteins. *Eur Heart J.* (2020) 41:2878–90. doi: 10.1093/eurheartj/ehaa383
100. Calkins H. A new diagnostic test for arrhythmogenic right ventricular cardiomyopathy: is this too good to be true? *Eur Heart J.* (2018) 39:3945–6. doi: 10.1093/eurheartj/ehy410

Conflict of Interest: The authors declare that the research was conducted in the absence of any commercial or financial relationships that could be construed as a potential conflict of interest.

Publisher's Note: All claims expressed in this article are solely those of the authors and do not necessarily represent those of their affiliated organizations, or those of the publisher, the editors and the reviewers. Any product that may be evaluated in this article, or claim that may be made by its manufacturer, is not guaranteed or endorsed by the publisher.

frontiers in Cardiovascular Medicine

ORIGINAL RESEARCH
published: 17 December 2021
doi: 10.3389/fcvm.2021.761860

The Impact of Ischemia Assessed by Magnetic Resonance on Functional, Arrhythmic, and Imaging Features of Hypertrophic Cardiomyopathy

Sílvia Aguiar Rosa[1,2,3*], *Boban Thomas*[3], *António Fiarresga*[1], *Ana Luísa Papoila*[2,4], *Marta Alves*[2,4], *Ricardo Pereira*[3], *Gonçalo Branco*[3], *Inês Cruz*[5], *Pedro Rio*[1], *Luis Baquero*[3], *Rui Cruz Ferreira*[1], *Miguel Mota Carmo*[2] and *Luís Rocha Lopes*[6,7,8]

[1] Department of Cardiology, Santa Marta Hospital, Lisbon, Portugal, [2] NOVA Medical School, Faculty of Medical Science of Lisbon, New University, Lisbon, Portugal, [3] Heart Centre, Hospital Cruz Vermelha Portuguesa, Lisbon, Portugal, [4] Epidemiology and Statistics Unit, Research Centre, Centro Hospitalar Universitário de Lisboa Central and Centre of Statistics and its Applications, University of Lisbon, Lisbon, Portugal, [5] Department of Cardiology, Hospital Garcia de Orta, Almada, Portugal, [6] Inherited Cardiac Disease Unit, Bart's Heart Centre, St Bartholomew's Hospital, London, United Kingdom, [7] Centre for Heart Muscle Disease, Institute of Cardiovascular Science, University College London, London, United Kingdom, [8] Cardiovascular Centre, University of Lisbon, Lisbon, Portugal

OPEN ACCESS

Edited by:
Andrea Igoren Guaricci, Azienda Ospedaliero Universitaria Consorziale Policlinico di Bari, Italy

Reviewed by:
Carmen Chan, Queen Mary Hospital, Hong Kong SAR, China
Filippo Cademartiri, Gabriele Monasterio Tuscany Foundation (CNR), Italy

***Correspondence:**
Sílvia Aguiar Rosa
silviaguiarosa@gmail.com

Specialty section:
This article was submitted to Cardiovascular Imaging, a section of the journal Frontiers in Cardiovascular Medicine

Received: *20 August 2021*
Accepted: *22 November 2021*
Published: *17 December 2021*

Citation:
Aguiar Rosa S, Thomas B, Fiarresga A, Papoila AL, Alves M, Pereira R, Branco G, Cruz I, Rio P, Baquero L, Ferreira RC, Mota Carmo M and Lopes LR (2021) The Impact of Ischemia Assessed by Magnetic Resonance on Functional, Arrhythmic, and Imaging Features of Hypertrophic Cardiomyopathy. Front. Cardiovasc. Med. 8:761860. doi: 10.3389/fcvm.2021.761860

Aims: The aim of the study is to investigate the association between the degree of ischemia due to coronary microvascular dysfunction (CMD) and the left ventricular (LV) tissue characteristics, systolic performance, and clinical manifestations in hypertrophic cardiomyopathy (HCM).

Methods and Results: This prospective study enrolled 75 patients with HCM without obstructive epicardial coronary artery disease. Each patient underwent cardiovascular magnetic resonance (CMR) including parametric mapping, perfusion imaging during regadenoson-induced hyperemia, late gadolinium enhancement (LGE) and three-dimensional longitudinal, circumferential, and radial strains analysis. Electrocardiogram, 24-h Holter recording, and cardiopulmonary exercise testing (CPET) were performed to assess arrhythmias and functional capacity. In total, 47 (63%) patients were men with the mean age of 54.6 (14.8) years, 51 (68%) patients had non-obstructive HCM, maximum wall thickness (MWT) was 20.2 (4.6) mm, LV ejection fraction (LVEF) was 71.6 (8.3%), and ischemic burden was 22.5 (16.9%) of LV. Greater MWT was associated with the severity of ischemia (β-estimate:1.353, 95% CI:0.182; 2.523, $p = 0.024$). Ischemic burden was strongly associated with higher values of native T1 (β-estimate:9.018, 95% CI:4.721; 13.315, $p < 0.001$). The association between ischemia and LGE was significant in following subgroup analyses: MWT 15–20 mm (β-estimate:1.941, 95% CI:0.738; 3.143, $p = 0.002$), non-obstructive HCM (β-estimate:1.471, 95% CI:0.258; 2.683, $p = 0.019$), women (β-estimate:1.957, 95% CI:0.423; 3.492, $p = 0.015$) and age <40 years (β-estimate:4.874, 95% CI:1.155; 8.594, $p = 0.016$). Ischemia in ≥21% of LV was associated with LGE >15% (AUC 0.766, sensitivity 0.724, specificity 0.659). Ischemia was also associated with atrial fibrillation or flutter (AF/AFL) (OR-estimate:1.481, 95% CI:1.020; 2.152, $p = 0.039$), but no association

was seen for non-sustained ventricular tachycardia. Ischemia was associated with shorter time to anaerobic threshold (β-estimate: −0.442, 95% CI: −0.860; −0.023, $p = 0.039$).

Conclusion: In HCM, ischemia associates with morphological markers of severity of disease, fibrosis, arrhythmia, and functional capacity.

Keywords: hypertrophic cardiomyopathy, coronary microvascular dysfunction, cardiovascular magnetic resonance, tissue characteristics, functional capacity, arrhythmia

INTRODUCTION

Hypertrophic cardiomyopathy (HCM) is defined by unexplained left ventricular (LV) hypertrophy in the absence of abnormal loading conditions (1). In HCM, coronary microvascular dysfunction (CMD) and ischemia have been attributed to reduced capillary density, vascular remodeling, fibrosis, myocyte disarray, and extravascular compression (2, 3).

Myocardial fibrosis is a cardinal feature in HCM, with two patterns identified: replacement fibrosis and diffuse interstitial fibrosis (4, 5). Myocardial late gadolinium enhancement (LGE) by cardiac magnetic resonance (CMR) correlates with replacement fibrosis in HCM (4, 5). Native T1 mapping and extracellular volume (ECV) have shown to be more reliable to assess diffuse interstitial fibrosis (6), correlating with histological interstitial fibrosis in endomyocardial biopsy (7). ECV along with LGE can estimate the total fibrotic burden in patients with HCM. Native T1 also measures intracellular components and may reflect cellular abnormalities (8).

Increased myocardial fibrosis is frequently interpreted as a consequence of long-standing disease, including ischemia due to microvascular abnormalities. However, the association between fibrosis and small vessel disease is not completely established (9). Despite the important clinical implications myocardial ischemia may have, it is not a systematic evaluated parameter for clinical decision making in HCM.

We prospectively assessed CMD in patients with HCM by assessing myocardial perfusion defects using stress CMR and hypothesized that CMD impacts on tissues abnormalities, arrhythmias, and functional capacity. We also aimed to identify clinical and imaging characteristics associated with ischemic burden.

MATERIALS AND METHODS

Study Design and Sample

Multicenter prospective study with recruitment performed in Hospital de Santa Marta, Centro Hospital Universitário de Lisboa Central and Hospital Garcia de Orta, Almada, between December 2017 and August 2020. The CMR studies were performed at Heart Center, Hospital da Cruz Vermelha Portuguesa, and the remaining investigations took place in Hospital de Santa Marta.

The study included consecutive adult patients with HCM seen in a cardiomyopathy clinic who fulfilled the inclusion criteria and gave informed consent. The diagnosis of HCM was performed according to published guidelines (1); more specifically, anatomical inclusion criteria were a wall thickness ≥15 mm in one or more LV myocardial segments in probands or >13 mm in relatives or mutation carriers, measured by any imaging technique (echocardiography, CMR, or computed tomography), in the absence of another cardiac or systemic cause of LV hypertrophy. Genetic testing was performed according to the physicians' judgement for each particular case and was not considered for this study.

Patients with LV ejection fraction (LVEF) <50%, prior septal reduction therapy (myectomy or alcohol ablation), and epicardial coronary artery disease were excluded. Obstructive epicardial coronary artery disease was excluded by invasive coronary angiography or coronary computerized tomography in symptomatic patients or asymptomatic patients older than 40 years. In asymptomatic patients younger than 40 years and without cardiovascular risk factors, it was assumed a low likelihood of obstructive coronary artery disease. The investigation followed the principles outlined in the Declaration of Helsinki. The institutional ethics committee of the NOVA Medical School, Lisbon and Centro Hospital Universitário de Lisboa Central approved the study protocol. All patients provided written informed consent.

Clinical Evaluation

At baseline clinical visit, all patients were evaluated regarding symptoms and physical examination and underwent a 12-lead electrocardiogram and a comprehensive echocardiogram., following current guidelines (10). Obstructive HCM was defined by a systolic gradient of ≥30 mmHg in the LV outflow tract (LVOT) at rest or after provocative maneuvers.

Maximal symptom-limited treadmill cardiopulmonary exercise testing (CPET) was performed using a modified Bruce protocol. Oxygen uptake (VO_2), CO_2 production (VCO_2), and ventilation (VE) were measured. Peak VO_2 was analyzed as the percentage of predicted peak VO_2 according to age and gender. Minute VE/CO_2 production (VE/VCO_2) slope was calculated, and peak circulatory power was determined as peak VO_2 x peak systolic blood pressure. Arrhythmic response to exercise was defined as the presence of repetitive premature ventricular beats, non-sustained or sustained ventricular tachycardia. Abnormal blood pressure response to exercise was defined as a failure to increase systolic pressure by at least 20 mmHg from rest to peak exercise or a fall of >20 mmHg from peak pressure.

Twenty-four-hours Holter recording was performed to document the presence of permanent or paroxysmal

supraventricular arrhythmias [atrial fibrillation (AF) or atrial flutter (AFL)] and ventricular tachycardia.

CMR Acquisition Protocol and Analysis

All subjects underwent CMR performed on a 1.5T system (Sola, Siemens, Erlangen, Germany) and abstained from caffeine for at least 24 h. Using compressed sensing-based sequence, cine images in three long-axis planes and sequential short-axis slices spanning the entire left ventricle from the base to the apex were acquired. Basal, mid, and apical precontrast and postcontrast short axis T1 maps were generated using a modified look locker inversion sequence in a 5(3)3 configuration. Basal, mid, and apical precontrast short axis T2 maps were generated, using a single shot TrueFISP acquisition. The same three slices were used for stress perfusion CMR 90 s after hyperemia induced by regadenoson. Images were acquired apex to base during breath-hold at the first pass of contrast (60 measurements). A gradient echo sequence was used. LGE images were acquired using a breath-held segmented inversion-recovery steady-state-free precession sequence.

Microvascular dysfunction was considered present if a visual perfusion defect was observed. Perfusion defects were considered surrogates for ischemia. For perfusion assessment and semi-quantification, the myocardium was divided into 32 subsegments (16 American Heart Association (AHA) segments subdivided into an endocardial and epicardial layer). Ischemic burden for each patient was calculated based on the number of involved subsegments, assigning 3% of myocardium to each subsegment, as assessed in previous landmark studies (11, 12). Each segment was analyzed for the presence or absence of perfusion defect. Perfusion defects sparing the subendocardium and coincident with LGE were not considered, as subendocardial involvement is mandatory for microvascular dysfunction defects. The LGE was analyzed on a per-segment basis using a signal threshold vs. reference myocardium of $\geq$6 standard deviation, as previously validated with high reproducibility for HCM (13). Total LGE was expressed as a proportion of LV mass.

Native T1 and postcontrast T1 values of myocardium were measured from the three slices generating T1 maps. ECV was calculated according to the previous published formula (14) using patient haematocrit collected at the clinical evaluation, with an interval of <1 month between the evaluation and CMR study. T2 values of myocardium were measured from the three slices generating T2 maps. For each parameter, all 16 AHA segments were included in the analysis.

Three-dimensional longitudinal, circumferential, and radial strains were obtained using an automatic feature-tracking algorithm.

Statistical Analysis

An exploratory analysis of the variables under study was carried out with categorical variables being described by frequencies (percentages) and quantitative variables by the mean (standard deviation). Locally weighted scatterplot smoothers were used to study the association between MWT and ischemia and between ischemia and LGE.

To identify factors contributing to ischemia (dependent variable) and to study the association between ischemia (independent variable) and tissue characteristics, LV performance, and clinical manifestations, generalized linear regression models for continuous and binary response were applied. Univariable and multivariable models were included patients' characteristics which might potentially influence these outcomes, including age, gender, cardiovascular risk factors**,** maximum wall thickness (MWT), LV mass, the presence of LVOT obstruction, and other CMR findings.

All variables that in the univariable analysis attained a $p \leq 0.25$ were selected for the multivariable models. Crude and adjusted odds ratios (OR), and crude and adjusted regression coefficients (β) were estimated with corresponding 95% confidence intervals (95% CI). For the linear regression models, the normality assumption of the residuals was verified using Shapiro–Wilk test. To check the assumption of linearity to the logit for the continuous independent variables in the logistic regression analyses, generalized additive regression models for binary response were used.

Considering the outcome LGE as a binary variable (LGE $>$ 15%; LGE $\leq$ 15%), a cutoff point was determined for ischemia using the criterion that maximizes sensitivity and specificity.

For LGE, a stratified analysis by some groups (MWT, obstructive HCM, gender, and age) was also performed using linear regression models.

The level of significance $\alpha = 0.05$ was considered, although *p*-values greater than 0.05 and lower than 0.1 (weak evidence of the difference or association) were still considered.

Data were analyzed using the Statistical Package for the Social Science for Windows, version 25.0 (IBM Corp. Released 2017. IBM SPSS Statistics for Windows, version 25.0. Armonk, NY: IBM Corp.) and R (R: A Language and Environment for Statistical Computing, R Core Team, R Foundation for Statistical Computing, Vienna, Austria, year = 2021, http://www.R-project.org.).

RESULTS

Study Population

Seventy-five patients were recruited, mean age 54.6 (14.8) years, 47 (63%) of whom were male. The pattern of hypertrophy was asymmetric septal in 48 (64%), apical in 22 (29%), and concentric in 5 (7%). Fifty-one patients (68%) had non-obstructive HCM and MWT was 20.2 (4.6) mm. An apical aneurysm was noted in four patients, perfusion defect in at least one segment was noted in 68 (91%) patients, ischemic burden was, on average, 22.5 (16.9%) of LV in the overall population, and LGE was detected in 70 (93%) patients. Baseline characteristics are shown in **Tables 1**, **2**.

Stress perfusion images were interpretable in all patients. LGE images were not interpretable in one patient due to artifact. Also, in one patient, it was not possible to interpret CPET parameters due to intolerance to the face mask leading to inaccurate analysis of expired gases; four patients refused to do CPET.

TABLE 1 | Baseline characteristics of the study participants.

	***n* = 75**
Male gender, *n* (%)	47 (63)
Age (years), mean (SD)	54.6 (14.8)
BSA (m^2), mean (SD)	1.93 (0.21)
Hypertension, *n* (%)	38 (51)
Diabetes, *n* (%)	12 (16)
Dyslipidaemia, *n* (%)	30 (40)
Current smoker, *n* (%)	11 (15)
Family history of HCM, *n* (%)	21 (28)
Beta-blocker, *n* (%)	54 (72)
Calcium channel blocker, *n* (%)	18 (24)
Angiotensin converting enzyme inhibitors, *n* (%)	13 (17)
Angiotensin receptor blockers, *n* (%)	18 (24)
Spironolactone, *n* (%)	3 (4)
Non-obstructive HCM, *n* (%)	51 (68)
NYHA I, *n* (%)	41 (55)
NYHA II-III, *n* (%)	34 (45)
Angina, *n* (%)	25 (33)
Syncope, *n* (%)	2 (3)
Palpitations, *n* (%)	24 (32)

BSA, body surface area; HCM, hypertrophic cardiomyopathy; NYHA, New York Heart Association; SD, standard deviation.

TABLE 2 | Imaging, arrhythmic, and functional findings.

	***n* = 75**
CMR findings	
MWT (mm), mean (SD)	20.2 (4.6)
LV mass indexed (g/m2), mean (SD)	97.2 (30.5)
LVEDV(mL/m2), mean (SD)	60.7 (15.3)
LVESV (mL/m2), mean (SD)	18.3 (8.9)
LVEF (%), mean (SD)	71.6 (8.3)
Ischemia (% of LV), mean (SD)	22.5 (16.9)
Native T1 mapping (ms), mean (SD)	1024.1 (35.8)
ECV (%), mean (SD)	26.7 (4.1)
T2 mapping (ms), mean (SD)	50.5 (2.4)
LGE (% of LV mass), mean (SD)	12.7 (8.6)
Global longitudinal strain (%), mean (SD)	−6.15 (4.79)
Global radial strain (%), mean (SD)	24.26 (9.87)
Global circumferential strain (%), mean (SD)	−17.07 (3.78)
Arrhythmic findings	
Sinus rhythm, *n* (%)	59 (79)
AF/AFL, *n* (%)	16 (21)
AF	14
AFL	2
Non-sustained ventricular tachycardia, *n* (%)	17 (23)
CPET parameters	
Peak VO_2 (ml/kg/min), mean (SD)	21.07 (6.68)
predicted peak VO_2 (%), mean (SD)	84.17 (22.49)
VE/VCO_2 slope, mean (SD)	29.12 (5.23)
Circulatory power (mmHg.ml/kg/min), mean (SD)	3596.5 (1397.4)
Time to anaerobic threshold (min), mean (SD)	5.9 (3.5)
Peak VO_2 at anaerobic threshold (ml/kg/min)	14.13 (3.58)

CMR, cardiovascular magnetic resonance; CPET, cardiopulmonary exercise testing; LV, left ventricular; LGE, late gadolinium enhancement; LVEDV, left ventricular end-diastolic volume; LVEF, left ventricular ejection fraction; LVESV, left ventricular end-systolic volume; SD, standard deviation; VCO_2, CO_2 production; VE, ventilation; VO_2, oxygen uptake.

TABLE 3 | Univariable linear regression for factors related to ischemia.

	Univariable		
	β-estimate	**95% confidence interval**	***p*-value**
Female	2.084	−6.015 to 10.183	0.610
Age (years)	−0.105	−0.371 to 0.162	0.436
MWT (mm)	1.788	1.033 to 2.542	<0.001
LV mass (g/m2)	0.241	0.124 to 0.358	<0.001
Non-obstructive HCM	−1.132	−9.541 to 7.276	0.789
Hypertension	3.081	−4.736 to 10.898	0.435
Diabetes	2.702	−7.984 to 13.389	0.616
Dyslipidemia	−0.300	−8.310 to 7.710	0.941
Current smoker	3.379	−7.686 to 14.444	0.545
HCM risk-SCD score	1.355	−0.350 to 3.060	0.117

HCM, hypertrophic cardiomyopathy; LV, left ventricle; SCD, sudden cardiac death.

Association Between Baseline Clinical and Imaging Characteristics and Ischemic Burden

Clinically relevant baseline characteristics, potentially linked with CMD, were tested for the association with ischemia in patients with HCM (**Table 3**).

In univariable analysis, the severity of LV hypertrophy, measured by MWT and LV mass, was associated with more extensive ischemia (MWT β-estimate:1.788, 95% CI:1.033; 2.542, $p < 0.001$; LV mass β-estimate:0.241, 95% CI: 0.124; 0.358, $p < 0.001$). No difference in ischemic burden was found between patients with non-obstructive and obstructive HCM. Demographic factors or cardiovascular risk factors such as diabetes and hypertension were not associated with ischemia. In the multivariable analysis, only MWT is associated with ischemia with a mean increase in LV ischemia of 1.79% for each 1 mm increase in MWT. The association between MWT and ischemia is approximately linear and is graphically represented in **Figure 1A**.

Association Between Ischemia and Other CMR Parameters

In this section, the univariable analysis considering the relevant clinical and imaging characteristics is shown in the **Supplementary Tables S1**, **S2**.

CMR images of the different acquisitions are shown in **Figure 2**.

The extent of ischemia was associated with higher values of native T1 in multivariable analysis (**Table 4**). For each 10% increase in LV ischemia, there was a mean increase of 9 ms in the value of native T1.

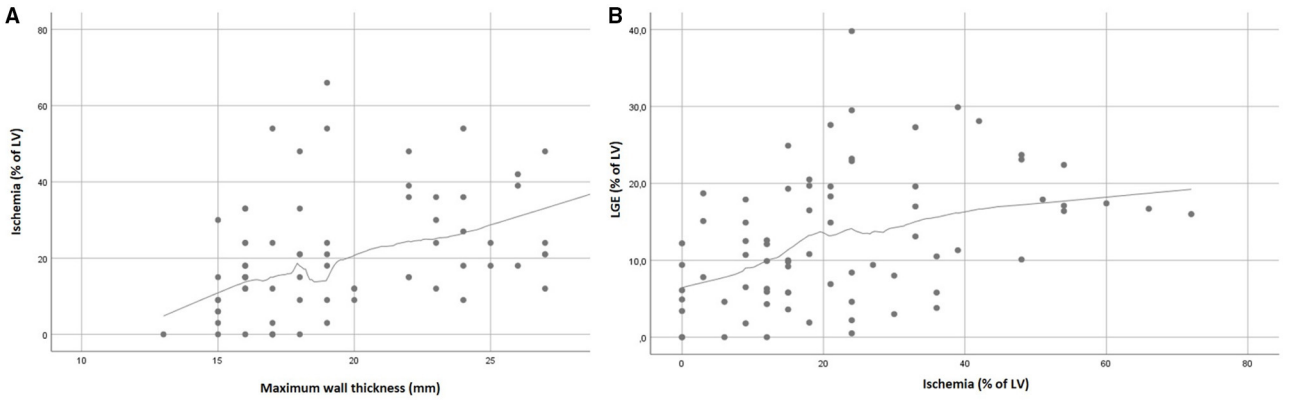

FIGURE 1 | Relationship between MWT and LV ischemia **(A)**, and ischemia and LGE **(B)**.

Ischemia had a weak evidence of association with ECV in univariable analysis (**Supplementary Table S1**), and no association was found after adjusting for baseline characteristics ($p = 0.566$).

Higher ischemic burden was associated with the extent of LGE in univariable analysis (β-estimate:2.02, 95% CI:0.93; 3.10, $p < 0.001$) (**Figure 1B**). Discretizing LGE into a binary variable (LGE > 15%; LGE ≤ 15%), higher ischemia values were obtained for LGE >15%, with an area under the ROC curve of 0.766 (**Supplementary Figure S1**). At the ischemia estimated cutoff point at 21%, a sensitivity of 0.724 and a specificity of 0.659 were achieved. In the multivariable analysis, ischemia showed only a weak evidence of association with LGE (β-estimate:1.070, 95% CI: −0.106; 2.245, $p = 0.074$) (**Table 4**).

Because LGE is an important prognostic marker of the disease, a subgroup analysis was further performed to clarify the association between ischemia and LGE. This association was found in individuals with MWT 15–20 mm, non-obstructive HCM, women and age <40 years (**Table 4**, **Figure 3**).

In multivariable analysis, ischemia had a weak evidence of association with T2 (β-estimate:0.280, 95% CI: −0.010; 0.580, $p = 0.061$) (**Table 4**).

Among the other imaging findings, MWT was most prominently related to tissue characteristics, associated with increased values of native T1, ECV, and LGE (**Table 4**).

In univariable analysis, ischemia was associated with impaired global longitudinal strain (β-estimate: 0.085, 95% CI: 0.020; 0.151, $p = 0.011$) and global radial strain (β-estimate: −0.169, 95% CI: −0.304; −0.034, $p = 0.015$). In multivariable analysis, only LV mass and MWT were independently associated with impairment in myocardial deformation parameters (**Supplementary Table S2**).

Impact of Ischemia on Arrhythmias and Functional Capacity

In this section, the univariable analysis considering the relevant clinical and imaging characteristics is shown in the **Supplemental Tables S3**, **S4**.

Supraventricular arrhythmias were documented in 16 patients (21%) of whom 6 had permanent AF, 8 paroxysmal AF, and 2 paroxysmal AFL on ECG or Holter monitoring. NSVT was reported in 17 patients (23%), on Holter monitoring.

During CPET, two patients had NSVT and 12 had premature ventricular beats during exercise or recovery phase; four patients presented abnormal BP response.

Regarding ECG abnormalities, namely voltage criteria for LV hypertrophy, QRS fragmentation, and the presence of Q wave and T wave inversion, ischemia was only independently associated with voltage criteria for LV hypertrophy (OR: 1.072, 95% CI: 1.013; 1.135, $p = 0.017$) (**Supplementary Table S3**).

Ischemia (OR:1.669, 95% CI: 1.082; 2.574, $p = 0.021$) and left atrial volume (OR:1.105,95% CI:1.050; 1.164, $p < 0.001$) were independently associated with supraventricular arrhythmias, mainly AF. No association was verified between ischemia and NSVT (**Table 5**).

Regarding CPET parameters, ischemia was associated with shorter time to anaerobic threshold (β-estimate: −0.442, 95% CI: −0.860; −0.023, $p = 0.039$).

Older age (β-estimate: −0.202, 95% CI: −0.290; −0.114, $p < 0.001$) and female gender (β-estimate: −4.907, 95% CI: −7.580; −2.234, $p < 0.001$) were the characteristics associated with lower peak VO_2 and lower VO_2 at anaerobic threshold, whereas LVEF (β-estimate: 0.618, 95% CI: 0.007; 1.228, $p < 0.047$) and LGE (β-estimate: −0.815, 95% CI: −1.478; −0.153, $p = 0.017$) were independently associated with predicted peak VO_2.

Older age and more extensive LGE were associated with higher VE/VCO_2 slope whereas older age, female gender, and more extensive LGE showed association with worse circulatory power (**Table 5**).

DISCUSSION

In this study, we showed that ischemia had a transversal impact through the pathophysiological aspects of HCM, from the tissue characteristics to the clinical manifestations. Increased severity of ischemia was associated with higher values of native T1

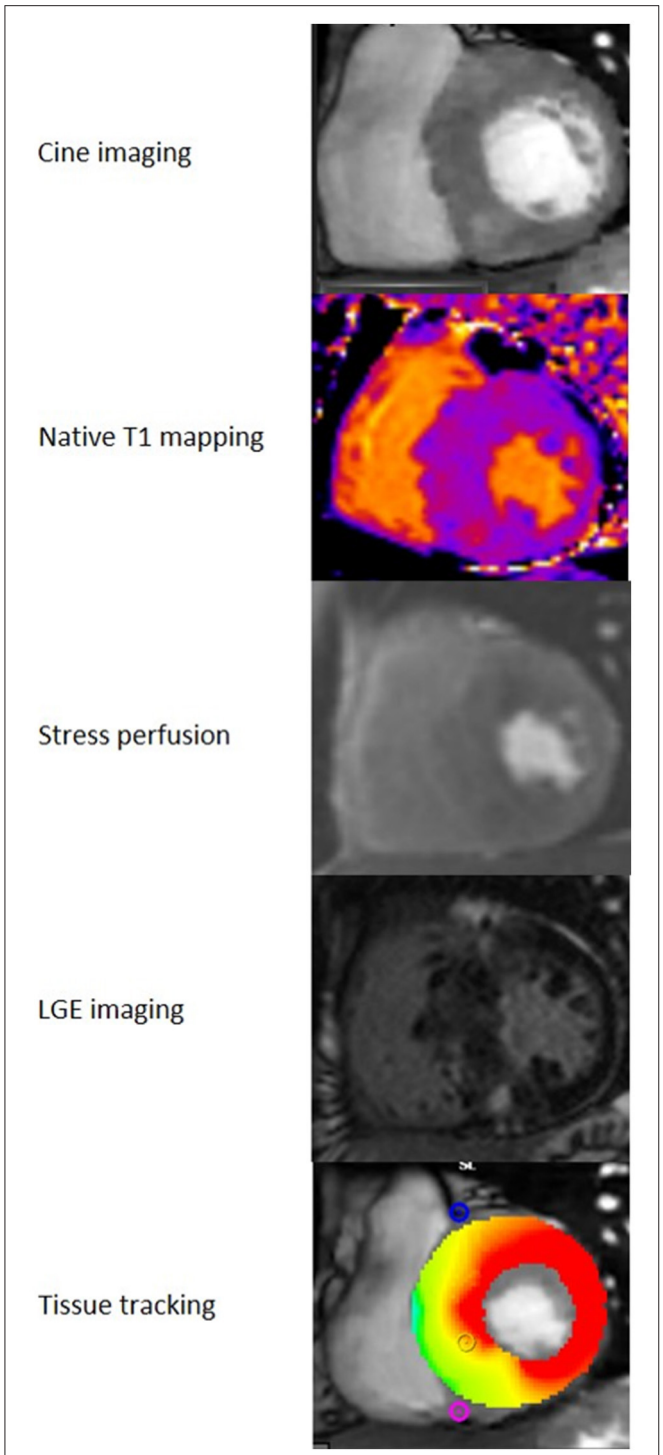

FIGURE 2 | CMR analysis. CMR images from a patient with HCM. Note the asymmetrical septal hypertrophy in the cine images, perfusion defects in the most hypertrophied segments in the stress perfusion acquisition and midwall LGE in the septum and right ventricle insertion points.

and more extensive LGE and increased the risk of AF/AFL. Patients with ischemia reached anaerobic threshold earlier on CPET.

TABLE 4 | Multivariable linear regression for factors related to tissue characteristics.

	Multivariable		
	β-estimate	**95% confidence interval**	***p*-value**
Native T1 (ms)			
Ischemia (% of LV)*	9.018	4.721; 13.315	<0.001
MWT (mm)	2.569	0.981; 4.157	0.002
ECV (%)			
Ischemia (% of LV)*	0.002	−0.005; 0.009	0.566
MWT (mm)	0.003	0.001; 0.005	0.016
LGE (%of LV)			
Ischemia (% of LV)*	1.070	−0.106; 2.245	0.074
MWT (mm)	0.716	0.276; 1.155	0.002
Subgroup analysis			
MWT 15–20 mm			
Ischemia (% of LV)*	1.941	0.738; 3.143	0.002
LV mass (g/m^2)	0.122	0.012; 0.231	0.031
MWT ≥21mm			
Ischemia (% of LV)*	0.050	−2.213; 2.314	0.964
Nonobstructive HCM			
Ischemia (% of LV)*	1.471	0.258; 2.683	0.019
MWT (mm)	0.553	0.068; 1.038	0.026
Obstructive HCM			
Ischemia (% of LV)*	−1.073	−4.161; 2.015	0.476
MWT (mm)	1.284	0.307; 2.262	0.013
Male			
Ischemia (% of LV)*	0.436	−1.287; 2.159	0.613
MWT (mm)	0.939	0.312; 1.566	0.004
Female			
Ischemia (% of LV)*	1.957	0.423; 3.492	0.015
Age <40years			
Ischemia (% of LV)*	4.874	1.155; 8.594	0.016
MWT (mm)	1.380	0.608; 2.153	0.003
Age ≥40 years			
Ischemia (% of LV)*	1.145	−0.141; 2.431	0.080
MWT (mm)	0.515	−0.004; 1.034	0.052
T2(ms)			
Ischemia (% of LV)*	0.280	−0.010; 0.580	0.061
Non-obstructive HCM	−1.294	−2.389; −0.199	0.021

ECV, extracellular volume; HCM, hypertrophic cardiomyopathy; LGE, late gadolinium enhancement; LV, left ventricle; MWT, maximum wall thickness.
**For each 10% increment of ischemia.*

Studies previously published using CMR and positron emission tomography to study CMD in HCM pointed out that CMD is associated mostly with LV hypertrophy and LGE and linked with worse outcome (**Supplementary Table S5**).

Our study performed a comprehensive assessment of the impact of CMD among important points of the disease pathophysiology.

In HCM, CMD represents an intrinsic feature, being present in various stages of the disease (15). CMD is mainly caused by

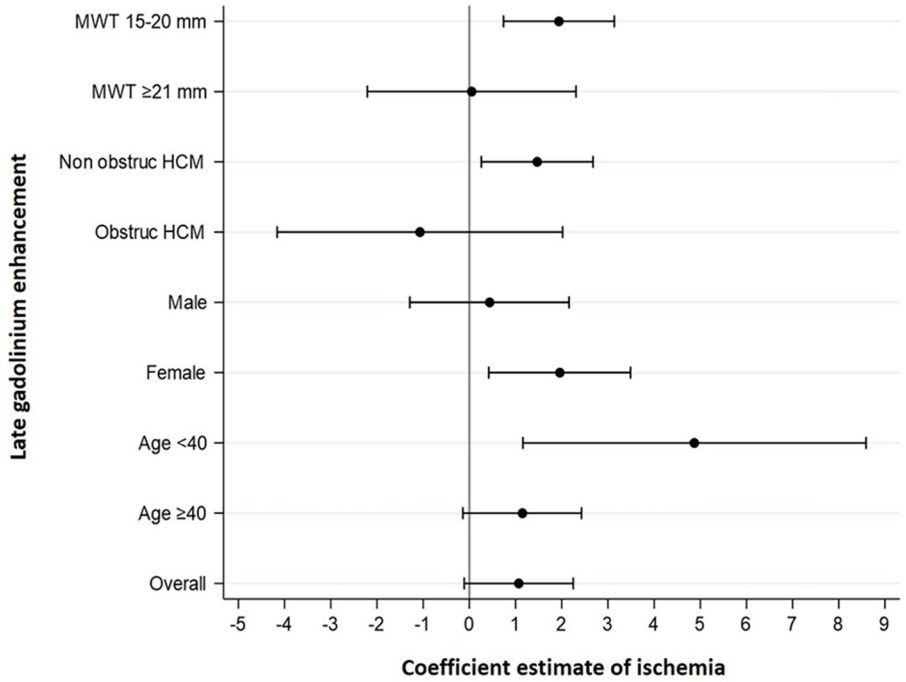

FIGURE 3 | Forest plots for the association between ischemia and LGE. The severity of ischemia was associated with the extent of LGE in patients with MWT 15–20 mm, nonobstructive HCM, women, and age <40 years. Coefficients' estimates and corresponding 95% confidence intervals were obtained by multivariable linear regression models for LGE. MWT, maximum wall thickness; obstruct HCM, obstructive hypertrophic cardiomyopathy.

intrinsic structural abnormalities in intramural small coronary arteries (3) and by extrinsic compression secondary to LV hypertrophy, LVOT obstruction, and diastolic dysfunction. Despite the identification of these pathophysiological factors, it is not clear which patients with HCM will develop functionally significant CMD.

We found greater ischemic burden in patients with more severe LV hypertrophy, without significant association with the presence of LVOT obstruction. The presence of concomitant comorbidities, previously described as associated with CMD, such as hypertension and diabetes (16, 17) was not associated with the presence of ischemia in our cohort.

Ischemia and Tissue Characteristics

Ischemia and the severity of LV hypertrophy were the major factors associated with tissue changes. Ischemia was associated with slightly increased native T1, but not with ECV. We hypothesize that this observation is due to CMD having a greater association with intracellular changes rather than interstitial diffuse fibrosis. Regarding intracellular compartment, the elevation of native T1 in HCM probably depicts intracellular changes, namely altered calcium cycling and sarcomeric calcium sensitivity, disturbed biomechanical stress sensing, and impaired cardiac energy homeostasis (18). Abnormal development of coronary circulation may be secondary to the exposure of coronary precursors to abnormal mechanical stimuli by mutated cardiomyocytes (19), contributing for the association between intracellular abnormalities and CMD.

Despite a significant association between ischemia and LGE in univariable analysis, with an increase of 2% in the extent of LGE verified for each 10% increase of ischemia, this association became weak when adjusting for MWT, which was the most important independent factor associated with LGE in the overall population. CMR studies have demonstrated that the severity of LV hypertrophy is linked to the extent of LGE (20, 21), and higher MWT is independently associated with increased LGE progression rate during the follow-up (22).

However, in the subgroup analyses, ischemia was strongly associated with the extent of LGE among the individuals with MWT 15–20 mm, non-obstructive HCM, women and age <40 years. The recognition of the association between ischemia and LGE in particular subgroups raises important points. The ischemic burden was independently associated with the extent of LGE in subgroups classically associated with lower risk of sudden cardiac death, such as MWT 15–20 mm and non-obstructive HCM (1). Despite the development of different approaches for risk stratification, sudden cardiac death prediction is still characterized by a significant amount of unpredictability (23). LGE is associated with sudden cardiac death (20, 24); therefore, the recognition of features associated with fibrosis has the potential to improve the accuracy of risk stratification in these subsets of patients. In younger patients, ischemia had strong correlation with LGE, independently of MWT, which could explain, at least in part, the heterogeneity in the extent of fibrosis found among younger patients. The recognition of an important precursor of the interstitial fibrotic process may allow

TABLE 5 | Multivariable logistic and linear regression for factors related to arrhythmias and functional capacity.

	Multivariable		
	OR estimate	**95% confidence interval**	***p*-value**
AF/AFL			
Ischemia (% of LV)*	1.669	1.082; 2.574	0.021
Left atrial volume (ml/m^2)	1.105	1.050; 1.164	<0.001
Nonsustained ventricular tachycardia			
Ischemia (% of LV)*	0.864	0.571; 1.307	0.489
Non-obstructive HCM	0.196	0.052; 0.733	0.015
LGE (% of LV)	1.096	1.004; 1.197	0.041
	β-estimate	95% confidence interval	*p*-value
Peak VO_2			
Ischemia (% of LV)*	−0.170	−0.887; 0.547	0.637
Female	−4.907	−7.580; −2.234	<0.001
Age (years)	−0.202	−0.290; −0.114	<0.001
Predicted Peak VO_2			
Ischemia (% of LV)*	1.084	−2.133; 4.301	0.503
LVEF (%)	0.618	0.007; 1.228	0.047
LGE (% of LV)	−0.815	−1.478; −0.153	0.017
VE/VCO_2 slope			
Ischemia (% of LV)*	−0.102	−0.716; 0.512	0.741
LGE (% of LV)	0.195	0.069; 0.320	0.003
Age (years)	0.147	0.076; 0.217	<0.001
Diabetes	4.423	1.551; 7.295	0.003
Time to anaerobic threshold			
Ischemia (% of LV)*	−0.442	−0.860; −0.023	0.039
Non-obstructive HCM	−1.727	−3.255; −0.198	0.027
Age (years)	−0.083	−0.135; −0.031	0.002
Diabetes	−2.330	−4.436; −0.225	0.031
VO_2 at anaerobic threshold			
Ischemia (% of LV)*	−0.159	−0.590; 0.271	0.462
Female	−1.916	−3.534; −0.298	0.021
Age (years)	−0.100	−0.153; −0.046	<0.001
Circulatory power			
Ischemia (% of LV)*	−10.730	−196.200; 174.741	0.908
MWT (mm)	103.970	29.553; 178.387	0.007
LGE(% of LV)	−67.439	−104.494; −30.383	0.001
Female	−887.509	−1502.111; −272.907	0.005
Age (years)	−20.882	−40.255; −1.510	0.035
Beta-blocker	−758.485	−1364.217; −152.753	0.015

HCM, hypertrophic cardiomyopathy; LGE, late gadolinium enhancement; LV, left ventricle; MWT, maximum wall thickness; OR, odds ratio; VCO_2, CO_2 production; VE, ventilation; VO_2, oxygen uptake.
**For each 10% increment of ischemia.*

the development of targeted therapies with significant impact on the disease natural history and prognosis. In HCM, women present less MWT than men (25), and this fact may explain the higher preponderance of ischemia in the fibrotic process, as hypertrophy is not so pronounced. Conversely, MWT was the most important factor associated with LGE in men.

Coronary microvascular dysfunction leads to repetitive episodes of ischemia resulting in myocyte death and fibrotic replacement (26). Postmortem studies in patients with HCM showed different phases of ischemic lesions, including an acute phase with coagulative necrosis and neutrophilic infiltrate to postnecrotic replacement-type fibrosis (2). Interstitial fibrosis derives from fibroblast activity that leads to increased numbers and thickness of collagen fiber, arranged in disorganized patterns (27). The two types of fibrosis reflect different phases of the disease. Whereas interstitial fibrosis is associated with myocyte disarray and predominates at the earliest stages, replacement fibrosis is typically acquired later in the natural history of the disease (28). Histologically, the abnormalities in intramural small vessels closely colocalize to the fibrotic scars, but this association is less stronger with interstitial fibrosis (2, 5, 15). Our findings are in accordance with these published features, as we noted a relationship between ischemia and LGE but not with ECV. High-resolution quantitative perfusion analysis demonstrated a higher ischemic burden in patients with LGE (29), and perfusion mapping confirmed that stress myocardial blood flow was lowest in the fibrotic segments (30). Hyperemic myocardial flow is impaired in areas with LGE and its immediate vicinity compared with remote areas (31). These findings suggested that LGE corresponds, at least in part, to replacement fibrosis secondary to CMD and myocardial ischemia.

Taking into consideration that LGE >15% is a marker of worse outcome (24), we found that ischemia ≥21% of LV has good sensitivity and specificity for the association with LGE >15%.

Myocardial edema evaluated by T2-weighted imaging has been described in patients with HCM, associated with signs of advanced disease, such as higher LV mass, lower ejection fraction, and greater LGE extent (32). Furthermore, high T2 was associated with postexercise troponin rise in patients with HCM, identifying a subset of individuals more vulnerable to myocardial injury after a situation of high oxygen demand (33). In our cohort, ischemia had a weak evidence of association with higher T2 values, whereas non-obstructive HCM was associated with lower T2 compared to obstructive HCM.

CMD, Arrhythmias, and Functional Capacity

Coronary microvascular dysfunction had strong evidence of association with the presence of supraventricular arrhythmia, mainly AF. For each 10% increase in ischemia, there was an increase of 67% in the odds of AF/AFL, and this association was independent of other well-known predictors of AF such as age and left atrial volume or other markers of the disease severity, such as MWT and LVOT obstruction. Although the atrial wall cannot be accurately assessed by CMR, we hypothesize that this link between AF/AFL and ischemic burden may reflect advanced disease, involving atrial myocardium beyond LV myocardium, contributing for atrial dysfunction and arrhythmogenicity. Furthermore, recurrent episodes of ischemia may contribute

to LV diastolic dysfunction and consequent increase in atrial pressures and stretch. In HCM, the relationship between CMD and AF has been previously described even in low-risk patients, independently of atrial dimension (34).

Despite the association between CMD and LGE, and the latest with NSVT, ischemia was not directly linked to NSVT in our cohort. Therefore, this proarrhythmic effect seems to be driven by fibrosis *per se*, without significant contribution from its ischemic precursor.

Age, female gender, and LGE were the most important factors associated with worse functional capacity objectively assessed by CPET. Ischemia was only associated with shorter time to anaerobic threshold. Older age and female gender were associated with lower peak VO_2 and lower VO_2 at anaerobic threshold, in line with previous studies (35). Lower peak VO_2 is associated with increased risk of severe symptoms (36). In HCM, women have shown 50% greater risk of progression to advanced heart failure compared with men, which may be explained by greater prevalence of LV outflow obstruction, smaller LV cavity dimensions, and enhanced susceptibility to LV remodeling (25). In our study, when adjusted to age and gender, LGE became an independent factor associated with predicted peak VO_2, being also associated with higher VE/VCO_2 slope and lower peak circulatory power. Higher VE/VCO_2 slope and worse peak circulatory power, and also the extension of fibrosis (5), have been described markers of worse outcome, including progression to heart failure (37). Our nuanced findings reinforce the link between extensive fibrosis and declined functional capacity.

Besides peak VO_2 and VE/VCO_2 slope, anaerobic threshold was found to be a predictor of all-cause mortality or progression to heart transplant in patients with HCM (35, 38). Interestingly, we found a relationship between greater ischemic burden and shorter time to anaerobic threshold. Older patients with non-obstructive HCM and diabetic had a shorter time to anaerobic threshold and therefore more severe ischemia.

We found a significant relationship between LGE and functional capacity, whereas the association between CPET parameters and ischemia was less pronounced. Whereas the progression of myocardial fibrosis is documented in patients who development heart failure and systolic dysfunction, CMD may remain unchanged compared with earlier phases of the disease (15).

The association between diabetes and higher VE/VCO_2 slope and shorter time to anaerobic threshold was likely in relation to the fact that diabetic patients were older and mostly women.

In our sample, older patients had lower MWT, which may explain the association found between higher MWT and greater circulatory power.

Limitations

An important limitation of our study is the relatively small sample size and low number of events, which limits the achievement of statistical significance in some associations. There was not a validation of tissue characteristics with histological samples. Perfusion defects on CMR are considered as surrogates for ischemia, similar to several other studies in multiple conditions. We decided to adopt a semi-quantitative analysis of ischemia, based on the presence of visual perfusion defects in 32 segments because it was used in a previous landmark study which compared stress CMR with the gold standard of invasive evaluation by fractional flow reserve (11), and it provides an easily applicable and available method for clinical practice. This approach has the inherent limitation of the visual assessment and the total of LV evaluated is 96% (3% for each segment).

Six patients were in AF during CMR scan, which may interfere in the values obtained for parametric mapping.

CONCLUSION

In HCM, ischemia is related to the severity of LV hypertrophy and impacts various pathological and clinical features, encompassing tissue abnormalities and arrhythmic events. Our findings highlight the potential additional role of the evaluation of ischemia in the approach of the patients with HCM and their risk stratification.

DATA AVAILABILITY STATEMENT

The raw data supporting the conclusions of this article will be made available by the authors, without undue reservation.

ETHICS STATEMENT

The studies involving human participants were reviewed and approved by NOVA Medical School, Lisbon Centro Hospital Universitário de Lisboa Central. The patients/participants provided their written informed consent to participate in this study.

AUTHOR CONTRIBUTIONS

SA, AF, MM, and LL contributed to conception and design of the study and interpretation of data. SA, BT, AF, RP, GB, IC, PR, LB, and RF contributed to acquisition and analysis or interpretation of data. AP and MA performed the statistical analysis. SA wrote the first draft of the manuscript. All authors contributed to manuscript revision, read, and approved the submitted version.

FUNDING

LL is supported by an MRC UK clinical academic partnership award (CARP) MR/T005181/1.

SUPPLEMENTARY MATERIAL

The Supplementary Material for this article can be found online at: https://www.frontiersin.org/articles/10.3389/fcvm.2021.761860/full#supplementary-material

REFERENCES

1. Zamorano JL, Anastasakis A, Borger MA, Borggrefe M, Cecchi F, Charron P, et al. 2014 ESC guidelines on diagnosis and management of hypertrophic cardiomyopathy: The task force for the diagnosis and management of hypertrophic cardiomyopathy of the European Society of Cardiology (ESC). *Eur Heart J.* (2014) 35:2733–79. doi: 10.1093/eurheartj/ehu284
2. Basso C, Thiene G, Corrado D, Buja G, Melacini P, Nava A. Hypertrophic cardiomyopathy and sudden death in the young: pathologic evidence of myocardial ischemia. *Hum Pathol.* (2000) 31:988–98. doi: 10.1053/hupa.2000.16659
3. Maron BJ, Wolfson JK, Epstein SE, Roberts WC. Intramural ("small vessel") coronary artery disease in hypertrophic cardiomyopathy. *J Am Coll Cardiol.* (1986) 8:545–57. doi: 10.1016/S0735-1097(86)80181-4
4. Moon JCC, Reed E, Sheppard MN, Elkington AG, Ho SY, Burke M, et al. The histologic basis of late gadolinium enhancement cardiovascular magnetic resonance in hypertrophic cardiomyopathy. *J Am Coll Cardiol.* (2004) 43:2260–4. doi: 10.1016/j.jacc.2004.03.035
5. Galati G, Leone O, Pasquale F, Olivotto I, Biagini E, Grigioni F, et al. Histological and histometric characterization of myocardial fibrosis in end-stage hypertrophic cardiomyopathy. *Circ Heart Fail.* (2016) 9:e003090. doi: 10.1161/CIRCHEARTFAILURE.116.003090
6. Moon JC, Messroghli DR, Kellman P, Piechnik SK, Robson MD, Ugander M, et al. Myocardial T1 mapping and extracellular volume quantification: a Society for Cardiovascular Magnetic Resonance (SCMR) and CMR Working Group of the European Society of Cardiology consensus statement. *J Cardiovasc Magn Reson.* (2013) 15:1–12. doi: 10.1186/1532-429X-15-92
7. Miller CA, Naish JH, Bishop P, Coutts G, Clark D, Zhao S, et al. Comprehensive validation of cardiovascular magnetic resonance techniques for the assessment of myocardial extracellular volume. *Circ Cardiovasc Imaging.* (2013) 6:373–83. doi: 10.1161/CIRCIMAGING.112.000192
8. Messroghli DR, Moon JC, Ferreira VM, Grosse-Wortmann L, He T, Kellman P, et al. Clinical recommendations for cardiovascular magnetic resonance mapping of T1, T2, T2 and extracellular volume: a consensus statement by the Society for Cardiovascular Magnetic Resonance (SCMR) endorsed by the European Association for Cardiovascular Imagin. *J Cardiovasc Magn Reson.* (2017) 19:75. doi: 10.1186/s12968-017-0389-8
9. Varnava AM, Elliott PM, Sharma S, McKenna WJ, Davies MJ. Hypertrophic cardiomyopathy: the interrelation of disarray, fibrosis and small vessel disease. *Heart.* (2000) 84:476–82. doi: 10.1136/heart.84.5.476
10. Lang RM, Badano LP, Mor-Avi V, Afilalo J, Armstrong A, Ernande L, et al. Recommendations for cardiac chamber quantification by echocardiography in adults: An update from the American society of echocardiography and the European association of cardiovascular imaging. *Eur Heart J Cardiovasc Imaging.* (2015) 16:233–71. doi: 10.1093/ehjci/jev014
11. Nagel E, Greenwood JP, McCann GP, Bettencourt N, Shah AM, Hussain ST, et al. Magnetic resonance perfusion or fractional flow reserve in coronary disease. *N Engl J Med.* (2019) 380:2418–28. doi: 10.1056/NEJMoa1716734
12. Maron DJ, Hochman JS, Reynolds HR, Bangalore S, O'Brien SM, Boden WE, et al. Initial invasive or conservative strategy for stable coronary disease. *N Engl J Med.* (2020) 382:1395–407. doi: 10.1056/NEJMoa1915922
13. Harrigan CJ, Peters DC, Gibson CM, Maron BJ, Manning WJ, Maron MS, et al. Hypertrophic cardiomyopathy: quantification of late gadolinium enhancement with contrast-enhanced cardiovascular MR imaging. *Radiology.* (2011) 258:128–33. doi: 10.1148/radiol.10090526
14. Haaf P, Garg P, Messroghli DR, Broadbent DA, Greenwood JP, Plein S. Cardiac T1 Mapping and Extracellular Volume (ECV) in clinical practice: a comprehensive review. *J Cardiovasc Magn Reson.* (2016) 18:89. doi: 10.1186/s12968-016-0308-4
15. Foà A, Agostini V, Rapezzi C, Olivotto I, Corti B, Potena L, et al. Histopathological comparison of intramural coronary artery remodeling and myocardial fibrosis in obstructive versus end-stage hypertrophic cardiomyopathy. *Int J Cardiol.* (2019) 291:77–82. doi: 10.1016/j.ijcard.2019.03.060
16. Hamasaki S, Al Suwaidi J, Higano ST, Miyauchi K, Holmes DR, Lerman A. Attenuated coronary flow reserve and vascular remodeling in patients with hypertension and left ventricular hypertrophy. *J Am Coll Cardiol.* (2000) 35:1654–60. doi: 10.1016/S0735-1097(00)00594-5
17. Di Carli MF, Janisse J, Grunberger G, Ager J. Role of chronic hyperglycemia in the pathogenesis of coronary microvascular dysfunction in diabetes. *J Am Coll Cardiol.* (2003) 41:1387–93. doi: 10.1016/S0735-1097(03)00166-9
18. Frey N, Luedde M, Katus HA. Mechanisms of disease: hypertrophic cardiomyopathy. *Nat Rev Cardiol.* (2012) 9:91–100. doi: 10.1038/nrcardio.2011.159
19. Olivotto I, Girolami F, Sciagr R, Ackerman MJ, Sotgia B, Bos JM, et al. Microvascular function is selectively impaired in patients with hypertrophic cardiomyopathy and sarcomere myofilament gene mutations. *J Am Coll Cardiol.* (2011) 58:839–48. doi: 10.1016/j.jacc.2011.05.018
20. Mentias A, Raeisi-Giglou P, Smedira NG, Feng K, Sato K, Wazni O, et al. Late gadolinium enhancement in patients with hypertrophic cardiomyopathy and preserved systolic function. *J Am Coll Cardiol.* (2018) 72:857–70. doi: 10.1016/j.jacc.2018.05.060
21. Kwon DH, Smedira NG, Rodriguez ER, Tan C, Setser R, Thamilarasan M, et al. Cardiac magnetic resonance detection of myocardial scarring in hypertrophic cardiomyopathy. correlation with histopathology and prevalence of ventricular tachycardia. *J Am Coll Cardiol.* (2009) 54:242–9. doi: 10.1016/j.jacc.2009.04.026
22. Habib M, Adler A, Fardfini K, Hoss S, Hanneman K, Rowin EJ, et al. Progression of myocardial fibrosis in hypertrophic cardiomyopathy: a cardiac magnetic resonance study. *JACC Cardiovasc Imaging.* (2021) 14:947–58. doi: 10.1016/j.jcmg.2020.09.037
23. Weissler-Snir A, Allan K, Cunningham K, Connelly KA, Lee DS, Spears DA, et al. Hypertrophic cardiomyopathy-related sudden cardiac death in young people in Ontario. *Circulation.* (2019) 140:1706–16. doi: 10.1161/CIRCULATIONAHA.119.040271
24. Chan RH, Maron BJ, Olivotto I, Pencina MJ, Assenza GE, Haas T, et al. Prognostic value of quantitative contrast-enhanced cardiovascular magnetic resonance for the evaluation of sudden death risk in patients with hypertrophic cardiomyopathy. *Circulation.* (2014) 130:484–95. doi: 10.1161/CIRCULATIONAHA.113.007094
25. Olivotto I, Maron MS, Adabag AS. Gender-related differences in the clinical presentation and outcome of hypertrophic cardiomyopathy. *ACC Curr J Rev.* (2005) 14:34. doi: 10.1016/j.accreview.2005.10.042
26. Maron MS, Olivotto I, Maron BJ, Prasad SK, Cecchi F, Udelson JE, et al. The case for myocardial ischemia in hypertrophic cardiomyopathy. *J Am Coll Cardiol.* (2009) 54:866–75. doi: 10.1016/j.jacc.2009.04.072
27. Shirani J, Pick R, Roberts WC, Maron BJ. Morphology and significance of the left ventricular collagen network in young patients with hypertrophic cardiomyopathy and sudden cardiac death. *J Am Coll Cardiol.* (2000) 35:36–44. doi: 10.1016/S0735-1097(99)00492-1
28. Finocchiaro G, Sheikh N, Leone O, Westaby J, Mazzarotto F, Pantazis A, et al. Arrhythmogenic potential ofmyocardial disarray in hypertrophic cardiomyopathy: genetic basis, functional consequences and relation to sudden cardiac death. *Europace.* (2020) 2:1–11. doi: 10.1093/europace/euaa348
29. Villa ADM, Sammut E, Zarinabad N, Carr-White G, Lee J, Bettencourt N, et al. Microvascular ischemia in hypertrophic cardiomyopathy: new insights from high-resolution combined quantification of perfusion and late gadolinium enhancement. *J Cardiovasc Magn Reson.* (2016) 18:4. doi: 10.1186/s12968-016-0223-8
30. Camaioni C, Knott KD, Augusto JB, Seraphim A, Rosmini S, Ricci F, et al. Inline perfusion mapping provides insights into the disease mechanism in hypertrophic cardiomyopathy. *Heart.* (2019) 106:824–29. doi: 10.1136/heartjnl-2019-315848
31. Sotgia B, Sciagrà R, Olivotto I, Casolo G, Rega L, Betti I, et al. Spatial relationship between coronary microvascular dysfunction and delayed contrast enhancement in patients with hypertrophic cardiomyopathy. *J Nucl Med.* (2008) 49:1090–6. doi: 10.2967/jnumed.107.050138
32. Todiere G, Pisciella L, Barison A, Del Franco A, Zachara E, Piaggi P, et al. Abnormal T2-STIR magnetic resonance in hypertrophic cardiomyopathy: a marker of advanced disease and electrical myocardial instability. *PLoS ONE.* (2014) 9:e111366. doi: 10.1371/journal.pone.0111366

33. Cramer GE, Gommans DHF, Dieker HJ, Michels M, Verheugt F, De Boer MJ, et al. Exercise and myocardial injury in hypertrophic cardiomyopathy. *Heart.* (2020) 106:1169–75. doi: 10.1136/heartjnl-2019-315818
34. Sciagrà R, Sotgia B, Olivotto I, Cecchi F, Nistri S, Camici PG, et al. Relationship between atrial fibrillation and blunted hyperemic myocardial blood flow in patients with hypertrophic cardiomyopathy. *J Nucl Cardiol.* (2009) 16:92–6. doi: 10.1007/s12350-008-9005-5
35. Coats CJ, Rantell K, Bartnik A, Patel A, Mist B, McKenna WJ, et al. Cardiopulmonary exercise testing and prognosis in hypertrophic cardiomyopathy. *Circ Hear Fail.* (2015) 8:1022–31. doi: 10.1161/CIRCHEARTFAILURE.114.002248
36. Sorajja P, Allison T, Hayes C, Nishimura RA, Lam CSP, Ommen SR. Prognostic utility of metabolic exercise testing in minimally symptomatic patients with obstructive hypertrophic cardiomyopathy. *Am J Cardiol.* (2012) 109:1494–8. doi: 10.1016/j.amjcard.2012.01.363
37. Magrì D, Re F, Limongelli G, Agostoni P, Zachara E, Correale M, et al. Heart failure progression in hypertrophic cardiomyopathy - Possible insights from cardiopulmonary exercise testing. *Circ J.* (2016) 80:2204–11. doi: 10.1253/circj.CJ-16-0432
38. Finocchiaro G, Haddad F, Knowles JW, Caleshu C, Pavlovic A, Homburger J, et al. Cardiopulmonary responses and prognosis in hypertrophic cardiomyopathy. A potential role for comprehensive noninvasive hemodynamic assessment. *JACC Hear Fail.* (2015) 3:408–18. doi: 10.1016/j.jchf.2014.11.011

Conflict of Interest: The authors declare that the research was conducted in the absence of any commercial or financial relationships that could be construed as a potential conflict of interest.

Publisher's Note: All claims expressed in this article are solely those of the authors and do not necessarily represent those of their affiliated organizations, or those of the publisher, the editors and the reviewers. Any product that may be evaluated in this article, or claim that may be made by its manufacturer, is not guaranteed or endorsed by the publisher.

Advantages of publishing in Frontiers

OPEN ACCESS
Articles are free to read for greatest visibility and readership

FAST PUBLICATION
Around 90 days from submission to decision

HIGH QUALITY PEER-REVIEW
Rigorous, collaborative, and constructive peer-review

TRANSPARENT PEER-REVIEW
Editors and reviewers acknowledged by name on published articles

Frontiers
Avenue du Tribunal-Fédéral 34
1005 Lausanne | Switzerland

Visit us: www.frontiersin.org
Contact us: frontiersin.org/about/contact

REPRODUCIBILITY OF RESEARCH
Support open data and methods to enhance research reproducibility

DIGITAL PUBLISHING
Articles designed for optimal readership across devices

FOLLOW US
@frontiersin

IMPACT METRICS
Advanced article metrics track visibility across digital media

EXTENSIVE PROMOTION
Marketing and promotion of impactful research

LOOP RESEARCH NETWORK
Our network increases your article's readership